DOE/NV/10461--T76

EVALUATION OF THE GEOLOGIC RELATIONS AND SEISMOTECTONIC STABILITY OF THE YUCCA MOUNTAIN AREA NEVADA NUCLEAR WASTE SITE INVESTIGATION (NNWSI)

PROGRESS REPORT

30 SEPTEMBER 1995

CENTER FOR NEOTECTONIC STUDIES

MACKAY SCHOOL OF MINES

UNIVERSITY OF NEVADA, RENO

CONTENTS

SECTION I

Annual Progress Report----General Task
Prepared by Steven G. Wesnousky

October 1, 1994 to September 30, 1995

Introduction

This report provides a summary of progress for the project "Evaluation of the Geologic Relations and Seismotectonic Stability of the Yucca Mountain Area, Nevada Nuclear Waste Site Investigation (NNWSI)." A similar report was previously provided for the period of 1 October 1993 to 30 September 1994. The report initially covers the activities of the General Task and is followed by sections that describe the progress of the other ongoing Tasks which are listed below.

Task 1:	Quaternary Tectonics
Task 3:	Mineral Deposits, Volcanic Geology
Task 4:	Seismology
Task 5:	Tectonics
Task 8:	Basinal Studies

General Task

Staff

Steven G. Wesnousky, Project Director; Nina G. Krob, Administrative Assistant

Administrative Activities

The General Task continued the (1) coordination and oversight of the research of Tasks 1, 3, 5, and 8, the (2) oversight of budgets and (3) the collation and preparation of required monthly reports. As well, Dr. Wesnousky has continued to represent NWPO at meetings with the National Academy of Sciences, the Nuclear Regulatory Commission, and the Department of Energy.

Steven G. Wesnousky attended the following meetings and provided the following seminars for NWPO:

January 26, 1994, NRC/DOE Technical Exchange on Seismic Hazard Assessment and Seismic Design, Las Vegas, NV

February 2-5, 1995, NWPO field trip to examine faults in the Yucca block, precarious rocks, and the Rock Valley fault.

May 5 - 6, 1995, Examine Crater Flat and Rock Valley Trenches.

May 16-17, 1995, NRC-DOE technical exchange at FOC, Yucca Mountain.

June 15, 1995, Technical Contractors Meeting at Carson City.

Technical Activities

Projects Completed:

Scaling Laws relating earthquake size, fault slip rate, and earthquake magnitude: This project was implemented in the preceding fiscal year, completed during this fiscal year, and submitted and accepted for publication this fiscal year. Estimation of the size of expected earthquakes along mapped faults is generally determined from empirically derived relationships between fault length and seismic moment or magnitude for historical earthquakes. There are numerous of these compilations, including a most recent by Wells and Coppersmith (BSSA, v.84, 974-1003, 1994). Many of these compilations and resulting regressions of earthquake size versus fault length tend to ignore an observation that has been in the seismological literature for some time, which is that the relationship of earthquake size versus rupture length in earthquakes is a function of the repeat time or fault slip rate on which the earthquake occurs (e.g. Scholz et al, BSSA, v. 76, 65-70, 1986; Kanamori and Allen, in Earthquake Source Mechanics, v. 6, 1985; Wesnousky, JGR, v. 91, 12,587-12,631, 1986). We show that slow slipping faults will generally produce a larger moment-magnitude earthquake than a faster slipping fault, by as much as .3 to .4 magnitude units when considering faults slipping at .01 to 10 mm/yr, respectively.

Earthquake Frequency Statistics: Whether or not seismicity on a particular fault satisfies the Gutenberg-Richter or characteristic earthquake distribution is important to seismic hazard analysis at Yucca Mountain. Study of the question is hampered by limited historical, geological, and instrumental data. We initially used a well-defined data set in southern California and extended the research to a global data set of faults to empirically examine the question. The results are published or now in press in Wesnousky (1994), Stirling et al, (1995), and Wesnousky (1995).

Meetings and Abstracts:

1994 AGU Annual Fall Meeting, San Francisco, CA

Adams, K. D. and S. G. Wesnousky, Isostatic Rebound of the Pluvial Lake Lahontan Basin, Nevada and California: Progress Report, EOS supplement, Nov 1, 1994, p.581.

Kumamoto, T. and S. G. Wesnousky, Review of Japanese Paleoearthquake Data: Observations Bearing on the Characteristic of Earthquake Recurrence along Japanese Intraplate Faults, EOS supplement, Nov 1, 1994, p. 452.

Stirling, M., S. G. Wesnousky, and K. Shimazaki, Fault Trace Complexity, Cumulative Slip and the Shape of the Magnitude-Frequency Distribution fort Strike-Slip Faults: A Global Survey, EOS supplement, Nov 1, 1994, p. 437.

1995 SSA Annual Meeting, El Paso, TX

Anderson, J. G., S. G. Wesnousky, M. W. Stirling, M. P. Sleeman, and T. Kumamoto, Regressions for Magnitude of Earthquakes incorporating fault slip rate as an independent parameter.

1995 Cordilleran Section of the Geological Society of America, Boise, Idaho.

Adams, K. D., and S. G. Wesnousky, The age and synchroneity of the Highest Lake Lahontan Shoreline Features, Northwestern Nevada and Northeastern California.

1995 Int. Union. Quaternary Research (INQUA), 14th Congress, Aug 3-10, Berlin, 1995

Johnson, D. L., S. G. Wesnousky, and L. Abbott, Rapid, time-constrained pedogenesis and diagenesis following natural (1811-12 Earthquakes) and human-caused (1916 Watertable lowering) events, New Madrid Seismic Zone, Midcontinental USA.

Wesnousky, S. G., Johnson, D. L., and L. Abbott, Paleosol and C-14 evidence for two pre-1811 large magnitude earthquakes in the New Madrid Seismic Zone, Midcontinental USA.

1995 Y. M. Goldschmidt Conference, Penn State University, University Park, PA. May 24-26

Johnson, D. L., and S. G. Wesnousky, Origins and ages of iron concretions formed in sand, New Madrid seismic zone, Midcontinental USA.

Publications

Wesnousky, S. G., The Gutenberg-Richter or Characteristic Earthquake Distribution, Which is it? (1994) Bulletin of the Seismological Society of America, 84, 1940-1959.

Working Group on California Earthquake Probabilities (Contributor), Seismic Hazards in Southern California: Probable Earthquakes, 1994 to 2024 (1995), Bulletin of the Seismological Society of America, 85, 379-439.

Kumamoto, T., S. G. Wesnousky, M. Okamura, H. Tsutsumi, N. Chida, K. Shimazaki, and T. Nakata (1995), Active Faults in Lake Tahoe, Western Part of the United States--a Preliminary Report, Active Fault Research, v. 13, 47-53.

Caskey, S. J., S. G. Wesnousky, P. Zhang, and D. B. Slemmons, Surface Faulting and Mechanical Aspects of the 1954 Fairview Peak (Ms = 7.2) and Dixie Valley (Ms=6.9) Earthquakes, Central Nevada, accepted for publication in the Bulletin of the Seismological Society of America.

Caskey, S. J., Geometric relations of dip slip to a faulted ground surface: new nomograms for estimating components of fault displacement, Journal of Structural Geology, 17, 1197-1202, 1995.

Anderson, J. G., S. G. Wesnousky, M. W. Stirling, M. P. Sleeman, and T. Kumamoto, Earthquake Size as a Function of Fault Slip Rate, submitted to Bulletin of the Seismological Society of America.

Stirling, M. W., S. G. Wesnousky, Fault trace complexity, cumulative slip, and the shape of the magnitude-frequency distribution for strike-slip faults: a global survey, accepted for publication in the Geophysical Journal of the Royal Astronomical Society.

Hirabayashi, C. K., T. K. Rockwell, S. G. Wesnousky, M. W. Stirling, and F. Suarez-Vidal, A Neotectonic Study of the San Miguel-Vallecito fault, Baja California, Mexico, accepted for publication in the Bulletin of the Seismological Society of America.

SECTION II

TASK 1 QUATERNARY TECTONICS

PROGRESS REPORT

1 October 1994 to 30 September 1995

John W. Bell
Principal Investigator

Craig M. dePolo
Co-Investigator

SUMMARY OF ACTIVITIES CONDUCTED DURING THE CONTRACT PERIOD

During the contract period, the following activities were conducted by Task 1:

** J.W. Bell completed and published with F.F. Peterson, R.I. Dorn, A.R. Ramelli, and T.L. Ku the paper "Late Quaternary geomorphology and soils in Crater Flat, Yucca Mountain area, southern Nevada" in the Geological Society of America *Bulletin*, v. 107, no. 4, p. 379-395.

** J.W. Bell completed and submitted the map "Quaternary Geologic Map of the Mina Quadrangle, Nevada" which is being published as Nevada Bureau of Mines and Geology Field Studies Map 10 (in press).

** C.M. dePolo together with A.R. Ramelli and J.W. Bell published "The 1932 Cedar Mountain earthquake, central Nevada, USA: a Major Basin and Range Province Earthquake That Had a Widely Distributed Surface Rupture Faulting Pattern" in Proceedings of the Workshop on Paleoseismology: U.S. Geological Survey Open-file Report 94-568, p. 50-52.

** C.M. dePolo published "Estimating Fault Slip Rates in the Great Basin, USA" in Proceedings of the Workshop on Paleoseismology: U.S. Geological Survey Open-file Report 94-568, p. 48-49.

** C.M. dePolo together with J.W. Bell and A.R. Ramelli completed the draft manuscript "Surface Faulting Associated with the December 21, 1932 Cedar Mountain, Nevada Earthquake and Implications for Seismic Hazard Studies" for publication as a Nevada Bureau of Mines and Geology Special Publication.

** J.W. Bell and C.M. dePolo began preparation of the journal paper "Paleoseismic History of the 1932 Cedar Mountain Earthquake Zone".

** C.M. dePolo and J.W. Bell reviewed the DOE Topical Report "Methodology to Assess Fault Displacement and Vibratory Ground Motion Hazards at Yucca Mountain".

** J.W. Bell reviewed the DOE Topical Report "Evaluation of the Potentially Adverse Condition 'Evidence of Extreme Erosion During the Quaternary Period' at Yucca Mountain, Nevada".

** J.W. Bell reviewed DOE quality assurance data for trench review at Yucca Mountain.

** J.W. Bell and C.M. dePolo attended a DOE/NRC videoconference meeting in Las Vegas held to address seismic hazard and design.

** J.W. Bell organized a three-day field review of fault trenches at Yucca Mountain for NWPO and other State participants.

** J.W. Bell and C.M. dePolo attended a two-day USGS-sponsored workshop in Denver held

to formulate deterministic ground motion models for Yucca Mountain.

** J.W. Bell attended the meeting in Salt Lake City of the DOE Expert Panel on Probabilistic Seismic Hazard and made the presentation "Overview of Nevada Bureau of Mines and Geology Research Activities at Yucca Mountain".

** J.W. Bell attended the annual NRC/DOE field review at Yucca Mountain.

** J.W. Bell was co-chairman for the session "Field Data Acquisition and Analysis for Ground Motion and Faulting" at the American Nuclear Society FOCUS 95 Meeting "Methods of Seismic Hazards Evaluation".

** J.W. Bell and C.M. dePolo conducted field activities at Yucca Mountain:

Logging of Ghost Dance fault exposure at UZ-7a drillpad.
Logging of Whale Back Ridge trench
Field examination of Ghost Dance-Abandoned Wash-Dune Wash fault system
Review of USGS Crater Flat trenches 1,2,3 and 4
Review of Bare Mountain trench 3
Review of Solitario Canyon trenches 8 and SCFT-3

** J.W. Bell and C.M. dePolo completed field investigations in the 1932 Cedar Mountain earthquake area:

Completion of mapping of 1932 surface ruptures
Completion and review of trenches 3 and 6
Radiocarbon dating of samples from trench 6
Compilation of logs for trenches 3, 6, and 8

** C.M. dePolo and J.W. Bell conducted field investigations of ground cracking associated with the 1994 Double Spring Flat earthquake (M_s6.3).

TECHNICAL REPORT

Paleoseismic Studies in the 1932 Cedar Mountain Earthquake Area

Several components of the on-going studies in the 1932 Cedar Mountain area were brought to completion during the contract period. These included compilation of late Quaternary and historic faulting in the region, finalization of Quaternary stratigraphic relations and ages, and radiocarbon dating of deposits exposed in trenches.

Distribution of late Quaternary and historic surface faulting

Large-scale (1:24,000) mapping of surface ruptures associated with the 1932 Cedar Mountain event was completed, and the maps will be published as a Nevada Bureau of Mines and Geology Special Publication titled "Surface Faulting Associated with the December 21, 1932 Cedar Mountain, Nevada Earthquake and Implications for Seismic Hazard Studies". A journal paper titled "Paleoseismic History of the 1932 Cedar Mountain Earthquake Area" is being prepared which will synthesize the results of stratigraphic, trenching and dating studies.

The 1932 Cedar Mountain rupture zone consisted of three separate distributive rupture sets (Fig. 1): 1. right-lateral faulting in Monte Cristo Valley; 2. apparent right-lateral faulting in Stewart Valley, and 3. normal faulting in Gabbs Valley. The main epicenter was located in the southern Gabbs Valley area and a second event was placed slightly west of the main event (Byerly, 1935; Doser, 1988). Based on seismic moment and the extent of right-lateral faulting occurring in Monte Cristo Valley, it is likely that a third and possibly a fourth subevent also occurred in the southern portion of the rupture zone (dePolo and others, 1994)

Figure 1 shows the relation between the 1932 ruptures and other historical and late Quaternary faults in the region. The northern portion of the rupture zone overlaps the southern portion of the 1954 Fairview Peak surface faulting which extended along the eastern flank of Mt. Annie. In the epicentral area, minor normal 1932 faulting occurred along Holocene and late Pleistocene scarps of the Paradise Range fault zone. Although Doser (1988) believed the location of the 1932 subevent to be poorly defined, she placed it close to the trace of the Petrified Spring fault, a large northwest-trending late Quaternary fault of the Walker Lane system. Other principal, active, late Quaternary faults include the Benton Spring, Gumdrop Hills, and Indian Head faults. The Excelsior Mountains fault zone ruptured in 1934 (M6.3) with about 15-30 cm of secondary surface displacement.

Quaternary Stratigraphic Studies in the 1932 Cedar Mountain Area

Detailed Quaternary stratigraphic studies were completed in the Mina and Monte Cristo Valley areas (Figs. 2,3, and 4; Bell, 1995). These studies form the basis for defining the paleoseismic relations in the Monte Cristo Valley rupture zone.

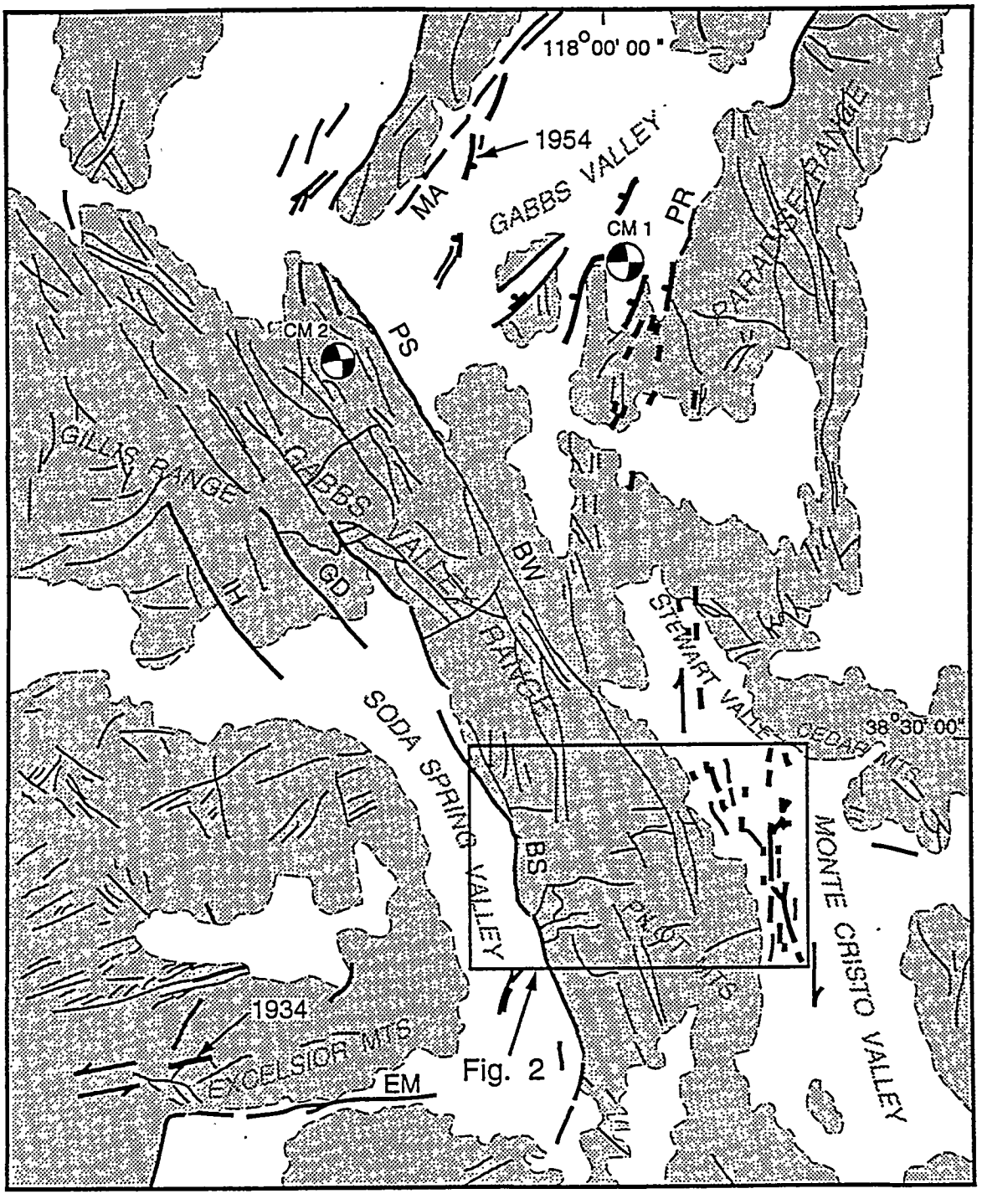

Figure 1. Regional fault map of the 1932 Cedar Mountain earthquake area. Principal regional faults include the Excelsior Mountain (EM), Benton Spring (BS), Indian Head (IH), Gumdrop Hills (GD), Bettles Well (BW), Petrified Spring (PS), Paradise Range (PR), and Mount Annie (MA) faults. Location of Figure 2 is shown by box.

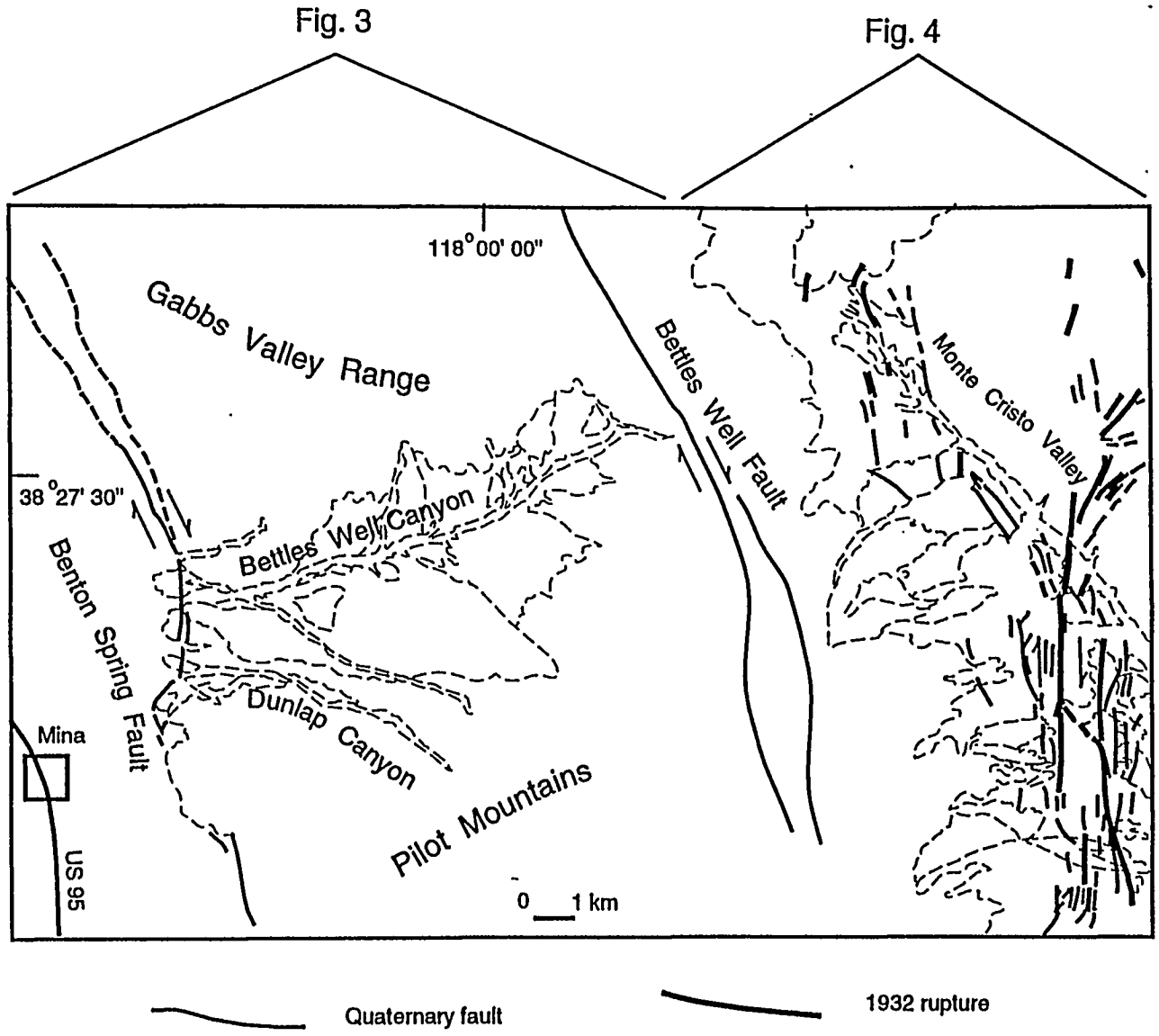

Figure 2. Generalized location map showing distribution of Quaternary deposits and faults in the Benton Spring and Monte Cristo Valley areas. Regional stratigraphic relations were developed within this region to establish a chronostratigraphy for defining the paleoseismic history of the 1932 Cedar Mountain fault zone. Detailed stratigraphic relations and dating location sites are shown on Figures 3 and 4.

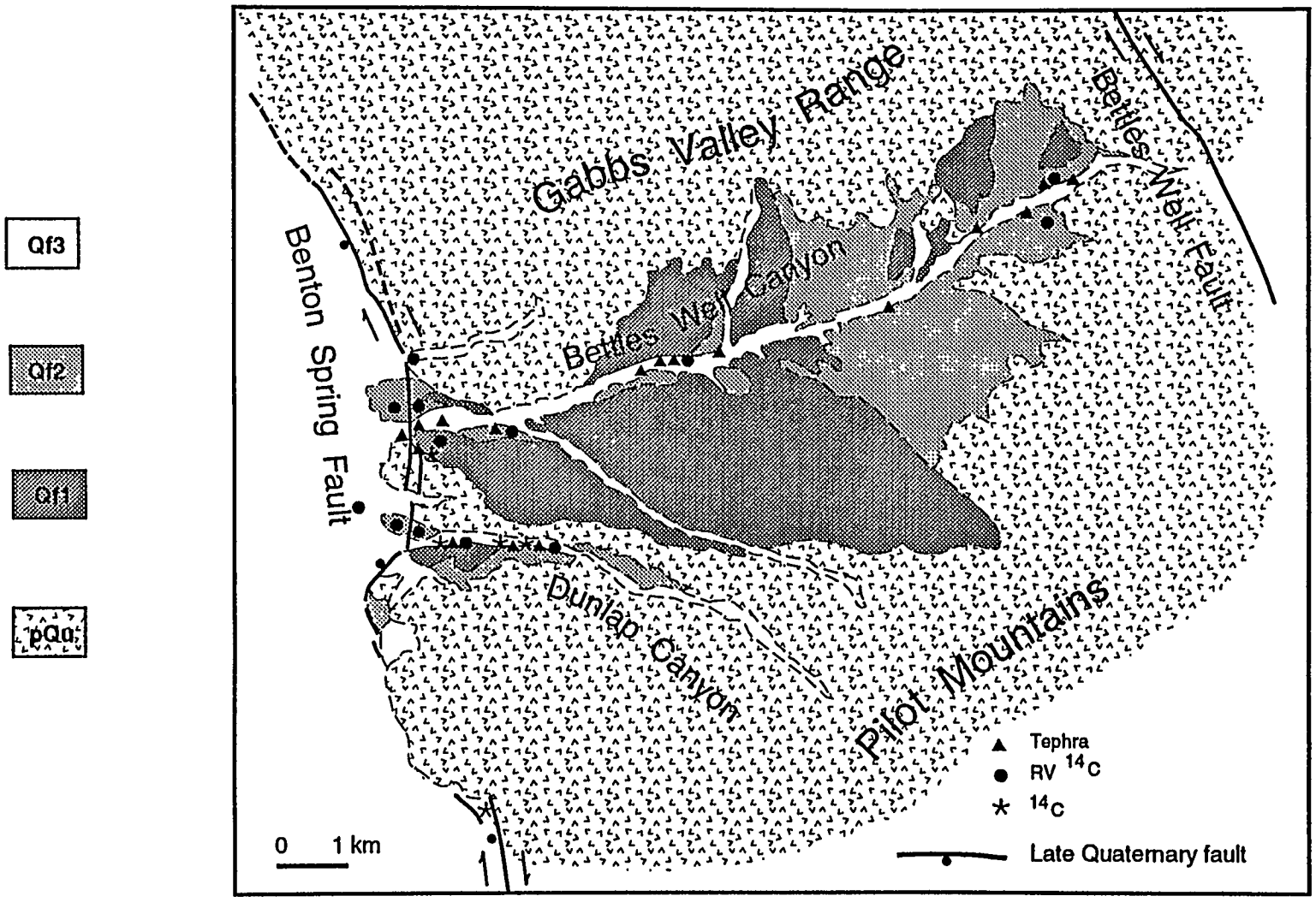

Figure 3. Generalized surficial geology of the Benton Spring fault region showing Quaternary stratigraphy and dating locations.

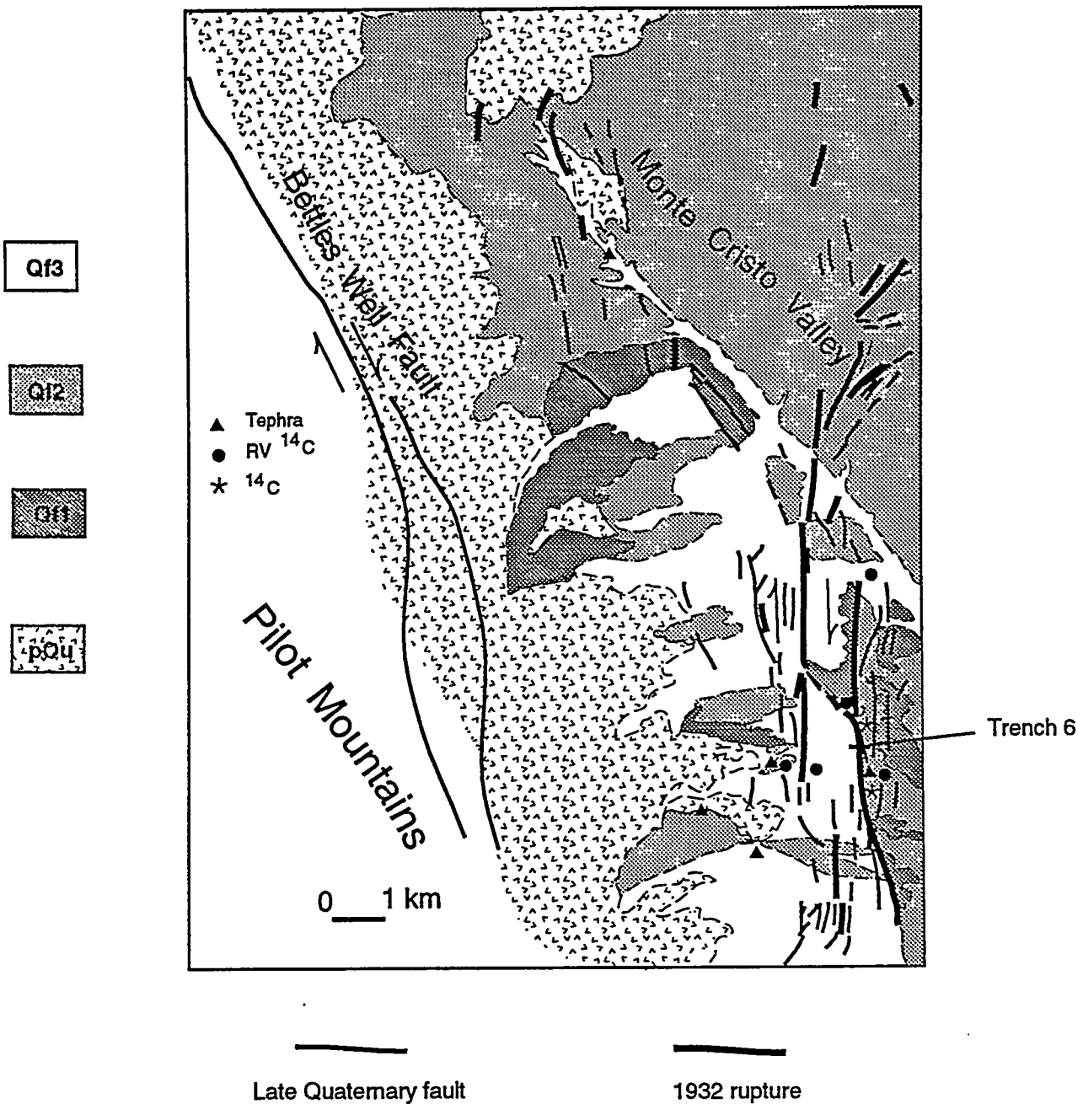

Figure 4. Generalized surficial geology of the Monte Cristo Valley fault zone region showing Quaternary stratigraphy and dating locations.

Three principal allostratigraphic units are defined based upon broad geomorphic relations (Qf1, Qf2, and Qf3). The latter two units are further subdivided on the basis of soils, rock varnish, tephrochronology, and conventional ^{14}C dating: Qf2a, Qf2b, Qf3a, Qf3b, and Qf3c. The generalized distribution of these units is shown on Figs. 3 and 4. Detailed 1:24,000-scale mapping conducted in the Mina quadrangle provides the primary basis for defining numerical age relations. This detailed mapping is included as Appendix A.

Sampling locations for volcanic tephra, rock varnish, and conventional ^{14}C analysis are shown on Figs. 3 and 4. A tabulation of tephra glass chemistry and identification and a listing of conventional ^{14}C dates are provided in Appendix A. Rock varnish data are provided in Table 1.

Radiocarbon Dating of Trench 6 Deposits

Trench 6 is located across the principal trace of the Monte Cristo Valley segment of the 1932 rupture (Fig. 4). A sequence of late Pleistocene and Holocene ponded, colluvial, and alluvial-fan sediments are faulted against bedded tuffaceous sediments of the Tertiary Esmeralda formation (Fig. 5). The 1932 event vertically offset this sequence about 1m; horizontal slip is estimated to have been 1-2 m. The presence of weakly developed paleosols and stone lines in association with colluvial wedges buttressed against the fault indicate recurrent offset along this trace.

Nine samples of organic soil material were collected from Trench 6 (Table 2). Soils developed within Trench 6 deposits are weakly developed, gray, massive to weakly vesicular A-horizons ranging in thickness from 5-10 cm. The soils were submitted to Geochron Laboratories for bulk sample radiocarbon analysis. The radiocarbon dating of bulk soil samples provides a minimum age (mean residence time) for the deposit based on the cumulative nature of carbon accumulation in the near surface. In applying the bulk soil dating approach to the buried paleosols here, we assume that the decalcified organic material contained in the buried soil is an accumulation of humus originating when the soil formed at the ground surface. We further assume that once isolated through burial, the organic matter decayed under closed system conditions. Four of the soil samples had sufficient organic matter to allow conventional radiocarbon analysis; the remaining five samples had insufficient organic matter and required dating by accelerator mass spectrometry (AMS) analysis.

TABLE 1

CEDAR MOUNTAIN AREA ROCK VARNISH DATA
(R.I. Dorn, 1993)

Unit	Sample #	^{14}C date in yrs BP (Lab #)	Cation ratio (K + Ca/Ti)
Qf3c	BS34	625 ± 75 (NZA 1382)	9.07 ± 0.20
Qf3c	BS46	823 ± 66 (NZA 2929)	8.95 ± 0.12
Qf3c	BS9 (1990)	--	9.27 ± 0.60
Qf3c	BS10	1134 ± 70 (NZA 2931)	8.66 ± 0.16
Qf3c	BS9(1992)	1267 ± 71 (NZA 2930)	8.66 ± 0.19
Qf3b	BS75	4347 ± 72 (NZA 2933)	7.31 ± 0.21
Qf3b	CM34	--	7.13 ± 0.15
Qf3b	CM35	5900 ± 90 (NZA 1380)	7.03 ± 0.10
Qf3a	BS42	8000 ± 100 (NZA 1368)	6.82 ± 0.15
Qf3a	CM33	11,250 ± 120 (NZA 1381)	6.59 ± 0.10
Qf2b	CM18	21,940 ± 360 (NZA 1377)	5.56 ± 0.23
Qf2b	BS39	--	5.52 ± 0.16
Qf2b	BS37	22,170 ± 370 (NZA 1360)	5.50 ± 0.11
Qf2b	CM22	22,740 ± 360 (NZA 1417)	5.50 ± 0.11
Qf2b	BS28	--	5.48 ± 0.12
Qf2b	BS27	25,430 ± 480	5.42 ± 0.09
Qf2b	BS8	25,020 ± 270 (NZA 2935)	5.41 ± 0.09
Qf2a	BS35	--	4.40 ± 0.14
Qf2a	BS43	>47,000 (NZA 2934)	4.33 ± 0.18
Qf1b	BS41	--	3.79-4.06

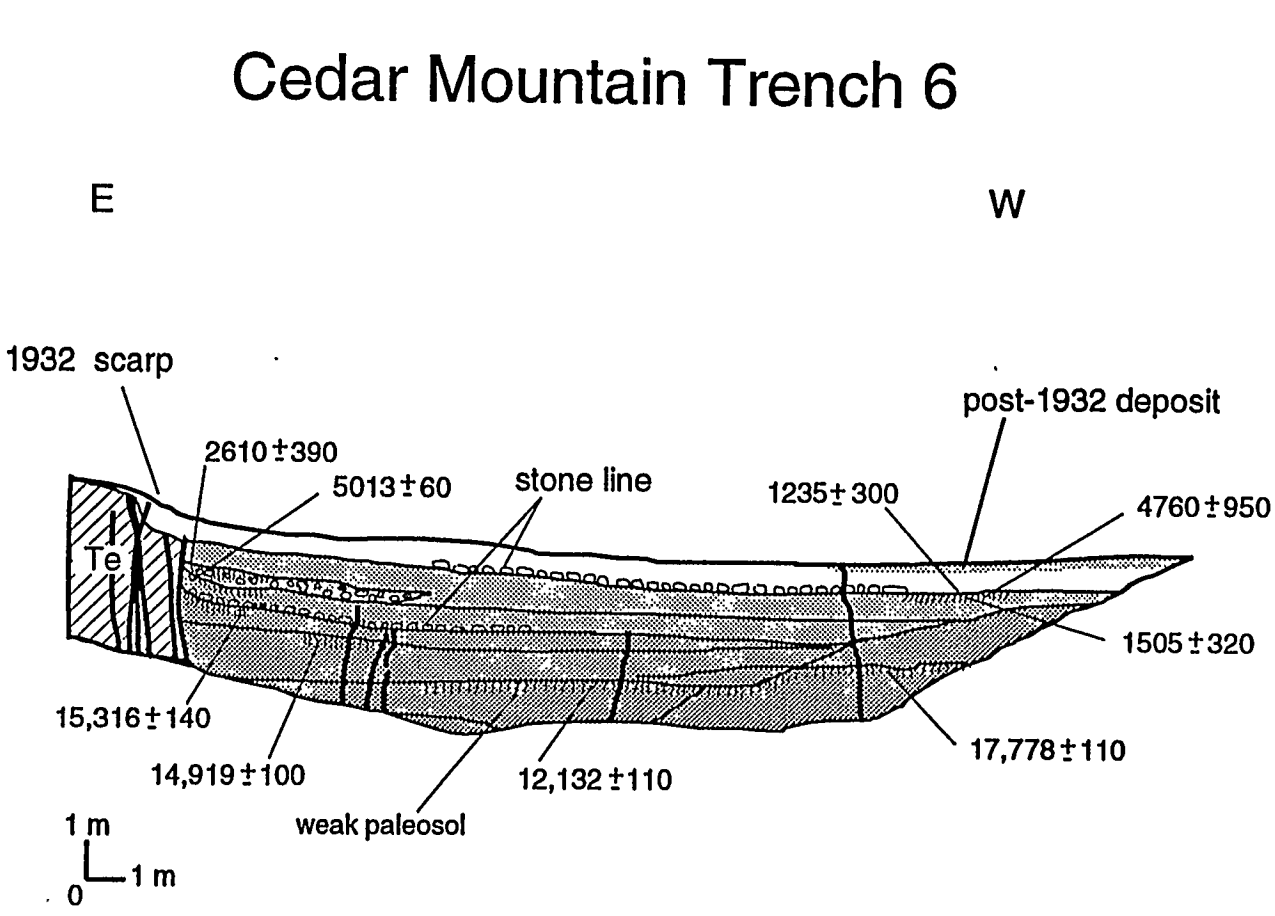

Figure 5. Generalized log of Cedar Mountain trench 6 showing location and ages of ^{14}C samples.

TABLE 2

Trench 6 ^{14}C Dates

Sample #	Material dated	^{14}C yrs (Lab#)	Calibrated yrs
CM-5	soil organics	4760 ± 950 (GX-18938)	5491^{+1261}_{-1018}
CM-6	soil organics	1505 ± 320 (GX-20327)	1388^{+290}_{-372}
CM-7	soil organics	2610 ± 390 (GX-20328)	2757^{+390}_{-462}
CM-8	soil organics	5013 ± 60 (GX-20329; AMS)	5755^{+73}_{-133}
CM-9	soil organics	15,316 ± 140 (GX-20330; AMS)	**
CM-10	soil organics	14,919 ± 100 (GX-20331; AMS)	**
CM-11	soil organics	17,778 ± 110 (GX-20332; AMS)	**
CM-12	soil organics	12,132 ± 110 (GX-20333; AMS)	**
CM-13	soil organics	1235 ± 300 (GX-20334)	1175^{+295}_{-245}

** Radiocarbon age beyond the range of calibration curve (8000 yrs)

EVIDENCE FOR QUATERNARY MOVEMENT ON THE GHOST DANCE FAULT

At the request of the Nuclear Waste Project Office, a study of surficial relations and trench exposures along the Ghost Dance fault was conducted in order to assess the evidence for Quaternary movement. The Ghost Dance fault is the principal through-going structural feature transecting the proposed repository block.

Background

Previous Work

The Ghost Dance fault appears on the first maps produced for the Yucca Mountain region, for example, the map of Lipman and McKay (1965). Scott and Bonk (1984) mapped the Ghost Dance fault and other faults of the Yucca Mountain system in detail (Fig. 6) , noting that carbonate breccias and adjacent, imbricate faults typify the zone. The Ghost Dance fault is described by Scott and Bonk (1984) as a down-to-the-west fault with 20 to 30 m of offset of the nonwelded unit of the Tiva Canyon member of the Paintbrush tuff.

Scott (1990) provided a detailed structural interpretation of Yucca Mountain. An important aspect of the Ghost Dance fault is the imbricate fault zone, lying to the east and south of the main fault. The imbricate zone is made up of "closely spaced, steep, west-dipping faults with minor, down-to-the-west offsets of a few meters or less" (Scott, 1990).

O'Neill and others (1992) were the first to note the relationship between the Ghost Dance fault and the multiple zones of deformation along its southern reach. They identified the Abandoned Wash fault and a series of northwest-trending faults, here referred to the Western Dune Wash fault zone, as southern extensions of the Ghost Dance fault. They characterized the geomorphic expression of the central part of the Ghost Dance fault as "a series of colinear topographic features that cut across east-trending ridges ...". They note that although the fault is easily mappable on the ground, it is less obvious on the aerial photographs.

Spengler and others (1993) conducted detailed structural mapping of the Ghost Dance fault at Antler Ridge. They found that in addition to the recognized singular trace of the fault originally mapped by Scott and Bonk (1984), a zone of secondary faulting, fractured rock, and stratal flexing cumulatively comprising a shear zone as much as 213 m wide characterized the fault. These secondary faults were found to be parallel to the principal Ghost Dance fault and contained near-vertical features commonly spaced at about 15 to 46 m intervals, with 3 to 6 m of individual down-to-the-west offsets. A cross section by Spengler and others (1993) showed the main trace of the Ghost Dance fault at Antler Ridge having about 16 m of vertical separation in tuffs of the Tiva Canyon member, with about 30 m of cumulative separation across the entire zone of faulting. Thus, the zone of secondary faulting appears to account for about half of the overall displacement. Spengler and others (1993) noted that the Ghost Dance fault dies out to the north into highly brecciated and fractured rock. They also noted that the Swadley and others

Figure 6. Geologic map of the repository block portion of Yucca Mountain (from Scott and Bonk, 1984).

(1984) trenches were inconclusive and that "the age of latest movements along the Ghost Dance fault remains unknown".

Spengler and others (1994) conducted additional mapping of the zone around the Ghost Dance fault, ultimately expanding the mapped width of the zone to 366 m. They noted:

> "The width of the Ghost Dance fault system is consistent with the width of the area where north- to northeast-trending faults had been previously mapped on either side of the Ghost Dance fault by Scott and Bonk (1984). These ancillary faults were previously interpreted to have northern terminations near the crest of Broken Limb Ridge at the southeastern margin of the proposed repository area."

Spengler and others (1994) also found that field observations indicated that the Ghost Dance fault is offset right-laterally at least 52 m along its northern part by a northwest-trending fault they named the Sundance fault zone. They noted that relative age relationships remained unresolved.

Pezzopane and others (1994) characterized the Ghost Dance fault as "one of the smaller intra-block faults within the potential repository block." They further noted that "the fault lacks a youthful geomorphic expression, and no displacement of late Quaternary alluvium is apparent in trenches across the fault trace." They estimated the length of the Ghost Dance fault to be 3 km, with a maximum of 7 km possible if structural connections are considered. They questioned whether the Ghost Dance fault extends to seismogenic depths, suggesting a possible structural connection with more prominent Quaternary faults. They noted that the fault length is proportional to a magnitude 6 to 6.5 earthquake, but concluded that it is more likely that the fault is structurally attached to other larger seismogenic features such as the Paintbrush Canyon or Solitario Canyon faults.

Simonds and others (1995) included the Ghost Dance fault on their fault compilation map of the Yucca Mountain site area and provided map notations regarding geomorphic characteristics of the fault. They described the Ghost Dance fault as the "main structure in a diffuse zone of minor bedrock faults and fractured rock east of Yucca Crest". They estimated the overall fault length of the Ghost Dance fault at 9 km if the longest bedrock splay is connected to it; this splay merges with the Iron Ridge fault at it south end. The Ghost Dance fault and possible related faults are annotated as "bedrock faults" by Simonds and others (1995). At Whale Back Ridge, however, they noted the existence of geomorphic scarps of unknown age in bedrock as much as 0.5 to 2 m in height. Similarly, along the Western Dune Wash fault zone (Fig. 7), several parallel fault traces exhibit subtle degraded bedrock scarps of unknown age. They also noted that a graben forms a low swale approximately 25 m wide in this area.

Swadley and others (1984) reported on five trench exposures across the projections of the Ghost Dance and Abandoned Wash faults: trenches 1, 2, 4, 6, and 9 (Fig. 7). A discussion of relations exposed in these trenches is presented below.

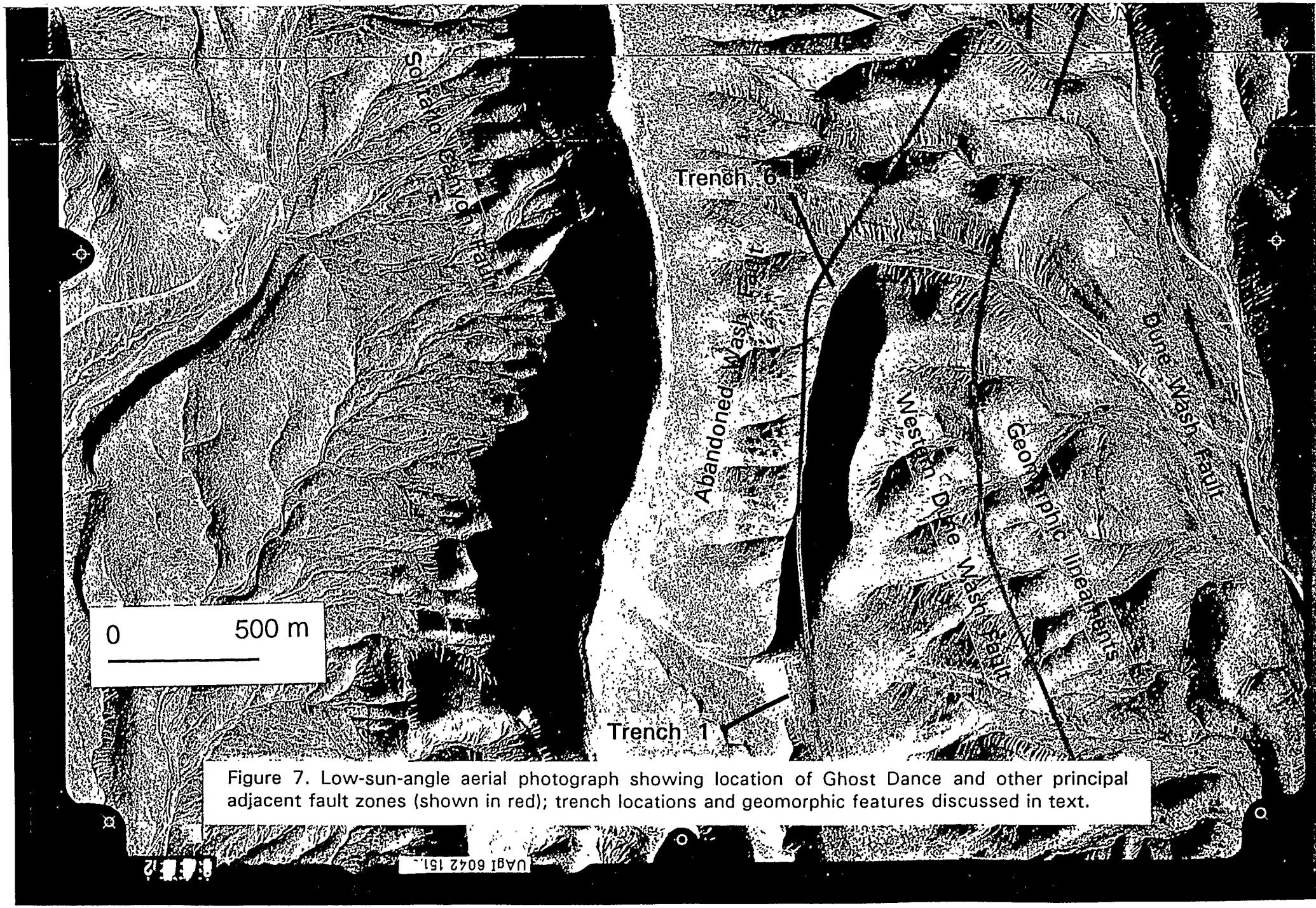

Figure 7. Low-sun-angle aerial photograph showing location of Ghost Dance and other principal adjacent fault zones (shown in red); trench locations and geomorphic features discussed in text.

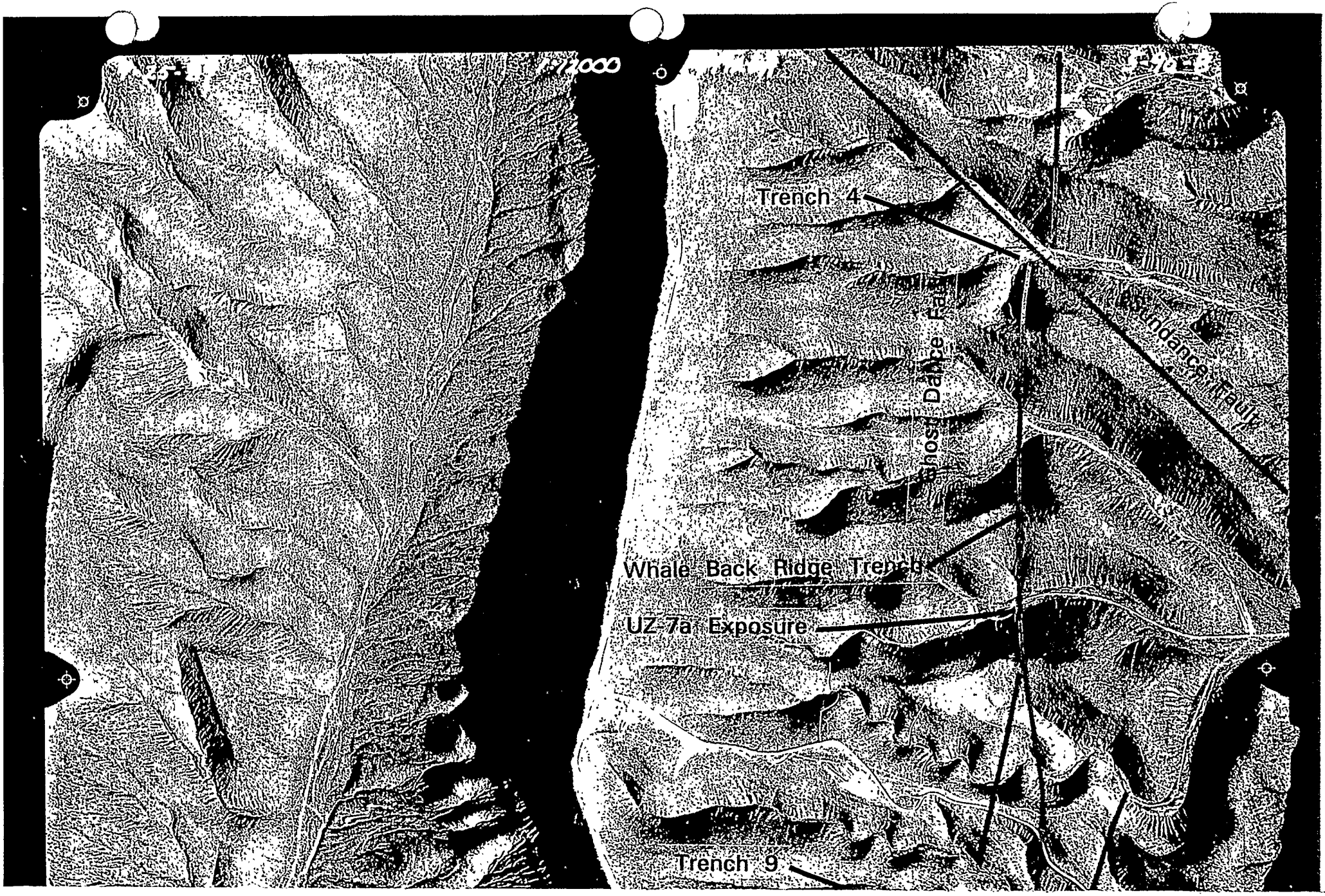
Trench 4
Ghost Dance Fault
Sundance Fault
Whale Back Ridge Trench
UZ-7a Exposure
Trench 9

Taylor and others (1995) described results of trenching across projections of the Ghost Dance fault and concluded that there was no evidence of offset in any of the Quaternary deposits exposed in the trenches. The trenches included reexcavation of the Swadley and others (1984) trench 4 and a new excavation across the main trace of the Ghost Dance fault on Whale Back Ridge. Topographic slope profiles across the Ghost Dance fault at Whale Back Ridge, Antler Ridge, and Split Wash led Taylor and others (1995) to conclude "No features are preserved that suggest either a Quaternary or bedrock [scarp]."

Description of the Ghost Dance fault system

The Ghost Dance fault is part of a complex system of anastomosing and interconnected faults within the Yucca Mountain block (cf., Scott, 1990; Fig. 6). This system of faults extends from the Iron Ridge and Paintbrush Canyon faults, northward to northwest-trending faults in Drill Hole Wash and possibly as far north as similar faults in Pagany Wash. The system is dominantly normal slip, down-to-the-west, but a significant splay southeast of the Ghost Dance fault is likely down-to-the-east. The faults that comprise this system are listed in Table 3. As noted by Scott (1990) the number of normal faults and the amount of displacement increases to the south. Fitting this pattern, the main trace of the Ghost Dance fault appears to increase in displacement from minor offsets on the north to 30 m at its southern end near Whale Back and Highway Ridges. Recent deep seismic reflection data suggest that the Ghost Dance fault has as much as 1 km of vertical throw across the Tertiary-Paleozoic contact (T. Broecker, U.S. Geological, 1995 presentation to the Nuclear Regulatory Commission).

TABLE 3

Fault	Sense of Displacement
Ghost Dance fault	normal; down to west
Sundance fault zone	right lateral
Abandoned Wash fault	normal; down to west
Western Dune Wash fault zone	normal; down to east?
Abandoned Wash southeast splay	normal; down to west
imbricate fault zone	normal; down to west

The northern end of the Ghost Dance fault appears to progressively die out in displacement, intersecting a set of northwest-trending faults: the Sundance, Drill Hole Wash, and possibly the Pagany Wash faults. Near the Swadley and others (1984) Trench 2, a synthetic fault lies 500 m

west-northwest of the northern end of the Ghost Dance fault, and it may be a structural continuation of the fault zone.

The southern end of the Ghost Dance fault lies within an area of considerable structural complexity, and we believe that there is substantial uncertainty regarding the exact location of this portion of the fault zone. Four possible structural connections to the south can be hypothesized. In these four models, we assume that displacement will be conserved in dominantly normal-slip systems through non-direct ways (such as structurally compatible overlapping normal faults).

The most direct extension of the Ghost Dance fault to the south (and the presently preferred USGS interpretation) is to a series of down-to-the-west faults within the Abandoned Wash fault system. This connection is illustrated in Figure 13 of Scott (1990) where he combined the two faults as the Ghost Dance-Abandoned Wash fault system.

A second possible southern extension of the Ghost Dance fault, however, could involve the eastern splay of the fault which extends south from the UZ-7a exposure to a series of traces bounding the eastern side of the unnamed ridge along the east side of Abandoned Wash (Fig. 7). This set of north-northwest-trending faults consists of several subparallel down-to-the-east traces and grabens and is here named the Western Dune Wash fault zone. Photographic and ground examination indicate that this zone contains some of the most youthful-looking and prominent structural-geomorphic features within the repository block. Sharp, linear, erosional fault contacts, linear troughs and topographic lineaments, and bedrock-alluvial scarps suggest that this zone is more recently active than the Abandoned Wash trace.

A third alternative model would involve connecting the Ghost Dance fault to the Dune Wash fault through a series of east-stepping normal faults. The northwest-trending Dune Wash fault bounds the west flank of Boundary Ridge and intersects the Ghost Dance fault system near Highway Ridge (Scott and Bonk, 1984).

The fourth model would involve volume deformation rather than brittle rupture along discreet faults. Part of the structural complexity at the southern end of the Ghost Dance fault is largely due to intense imbricate faulting present in this area (Scott and Bonk, 1984). As discussed above, Spengler and others (1993) identified a significant zone of faults adjacent to the Ghost Dance fault that collectively account for about half of the overall fault displacement. This zone, or elements of it, may become important as a transfer system of deformation to the imbricate fault zone to the south. Given the structural intimacy of faults at Yucca Mountain, a structural relationship with a combination of some, or all, of these faults is possible, and is perhaps likely.

Excavation Exposure At Drillpad UZ-7a

At Drill Pad UZ-7a (Fig. 7) the main trace of Ghost Dance fault zone is exposed in the south wash wall. For this study we examined and logged the 6-m high exposure in order to document the evidence for Quaternary faulting (Fig. 8). The main fault trace, which displaces non-lithophysal beds against lithophysal beds of the Tiva Canyon tuff, is characterized by a 1.7 m to 3 m wide zone of carbonate-cemented and loose fault breccia and gouge. Based on breccia and cementation characteristics, at least three, and possibly four, different episodes of fault movement can be identified. Decreasing degrees of secondary carbonate content and cementation from east to west correspond to successively younger faulting events. The youngest recognized event is marked by a narrow, silt-filled shear zone lacking any significant secondary carbonate, and its loose, friable character strongly suggests that the age of the event is of late Quaternary age.

Six trench log units (Fig. 9) are differentiated. Units 1, 2 and 3 are the oldest shear units exposed, having abundant evidence of the deposition of secondary carbonate, and Units 4 and 5 are the youngest parts of the fault zone.

Unit 1 is a light gray to white, strongly-carbonate-cemented fault breccia. The unit is a matrix-supported cobbly, gravelly pebble sand. Footwall lithology (Tiva Canyon lower lithophysal unit) is common in breccia clasts that are nominally 3 to 5 cm in diameter.

Unit 2 is a medium gray, open-matrix cobble gravel fault breccia. Clasts are dominantly from the footwall, are nominally 5 to 10 cm in diameter, and are partly carbonate-coated on their surfaces. Sandy fillings in the matrix are loose and the gravel ravels easily. There are numerous voids within the matrix.

Unit 3 is a medium gray to tan, slightly to moderately carbonate-cemented fault breccia. Clasts are mostly from the footwall and are nominally 3 to 5 cm in diameter. The unit is a matrix-supported, pebbly, cobbly sand.

Unit 4 is a fault-parallel seam of loose, brown silty sand fault breccia that likely represents the last fault activity. This seam is very friable, lacking any cementation and contains only slight secondary carbonate coatings. About midway down the exposure the seam is somewhat more carbonate rich, probably reflecting the incorporation of units 2 and 3 into 4.

Unit 5 is gray, brecciated and fractured hanging-wall bedrock (Tiva Canyon non-lithophysal unit) surrounded by a matrix-dominated gravelly silty sand breccia. Clasts are angular fragments with local shear fabric. Some carbonate coatings occur on clasts. The matrix of this unit is friable and loose, and clasts pull out of the unit easily. Oxidized iron staining is common in this unit indicating that water permeates through this unit.

Unit 6 is a brown wedge of matrix-dominated breccia near the top of the exposure, immediately above unit 5. The unit is similar to unit 5, except it is more matrix dominated and contains

Figure 8. Photograph of main shear zone of Ghost Dance fault exposed on south wall of UZ-7a drillpad. Close-up view of most recent event is shown in Figure 10. Rock hammer at lower center for scale.

UZ-7a Drillpad Exposure

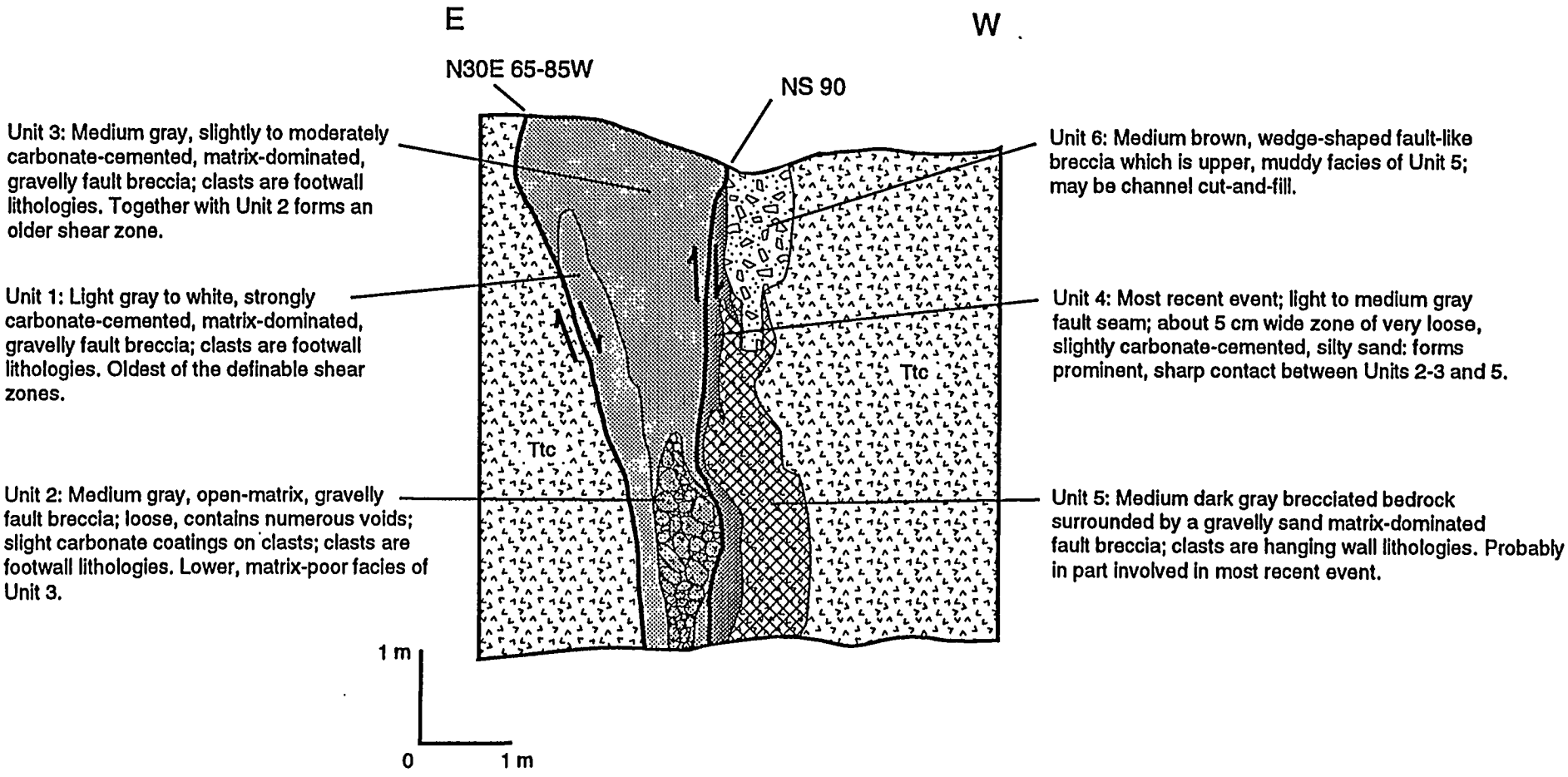

Figure 9. Log of main trace of the Ghost Dance fault exposed on the south wall of the UZ-7a drillpad. Area mapped approximately corresponds that shown in Figure 8.

more mud. This unit truncates Unit 4. The origin of this unit is unclear; it may be a fault breccia or fault fissure fill, but it may also be a cut and fill deposit resulting from slope runoff and erosion seen on the bedrock slope above the wash exposure.

The hanging wall adjacent to units 5 and 6 is highly brecciated with clasts that pull out relatively easily. Recent mapping by the USGS suggests that the hanging wall is cut by high-angle and radial fractures with right-lateral slip across low-angle fracture planes. The footwall, although jointed and having some minor, carbonate filled faults, is relatively unbrecciated.

Two fault planes are present within the shear zone. The east side of the fault zone, at the contact with the footwall, trends N30°E, dipping 65° to 85° to the west. A second fault plane occurs on the west side of a carbonate seam along unit 3 that has a north-south orientation and dips vertically. This fault plane is the likely location for the most recent slip. The N30°E fault merges with, or is truncated by, the north-south fault a few meters south of the exposure.

Age of the most recent faulting event at the UZ-7a exposure

Although the exact age of the most recent faulting event is not known, the loose, friable, silt-filled nature of Units 4 and 5 is striking (Figure 10) and it is strongly suggestive of late Quaternary offset. The correspondence between the degree of secondary carbonate content in the shear zone and the age of faulting is a consistent pattern seen in many of the dated trench exposures at Yucca Mountain (c.f., Menges and others, 1994). As in the progressive development of calcic soils, the degree of carbonate present in a shear zone is some measure of the age of faulting.The progressive decrease in carbonate cementation from east to west through the fault zone exposure provides a relative age relation with the oldest shear zone deposits being the most strongly cemented. The carbonate-poor silt present in Unit 4 is similar to other silt-filled fissures found along other Yucca Mountain faults estimated to have late Quaternary movement. For example, the carbonate-poor, uncemented character of the 60-80 ka basaltic ash- and silt-filled fissures along several of the Yucca Mountain faults (e.g., Solitario Canyon and Bow Ridge faults) supports this interpretation.

It is unlikely that the lack of secondary carbonate in Units 4 and 5 can be attributed to dissolution. Although surface water may percolate through the fault zone, the fact that each shear zone unit contains a different degree of carbonate cementation argues against differential dissolution.

Figure 10. Close-up photograph of loose, carbonate-poor, silt-filled fault seam that marks the trace of the most recent faulting event.

Whale Back Ridge Trench

A trench excavated by the USGS across the Ghost Dance fault on Whale Back Ridge (Fig. 11) was examined and partially logged in order to compare fault-stratigraphic relations and to further document ages of fault offset. Previous studies by Taylor and others (1995) concluded that slope wash and eolian deposits are unfaulted. An unfaulted carbonate laminae yielded a uranium-series age of 80-90 ka.

The principal trace of the Ghost Dance fault on Whale Back Ridge is located at the eastern end of the trench (Fig. 12). Faulted Tiva Canyon tuffs are overlain by a thin veneer of soil and eolian cap. At least three episodes of faulting are identifiable within the carbonate-cemented shears of the 1.5-m wide main fault zone. A strongly cemented, carbonate-engulfed fault breccia (Unit 1) abuts highly fractured, massively cemented tuff of the hanging wall. This breccia is cut by a less well cemented shear zone (Unit 2) that does not offset laminar calcrete 1-5 cm thick. The youngest fault trace (Unit 3) occurs between the moderately cemented shear zone (Unit 2) and the tuffs of the footwall, and it offsets all calcrete horizons of the shear zone except the uppermost thin (<1 cm) laminae. The unfaulted calcrete laminae dated by Taylor and others (1995) is located about 1m west of this trace (Fig. 13).

The fault zone is overlain by a strongly developed argillic Bt horizon that is not visibly broken, but it noticeably thickens at the fault zone. A topographic profile surveyed across the natural terrain on the south edge of the trench indicates that a subtle scarp about 20-30 cm in height is coincident with the fault zone. A similar deflection across the top of the Bt horizon also occurs at this location and coincides with the thickening of the Bt. The degree of development and thickness of the Bt horizon are similar to soils of Early Black Cone age (about 150 ka; Peterson and others, 1995).

Age of Most Recent Faulting Event at Whale Back Ridge

The youngest fault trace (Fig. 13) is overlain by a thin, unfaulted calcrete laminae estimated by Taylor and others (1995) to be between 80-90 ka based on uranium-series dating. The actual age of the faulting is unknown, but we believe that the most recent event is not substantially older than this age based on several lines of evidence. The small topographic scarp overlying the fault and the coincident deflection of the argillic Bt horizon together are suggestive of surface offset. This is supported by the thickening of the Bt horizon across the fault zone, forming a small colluvial wedge. Such small, subtle surface offsets appear common at Yucca Mountain. At trench 14 across the Bow Ridge fault, for example, a subtle surface scarp and lineament visible on aerial photography correspond to a small faulting event dated at about 66 ka (Menges and others, 1994).

Figure 11. Photograph of main trace of Ghost Dance fault exposed at east end of the south wall of Whale Back Ridge trench. The 20-30 cm step across the bedrock-calcrete contact corresponds to a similar topographic inflection on the ground surface.

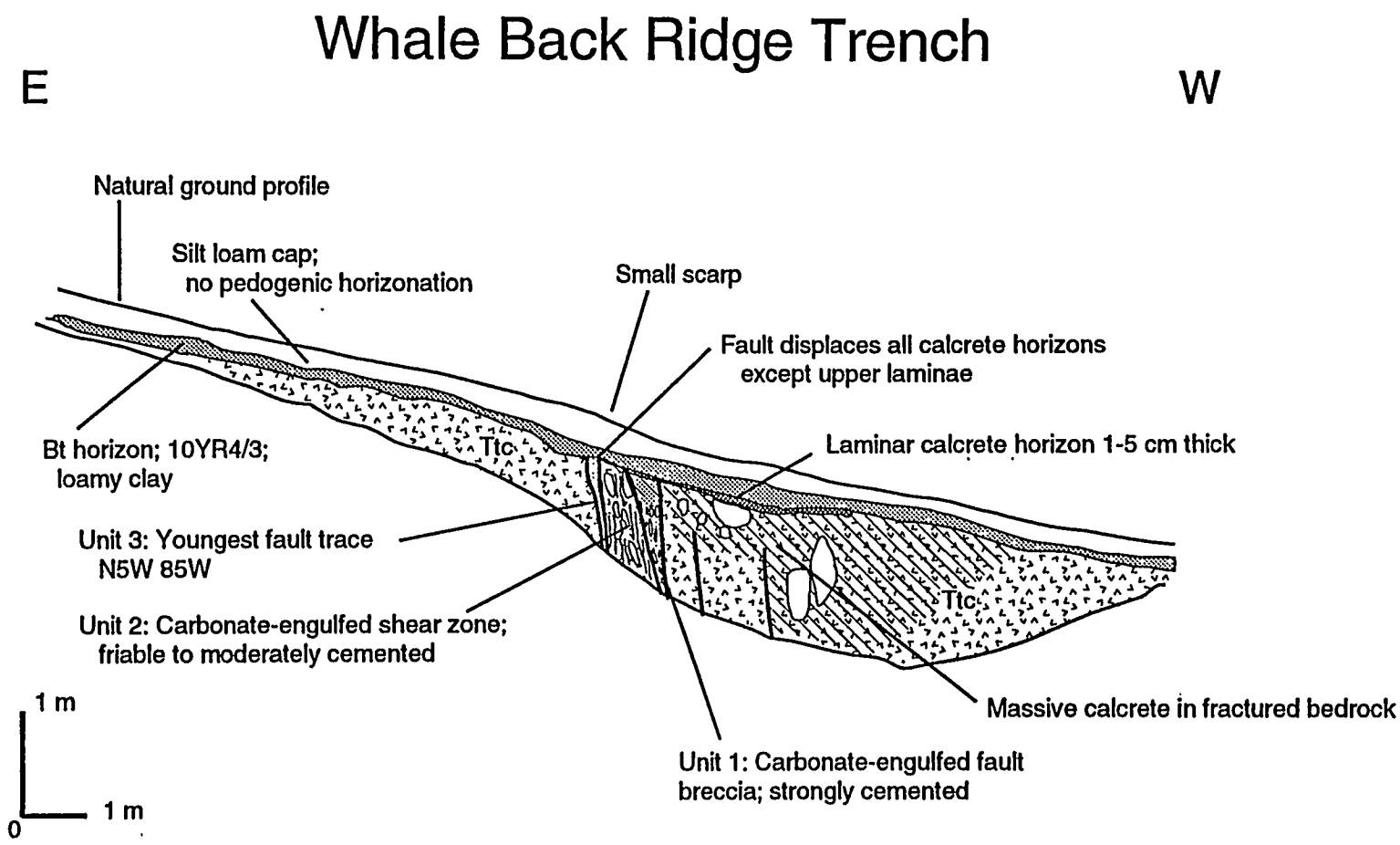

Figure 12. Log of main trace of Ghost Dance fault at east end of south wall of Whale Back Ridge trench.

Figure 13. Close-up of main trace of Ghost Dance fault exposed at east end of south wall of Whale Back Ridge trench. Most recent faulting cuts all calcrete units except uppermost, thin carbonate laminae.

Geomorphic Features along the Western Dune Wash fault zone

In order to further investigate the evidence for Quaternary activity on the Ghost Dance fault, we examined faults extending south from the UZ-7a site. We found that some of the best photolineaments and tectonogeomorphic features within the eroded bedrock terrain of the Yucca Mountain block are located along the 350-400 m wide set of faults that make up the possible southern extension of the Ghost Dance fault that we have named the Western Dune Wash fault zone. Bedrock-alluvial scarps, broad grabens and troughs, hilltop depressions, alluvial and bedrock vegetation and erosional lineaments, and linear outcrops of cemented secondary carbonate occur along the Western Dune Wash fault zone.

Although distinct alluvial scarps are absent and the age of the most recent movement on the Western Dune Wash fault is unknown, these lineaments and geomorphic features are strongly suggestive of late Quaternary movement. Small (½-1 m) bedrock-alluvial scarps are common in the northern portion of the Western Dune Wash fault zone (Fig. 7) and they coincide with surface outcrops of carbonate-cemented fault breccia. These scarps commonly bound grabens, troughs and hilltop depressions formed within unconsolidated colluvial deposits. Exploratory trenching is necessary to completely characterize these features, but we can nonetheless infer that their youthful geomorphic expression is a strong indicator of late Quaternary offset.

Evaluation of Relations Exposed in Existing USGS Trenches

Trench 1 (Fig. 6) is located in Abandoned Wash; it was described by Swadley and others (1984) as a locality along the Abandoned Wash fault where Quaternary deposits were thin or absent, and they did not pursue additional study at this site. Our investigation indicates that the trench probably does not directly overlie the principal fault trace.

Trench 2 is located in Drillhole Wash and is likely a secondary fault within the Ghost Dance fault zone. This fault trace lies about 500 m to the west and northwest of the northern part of the main Ghost Dance fault, and it may be structurally connected with the Sundance fault. Although this trench lies across a vegetation lineament visible on aerial photography, the trench log of Swadley and others (1984) showed unfaulted Pleistocene and Holocene deposits. Since the trench lies across a secondary trace of the Ghost Dance fault, the relation between the lack of faulting observed in the trench and activity of the northern end of the Ghost Dance fault is inconclusive.

Trench 4 is located in the alluvium of Split Wash, a location estimated by Swadley and other (1984) to be where the Ghost Dance fault projected across the wash. No surficial evidence of faulting is evident in the field or on aerial photography. This trench has recently been lengthened and deepened (Taylor and others, 1995). As originally logged by Swadley and others (1984), undisturbed Holocene sediments comprise the trench exposure. Our review of the deepened

trench found that no faults are exposed in the trench, and that all of the deposits are of probable Holocene age. Soils formed within these deposits are only minimally developed, and the deposits are likely related to the Holocene alluviation seen in many of the Yucca Mountain alluvial channels. Taylor and others (1995) estimated these deposits to be of late Pleistocene to early Holocene age.

Trench 6 is located in Quaternary deposits along the western sideslope of Abandoned Wash. One of the major strands of the Abandoned Wash fault as mapped by Scott and Bonk (1984) is located on the west side of the wash, but it lies beyond the west end of the trench. The trench ended near the active wash; thus, the eastern side of Abandoned Wash was not trenched and it is uncertain if the main trace of the Abandoned Wash fault was crossed. Swadley and others (1984) concluded that Trench 6 lies across the projection of the fault, but we believe that their trenching results are inconclusive due to the location of the trench on the sideslope deposits of Abandoned Wash. Deposits exposed in the trench are Holocene age based on lack of soil development. No faulting is visible in the trench.

Although Swadley and others (1984) showed Trench 9 crossing the Ghost Dance-Abandoned Wash fault, our examination of the Scott and Bonk (1984) map indicates this trench is actually located west of the main fault trace. Thus, we conclude that the lack of faulting seen in trench 9 deposits is inconclusive.

Conclusions Regarding Quaternary Activity along the Ghost Dance Fault

Based on examination of field and trench relations along the Ghost Dance-Abandoned Wash fault zone, we conclude that there is both direct and circumstantial evidence indicating that there have been at least several episodes of Quaternary movement on the Ghost Dance fault. There is no substantive evidence for Holocene movement. Although we do not know the actual numerical age of the last event, trench exposures and tectonogeomorphic features along the fault are consistent with an age of about 100 ka or less. We further conclude that the previous USGS trench locations either lie across estimated projections of the fault or do not directly overlie the fault, and thus they are inconclusive for determining fault slip histories. None of the previous trenches have exposed the main trace of the Ghost Dance fault, and only the recently excavated exposures on Whale Back Ridge and at drillpad UZ-7a reveal the main trace of the fault.

Evidence that supports a late Quaternary age for most recent movement on the Ghost Dance fault includes:

1. The fault cuts all Quaternary-age secondary carbonate (calcrete) in the Whale Back Ridge trench except for the uppermost thin laminae of carbonate dated at 80-90 ka. Although a 150 ka argillic soil is not visibly ruptured, a small surface scarp and thickening of the Bt horizon over the fault are suggestive of offset.

2. Three distinct episodes of faulting are visible in the carbonate-engulfed fault zone exposed at

the UZ-7a drillpad. The youngest event is characterized by a very loose, carbonate-poor, silt-filled shear fabric that is strongly suggestive of a late Quaternary age.

3. Tectonogeomorphic features along the Western Dune Wash fault, a possible southern extension of the Ghost Dance fault, include bedrock-alluvial scarps, vegetation and topographic lineaments, grabens, and hilltop depressions, all suggestive of late Quaternary movement.

4. The surficial and trenching evidence along the Ghost Dance fault is similar to that displayed by the Bow Ridge fault, an adjacent repository block fault. Although no distinct surficial or bedrock scarps are visible along the Bow Ridge fault, trenching data from Exile Hill (trench 14) indicate that the most recent movement on the fault occurred about 66 ka.

We conclude that the Ghost Dance fault has not been completely characterized by DOE with respect to extent, age, and seismogenic potential. The Ghost Dance fault is an intrablock fault that appears to be structurally connected to other Yucca Mountain faults exhibiting late Quaternary activity: the Bow Ridge, Paintbrush Canyon, and Solitario Canyon faults. Like these other faults, it is part of a system that increases in displacement towards the south, where it merges with bounding faults. In particular, the Bow Ridge fault may serve as a good analogue for the Ghost Dance fault. The Bow Ridge fault is predominantly a bedrock structure which exhibits little surficial evidence of Quaternary faulting. However, Menges and others (1994) concluded that the most recent event on the Bow Ridge fault was about 66 ka old based on detailed trenching investigations.

Part of the difficulty in characterizing the Quaternary slip history of the Ghost Dance fault can be attributed to the lack of a complete Quaternary stratigraphic section along the trace of the fault. All wash deposits which cross the trace of the fault, and which are exposed in all previous trenches, are of Holocene age or latest Pleistocene age at the oldest. The oldest unfaulted stratigraphy overlying the fault is thus on the order of 10 ka or less. Only in the Whale Back Ridge trench is there pre-Holocene stratigraphic age control. Due to the fact that a number of the previous trench excavations were situated either off the principal trace of the fault or located across projections of the fault through the Holocene channel fills, the older trenching data provide only very minimal information. The fact that none of the previous trenches, with the exception of the Whale Back Ridge trench, exposes the main trace of the Ghost Dance fault creates substantial uncertainty regarding the actual location of the principal trace of the fault.

We believe that the studies conducted to date by DOE have not adequately considered the possibility that the most active southern portion of the Ghost Dance fault is connected with Western Dune Wash fault rather than with the Abandoned Wash fault. Although the Ghost Dance fault has consistently been connected by previous studies to the Abandoned Wash fault, it is possible that the Western Dune Wash fault is a southern extension of the Ghost Dance fault based on several lines of evidence. The Western Dune Wash fault has numerous tectonogeomorphic features suggestive of Quaternary activity, but this fault to date remains unstudied.

Recommendations for Future Study

We recommend that future studies of the Ghost Dance fault system include the following:

1. Excavate additional trenches across the Ghost Dance fault where it transects the east-trending ridge crests. In the absence of pre-Holocene wash deposits across the trace of the fault, trenching on the bedrock interfluves could provide a longer structural-stratigraphic record than wash exposures. In addition, the principal trace of the fault can be more precisely located, and is at present better known, on the ridge crests than across the wash bottoms where fault locations are based solely on projections. The Whale Back Ridge trench demonstrates that a substantial late Quaternary record, as well as datable stratigraphy, can be obtained from trenching such locations. Additional trench locations could include Antler Ridge, the UZ-7a ridge, Highway Ridge, and the unnamed ridge immediately north of Abandoned Wash.

2. Investigate more fully the extent, structural relations and age of the Western Dune Wash fault system. As noted, this system contains some of the youngest tectonogeomorphic features of any of the repository block faults. Detailed surficial mapping and exploratory trenching across one or more splays of the fault system can likely provide important new data regarding the structural-tectonic history of Yucca Mountain. Field investigation indicates that several of the youngest features transect Quaternary hillslope deposits that have a high potential for preserving late Quaternary structural-stratigraphic relations.

3. Conduct additional uranium-series dating of carbonate deposits in the Whale Back Ridge trench and at the UZ-7a exposure. The previous uranium-series date obtained by the USGS from the Whale Back Ridge trench was taken from an off-fault location, and additional dating of the unfaulted laminae directly overlying the fault trace would provide a more accurate constraint. At the UZ-7a exposure, a complete suite of samples from the separate shear zones could provide a long-term Quaternary slip history.

References

Bell, J.W., 1995, Quaternary geologic map of the Mina quadrangle: Nevada Bureau of Mines and Geology Field Studies Map 10 (in press).

Byerly, P. 1935, The first preliminary waves of the Nevada earthquake of December 20, 1932: Seismological Society Bulletin, v. 25, p. 161-168.

dePolo, C.M., Ramelli, A.R., and Bell, J.W., 1994, Surface faulting from the 1932 Cedar Mountain earthquake, central Nevada: Seismological Research Letters, v. 65, p. 68.

Doser, D.I., 1988, Source parameters of earthquakes in the Nevada Seismic Zone, 1915-1943: Journal of Geophysical Research, v. 93, no. B12, p. 15,001-15,015.

Lipman, P.W. and McKay E.J., 1965, Geologic map of the Topopah Spring SW Quadrangle, Nye County, Nevada: U.S. Geological Survey, Geologic Quadrangle Map, GQ-439 (scale 1:24,000).

Menges, C.M., Wesling, J.R., Whitney, J.W., Swan, F,H, Coe, J.A., Thomas, A.P., and Oswald, J.A., 1994, Preliminary results of paleoseismic investigations of Quaternary faults on eastern Yucca Mountain, Nye County, Nevada: Proceedings, 5th International Conference on High-level Radioactive Waste Management, v. 4, p. 2372-2390.

O'Neill, J.M., Whitney, J.W., and Hudson, M.R., 1992, Photographic and kinematic analysis of lineaments at Yucca Mountain, Nevada: implications for strike-slip faulting and oroclinal bending: U.S. Geological Survey, Open-File Report 91-623, 23 p. (map scale 1:24,000)

Peterson, F.F., Bell, J.W., Dorn, R.I., Ramelli, A.R., and Ku, T.L., 1995, Late Quaternary geomorphology and soils in Crater Flat, Yucca Mountain area, southern Nevada: Geological Society of America Bulletin, v. 107, p. 379-395.

Pezzopane, S.K., Menges, C.M., and Whitney, J.W., 1994, Quaternary paleoseismology and Neogene tectonics at Yucca Mountain, Nevada, in ICL-USGS Workshop on Paleoseismology, proceedings: U.S. Geological Survey, Open-File Report 94-568, p. 149-151.

Scott, R.B., 1990, Tectonic setting of Yucca Mountain, southwest Nevada, in Wernicke, B.P., ed., Basin and Range extensional tectonics near the latitude of Las Vegas, Nevada: Geological Society of America, Memoir 176, p. 251-282.

Scott, R.B. and Bonk, J., 1984, Preliminary geologic map of Yucca Mountain, Nye County, Nevada, with cross sections: U.S. Geological Survey, Open-File Report 84-494, 9 p. and 3 plates (1:12,000).

Simonds, F.W., Whitney, J.W., Fox, K.F., Ramelli, A.R., Yount, J.C., Carr, M.D., Menges, C.M., Dickerson, R.P., and Scott, R.B., 1995, Map showing fault activity in the Yucca Mountain area, Nye County, Nevada: U.S. Geological Survey, Map I-2520, (scale 1:24,000).

Spengler, R.W., Braun, C.A., Linden, R.M., Martin, L.G., Ross-Brown, D.M., and Blackburn, R.L., 1993, Structural character of the Ghost Dance fault, Yucca Mountain, Nevada, in, Fourth International High Level Radioactive Waste Management Conference, Las Vegas: American Nuclear Society, Proceedings Volume, p. 653-659.

Spengler, R.W., Braun, C.A., Martin, L.G., and Weisenberg, C.W., 1994, The Sundance fault: a newly recognized shear zone at Yucca Mountain, Nevada: U.S. Geological Survey, Open-File Report 94-49, 11 p.

Swadley, W.C., Hoover, D.L., and Rosholt, J.N., 1984, Preliminary report on late Cenozoic faulting and stratigraphy in the vicinity of Yucca Mountain, Nye County, Nevada: U.S. Geological Survey Open-file Report 84-788, 42 p.

Taylor, E., Menges, C., and Whitney, J.W., 1995, Preliminary results of trenching Quaternary deposits that intersect projections of the Ghost Dance and Sundance faults: Unpublished presentation to the Nuclear Regulatory Commission, 8 p.

Appendix A

Quaternary Geologic Map of the Mina Quadrangle

QUATERNARY GEOLOGIC MAP OF THE MINA QUADRANGLE, NEVADA

John W. Bell

1995

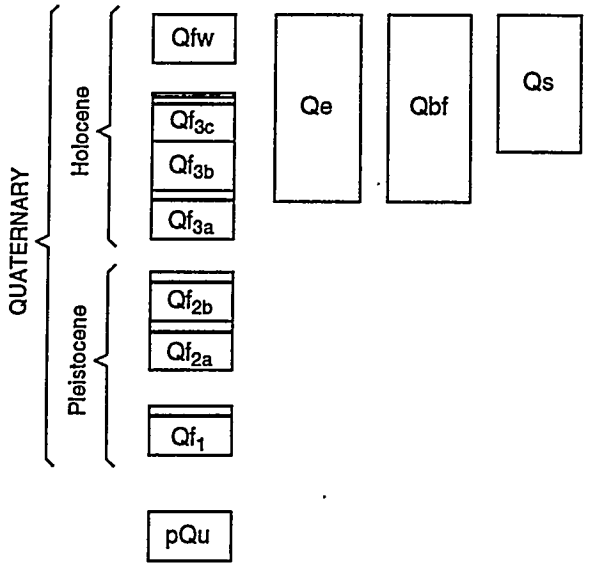

Contact Dashed where approximately located.

Quaternary fault Dashed where approximately located, dotted where inferred, ball on downthrown side.

RV9□ Rock varnish sample

RC2○ ^{14}C sample

T4△ Tephra

Office review by:
Jim Yount, USGS
Alan Ramelli, NBMG
Jim Rigby, NBMG

First edition, first printing, 1995
Printed by DynaGraphics, Reno, Nevada
Edited by Dick Meeuwig
Cartography by Susan Tingley

Nevada Bureau of Mines and Geology
University of Nevada, Mail Stop 178
Reno, Nevada 89557-0088

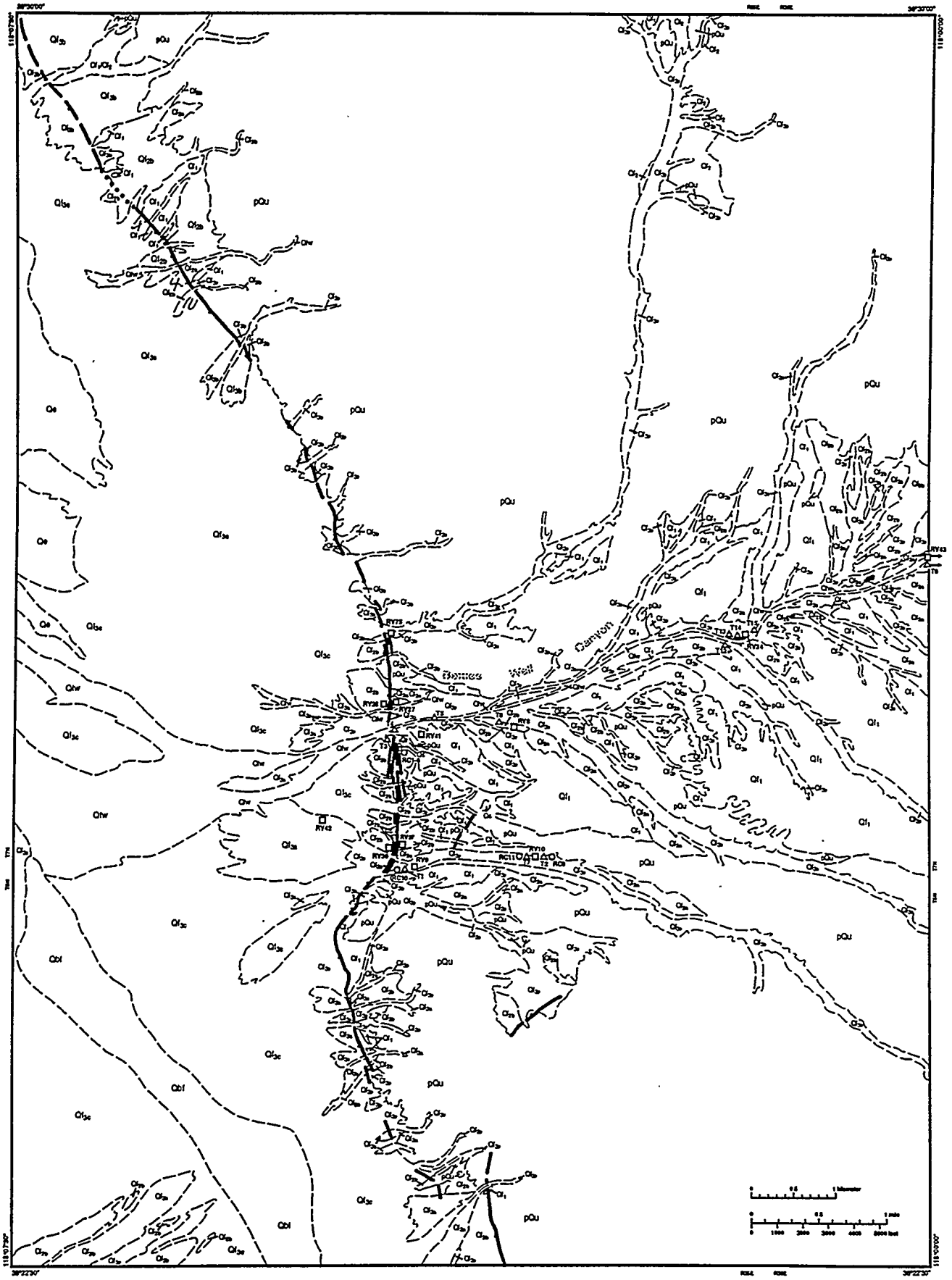
Canyon
Qf3a
Qf3b
Qf3c
Qf2a
Qf2b
Qf1
pQu
Qbf
Qhw
Qe

Qfw **Modern active wash deposits** Very pale-brown to grayish- brown muddy, sandy gravel and gravelly sand; poorly to moderately stratified; uncemented. Includes numerous recent water-flood and debris-flow deposits radiating from mouths of canyons along the Gabbs Valley Range and Pilot Mountains.

Qe **Eolian sand deposits** Very pale-brown sand; well sorted; loose, uncemented. Includes sand sheets and inactive dunes of mid to late Holocene age.

Qbf **Basin-fill deposits** White to very pale-brown silty sand and sandy silt; moderately well stratified; poorly cemented. Unit is basin-floor (playa) facies of mid to late Holocene alluvial fan (Qf_3) deposits.

Qs **Spring deposits** Light-gray to black sandy silt; loose, uncemented. At mouth of Bettles Well Canyon, deposits consist of interbedded volcanic ash (**Qty**) and peat. Eight ^{14}C dates on the peat range from 435 to 1,550 yr BP (RC1 through RC8).

Qf_3 **Holocene fan-piedmont and wash terrace remnants** Composed dominantly of volcanic andesite, tuff, and basalt clasts with minor to moderate concentrations of limestone, sedimentary, and metamorphic clasts in units near the Pilot Mountains. Qf_{3c} Very pale-brown to grayish-brown muddy, sandy gravel to gravelly sand; poorly to moderately stratified; uncemented. Fresh-looking distributive bar-and-channel microtopography with discrete debris flows distinguishable on aerial photography. Unit forms bulk of the piedmont flanking the west side of the Gabbs Valley Range and Pilot Mountains. Soil varies from A-C profile with no visible horizonation to A-C profile with incipient to very weak B-horizon development; carbonate, if present, is weak Stage I. Incipient desert pavement; weak to no rock varnish. Contains several chemically indistinguishable Mono Craters tephra (**Qty**) ranging in age between about 900 and 1950 yr BP. Three ^{14}C dates from charcoal and organics in deposits from Dunlap Canyon range between 1,505 and 2,355 yr BP (RC9, 10, 11). Rock varnish ^{14}C AMS dates from clasts overlying the tephra in Dunlap and Bettles Well Canyon (RV9, 10, 34) range between 625 and 1267 yr BP. Qf_{3b} Light-gray to grayish-brown muddy, sandy gravel to gravelly sand; poorly to moderately stratified; uncemented to slightly cemented. Surfaces exhibit distributive bar-and-channel microtopography slightly more subdued than Qf_{3c}. Soil is A-C profile typically with 5 cm Av and 30 cm Bk horizon (Stage I coatings). Incipient to weak desert pavement; moderately dark rock varnish; moderately etched limestone clasts. A rock varnish ^{14}C AMS date of 4,347 yr BP was obtained from surface clasts at the mouth of Volcano Canyon (RV75). Qf_{3a} Light-gray to grayish-brown muddy, sandy gravel to gravelly sand; poorly to moderately stratified; slightly cemented. Relatively broad, flat, slightly dissected remnants stand only slightly topographically higher (<1 m) than younger Qf_3 remnants; bar-and-channel microtopography has been subdued and smoothed. Soils are camborthids typically containing 7 cm Av, 15 cm Bw (10 YR), and 30 cm Bk (stage I-II) horizons. Moderately well developed desert pavement and rock varnish. Just east of quadrangle along Bettles Well Canyon, unit contains a Mono Craters tephra (**Qtc**; T9) estimated to be about 7.2 ka where dated at Crooked Meadows, California. A rock varnish ^{14}C AMS date of 8,000 yr BP was obtained from surface clasts near the mouth of Dunlap Canyon (RV42).

Qf_2 **Late Pleistocene fan-piedmont remnants** Forms prominent series of broad, flat surfaces inset slightly below (1-2 m) unit Qf_1 in Bettles Well Canyon. Composed dominantly of volcanic andesite, tuff, and basalt clasts with minor to moderate concentrations of limestone, sedimentary, and metamorphic clasts in units near the Pilot Mountains. Qf_{2b} Light-brownish-gray to pale-brown muddy, sandy gravel to gravelly sand; poorly to moderately stratified; slightly to moderately cemented. Soils are haplargids typically with 7 cm Av, 25 cm Bt (7.5 YR), and 50-60 cm Bk (stage II-III) horizons. Well-developed desert pavement and dark rock varnish on broad, flat interfluves give unit distinctive aerial photographic appearance. Contains the Wilson Creek tephra (**Qtw**, T6; 36 ka) in a side-stream exposure along Bettles Well Canyon. Rock varnish ^{14}C AMS dates from clasts above ash and from surfaces at mouths of Bettles Well and Dunlap Canyons yielded ages ranging between 22 and 25 ka (RV27, 28, 37, 39). Qf_{2a} Light-brownish-gray to pale-brown muddy, sandy gravel to gravelly sand; poorly to moderately stratified; moderately to well cemented. Soils are haplargids and durargids with typically 7 cm Av, 7 to 10 cm Bt (7.5 YR), and 60 to 100 cm Bk or Bqkm (stage III-IV) horizons. Well-developed desert pavement and dark rock varnish on moderately dissected interfluvial remnants; remnants are geomorphically similar to Qf_{2b} and generally are only slightly topographically higher. The Mono Craters Negit Causeway tephra (**Qtn**, T3; 60-100 ka) occur in faulted paludal deposits within Qf_{2a} deposits at the mouth of Bettles Well Canyon and in Qf_{2a} gravels exposed in a roadcut along Bettles Well Canyon just off the quadrangle to the east. A rock varnish ^{14}C date from clasts overlying the tephra was infinite: >47,000 yr BP (RV43).

Qf_1 **Early to mid Pleistocene fan-piedmont remnants** A prominent series of high-level, well-dissected, digitate remnants which comprise the bulk of the fan-piedmont complex in Bettles Well Canyon. Along Dunlap and Cinnabar Canyons, unit lies directly on Tertiary sedimentary and volcanic rocks. Light-brownish-gray to brown muddy, sandy gravel to gravelly sand; poorly to moderately well stratified; well indurated to massively cemented. Soils are durargids with remnantal Bt horizons overlying strongly cemented Bqkm (stage IV) horizons in excess of 1 m thick. In Monte Cristo Valley to the east of the quadrangle, unit contains Bishop-Glass Mountain G tephra (**Qtb**, 0.73-1.0 Ma). Rock varnish cation ratios from clasts at mouth of Bettles Well Canyon indicate unit is >>47,000 yr BP (RV41).

pQu **Pre-Quaternary rocks, undivided** See companion map by Oldow and Dockery (1993).

Neotectonic History of the Benton Spring Fault

The Benton Spring fault is one of several prominent northwest-trending faults which comprise the central Walker Lane belt; the others include the Bettles Well, Indian Head, Petrified Spring, and Gumdrop Hills faults. These faults form a large right-slip fault system through and bounding the Gillis and Gabbs Valley Ranges and the Pilot Mountains, with the Benton Spring fault offsetting the Tertiary volcanic section as much as 8 km (Ekren and Byers, 1984). North- and northeast-trending conjugate faults in Monte Cristo and Gabbs Valleys ruptured during a large magnitude (M7.2) earthquake in 1932. Right-slip faulting of as much as 2 m associated with the earthquake was attributed to wrench fault tectonics of the Walker Lane belt by Gianella and Callaghan (1934).

The Benton Spring fault displays recurrent Quaternary offset in the Mina Quadrangle. At the mouths of Dunlap and Bettles Well Canyons, the late Wisconsin (>22-25 ka) $\mathbf{Qf_{2b}}$ fan-piedmont remnants are vertically offset as much as 3.8 m, and the older (60-100 ka) $\mathbf{Qf_{2a}}$ surfaces are vertically offset about 7.6 m. No geomorphic evidence of lateral offset (for example, offset stream channels) is visible within the faulted alluvium, and the component of Quaternary right slip is not precisely known. Slickensides along the Pilot Mountains bedrock-alluvial fault contact at the southern edge of the quadrangle, however, plunge 25 to 35° N and represent a horizontal to vertical slip ratio of between about 1.5:1 to 2:1. The most recent faulting event had a maximum vertical offset of about 1 m; it displaced $\mathbf{Qf_{3b}}$ deposits, but predated the deposition of $\mathbf{Qf_{3c}}$ deposits. Thus, the age of the most recent event is constrained between about 900 and 4,300 yr BP based on tephra and rock-varnish age control. One or more older events are preserved in the 3.8 m offset in the >22 to 25 ka $\mathbf{Qf_{3b}}$ deposits at Dunlap and Bettles Well Canyons, but additional study, including exploratory trenching, is necessary to resolve these older slip histories. Based on a 1.5:1 to 2:1 horizontal to vertical slip ratio, 6.6 to 9.0 m of net slip is estimated to have occurred in the last 22 to 25 ka, yielding a slip rate of about 0.26 to 0.41 mm/yr. Similarly, a slip rate of between 0.13 and 0.30 mm/yr is estimated from a 13.2 to 18.0 m net offset of $\mathbf{Qf_{2a}}$ deposits (60-100 ka).

Acknowledgments

The author thanks C.M. dePolo, A.R. Ramelli, J.C. Yount, and P.A. Glancy for field assistance and review. Field work and sample analyses were supported by funding from the Nevada Nuclear Waste Project Office to the Center for Neotectonic Studies, University of Nevada, Reno.

References

Ekren, E.B., and Byers, F.M., 1984, The Gabbs Valley Range—a well-exposed segment of the Walker Lane in west-central Nevada, *in* Lintz, J., ed., Western Geological Excursions, v. 4: Field Guide for 1984 Annual Meeting Geological Society of America, Reno, Nevada, p. 203-215.

Gianella, V.P., and Callaghan, E., 1934, The earthquake of December 20, 1932, at Cedar Mountain, Nevada, and its bearing on the genesis of Basin-Range structure: Journal of Geology, v. 42, p. 1-22.

Oldow, J.S., and Dockery, H.A., 1993, Geologic map of the Mina Quadrangle, Nevada: Nevada Bureau of Mines and Geology Field Studies Map 6.

Stuiver, M., and Pearson, G.W., 1986, High precision calibration of radiocarbon time scale, AD1950-500BC: Radiocarbon, V. 28, p. 805-838.

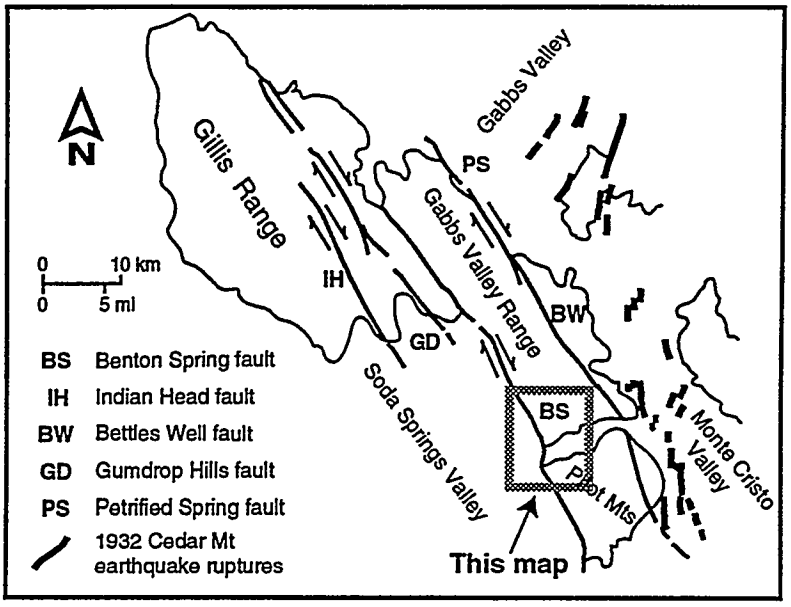

Glass Chemistry of Volcanic Tephra

(Microprobe data and tephra identification by A. Sarna-Wojcicki, 1992)

Tephra	SiO_2	Al_2O_3	Fe_2O_3	MgO	MnO	CaO	TiO_2	Na_2O	K_2O	Total
Qty (T1)	76.70	12.80	1.06	0.02	0.04	0.54	0.06	4.05	4.72	99.99
Qty (T2)	76.56	12.91	1.12	0.02	0.04	0.53	0.08	4.04	4.72	100.0
Qty (T4)	76.75	12.83	1.04	0.03	0.06	0.55	0.06	3.95	4.73	100.0
Qty (T5)	76.69	12.91	1.08	0.02	0.05	0.55	0.09	3.90	4.70	99.99
Qty (T7)	76.73	12.89	1.10	0.03	0.05	0.54	0.06	3.91	4.69	100.0
Qty (T12)	76.51	12.85	1.11	0.03	0.08	0.54	0.05	4.16	4.67	100.0
Qty (T15)	76.59	12.83	1.08	0.03	0.07	0.54	0.04	4.23	4.59	100.0
Qty (T13)	76.49	12.83	1.08	0.03	0.08	0.53	0.06	4.26	4.64	100.0
Qty (T14)	76.55	12.82	1.11	0.02	0.07	0.55	0.06	4.20	4.62	100.0
Qtc (T9	76.42	12.92	1.10	0.01	0.08	0.55	0.05	4.22	4.65	100.0
Qtw (T6)	76.39	13.29	0.83	0.04	0.06	0.71	0.06	3.88	4.74	100.0
Qtn (T3)	76.16	13.29	0.85	0.08	0.04	0.81	0.08	3.65	5.04	100.0
Qtb (Monte Cristo Valley)	77.55	12.62	0.75	0.05	0.05	0.41	0.06	3.67	4.86	100.0

Radiocarbon Dates

Sample	Material dated	^{14}C yrs (Lab #)	Calibrated years*
RC1	peat	995 ± 110 (GX-17250)	935^{+145}_{-65}
RC2	peat	535 ± 150 (GX-17251)	547^{+123}_{-77}
RC3	peat	1260 ± 145 (GX-17252)	1199^{+111}_{-189}
RC4	peat	435 ± 110 (GX-17253)	503^{+47}_{-153}
RC5	peat	790 ± 105 (GX-17254)	706^{+94}_{-36}
RC6	peat	1025 ± 65 (GX-17255)	950^{+40}_{-35}
RC7	peat	1110 ± 110 (GX-17256)	1008^{+152}_{-68}
RC8	peat	1550 ± 110 (GX-17257)	1433^{+127}_{-103}
RC9	charcoal	1605 ± 120 (GX-17566)	1522^{+108}_{-152}
RC10	organics	1505 ± 200 (GX-18939)	1388^{+222}_{-128}
RC11	organics	2355 ± 405 (GX-18940)	2361^{+498}_{-461}

*Calibrated from Stuiver and Pearson (1986)

Rock Varnish ^{14}C Dates and Cation Ratios
(Analyses by R.I. Dorn, 1993)

Sample (Unit)	Age (^{14}C yrs; Lab #)	Cation ratio
RV34 (Qf_{3c})	625 ± 75 (NZA 1382)	9.07 ± 0.20
RV10 (Qf_{3c})	1134 ± 70 (NZA 2931)	8.66 ± 0.16
RV9 (Qf_{3c})	1267 ± 71 (NZA 2930)	8.66 ± 0.66
RV75 (Qf_{3b})	4347 ± 72 (NZA 2933)	7.31 ± 0.21
RV42 (Qf_{3a})	8000 ± 100 (NZA 1368)	6.82 ± 0.15
RV37 (Qf_{2b})	22,170 ± 370 (NZA 1417)	5.50 ± 0.11
RV39 (Qf_{2b})	—	5.52 ± 0.16
RV8 (Qf_{2b})	25,020 ± 270 (NZA 2935)	5.41 ± 0.09
RV27 (Qf_{2b})	25,430 ± 480 (NZA 1379)	5.42 ± 0.09
RV28 (Qf_{2b})	—	5.48 ± 0.12
RV43 (Qf_{2a})	>47,000 (NZA 2934)	4.33 ± 0.18
RV41 (Qf_1)	—	3.79 – 4.06

SECTION III

TASK 3: EVALUATION OF MINERAL RESOURCE POTENTIAL, CALDERA GEOLOGY, AND VOLCANO-TECTONIC FRAMEWORK AT AND NEAR YUCCA MOUNTAIN

PROGRESS REPORT FOR OCTOBER, 1994 - SEPTEMBER, 1995

Steven I. Weiss,[1] Donald C. Noble,[2] and Lawrence T. Larson[3]

Department of Geological Sciences, Mackay School of Mines, University of Nevada, Reno

[1] Research Associate
[2] Co-principal Investigator and Professor of Geology and Economic Geology
[3] Co-principal Investigator and Professor of Economic Geology

INTRODUCTION

This report summarizes the work of Task 3 that was initially discussed in our monthly reports for the period October 1, 1994 through September 30, 1995, and is contained in our various papers and abstracts, both published and in press or currently in revision (see appendices). Our efforts during this period have involved the continuation of studies begun prior to October, 1994, focussed mainly on aspects of the magmatic activity, hydrothermal mineralization and extensional tectonics of the western and central parts of the southwestern Nevada volcanic field (SWNVF), studies of the subsurface rocks of Yucca Mountain utilizing drill-hole samples obtained in 1991 and 1992, supplemented by the examination of core from newly completed drill holes, and studies of rocks obtained recently from the Exploratory Studies Facility in Yucca Mountain.

Much effort during the period of this report has been concentrated on the production and publication of documents summarizing many of the data, interpretations and conclusions of Task 3 studies pertaining to hydrothermal activity and mineralization in the Yucca Mountain region and their relations to volcanism and tectonic activity. One manuscript is currently in press with the journal *Economic Geology* and a second, much longer manuscript is in revision following peer review (see below).

Our manuscript entitled *Pyritic ash-flow tuff, Yucca Mountain, Nevada--A discussion* was recast as a scientific communication entitled *Hydrothermal origin and significance of pyrite in ash-flow tuffs at Yucca Mountain, Nevada* and is in press with *Economic Geology* (Appendix A, Weiss et al., 1995) This paper disputes the interpretation of Castor et al. (1994) that pyrite in units of ash-flow tuff in Yucca Mountain is mainly xenolithic material derived from previously altered wallrocks and incorporated during the eruptions of the tuffs. Based on our studies of core and cuttings from 12 drill holes in Yucca Mountain, and detailed studies by personnel of the Los Alamos National Laboratory and the U. S. Geological Survey, we summarize our new information on the subsurface lateral and vertical distribution and textural characteristics of the pyrite, and consider phase stability relations and the conditions of major ash-flow eruptions that are inconsistent with the "lithic" origin of Castor et al. (1994). Our paper provides what we believe to be compelling arguments for the *in-situ* formation of pyrite from hydrothermal fluids containing small, but geochemically significant, amounts of reduced sulfur. We point out that such fluids are capable of transporting and depositing precious metals, that trace-elements associated with epithermal types of hydrothermal mineralization (e.g., As, Sb, Hg, Bi) are locally elevated with respect to fresh, unaltered rhyolitic ash-flow tuff at Yucca Mountain, and that the

existing and planned deep drill holes are too widely spaced to rule out the presence of potentially attractive mineral resources beneath the proposed repository.

The second and much longer manuscript, intended for publication in the journal *Economic Geology*, is entitled *Multiple episodes of hydrothermal activity and epithermal mineralization in the southwestern Nevada volcanic field and their relations to magmatic activity, volcanism and regional extension* (Weiss et al., 1996). An earlier version of this paper, providing important general information, and a large amount of specific and detailed decriptive information, radiometric age data and our interpretations concerning the nature and timing of hydrothermal activity and associated mineralization in the Yucca Mountain region, was included in our report for 1993-1994 and was submitted to the journal *Economic Geology*. Numerous revisions made following peer-review for *Economic Geology* have substantially improved the manuscript. However, in its current form the manuscript remains too lengthy for publication in *Economic Geology*. Moreover, one of the reviewers (Dr. David A. Sawyer of the U.S.G.S.) expressed the opinion that the spatial and temporal correspondence between magmatic-volcanic and hydrothermal activity were insufficient to support our inference of a genetic relation. Instead, Dr. Sawyer believes that hydrothermal activity in the southwestern Nevada volcanic field better correlates with, and was probably genetically related to, pulses of extensional tectonic activity. We disagree and consider magmas of the southwestern Nevada volcanic field to be the primary sources of heat for generating the middle and late Miocene, upper-crustal hydrothermal systems exposed in southwestern Nevada. Addressing this issue will require additional discussion which must yet be added to the already lengthy paper. In order to preserve the data and detailed discussions of the many known areas of hydrothermal activity and mineralization in the Yucca Mountain region of the volcanic field, which will need to to be removed for shortening the paper for *Economic Geology*, we include the current, revised draft in this report as Appendix B (Weiss et al., 1996).

A substantial amount of time was devoted to the preparation of an entirely new, but currently incomplete manuscript concerning the geology, alteration, geochemistry, age and origin of disseminated gold deposits in the Bare Mountain district, 15 km west of the repository site. This paper, provisionally entitled *Disseminated Gold Deposits Above a Large Miocene Magma System, Bare Mountain, Nevada* emphasises the similarities of the deposits in Bare Mountain to Carlin-type, sediment-hosted gold deposits and argues that they formed from hydrothermal systems related to the waning stages of a large, porphyry-type magmatic system of middle Miocene age. Much work remains to be done to produce the necessary figures and to complete the analy-

sis and interpretation of geochemical data obtained from the Mother Lode deposit at the north end of Bare Mountain. Portions of the paper concerning the evidence for a large, buried, porphyry magmatic system in Bare Mountain and the absolute and relative ages of igneous and hydrothermal events are presented with minor modifications below.

EVIDENCE FOR A LARGE, BURIED PORPHYRY-TYPE MAGMATIC SYSTEM AT BARE MOUNTAIN, NEVADA

The Bare Mountain (Fluorine) mining district in southern Nye County, Nevada, has been a source of fluorite, gold and small amounts of mercury since 1905. Production of gold from disseminated deposits at the currently operating Sterling mine and the recently producing Mother Lode mine has totalled approximately 5.12 tonnes (165,000 oz.) from 1980 through 1994 (RANDOL, 1993; Bonham and Hess, 1995) and accounts for nearly all of the recorded gold production of the district. Additional, currently subeconomic disseminated gold deposits are present near the Diamond Queen/Goldspar fluorite mine, at the Mother Lode mine, in Joshua Hollow, and in the vicinity of the Daisy fluorite mine (see Figure 2 of Appendix B). Previous workers have reported on fluorite deposits in the district (Cornwall and Kleinhampl, 1964; Papke, 1979) and the geology, alteration mineralogy and geochemistry of ore zones at the Sterling mine (Odt, 1983). Tingley (1984) investigated trace-element associations within the district. Noble et al. (1989; 1991) and Weiss et al. (1996) discussed the timing of hydrothermal and magmatic activity in the district in relation to other areas of mineralization in the Miocene southwestern Nevada volcanic field. Castor and Weiss (1992) compared the style and trace-element associations of gold and fluorite deposits in Bare Mountain with precious-metal deposits of the Wahmonie, Mine Mountain and Bullfrog districts.

The disseminated gold deposits at Bare Mountain share a number of geologic and geochemical similarities with the broad class of sedimentary rock-hosted precious-metals deposits referred to as Carlin-type and Carlin-like deposits elsewhere in the Great Basin (Noble et al., 1991; Castor and Weiss, 1992; Weiss et al., 1993), and differ markedly from the volcanic rock-hosted, gold-silver fissure vein deposits of middle Miocene age in the nearby Bullfrog district, about 15 km to the west (Ransome et al., 1910; Weiss et al., 1991; 1996). Although the exact ages and the origin of Carlin-type mineralization in the western United States remain controversial (e.g. Arehart et al., 1993; Ilchick, 1995; Kuehn and Rose, 1995), disseminated gold mineralization at Bare Mountain is in large part spatially associated with, and about 1.5 m.y. younger than a swarm of silicic porphyry dikes of middle Miocene age. We infer that hydrothermal

activity related to a late stage of this magmatic-hydrothermal system was responsible for the fluorite and disseminated gold mineralization. Such a genetic connection supports the idea that hydrothermal systems related to porphyry magmatic activity in some cases may approximate the conditions and processes responsible for the formation of Carlin-type deposits, although perhaps on a smaller scale.

Four separate, but related lines of evidence indicate that the gold and fluorite deposits of the Bare Mountain mining district are underlain by a large, porphyry-type magma system. The low-grade metasedimentary rocks of pre-Cenozoic age in Bare Mountain and the Late Oligocene(?)-Early Miocene(?) rocks of Joshua Hollow are intruded by an aerially extensive set of north-trending, steeply dipping, silicic porphyry dikes, which have been variously termed dacite and rhyodacite porphyry (Cornwall and Kleinhampl, 1961), porphyritic quartz-latite (Carr et al., 1986) and biotite-rhyolite (Noble et al., 1989). The dikes are generally less than 8 m in width and are pervasively, but variably hydrothermally altered in nearly all exposures. Prior to alteration the dikes contained phenocrysts of plagioclase, biotite, and sanidine, ± quartz, ± hornblende, and traces of sphene and zircon, surrounded by a coarsely granophyric groundmass of potassium feldspar and quartz. Individual dikes are in some cases compositionally zoned inward from biotite-rich, quartz-poor margins to interiors rich in quartz and having little biotite. The dikes are considered to be of middle Miocene age based on K-Ar ages on biotite of about 13.8, 13.9 and 14.9 Ma (Marvin et al., 1989; Noble et al., 1991; Monsen et al., 1992) and on a single-crystal $^{40}Ar/^{39}Ar$ age on sanidine of 14.4 ± 0.09 Ma (Table 1, see below). Carr et al. (1986) believed the dikes to be related to rhyolitic lava underlying the Lithic Ridge Tuff at Tram Ridge, 7 km north of the Mother Lode mine, based on similarities in phenocryst assemblage and on two K-Ar ages of 13.9 ±0.5 Ma on biotite from the lava. Sawyer et al. (1994) report an $^{40}Ar/^{39}Ar$ age of 14.0 ±0.13 Ma on biotite from the lava at Tram Ridge and include the porphyry dikes in Bare Mountain in a formal stratigraphic unit they refer to as the Lava of Tram Ridge.

Individual porphyry dikes are thin and laterally discontinuous, but virtually all contain coarse, granophyric groundmass textures. Granophyric textures include hypidiomorphic, inequigranular and blocky to micrographic intergrowths of potassium feldspar and quartz, ± small grains of biotite. Sparse to abundant, acicular and lath-shaped grains of potassium feldspar are arranged in a distinctive "bowtie" habit within the groundmass of most of the dikes (Fig. 1). Only rarely are the dike margins aphanitic, although in certain dikes the groundmass of the interiors is distinctly coarser than along the margins. Average grain-size of the groundmass minerals in most of the dikes is in the range of 0.05 to 0.1 mm, sufficiently

coarse to be termed "aplite porphyry" as used by Carten et al. (1988) to describe bodies of the Henderson-Urad intrusive complex. Such textures are characteristic of porphyry-type intrusions and commonly are attributed to quenching at subvolcanic depths due to the escape of a hydrous magmatic volatile phase (e.g., Carten et al., 1988).

High-temperature, highly saline fluids of magmatic origin are an important component and distinguishing characteristic of porphyry systems. The presence of such fluids at Bare Mountain is demonstrated by sparse, but ubiquitous, high-salinity, secondary fluid inclusions containing one or more daughter minerals in quartz phenocrysts in the dikes near the Sterling, Diamond Queen/Goldspar, Telluride and Mother Lode mines and in Tarantula Canyon (Noble et al., 1989; 1991). These are associated with a much larger number of liquid+vapor and vapor-rich inclusions (Fig. 2). Daughter minerals include halite, sylvite(?), calcite, hematite and other, unidentified phases. The presence of these daughter crystals indicates that the inclusions formed from fluids having salinities in excess of 26 weight percent NaCl equivalent. Heating-stage measurements on nine inclusions containing multiple daughter minerals from the dike between the Telluride and Mother Lode mines demonstrate very high temperatures of trapping. At 500° C, the limit of our heating stage, all nine inclusions contained 2 or more daughter minerals, and in six a vapor bubble remained as well. In three inclusions the vapor disappeared between 400° and 430° C. Such fluid temperatures would be difficult to maintain through long flow paths considering the narrow widths of the dikes and the lack of strong metamorphism in the wallrocks. Evaporite beds are not present in the district. The high temperatures and lack of nearby sedimentary salt beds implies that the inclusions formed from fluids released during crystallization of the dikes, and(or) from crystallization of magmas at greater depths.

The group of trace elements associated with hydrothermally altered rocks and gold and fluorite deposits in eastern and northern Bare Mountain consistently includes abundant fluorine and molybdenum (Tingley, 1984)), and, where data are available, at least locally elevated bismuth and tellurium (Weiss et al., 1993b; 1994a, Appendix C, Part II). These elements are commonly concentrated within and above porphyry molybdenum and copper-gold deposits and related systems such as gold-rich skarns and high sulfidation-type, or enargite-type, epithermal precious metals deposits.

Steeply dipping dikes of hydrothermal breccia < 2 m in width cut Paleozoic carbonate rocks northeast of Joshua Hollow and along the west margin of the porphyry dike near the Telluride mine. Clasts include angular to well-rounded fragments of sedimentary and volcanic

rocks and fragments of the porphyry dike. Dikes of hydrothermal breccia are commonly observed above and adjacent to porphyry-type intrusions. In northern Bare Mountain the breccia dikes formed either before, or during, gold-related hydrothermal activity as demonstrated by the presence of elevated concentrations of Au, Ag, As, Sb, Hg, Te and Mo in the breccia dike near the Telluride mine (Weiss et al., 1994a, Appendix C, Part II).

The silicic porphyry dikes crop out over a distance of 12.5 km along strike. Their large lateral extent and narrow widths require that the dikes were fed by a large, underlying magma body, or conceivably by multiple, stock-like or tabular intrusions aligned north-south and consisting of compositionally and mineralogically similar, porphyry-type magmas. Although the dikes are altered, petrographic characteristics and reconnaissance analyses of selected immobile, major- and trace-element contents and $^{87}Sr/^{86}Sr$ ratios (Table 2) show that the magmas were not homogeneous, and that isotopically distinct, more and less evolved magmas were present (Fig. 3). Strontium isotopic compositions of the dikes are significantly less radiogenic than those of the weakly to strongly peraluminous granitic plutons of late Cretaceous age that are associated with lithophile-element mineralization in the eastern Great Basin (Barton, 1990) and are within the range of values reported for the Bullfrog Tuff and the upper, less evolved rhyolitic portions of the Rainier Mesa and Tiva Canyon Tuffs of the southwestern Nevada volcanic field (Farmer et al., 1991).

Timing of Porphyry-type Igneous Activity, Hydrothermal Alteration and Fluorite and Disseminated Gold Mineralization

Pervasive hydrothermal alteration of the dikes complicates the interpretation of the K-Ar ages determined on biotite from the dikes (Marvin et al., 1989; Noble et al., 1991; Monsen et al., 1992) and makes it difficult to unequivocally establish the exact age, or ages, of igneous actvity. However, results of $^{40}Ar/^{39}Ar$ experiments on clear sanidine, turbid sanidine and hornblende from a single specimen of the dike between the Mother Lode and Telluride mines provide limits on the timing of crystallization of the dikes and subsequent alteration and mineralization. Relict hornblende from this dike gives a strongly saddle-shaped step-heating argon release pattern characteristic of excess radiogenic ^{40}Ar with a minimum at about 19.2 Ma (Fig. 4). This minimum in the release spectrum is best interpreted as a maximum possible age for the dike. Laser-fusion determinations on single crystals of clear sanindine from the same specimen give an apparent age of 14.39 $\pm$0.09 Ma (Table 1). Step-heating of turbid sanidine from this specimen gives an isochron age of 14.08 $\pm$0.06 Ma from a slightly rising release

spectrum (Table 1, Fig. 5). The release spectrum is consistent with an incomplete resetting event at about 14.1 Ma of slightly older, *ca.* 14.5 Ma sanidine. There is no evidence for significantly younger resetting, or for a sanidine component significantly older than about 14.5 Ma. Taken together, the results from clear and turbid sanidine suggest that initial cooling of the dike occurred at about 14.5 Ma and was followed at about 14.1 Ma by reheating(?) and recrystallization under sanidine-and biotite-stable conditions.

The K-Ar age on biotite of 13.9 ±0.5 Ma from a dike in Tarantula Canyon (Marvin et al., 1989) overlaps the clear sanidine age of 14.4 ±0.1 Ma, within the limits of the analytical uncertainty, but the biotite ages of 13.8 ±0.2 and 13.9 ±0.1 Ma (Monsen et al., 1992) are younger. In view of the hornblende results, it may be possible that the biotite contains excess radiogenic argon as well (e.g., McDougall and Harrison, 1988) and represent maximum ages. This possibility is not consistent with the sanidine data and it seems more reasonable to interpret the biotite ages as having been reset, consistent with the turbid sanidine age of 14.1 ±0.06 Ma. This resetting may reflect hydrothermal activity associated with magmatic activity at depth.

At the Sterling, Diamond Queen/Goldspar, and Mother Lode mines the argillic alteration and associated gold and fluorite mineralization overprint the biotite- and feldspar-stable alteration of the dikes and are therefore younger than 14.5 to 14.1 Ma. Two lines of evidence show that this alteration and mineralization occurred after about 12.8 Ma. Argillically altered and fluorite-bearing fragments of welded ash-flow tuffs of the Crater Flat and Paintbrush Group are present in gold- and fluorite-bearing breccia at the Diamond Queen/Goldspar mine, demonstrating that gold- and fluorite-related hydrothermal activity is younger than about 12.8 Ma, the age of the oldest unit of the Paintbrush Group (Sawyer et al., 1994). Adularia that pseudomorphs igneous feldspar in the dike at the Diamond Queen/Goldspar mine has given ages of 12.9 ±0.9 and 12.9 ±0.4 Ma (Noble et al., 1991), consistent with this timing.

At the Mother Lode mine K-Ar ages of 13.1 ±0.3 and 12.2 ±0.4 Ma have been obtained on illite-smectite from the mineralized porphyry dike (Table 1). Illite-smectite separated from mineralized, decarbonatized tuffaceous limestone adjacent to the dike, however, gives an age of 26.9 ±0.6 Ma (Table 1). Systematic studies in the Jerritt Canyon district have demonstrated that illite in mineralized sedimentary rocks in Carlin-type deposits can remain sufficiently unaffected by the mineralizing fluids to give ages inherited from original and diagenetic illite (Folger et al., 1995). We interpret the 26.9 Ma age at the Mother Lode mine as an inherited, late Oligocene age and evidence that the rocks of Joshua Hollow are, indeed, part

of the Titus Canyon Formation. An average of the two younger illite ages, which were obtained from specimens collected from the same outcrop, gives a reasonable estimate of the age of gold mineralization at the Mother Lode deposit of about 12.7 Ma and agrees well with the timing of hydrothermal activity at the Diamond Queen/Goldspar mine. Ages of 12.2 $\pm$0.4 Ma and 11.2 $\pm$0.3 Ma determined on alunite near the Telluride mine (Jackson, 1988; McKee and Bergquist, 1993) may reflect continued and/or renewed hydrothermal activity in northern Bare Mountain (Weiss et al., 1996).

Timing similar to that of the Mother Lode mine is constrained by geological relations at the Secret Pass deposit. Mineralization must be younger than 13.3 Ma, the age of the host Bullfrog Tuff of the Crater Flat Group. In addition, the lower part of the 12.8 Ma Topopah Spring Tuff has locally been altered to adularia-bearing assemblages directly above the mineralized rocks of the Bullfrog Tuff. The deposit is truncated at depth by the Fluorspar Canyon fault (Greybeck and Wallace, 1991). Because most of the movement on this fault pre-dates deposition of the 11.6 Ma Rainier Mesa Tuff, mineralization is therefore bracketed between about 12.8 and 11.6 Ma.

STUDIES OF SPECIMENS FROM THE SUBSURFACE OF YUCCA MOUNTAIN

Observations from the Inspection of Core from New Drill Holes

To our knowledge, only four drill holes of the renewed Yucca Mountain drilling program of the last 3 years (1992-1995) were drilled to depths sufficient to recover samples of what might lie beneath the rhyolite of Calico Hills in the area of the proposed repository. Drill hole USW UZ14 was drilled to a depth of 2206' and penetrated into the Bullfrog Tuff. Drill hole UE25 UZ16 was drilled to a depth of 1686.2' and penetrated into the Prow Pass Tuff. USW SD9 was completed at a depth of 2223.1' and penetrated into the Prow Pass Tuff. Drill hole USW SD12 was completed at a depth of 2166' in the upper part of the Bullfrog Tuff. We examined the lower 100 to 200' of the rhyolite of Calico Hills in each drill hole and all of the Crater Flat Group tuffs in each drill hole. Initially glassy, non-welded to partially welded tuffs in each drill hole appear to have been replaced, to varying degrees, by zeolites and clay minerals. No evidence for hydrothermal alteration or mineralization were observed in rocks that had undergone primary crystallization in cores of any of the drill holes.

Drill hole USW SD12 is particularly important because it is the only drill hole within the repository block, besides USW G4, deep enough to penetrate into tuffs of the Crater Flat Group. These two drill holes, which provide the only direct view of what may actually underlie the

repository, are spaced more than 1 km apart. Unfortunately, SD12 was terminated after penetrating only 114' into the Bullfrog Tuff.

Exploratory Studies Facility

Two visits were made to the Exploratory Studies Facility. The tunnel provides an opportunity to observe many details of the volcanic and structural history of the Paintbrush Group Tuffs not readily observable in surface exposures. Of particular interest to Task 3 is an area about 1 km from the portal within the ash-fall and pyroclastic surge deposits between the top of the Topopah Spring Tuff and the base of the Pah Canyon Tuff. Over a horizontal distance of about 10 m in length, the tuffs are discolored to shades of reddish-brown and greyish-purple, apparently due to the presence of abundant iron and manganese(?) oxides. This zone is informally known at the site as the "mural". Glass shards and pumice fragments in tuffs at the "mural" are largely replaced by mixtures of smectite clay and Fe-Mn(?) oxides. It is unclear if the clay-oxide concentration is related to the primary cooling and degassing of the tuffs, or if it perhaps is a paleohydrologic feature, such as an initially permeable horizon invaded by hydrothermal fluids. We were unable to collect samples from the "mural" at the time of our first visit. Two clay-oxide rich specimens were collected during our second visit, which took place in September, 1995. Portions of these specimens have been pulverized and sent to U.S. Minerals Laboratories, Inc., for low-detection limit multi-element chemical analyses. The results and our interpretations of the chemical analyses will be forwarded to the Nuclear Waste Project Office on receipt.

UPDATE ON MINING AND MINERAL EXPLORATION

Barrick Gold Corporation, through their purchase of Lac Minerals Ltd., has taken over the operation of the Lac Bullfrog mine (now referred to as the Barrick Bullfrog mine) in the southern Bullfrog Hills. Production of gold and silver from the open pit was completed late in 1994, but production from the underground workings continues with projected mining rates of about 1000 ton/day for the next several years. Approximately 301,000 oz. gold were produced in 1994 from ores with an average grade of 3.59 g/tonne (Eng et al., 1995). Production of gold and silver began at the Montgomery-Shoshone mine utilizing open-pit operations and the existing mill and recovery facilities of the Barrick Bullfrog mine. As of the end of 1994, total reserves for the Bullfrog and Montgomery-Shoshone mines were estimated to be 13.0 million tonnes with an average grade of 2.49 g/tonne (1,042,000 oz); the majority of proven reserves lying in the underground Bullfrog deposit (Eng et al., 1995). Cumulative production plus reserves at the end

of 1994 total over 2,500,000 oz gold, demonstrating that the Barrick Bullfrog mine is one of the largest volcanic-rock hosted gold-silver mines in Nevada.

Faced with rapid depletion of reserves, Barrick has continued an aggressive progam of exploratory drilling in the southern Bullfrog Hills, and has resumed surface studies in the northern Bullfrog Hills. Barrick has begun the permitting process for mining an open-pit resource in Bonanza Mountain that has been defined by exploratory drilling during the past 2 years. Drilling is currently being carried out by Barrick on the Reward property, north of the Gold Ace mine in Bare Mountain, to test the extent and grade of disseminated mineralization hosted by early Paleozoic sedimentary rocks.

Underground mining of disseminated, sedimentary-rock hosted ores continues at the Sterling mine; production since 1980 has exceeded 100,000 oz gold. During the past year Cathedral Gold Corporation purchased Saga Exploration's remaining interest in the property.

Inter-Rock Gold and Rayrock Yellowknife Resources announced mineable proven and probable oxide reserves at the Secret Pass gold deposit, in Fluorspar Canyon 19 km west of the repository site, of 6.8 million tons with an average grade of 0.019 oz gold/ton (Northern Miner, 1994). The reserve is part of a geological resource of 32.8 million tons containing an average grade of 0.018 oz gold/ton, defined from extensive drilling carried out during the past seven years. Most of the deposit is hosted by rhyolite ash-flow tuffs of the Bullfrog Tuff, demonstrating unequivocally that ash-flow units present in Yucca Mountain are suitable hosts for disseminated precious-metal ores. Plans call for an estimated rate of production of 22,000 oz gold/year for five years using open-pit and cyanide heap-leaching techniques. Capital cost for the mine is estimated to be US$5.1 million and recoveries are expected to be 80% (Northern Miner, 1994). Construction of the mine had not begun as of mid-September, 1995, but mine-site permitting and procurement of an adequate water supply are currently underway. In part for the purpose of obtaining water supplies, Inter-Rock has purchased the nearby Mother Lode mine site from U.S. Precious Metals, Inc.

HG Mining Inc. of Beatty, NV. continues production of cut stone products from ash-flow tuffs quarried within the geographic limits of the Timber Mountain caldera complex. Ash-flow units from which cut stone is currently produced include the glassy, partially welded caprock of the Rainier Mesa Tuff of the Timber Mountain Group in northern Crater Flat, the lower, lithic-rich, unwelded part of the Ammonia Tanks Tuff of the Timber Mountain Group in the Transvaal Hills, the tuff of Cut-off Road in the Transvaal Hills and the Pahute Mesa and Rocket Wash Tuffs of the Thirsty Canyon Group in upper Oasis Valley.

REVIEWS, PUBLICATIONS AND PRESENTATIONS

Reviews

S. I. Weiss served as a reviewer for the Nevada Bureau of Mines on a field review of a geologic map of the Castle Mountains, San Bernadino County, California and Clark County, Nevada, by R. C. Capps and J. N. Moore. This map, submitted for possible publication by the Nevada Bureau of Mines and Geology, documents the geologic setting of the Castle Mountains (Hart district) gold deposits currently being mined by Viceroy Gold Corp. These deposits are of particular interest to Task 3 as they are bulk-mineable, relatively high-grade vein and breccia deposits hosted within a group of overlapping, high-silica rhyolite domes and associated, near-vent pyroclastic deposits of middle Miocene age. Gold mineralization appears to have been concurrent with the development of the dome complex, but pre-dates the eruption of the youngest domes of the complex. This situation is analogous to post-Ammonia Tanks Tuff hydrothermal activity in the Calico Hills, peripheral to the southern margin of the Timber Mountain caldera, where unaltered flows of the rhyolite of Shoshone Mountain overlie strongly altered rocks. K-Ar ages of about 10.4 ±0.3 Ma on alunite from the Calico Hills indicate that hydrothermal activity must be only slightly older than the rhyolite of the Calico Hills (Weiss et al., 1996).

Publications

The following abstracts and articles resulting from Task 3 studies were produced and(or) published during the period covered by this report, and are contained in the appendices as follows:

Appendix A:

Weiss, S. I., Noble, D. C., and Larson, 1995, Hydrothermal origin and significance of pyrite in ash-flow tuff at Yucca Mountain, Nevada (*Economic Geology*, in press).

Appendix B:

Weiss, S. I., Noble, D. C., Connors, K. A., Jackson, M. R., and McKee, E. H., Multiple episodes of hydrothermal activity and epithermal mineralization in the southwestern Nevada volcanic field and their relations to magmatic activity, volcanism and regional extension (in revision following peer-review for *Economic Geology*).

Appendix C:

Connors, K. A., Weiss, S. I., and Noble, D. C., 1995a, The problems with forming gold deposits by leaching of silicic volcanic sequences and the significance of low-level gold anomalies in silicic volcanic terranes [extended abs.]: *Geology and Ore Deposits of the American Cordillera, Symposium Program with Abstracts*, Geological Society of Nevada, Reno, p. A20.

Appendix D:

Connors, K. A., Weiss, S. I., and Noble, D. C., 1995b, The Oasis Valley fault: the principal breakaway structure and eastern limit of Late Miocene synvolcanic extension in the Bullfrog Hills, southwestern Nevada [extended abs.]: EOS Trans. Am. Geophys. Union, v. 76, p. S284.

Presentations

S. I. Weiss gave a presentation entitled *Potential for undiscovered mineral deposits at Yucca Mountain, NV: Host rocks, timing and spatial distribution of nearby mineralization and evidence for hydrothermal activity from deep drilling at the site*. The talk was presented at the University of Nevada, Reno, in the Spring, 1995, lecture series of the Center for Environmental Science and Engineering, and the Environmental Studies Program.

SUMMARY OF CONCLUSIONS AND RECOMMENDATIONS

It is appropriate to state again, as we did in our report for 1993-1994, that stratigraphic relations and radiometric age data demonstrate that multiple episodes of ore-forming and potentially ore-forming hydrothermal activity have occurred in large areas of the southwestern Nevada volcanic field, including the Yucca Mountain region (Weiss et al., 1996, Appendix B). The pyritic rocks penetrated by the deep drill holes in Yucca Mountain provide important evidence, in addition to the large body of textural and mineralogical data on rock alteration reported in various papers by personnel of the Los Alamos National Laboratory and the U. S. Geological Survey, that one or more of these episodes has affected rocks deep within Yucca Mountain. More importantly, the presence of pyrite in these rocks indicates that the fluids contained small, but geochemically significant amounts of reduced sulfur and were therefore capable of transporting and depositing precious metals. Considering the uneven lateral and vertical distribution of pyrite in rocks of Yucca Mountain (Weiss et al., 1995), the lack of pyrite-bearing alteration assemblages in core from drill hole USW SD12 reduces the probability of, but does not rule out,

possible pyritic alteration and/or epithermal mineralization deeper in the Crater Flat Group or older units beneath the proposed repository. It remains our opinion that additional drill holes, to depths of 5000+ feet, are necessary within and adjacent to the proposed repository if the issue of possible mineral resources is to be resolved with a reasonable level of uncertainty.

As a progressively better understanding of the conditions of transport and deposition of gold, both in magmatic and hydrothermal systems is obtained (e.g., Connors et al., 1993), it is clear that one critical factor in the formation of gold deposits is the existence of a relatively gold-rich hydrothermal solution (e.g., Bartos, 1993; Matsuhisa and Aoki, 1994; Connors et al., 1995). An important corollary of this recognition is that the *absence* of gold in altered rocks recovered from the widely spaced drill holes in Yucca Mountain does not demonstrate that a major deposit may not be present, contrary to the view held by the Department of Energy and their contractors (e.g., Castor et al., 1994). At present a group of geologists directed by S. B. Castor of the Nevada Bureau of Mines and Geology has essentially completed the first year of a two-year formal assessment of the potential for mineral, geothermal and hydrocarbon resources at Yucca Mountain, under a contract from the Department of Energy. We strongly recommend that the Nuclear Waste Project Office obtain careful scrutiny and review of the methods, data and interpretations of the Nevada Bureau of Mines resource assessment.

REFERENCES CITED AND OTHER PERTINENT LITERATURE

The following references were selected because of their direct bearing on the Cenozoic volcanic stratigraphy and caldera geology, hydrothermal activity, and mineral potential of Yucca Mountain and the surrounding region of the southwestern Nevada volcanic field. Additional pertinent references on mineral potential, and particularly unpublished data in files of the Nevada Bureau of Mines and Geology, are given by Bell and Larson (1982b). A compendium of information from the U.S. Geological Survey's Mineral Resource Data System is given by Bergquist and McKee (1991).

Ahern, R., and Corn, R.M., 1981, Mineralization related to the volcanic center at Beatty, Nevada: Arizona Geological Society Digest, v. XIV, p. 283-286.

Albers, J. P., and Stewart, J. H., 1972, Geology and mineral deposits of Esmeralda County, Nevada, Nevada Bur. Mines and Geol. Bull. 78, 80 p.

Ander, H.D., and Byers, F.M., 1984, Nevada Test Site field trip guidebook; Reno, Nevada, University of Nevada-Reno, Department of Geological Sciences, v. 2, 1984, 35 p.

Anderson, R.E., Ekren, E.B., and Healey, D.L., 1965, Possible buried mineralized areas in Nye and Esmeraldo Counties, Nevada: U.S. Geological Survey Professional Paper 525-D, p. D144-D150.

Anonymous, 1928, One strike of real importance made at Nevada's new camp: Engineering and Mining Journal, v. 125, no. 1, p. 457.

Arehart, G., B., Foland, K. A., Naeser, C. W., and Kesler, S. E., 1993, $^{40}Ar/^{39}Ar$, K/Ar, and fission-track geochronology of sediment-hosted disseminated gold deposits at Post-Betze, Carlin trend, northeastern Nevada: Economic Geology, v. 88, p. 622-646.

Aronson, J.L., and Bish, D.L., 1987, Distribution, K/Ar dates, and origin of illite/smectite in tuffs from cores USW G-1 and G-2, Yucca Mountain, Nevada, a potential high-level radioactive waste repository: Abstract of presentation at Clay Minerals Society Meeting, Socorro, NM, 1987.

Armstrong, R. L., Ekren, E. B., McKee, E. H., and Noble, D. C., 1969, Space-time relations of Cenozoic silicic volcanism in the Great Basin of the western United States: Am. Jour. Sci., v. 267, p. 478-490.

Bailey, E.H., and Phoenix, D.A., 1944, Quicksilver deposits in Nevada: Nevada Bureau of Mines and Geology Bulletin 41.

Barton, C.C., 1984, Tectonic significance of fractures in welded tuff, Yucca Mountain, Southwest Nevada: Geological Society of America, Abstracts with Programs, v. 16, p. 437.

Barton, M. D., 1990, Cretaceous magmatism, metamorphism, and metallogeny in the east-central Great Basin: *in* Anderson, J. L., ed., Geological Society of America Memoir 174, p. 283-302.

Barton, P. B., and Skinner, B. J., 1979, Sulfide mineral stabilities: *in* Barnes, H. L., ed., Geochemistry of Hydrothermal Ore Deposits, Wiley and Sons, New York, 798 p.

Bartos, P.J., 1993, Comparison of gold-rich and gold-poor quartz-base metal veins, western San Juan Mountains, Colorado: the Mineral Point area as an example: Society of Economic Geologists Newsletter, no. 15.

Bath, G.D., and Jahren, C.E., 1984, Interpretations of magnetic anomalies at repository site proposed for Yucca Mountain area, Nevada Test Site: U.S. Geological Survey Open-File Report 84-120, 40 p.

Bath, G.D., and Jahren, C.E., 1985, Investigation of an aeromagnetic anomaly on west side of Yucca Mountain, Nye County, Nevada: U.S. Geological Survey Open-File Report 85-459, 24 p.

Beck, B. A., 1984, Geologic and gravity studies of the structures of the northern Bullfrog Hills, Nye County, Nevada: California State University at Long Beach, unpublished MSc Thesis, 86 p.

Bedinger, M.S., Sargent, K.A., and Langer, W.H., 1984, Studies of geology and hydrology in the Basin and Range Province, Southwestern United States, for isolation of high-level radioactive waste; characterization of the Death Valley region, Nevada and California: U.S. Geological Survey Open-File Report 84-743, 173 p.

Bedinger, M.S., Sargent, K.A., and Langer, W.H., 1984, Studies of geology and hydrology in the Basin and Range Province, Southwestern United States, for isolation of high- level radioactive waste; evaluation of the regions: U.S. Geological Survey Open-File Report 84-745, 195 p.

Bell, E.J., and Larson, L.T., 1982a, Overview of energy and mineral resources of the Nevada Nuclear Waste Storage Investigations, Nevada Test Site, Nye County, Nevada: U.S. Department of Energy Report NVO-250 (DE83001418), 64 p. plus maps.

Bell, E.J., and Larson, L.T., 1982b, Annotated bibliography, Overview of energy and mineral resources for the Nevada Nuclear Waste Storage Investigations, Nevada Test Site, Nye County, Nevada: U.S. Department of Energy Report NVO-251 (DE83001263), 30 p.

Benson, L.V. and McKinley, P.W., 1985, Chemical composition of the ground water in the Yucca Mountain area, Nevada: U.S. Geological Survey Open-File Report 85-484, 10 p.

Bentley, C.B., 1984, Geohydrologic data for test well USW G-4, Yucca Mountain area, Nye County, Nevada: U.S. Geological Survey Open-File Report 84-63, 67 p.

Bergquist, J. R., and McKee, E. H., 1991, Mines, prospects and mineral occurrences in Esmeralda and Nye Counties, Nevada, near Yucca Mountain: U.S. Geological Survey Administrative Report to the Department of Energy, Yucca Mountain Project, 385 p.

Bish, D.L., 1987, Evaluation of past and future alteration in tuff at Yucca Mountain, Nevada based on clay mineralogy of drill cores USW G-1, G-2, and G-3: Los Alamos, New Mexico, Los Alamos National Laboratory Report LA-10667-MS, 42 p.

Bish, D. L., and Aronson, J. L., 1993, Paleogeothermal and paleohydrologic conditions in silicic tuff from Yucca Mountain, Nevada: Clays and Clay Minerals, v. 41, p. 148-161.

Bonham, H. F., Jr., and Garside, L. J., 1979, Geology of the Tonopah, Lone Mountain, Klondike and northern Mud Lake Quadrangles, Nevada: Nevada Bureau of Mines and Geology Bulletin 92, 142 p., 1:48,000.

Bonham, H. F., Jr., and Hess, R. H., 1995, Major precious-metal deposits: *in* The Nevada Mineral Industry--1994, Nevada Bureau of Mines and Geology Special Publication MI-1994.

Booth, M., 1988, Dallhold finalizes plans for huge Nevada mine: The Denver Business Journal, April 4, 1988, p. 10.

Boyle, R. W., 1979, The geochemistry of gold and its deposits: Geological Survey of Canada Bulletin 280, 584 p.

Boyle, R.W., and Jonasson, I.R., 1973, The geochemistry of arsenic and its use as an indicator element in geochemical prospecting: Journal of Geochemical Exploration, v. 2, p. 251-296.

Broxton, D. E., Vaniman, D., Caporuscio, F., Arney, B., and Heiken, G., 1982, Detailed petrographic descriptions and microprobe data fro drill holes USW-G2 and UE25b-1H, Yucca Mountain, Nevada: Los Alamos, New Mexico, Los Alamos National Laboratory Report LA-10802-MS, 168 p.

Broxton, D.E., Byers, F.M., Warren, R.G. and Scott, R.B., 1985, Trends in phenocryst chemistry in the Timber Mountain-Oasis Valley volcanic field, SW Nevada; evidence for isotopic injection of primitive magma into an evolving magma system: Geological Society of America, Abstracts with Programs, v. 17, p. 345.

Broxton, D. E., Warren, R. G., and Byers, F. M., Jr., 1989, Chemical and mineralogic trends within the Timber Mountain-Oasis Valley caldera complex, Nevada: Evidence for multiple cycles of chemical evolution in a long-lived silicic magma system: Journal of Geophysical Research, v. 94, p. 5961-5985.

Broxton, D.E., Warren, R.G., Byers, F.M., Jr., Scott, R.B., and Farner, G.L., 1986, Petrochemical trends in the Timber Mountain-Oasis Valley caldera complex, SW Nevada: EOS (American Geophysical Union Transactions), v. 67, p. 1260.

Broxton, D.E., Warren, R.G., Hagan, R.C. and Luedemann, G.,1986, Chemistry of diagenetically altered tuffs at a potential nuclear waste repository, Yucca Mountain, Nye County, Nevada: Los Alamos, New Mexico, Los Alamos National Laboratory Report LA-10802-MS, 160 p.

Byers, F. M., Jr., Carr, W. J., and Orkild, P. P., 1989, Volcanic centers of southwestern Nevada: evolution of understanding, 1960-1988: Journal of Geophysical Research, v.94, p. 5908-5924.

Byers, F.M., Jr., Carr, W.J., and Orkild, P.P., 1986, Calderas of southwestern Nevada-Evolution of understanding, 1960-1986: EOS (American Geophysical Union Transactions), v. 67, p. 1260.

Byers, F.M., Jr., Carr, W.J., Orkild, P.P., Quinlivan, W.D. and Sargent, K.A., 1976a, Volcanic Suites and related cauldrons of Timber Mountain-Oasis Valley caldera complex: U.S. Geological Survey Professional Paper 919, 70 p.

Byers, F.M., Jr., Carr, W.J., Christiansen, R.L., Lipman, P.W., Orkild, P.P., and Quinlivan, W.D., 1976b, Geologic map of the Timber Mountain Caldera area, Nye County, Nevada: U.S. Geological Survey Miscellaneous Investigations Series, I-891, sections, 1:48,000 scale.

Byers, F.M., Jr., Orkild, P.P, Carr, W. J., and Quinlivan, W.D., 1968, Timber Mountain Tuff, southern Nevada, and its relation to cauldron subsidence: Geological Society of America Memoir 110, p. 87-97.

Caporuscio, F., Vaniman, D.T., Bish, D.L., Broxton, D.E., Arney, D., Heiken, G., Byers, F.M., and Gooley, R., 1982, Petrologic studies of drill cores USW-G2 and UE25b-1H,Yucca Mountain, Nevada: Los Alamos, New Mexico, Los Alamos National Laboratory Report LA-9255-MS, 114 p.

Carr, M.D., and Monsen, S.E., 1988, A field trip guide to the geology of Bare Mountain: Geological Society of America Field Trip Guidebook, Cordilleran Section Meeting, Las Vegas, Nevada, p. 50-57.

Carr, M.D., Waddell, S.J., Vick, G.S., Stock, J.M., and Monsen, S.A., Harris, A.G., Cork, B.W., and Byers, F.M., Jr., 1986, Geology of drill hole UE25p-1: A test hole into pre-Tertiary rocks near Yucca Mountain, southern Nevada: U.S. Geological Survey Open File Report 86-175.

Carr, W.J., 1964, Structure of part of the Timber Mountain dome and caldera, Nye County, Nevada: U.S. Geological Survey Professional Paper 501-B, p. B16-B20.

Carr, W.J., 1974, Summary of tectonic and structural evidence for stress orientation at the NTS: U.S. Geological Survey Open-File Report 74-176, 53 p.

Carr, W.J., 1982, Volcano-tectonic history of Crater Flat, southwestern Nevada, as suggested by new evidence from drill hole USW-VH-1 and vicinity: U.S. Geological Survey Open-File Report 82-457, 23 p.

Carr, W.J., 1984a, Regional structural setting of Yucca Mountain, southwestern Nevada, and late Cenozoic rates of tectonic activity in part of the southwestern Great Basin, Nevada and California: U.S. Geological Survey Open-File Report 84-0854, 114 p.

Carr, W.J., 1984b, Timing and style of tectonism and localization of volcanism in the Walker Lane belt of southwestern Nevada: Geological Society of America, Abstracts with Programs, v. 16, p. 464.

Carr, W.J., 1988a, Styles of extension in the Nevada Test Site region, southern Walker Lane Belt: an integration of volcano-tectonic and detachment fault models: Geological Society of America, Abstracts with Programs, v. 20, p. 148.

Carr, W. J., 1988b, Volcano-tectonic setting of Yucca Mountain and Crater Flat, *in* Carr, M. D., and Yount, J. C., eds., Geologic and hydrologic investigations of a potential nuclear waste disposal site at Yucca Mountain, southern Nevada: U.S. Geol. Survey Bull. 1790, p. 35-49.

Carr, W.J., and Quinlivan, W.D., 1966, Geologic map of the Timber Mountain quadrangle, Nye County, Nevada: U.S. Geological Survey Geologic Quadrangle Map GQ-503, 1:24,000 scale, sections.

Carr, W.J., and Quinlivan, W.D., 1968, Structure of Timber Mountain resurgent dome, Nevada Test Site: Geological Society of America Memoir 110, p. 99-108.

Carr, W.J. and Parrish, L.D., 1985, Geology of drill hole USW VH-2, and structure of Crater Flat, southwestern Nevada: U.S. Geological Survey Open-File Report 85-475, 41 p.

Carr, W.J., Byers, F.M., and Orkild, P.P., 1984, Stratigraphic and volcano-tectonic relations of Crater Flat Tuff and some older volcanic units, Nye County, Nevada: U.S. Geological Survey Open-File Report 84-114, 97 p.

Carr, W.J., Byers, F.M., and Orkild, P.P., 1986, Stratigraphic and volcano-tectonic relations of Crater Flat Tuff and some older volcanic units, Nye County, Nevada: U.S. Geological Survey Professional Paper 1323, 28p.

Carten, R. B., Geraghty, E. P., Walker, B. M., and Shannon, J. R., Cyclical development of igneous features and their relationship to high-temperature hydrothermal features in the Henderson porphyry molybdenum deposit, Colorado: Economic Geology, v. 83, p. 266-296.

Castor, S. B., and Weiss, S. I., 1992, Contrasting styles of epithermal precious-metal mineralization in the southwestern Nevada volcanic field, USA: Ore Geology Reviews, v. 7, p. 193-223.

Castor, Feldman and Tingley, 1990, Mineral evaluation of the Yucca Mountain Addition, Nye County, Nevada: Nevada Bureau of Mines and Geology, Open-file Report 90-4, 80 pp.

Castor, Feldman and Tingley, 1990, Mineral potential report for the U.S. Department of Energy, Serial No. N-50250: Nevada Bureau of Mines and Geology, University of Nevada, Reno, 24 pp.

Castor, S. B., Tingley, J. V., and Bonham, H. F., Jr., 1991, Yucca Mountain Addition subsurface mineral resource analysis: unpub. proposal to Science Applications International Corp., 10 p.

Castor, S. B., Tingley, J. V., and Bonham, H. F., Jr., 1992, Subsurface mineral resource analysis, Yucca Mountain, Nevada, Preliminary Report 1: Lithilogic logs: Nevada Bureau of Mines and Geology Open-file report 92-4, 11 p. plus appendices.

Castor, S. B., Tingley, J. V., and Bonham, H. F., Jr., (*in review*), Pyritic ash-flow tuff in Yucca Mountain: manuscript submitted in 1992 to Geology.

Castor, S. B., Tingley, J. V., and Bonham, H. F., Jr., (*in press*), Pyritic ash-flow tuff in Yucca Mountain: manuscript submitted in 1993 to Economic Geology.

Castor, S. B., Tingley, J. V., and Bonham, H. F., Jr., 1994, Pyritic ash-flow tuff, Yucca Mountain, Nevada: Economic Geology, v. 89, p. 401-407.

Christiansen, R.L., and Lipman, P.W., 1965, Geologic map of the Topopah Spring NW quadrangle, Nye County, Nevada: U.S. Geological Survey Geologic Quadrangle Map GQ-444, 1:24,000 scale, sections.

Christiansen, R.L., Lipman, P.W., Carr, W.J., Byers, F.M., Jr., Orkild, P.P., and Sargent, K.A., 1977: Timber Mountain-Oasis Valley caldera complex of southern Nevada: Geological Society of America Bulletin, v. 88, p. 943-959.

Christiansen, R.L., Lipman, P.W., Orkild, P.P., and Byers, F.M., Jr., 1965, Structure of the Timber Mountain caldera, southern Nevada, and its relation to basin-range structure: U.S. Geological Survey Professional Paper 525-B, p. B43-B48.

Connors, K. A., (*in preparation*), Studies in silicic volcanic geology: Part I: Compositional controls on the initial gold contents of silicic volcanic rocks; Part II: Geology of the western margin of the Timber Mountain caldera complex and post-Timber Mountain volcanism in the Bullfrog Hills: unpublished PhD dissertation, University of Nevada, Reno.

Connors, K.A., Weiss, S.I., Noble, D.C., and Bussey, S.D., 1990, Primary gold contents of some silicic and intermediate tuffs and lavas: evaluation of possible igneous sources of gold: Geological Society of America Abst. with Programs, v. 22, p. A135.

Connors, K.A., Noble, D.C., Weiss, S.I., and Bussey, S.D., 1991a, Compositional controls on the gold contents of silicic volcanic rocks: 15th International Geochemical Exploration Symposium Program with Abstracts, p. 43.

Connors, K. A., Weiss, S. I., and Noble, D. C., 1995a, The problems with forming gold deposits by leaching of silicic volcanic sequences and the significance of low-level gold anomalies in silicic volcanic terranes [extended abs.]: Geology and Ore Deposits of the American Cordillera, Symposium Program with Abstracts, Geological Society of Nevada, Reno, p. A20.

Connors, K. A., Weiss, S. I., and Noble, D. C., 1995b, The Oasis Valley fault: the principal breakaway structure and eastern limit of Late Miocene synvolcanic extension in the Bullfrog Hills, southwestern Nevada [extended abs.]: EOS Trans. Am. Geophys. Union, v. 76, p. S284.

Connors, K. A., McKee, E. H., Noble, D. C., and Weiss, S. I., 1991, Ash-flow volcanism of Ammonia Tanks age in the Oasis Valley area, SW Nevada: Bearing on the evolution of the Timber Mountain calderas and the timing of formation of the Timber Mountain II resurgent dome [extended abs.]: EOS, Trans. Am. Geophys. Union., v. 72, p. 570.

Connors, K., A., Noble, D. C., Bussey, S., D., and Weiss, S. I., 1993, Initial gold contents of silicic volcanic rocks: bearing on the behavior of gold in magmatic systems: Geology, v. 21, p. 937-940.

Cornwall, H.R., 1962, Calderas and associated volcanic rocks near Beatty, Nye County, Nevada: Geological Society of America, Petrologic Studies, A.F. Buddington Volume, p. 357-371.

Cornwall, H.R., 1972, Geology and mineral deposits of southern Nye County, Nevada: Nevada Bureau of Mines and Geology Bulletin 77, p. 49.

Cornwall, H.R., and Kleinhampl, F.J., 1961, Geology of the Bare Mountain quadrangle, Nevada: U.S. Geological Survey Geologic Quadrangle Map GQ-157, 1:62,500 scale.

Cornwall, H.R., and Kleinhampl, F.J., 1964, Geology of the Bullfrog quadrangle and ore deposits related to the Bullfrog Hills caldera, Nye County, Nevada, and Inyo County, California: U.S. Geological Survey Professional Paper 454-J, 25 p.

Cornwall, H.R., and Norberg, J.R., 1978, Mineral Resources of the Nellis Air Force Base and the Nellis Bombing and Gunnery Range, Clark, Lincoln, and Nye Counties, Nevada: U.S. Bureau of Mines Unpublished Administrative Report, 118 p.

Craig, R.W. and Robinson, J.H., 1984, Geohydrology of rocks penetrated by test well UE-25p#1, Yucca Mountain area, Nye County, Nevada, U.S. Geological Survey Water-Resources Investigations 84-4248, 57 p.

Craig, R.W., Reed, R.L., and Spengler, R.W., 1983, Geohydrologic data for test well USW H-6, Yucca Mountain area, Nye County, Nevada: U.S. Geological Survey Open-File Report 83-856, 52 p.

Crowe, B.M., 1980, Disruptive event analysis: Volcanism and igneous intrusion: Batelle Pacific Northwest Laboratory Report PNL-2822, 28 p.

Crowe, B.M., and Carr, W.J., 1980, Preliminary assessment of the risk of volcanism at a proposed nuclear waste repository in the southern Great Basin: U.S. Geological Survey Open-File Report 80-357, 15 p.

Crowe, B.M., Johnson, M.E., and Beckman, R.J., 1982, Calculation of probability of volcanic disruption of a high-level radioactive waste repository within southern Nevada, USA: Radioactive Waste Management and the Nuclear Fuel Cycle, v. 3, p. 167-190.

Crowe, B.M., Vaniman, D.J., and Carr, W.J., 1983b, status of volcanic hazard studies for the Nevada nuclear waste storage investigations: Los Alamos, New Mexico, Los Alamos National Laboratory Report LA-9325-MS.

Dalrymple, G.B., and Lanphere, M.A., 1969, Potassium-argon dating-- principals, techniques and applications to geochronology: San Francisco, W.H. Freeman Co., 258 p.

Deino, A.L., Hausback, B.P., Turrin, B.T., and McKee, E.H., 1989, New $^{40}Ar/^{39}Ar$ ages for the Spearhead and Civet Cat Canyon Members of the of Stonewall Flat Tuff, Nye County, Nevada: EOS, Trans. American Geopphysical Union, v. 70, p. 1409.

Drexler, J. W., 1982, Mineralogy and geochemistry of Miocene volcanic rocks related to the Julcani Ag-Au-Cu-Bi deposit, Peru: Physiochemical conditions of a productive magma body: unpublished PhD dissertation, Houghton, Michigan Technical University, 250 p.

Eckel, E.B., ed., 1968, Nevada Test Site: Geological Society of America Memoir 110, 290 p.

Eichleberger, J. C., and Koch, F. G., 1979, Lithic fragments in the Bandelier Tuff, Jemez Mountains, New Mexico: Journal of Volcanology and Geothermal Research, v. 5, p. 115-134.

Ekren, E.B., and Sargent, K.A., 1965, Geologic map of Skull Mountain quadrangle at the Nevada Test Site, Nye County, Nevada: U.S. Geological Survey Geologic Quadrangle Map GQ-387.

Ekren, E.B., Anderson, R.E., Rodgers, C.L., and Noble, D.C., 1971, Geology of northern Nellis Air Force Base Bombing and Gunnery Range, Nye County, Nevada: U.S. Geological Survey Professional Paper 651, 91 p.

Eng, T., Boden, D. R., and Biggs, J. O., 1995, Geology and mineralization of the Bullfrog mine and vicinity, Nye County, Nevada: *in* Callicrate, T. E., ed., Gold Deposits of the Walker Lane, 1995 Symposium Field Trip I Giudebook, Reno, Geological Society of Nevada.

Farmer, G. L., Broxton, D. E., Warren, R. G., and Pickthorn, W., 1991, Nd, Sr, and O isotopic variations in metaluminous ash-flow tuffs and related volcanic rocks at the Timber Mountain/Oasis Valley caldera, SW Nevada: implications for the origin and evolution of large-volume silicic magma bodies: Contributions to Mineralogy and Petrology, v. 109, p. 53-68.

Feitler, S., 1940, Welded tuff resembling vitrophyre and pitchstone at Bare Mountain, Nevada: Geological Society of America Bulletin, v. 51, p. 1957.

Flood, T.P., and Schuraytz, B.C., 1986, Evolution of a magmatic system. Part II: Geochemistry and mineralogy of glassy pumices from the Pah Canyon, Yucca Mountain, and Tiva Canyon Members of the Paintbrush Tuff, southern Nevada: EOS Trans. American Geophysical Union, v. 67, p. 1261.

Foley, D., 1978, The geology of the Stonewall Mountain volcanic center, Nye County, Nevada: Ohio State University, Columbus Ohio, unpublished PhD Dissertation, 139 p.

Folger, H. W., Snee, L. W., Mehnert, H. H., Hofstra, A. H., and Dahl, A. R., 1995, Significance of K-Ar and $^{40}Ar/^{39}Ar$ dates from mica in Carlin-type gold deposits: evidence from the Jerritt Canyon district, Nevada [extended abs.]: Geology and Ore Deposits of the American Cordillera, Symposium Program with Abstracts, Geological Society of Nevada, Reno, p. A31.

Fouty, S.C., 1984, Index to published geologic maps in the region around the potential Yucca Mountain Nuclear Waste Repository site, southern Nye County, Nevada: U.S. Geological Survey Open-File Report 84-524, 31 p.

Fridrich, C. J., 1987, The Grizzly Peak cauldron, Colorado: structure and petrology of a deeply dissected resurgent ash-flow caldera: unpublished PhD dissertion, Stanford, Stanford University, 201 p.

Fridrich, C. J., Orkild, P. P., Murray, M., Price, J. R., Christiansen, R. L., Lipman, P. W., Carr, W. J., Quinlivan, W. D., and Scott, R. B., 1994, Geologic map of the East of Beatty Mountain Quadrangle, Nye County, Nevada: U.S. Geological Survey Open-file Report, 4 sheets, 1:12,000 (in review).

Frischknecht, F.C. and Raab, P.V., 1984, Time-domain electromagnetic soundings at the Nevada Test Site, Nevada, Geophysics, v. 49, p. 981-992.

Frizzell, Virgil, and Shulters, Jacqueline, 1986, Geologic map of the Nevada Test Site: EOS Trans. American Geophysical Union, v. 67, p. 1260.

Frizzell, Virgil, and Shulters, Jacqueline, 1990, Geologic map of the Nevada Test Site: U.S. Geological Survey Misc. Invest. Map I-2046, 1:100,000.

Gans, P. B., Mahood, G. A., and Schermer, E., 1989, Synextensional magmatism in the Basin and Range province; A case study from the eastern Great Basin: Geological Society of America Spec. Paper 233, 53 p.

Garside L.J. and Schilling, J.H., 1979, Thermal waters of Nevada: Nevada Bureau of Mines and Geology, Bulletin 91, 163 p.

Geehan, R.W., 1946, Exploration of the Crowell fluorspar mine, Nye County, Nevada: U.S. Bureau of Mines Report of Investigations 3954, 9 p.

Geldon, A. L., (in press) Preliminary hydrogeologic assessment of boreholes UE-25c #1, UE-25c #2 and UE-25c #3, Yucca Mountain, Nye County, Nevada: U.S. Geological Survey Water-Resources Investigations Report 91-XXX.

Greybeck, J. D., and Wallace, A. B., 1991, Gold mineralization at Fluorspar Canyon near Beatty, Nye County, Nevada: *in* Raines, G. L., Lisle,R. E., Shafer, R. W., and Wilkinson, W. W., eds., Geology and ore deposits of the Great Basin: Symposium Proceedings, Geol. Soc. of Nevada, sp. 935-946.

Hagstrum, J.T., Daniels, J.J., and Scott, J.H., 1980, Interpretation of geophysical well-log measurements in drill hole UE 25a-1, NTS, Radioactive Waste Program: U.S. Geological Survey Open-File Report 80-941, 32 p.

Hall, R.B., 1978, World nonbauxite aluminum resources--Alunite: U.S. Geological Survey Professional Paper 1076-A, 35 p.

Hamilton, W. B., 1988, Detachment faulting in the Death Valley region, California and Nevada, *in* Carr, M. D., and Yount, J. C., eds., Geologic and hydrologic investigations of a potential nuclear waste disposal site at Yucca Mountain, southern Nevada: U.S. Geol. Survey Bull. 1790, p. 51-86.

Hausback, B. P., and Frizzell, V. A. Jr., 1987, Late Miocene syntectonic volcanism of the Stonewall Flat Tuff, Nye County, Nevada [abs.]: Geological Society of America Abst. with Programs, v. 19, p. 696.

Hausback, B.P., Deino, A.L., Turrin, B.T., McKee, E.H., Frizzell, V.A., Noble, D.C., and Weiss, S.I., 1990, New $^{40}Ar/^{39}Ar$ ages for the Spearhead and Civet Cat Canyon Members of the Stonewall Flat Tuff, Nye County, Nevada: Evidence for systematic errors in standard K-Ar age determinations on sanidine: Isochron/West, No. 56, p. 3-7.

Harris, R.N., and Oliver, H.W., 1986, Structural implications of an isostatic residual gravity map of the Nevada Test Site, Nevada: EOS (American Geophysical Union Transactions), v. 67, p. 1262.

Heald, P., Foley, N.K., and Hayba, D.O., 1987, Comparative anatomy of volcanic-hosted epithermal deposits: acid-sulfate and adularia-sericite types: Economic Geology, v. 82, no. 1, p. 1-26.

Heikes, V.C., 1931, Gold, silver, copper, lead and zinc in Nevada--Mine report, in Mineral Resources of the U.S., 1928: U.S. Department of commerce, Bureau of Mines, pt. 1, p. 441-478.

Hildreth, E. W., 1977, The magma chamber of the Bishop Tuff: Gradients in temperature, pressure and composition: unpublished PhD dissertation, Univ. California-Berkely, 328 p.

Hill, J.M., 1912, The mining districts of the western U.S.: U.S. Geological Survey Bulletin 507, 309 p.

Hitchborn, A. D., Arbonies, D. G., Peters, S. G., McKee, E. H., Noble, D. C., Larson, L. T., and Beebe, J. S. (in preparation), Geology and gold deposits of the Bald Mountain mining district, White Pine County, Nevada: Geological Society of Nevada 1995 Symposium Volume, Geology and Ore Deposits of the American Cordillera.

Holmes, G.H., Jr., 1965, Mercury in Nevada, in Mercury potential of the United States: U.S. Bureau of Mines I.C., 8252, p. 215-300.

Hoover, D.L., Eckel, E.B., and Ohl, J.P., 1978, Potential sites for a spent unreprocessed fuel facility (SUREF), southwest part of the NTS: U.S. Geological Survey Open-File Report 78-269, 18 p.

Hoover, D. B., Chornack, M. P., Nervick, K. H., and Broker, M. M., 1982, Electrical studies at the proposed Wahmonie and Calico Hills Nuclear Waste Sites, Nye County, Nevada: U.S. Geol. Survey Open-File Rept. 82-466, 45 p.

Hudson, M. R., 1992, Paleomagnetic data bearing on the origin of arcuate structures in the Frenchman Peak - Massachusetts Mountain area of southern Nevada: Bull. Geol. Soc. Am., v. 104, p. 581-594.

Ilchik, R. P., 1995, $^{40}Ar/^{39}Ar$, K/Ar, and fission-track geochronology of sediment-hosted disseminated gold deposits at Post-Betze, Carlin trend, northeastern Nevada--A discussion: Economic Geology, v. 90, p. 208-209.

Ingamells, C. O., 1970, Lithium-metaborate flux in silicate analysis: Analytica Chimica Acta, v. 52, p. 323-334.

Jackson, M. J., 1988, The Timber Mountain magmato-thermal event: an intense widespread culmination of magmatic and hydrothermal activity at the southwestern Nevada volcanic field: University of Nevada, Reno - Mackay School of Mines, Reno, Nevada, unpublished MSc Thesis.

Jackson, M.R., Noble, D.C., Weiss, S.I., Larson, L.T., and McKee, E.H., 1988, Timber Mountain magmato-thermal event: an intense widespread culmination of magmatic and hydrothermal activity at the SW Nevada volcanic field, Geol. Soc. Am. Abstr. Programs, v. 20, p. 171.

Jorgensen, D. K., Rankin, J. W., and Wilkins, J., Jr., 1989, The geology, alteration and mineralogy of the Bullfrog gold deposit, Nye County, Nevada: Soc. Mining Eng. Preprint 89-135, 13 p.

Kane, M.F., and Bracken, R.E., 1983, Aeromagnetic map of Yucca Mountain and surrounding regions, southwest Nevada: U.S. Geological Survey Open-File Report 83-616, 19 p.

Kane, M.F., Webring, M.W., and Bhattacharyya, B.K., 1981, A preliminary analysis of gravity and aeromagnetic surveys of the Timber Mountain areas, southern Nevada: U.S. Geological Survey Open-File Report 81-189, 40 p.

Keith, J. D., Dallmeyer, R. D., Kim, Choon-Sik, and Kowallis, B. J., 1991, The volcanic history and magmatic sulfide mineralogy of latites of the central East Tintic Mountains, Utah: *in* Raines, G. L., Lisle,R. E., Shafer, R. W., and Wilkinson, W. W., eds., Geology and ore deposits of the Great Basin: Symposium Proceedings, Geol. Soc. of Nevada, p. 461-483.

Kistler, R.W., 1968, Potassium-argon ages of volcanic rocks on Nye and Esmeralda Counties, Nevada: Geological Society of America Memoir 110, P. 251-263.

Knopf, A., 1915, Some cinnabar deposits in western Nevada: U.S. Geological Survey Bulletin 620-D, p. 59-68.

Kral, V.E., 1951, Mineral resources of Nye County, Nevada: University of Nevada Bulletin, v. 45, no. 3, Geological and Mining Series 50, 223 p.

Kuehn, C. A., and Rose, A. W., 1995, Carlin gold deposits, Nevada: origin in a deep zone of mixing between normally pressured and overpressured fluids: Economic Geology, v. 90, p. 17-36.

Kullerude, G., and Yoder, H.S., 1959, Pyrite stability relations in the Fe-S sytem: Economic Geology, v. 54, p. 533-572.

Lahoud, R.G., Lobmeyer, D.H. and Whitfield, M.S., 1984, Geohydrology of volcanic tuff penetrated by test well UE-25b#1, Yucca Mountain, Nye County, Nevada: U.S. Geological Survey Water-Resources Investigations 84-4253, 49 p.

Larson, L. T., Noble, D. C., and Weiss, S. I., 1988, Task 3 report for January, 1987 - June, 1988: Volcanic geology and evaluation of potential mineral and hydrocarbon resources of the Yucca Mountain area: unpublished report to the Nevada Nuclear Waste Project Office, Carson City, Nevada.

Le Bas, M. J., Le Maitre, R. W., Streckheisen, A., and Zenettin, B., 1986, A chemical classification of volcanic rocks based on the total alkali-silica diagram: Journal of Petrology, v. 27, p. 745-750.

Lincoln, F.C., 1923, Mining districts and mineral resources of Nevada: Reno, Nevada, Nevada Newsletter Publishing Co., Reno, 295 p.

Lipman, P.W., Christiansen, R.L., and O'Connor, J.T., 1966, A compositionally zoned ash-flow sheet in southern Nevada: U.S. Geological Survey Professional Paper 524-F, p. F1-F47.

Lipman, P.W., and McKay, E.J., 1965, Geologic map of the Topopah Spring SW quadrangle, Nevada: U.S. Geological Survey Geologic Quadrangle Map GQ-439, 1:24,000 scale.

Lipman, P.W., Quinlivan, W.D., Carr, W.J., and Anderson, R.E., 1966, Geologic map of the Thirsty Canyon SE quadrangle, Nye County, Nevada: U.S. Geological Survey Geologic Quadrangle Map GQ-489, 1:24,000 scale.

Lobmeyer, D.H., Whitfield, M.S., Lahoud, R.G., and Bruckheimer, L., 1983, Geohydrologic data for test well UE-25bH, Nevada Test Site, Nye County, Nevada: U.S. Geological Survey Open-File Report 83-855, 54 p.

Luedke, R.G., and Smith, R.L., 1981, Map showing distribution, composition, and age of late Cenozoic volcanic centers in California and Nevada: U.S. Geological Survey Miscellaneous Investigation Series, I-1091-C, 2 sheets.

Maldonado, F., 1985, Late Tertiary detachment faults in the Bullfrog Hills, southwestern Nevada: Geol. Soc. Am. Abstr. Programs, 17, p. 651.

Maldonado, F., 1988, Geometry of normal faults in the upper plate of a detachment fault zone, Bullfrog Hills, southern Nevada: Geological Society of America, Abstracts with Programs, v. 20, P. 178.

Maldonado, F, 1990, Structural geology of the upper plate of the Bullfrog Hills detachment fault system, southern Nevada: Geological Society of America Bulletin, v. 102, p. 992-1006.

Maldonado, F, and Hausback, B.P., 1990, Geologic map of the northeastern quarter of the Bullfrog 15-minute quadrangle, Nye County, Nevada: U.S. Geological Survey Misc. Investigations Series Map I-2049, 1:24,000.

Maldonado, F, and Koether, S.L., 1983, Stratigraphy, structure, and some petrographic features of Tertiary volcanic rocks at the USW G-2 drill hole, Yucca Mountain, Nye County, Nevada: U.S. Geological Survey Open-File Report 83-732, 83 p.

Maldonado, F, Muller, D.C., and Morrison, J.N., 1979, Preliminary geologic and geophysical data of the UE25a-3 exploratory drill hole, Nevada Test Site, Nevada: U.S. Geological Survey Report, USGS-1543-6, 47 p.; available only from U.S. Department of Commerce, National Technical Information Service, Springfield, VA 22161.

Maldonado, Florian, Muller, D.C., and Morrison, J.N., 1979, Preliminary geologic and geophysical data of the UE25a-3 exploratory drill hole, Nevada Test Site, Nevada: U.S. Geological Survey Open-File Report 81-522.

Mapa, M.R., 1990 Geology and mineralization of the Mother Lode mine, Nye County, Nevada, *in* Hillmeyer, F., Wolverson, N., and Drobeck, P., 1990 spring fieldtrip guidebook, Volcanic-hosted gold deposits and structural setting of the Mohave region: Reno, Geol. Soc. Nevada, 4 p.

Marti, J., Diez-Gil, J. L., and Ortiz, R., 1991, Conduction model for the thermal influence of lithic clasts in mixtures of hot gases and ejecta: Journal of Geophysical Research, v. 96, p. 21,879-21,885.

Marvin, R.F., Byers, F.M., Mehnert, H.H., Orkild, P.P, and Stern, T.W., 1970, Radiometric ages and stratigraphic sequence of volcanic and plutonic rocks, southern Nye and western Lincoln Counties, Nevada: Geological Society of America Bulletin, v. 81, p. 2657-2676.

Marvin, R. F., and Cole, J. C., 1978, Radiometric ages: Compilation A, U.S. Geological Survey: Isochron/West, no. 22, p. 3-14.

Marvin, R. F., Mehnert, H. H., and Naeser, C. W., 1989, U.S. Geologic Survey radiometric ages - compilation "C", part 3: California and Nevada: Isochron/West, no. 52, p. 3-11.

Matsuhisa, Y., and Aoki, M., 1994, Temperature and oxygen isotope variations during formation of the Hishikari epithermal gold-silver veins, southern Kyushu, Japan: Economic Geology, v. 89, p. 1608-1613.

McDougall, I., and Harris, T. M., 1988, Geochronology and thermochronology by the $^{40}Ar/^{39}Ar$ method: New York, Oxford University Press, 212 p.

McKague, H.L. and Orkild, P.P., 1984, Geologic Framework of the Nevada Test Site: Geological Society of America, Abstracts with Programs, v. 16, p. 589.

McKay, E.J., 1963, Hydrothermal alteration in the Calico Hills, Jackass Flats quadrangle, Nevada Test Site: U.S. Geological Survey Technical Letter NTS-43, 6 p.

McKay, E.J., and Sargent, K.A., 1970, Geologic map of the Lathrop Wells quadrangle, Nye County, Nevada: U.S. Geological Survey Geologic Quadrangle Map GQ-883, 1:24,000 scale.

McKay, E.J., and Williams, W.P., 1964, Geology of Jackass Flats quadrangle, Nevada Test Site, Nevada: U.S. Geological Survey Geologic Quadrangle Map GQ-368, 1:24,000 scale.

McKee, E.H., 1983, Reset K-Ar ages: evidence for three metamorphic core complexes, western Nevada: Isocron/West, no.38, p 17-20.

McKee, E. H., and Bergquist, J. M., 1993, New radiometric ages related to alteration and mineraliztion in the vicinity of Yucca Mountain, Nye County, Nevada: U. S. Geological Survey Open-file Report 93-538, 26 pp.

McKee, E. H., Noble, D. C., and Weiss, S. I., 1989, Very young silicic volcanism in the southwestern Great Basin: The late Pliocene Mount Jackson dome field, SE Esmeralda County, Nevada: EOS, Trans. Am. Geophys. Union., v. 70, p. 1420.

McKee, E. H., Noble, D. C., and Weiss, S. I., 1990, Late Neogene volcanism and tectonism in the Goldfield segment of the Walker Lane belt: Geological Society of America Abstracts with Programs, v. 22, p. 66.

Miller, D.C. and Kibler, J.E., 1984, Preliminary analysis of geological logs from drill hole UE-25p#1, Yucca Mountain, Nye County, Nevada: U.S. Geological Survey Open-File Report 84-649, 17 p.

Mills, J.G., Jr., and Rose, T.P., 1986, Geochemistry of glassy pumices from the Timber Mountain Tuff, southwestern Nevada: EOS (American Geophysical Union Transactions), v. 67, p. 1262.

Monsen, S.A., Carr, M.D., Reheis, M.C., and Orkild, P.P., 1990, Geologic map of Bare Mountain, Nye County Nevada: U.S. Geological Survey Open-file Report 90-25, 1:24,000.

Monsen, S.A., Carr, M.D., Reheis, M.C., and Orkild, P.P., 1992, Geologic map of Bare Mountain, Nye County Nevada: U.S. Geological Survey Miscellaneous Investigations Map I-2201, 1:24,000.

Morton, J. L., Silberman, M. L., Bonham, H. F., Garside, L. J., and Noble, D. C., 1977, K-Ar ages of volcanic rocks, plutonic rocks, and ore deposits in Nevada and eastern California - Determinations run under the USGS-NBMG cooperative program: Isochron/West, n. 20, p. 19-29.

Noble, D. C., and Christiansen, R. L., 1974, Black Mountain volcanic center, in Guidebook to the geology of four Tertiary volcanic centers in central Nevada: Nevada Bur. Mines Geol. Rept. 19, p. 22-26.

Noble, D. C., McKee, E. H., and Weiss, S. I., 1988, Nature and timing of pyroclastic and hydrothermal activity and mineralization at the Stonewall Mountain volcanic center, southwestern Nevada: Isochron/West, No. 51, p. 25-28.

Noble, D. C., Weiss, S. I., and Green, S. M., 1989, High-salinity fluid inclusions suggest that Miocene gold deposits of the Bare Mtn. district, NV, are related to a large buried rare-metal rich magmatic system: Geological Society of America Abs. with Programs, v. 21, p. 123.

Noble, D. C., Weiss, S. I., and McKee, E. H., 1990a, Style, timing, distribution, and direction of Neogene extension within and adjacent to the Goldfield section of the Walker Lane structural belt: EOS, Trans. American Geophysical Union, v. 71, p. 618-619.

Noble, D. C., Weiss, S. I., and McKee, E. H., 1990b, Magmatic and hydrothermal activity, caldera geology and regional extension in the western part of the southwestern Nevada volcanic field: Great Basin Symposium, Program with Abstracts, Geology and ore deposits of the Great Basin, Geol. Soc. of Nevada, Reno, p. 77.

Noble, D. C., Weiss, S. I., and McKee, E. H., 1991a, Magmatic and hydrothermal activity, caldera geology, and regional extension in the western part of the southwestern Nevada volcanic field: *in* Raines, G. L., Lisle,R. E., Shafer, R. W., and Wilkinson, W. W., eds., Geology and ore deposits of the Great Basin: Symposium Proceedings, Geol. Soc. of Nevada, p. 913-934.

Noble, D. C., Worthington, J. E., and McKee, E. H., 1991b, Geologic and tectonic setting and Miocene volcanic stratigraphy of the Gold Mountain-Slate Ridge area, southwestern Nevada: Geol. Soc. America Abstr. with Prog., v. 23, p. A247.

Noble, D. C., Sargent, K. A., Ekren, E. B., Mehnert, H. H., and Byers, F. M., Jr., 1968, Silent Canyon volcanic center, Nye County, Nevada: Geological Society of America Spec. Paper 101, p. 412-413.

Noble, D.C., Vogel, T. A., Weiss, S.I., Erwin, J.W., McKee, E.H., and Younker, L.W., 1984, Stratigraphic relations and source areas of ash-flow sheets of the Black Mountain and Stonewall Mountain volcanic centers, Nevada: Journal of Geophysical Research, v. 89, p. 8593-8602.

Norberg, J.R., 1977, Mineral Resources in the vicinity of the Nellis Air Force Base and the Nellis Bombing and Gunnery Range, Clark, Lincoln, and Nye Counties, Nevada: U.S. Bureau of Mines Unpublished Report, 112 p.

Northern Miner, 1994, Rayrock study finds Secret Pass deposit viable: November 7, 1994, p. 3.

Orkild, P.P., 1968, Geologic map of the Mine Mountain quadrangle, Nye County, Nevada: U.S. Geological Survey Geologic Quadrangle Map GQ-746, 1:24,000 scale.

Orkild, P.P., and O'Connor, J.T., 1970, Geologic map of the Topopah Springs quadrangle, Nye County, Nevada: U.S. Geological Geologic Quadrangle Map GQ-849, 1:24,000 scale.

Odt, D. A., 1983, Geology and geochemistry of the Sterling gold deposit, Nye County, Nevada: Unpub. M.S. thesis, Univ. Nevada-Reno, 91 p.

Papike, J. J., Keith, T. E. C., Spilde, M. N., Galbreath, K. C., Shearer, C. K., and Laul, J. C., 1991, Geochemistry and mineralogy of fumarolic deposits, Valley of Ten Thousand Smokes, Alaska: bulk chemical and mineralogical evolution of dacite-rich protolith: American Mineralogist, v. 76, p. 1662-1673.

Papke, K.G., 1979, Fluorspar in Nevada: Nevada Bureau of Mines and Geology, Bulletin 93, 77 p.

Ponce, D.A., 1981, Preliminary gravity investigations of the Wahmonie site, Nevada Test Site, Nye County, Nevada: U.S. Geological Survey Open-File Report 81-522, 64 p.

Ponce, D.A., 1984, Gravity and magnetic evidence for a granitic intrusion near Wahmonie site, Nevada Test Site, Nevada, Journal of Geophysical Research, v. 89, p. 9401-9413.

Ponce, D.A., Wu, S.S. and Speilman, J.B., 1985, Comparison of survey and photogrammetry methods to positive gravity data, Yucca Mountain, Nevada: U.S. Geological Survey Open-File Report 85-36, 11 p.

Poole, F.G., 1965, Geologic map of the Frenchman Flat quadrangle, Nye, Lincoln, and Clark Counties, Nevada: U.S. Geological Survey Geological Quadrangle Map GQ-456, 1:24,000 scale.

Poole, F.G., Carr, W.J., and Elston, D.P., 1965, Salyer and Wahmonie Formations of south-eastern Nye County, Nevada: U.S. Geological Survey Bulletin 1224-A, p. A44-A51.

Poole, F.G., Elston, D.P., and Carr, W.J., 1965, Geologic map of the Cane Spring quadrangle, Nye County, Nevada: U.S. Geological Survey Geological Quadrangle Map GQ-455, 1:24,000 scale.

Powers, P.S. and Healey, D.L., 1985, Free-air gradient observations in Yucca Flat, Nye County, Nevada: U.S. Geological Survey Open-File Report 85-530, 18 p.

Quade, J., and Tingley, J.V., 1983, A mineral inventory of the Nevada Test Site and portions of the Nellis Bombing and Gunnery Range, southern Nye County, Nevada: DOE/NV/10295-1, U.S. Department of Energy, Las Vegas.

Quade, J., and Tingley, J.V., 1984, A mineral inventory of the Nevada Test Site, and portions of Nellis Bombing and Gunnery Range southern Nye County, Nevada: Nevada Bureau of Mines and Geology Open File Report 82-2, 40 p. plus sample descriptions and chemical analyses.

Quade, J., and Tingley, J.V., 1986a, Mineral inventory and geochemical survey Groom Mountain Range Lincoln County, Nevada: Nevada Bureau of Mines and Geology Open File Report 86-9, 66 p. plus sample descriptions and chemical analyses.

Quade, J., and Tingley, J.V., 1986b, Mineral inventory and geochemical survey appendices F., G., & H Groom Mountain Range, Lincoln County, Nevada: Nevada Bureau of Mines and Geology Open File Report 86-10.

Quinlivan, W.D., and Byers, F.M., Jr., 1977, Chemical data and variation diagrams of igneous rock from the Timber Mountain-Oasis Valley caldera complex, southern Nevada: U.S. Geological Survey Open-File Report 77-724, 9 p.

Ramelli, A. R., Bell, J. W., and dePolo, C. M., Late Quaternary faulting at Crater Flat and Yucca Mountain, southern Nevada: Nevada Bureau of Mines and Geology (in review).

RANDOL, 1993, Randol Mining Directory 1993/1994, U.S. mines and mining companies, Randol International, Ltd., Golden, Colorado, 734 p.

Raney, R. G., and Wetzel, N., Natural resource assessment methodologies for the proposed high-level nuclear waste repository at Yucca Mountain, Nye County, Nevada: U.S. Bureau of Mines report NRC FIN D1018, prepared for the Office of Nuclear Safety and Safeguards, U.S. Nuclear Regulatory Commission, 353 p.

Ransome, F.L., 1907, Preliminary account of Goldfield, Bullfrog, and other mining districts in southern Nevada: U.S. Geological Survey Bulletin 303, 98 p.

Ransome, F.L., Emmons, W.H., and Garrey, G.H., 1910, Geology and ore deposits of the Bullfrog district, Nevada: U.S. Geological Survey Bulletin 407, 130 p.

Reno Gazette-Journal, June 19, 1988, Gold report is favorable: Business page, Gold, J., Business editor.

Rhiele, J. R., 1973, Calculated compaction profiles of rhyolitic ash-flow tuffs: Geological Society of America Bulletin, v. 84, p. 2193-2216.

Richards, J. P., and McDougall, I., 1990, Geochronology of the Porgera gold deposit, Papua New Guinea: resolving the effects of excess argon on K-Ar and $^{40}Ar/^{39}Ar$ age estimates for magmatism and mineralization: Geochimica et Cosmochimica Acta, v. 54, p. 1397-1415.

Robinson, G.D., 1985, Structure of pre-Cenozoic rocks in the vicinity of Yucca Mountain, Nye County, Nevada; a potential nuclear-waste disposal site: U.S. Geological Survey Bulletin 1647, 22 p.

Rowe, J. J., and Simon, F. O., 1968, The determination of gold in geologic materials by neutron-activation analysis using fire assay for the radiochemical separations: U. S. Geological Survey Circular 559, 4 p.

Rush, F.E., Thordason, William, and Bruckheimer, Laura, 1983, Geohydrologic and drill-hole data for test well USW-H1, adjacent to Nevada Test Site, Nye County, Nevada: U.S. Geological Survey Open-File Report 83-141, 38 p.

Sander, M. V., 1988, Epithermal gold-silver mineralization, wall-rock alteration and geochemical evolution of hydrothermal fluids in the ash-flow tuff at Round Mountain, Nevada: Unpublished PhD. dissertation, Stanford University, Stanford, California, 283 p.

Sander, M. V., 1990, The Round Mountain gold-silver deposit, Nye County, Nevada: Geol. Soc. Nevada Symposium, Geology and Ore Deposits of the Great Basin, Field Trip Guidebook # 11, p. 108-121.

Sawyer, D. A., and Sargent, K. A., 1989, Petrologic evolution of divergent peralkaline magmas from the Silent Canyon caldera complex, southwestern Nevada volcanic field: Journal of Geophysical Research, v. 94, p. 6021-6040.

Sawyer, D. A., Fleck, R. J., Lanphere, M. A., Warren, R. G., and Broxton, D. E., 1990, Episodic volcanism in the southwest Nevada volcanic field: new $^{40}Ar/^{39}Ar$ geochronologic results: EOS, Transactions of the American Geophysical Union, v. 71, p. 1296.

Sawyer, D. A., Fleck, R. J., Lanphere, M. A., Warren, R. G., Broxton, D. E., and Hudson, M. R., 1994, Episodic caldera volcanism in the Miocene southwestern Nevada volcanic field: revised stratigraphic framework, $^{40}Ar/^{39}Ar$ geochronology, and implications for magmatism and extension: Geological Society of America Bulletin, *in press*.

Schoen, R., White, D.E., and Hemley, J.J., 1974, Argillization by decending acid at Steamboat Springs, Nevada: Clays and Clay Minerals, v. 22, p. 1-22.

Schneider, R. and Trask, N.J., 1984, U.S. Geological Survey research in radioactive waste disposal; fiscal year 1982: U.S. Geological Survey Water-Resource Investigation 84-4205, 116 p.

Schuraytz, B.C., Vogel, T.A., and Younker, L.W., 1986, Evolution of a magmatic system. Part I: Geochemistry and mineralogy of the Topopah Spring Member of the Paintbrush Tuff, southern Nevada: EOS, Transactions of the American Geophysical Union, v. 67, p. 1261.

Scott, R.B., 1984, Internal deformation of blocks bounded by basin-and-range-style faults: Geological Society of America, Abstracts with Programs, v. 16, p. 649.

Scott, R.B., 1986a, Rare-earth element evidence for changes in chemical evolution of silicic magmas, southwest Nevada: Transactions of the American Geophysical Union, v. 67, p. 1261.

Scott, R. B., 1986b, Extensional tectonics at Yucca Mountain, southern Nevada [abs.]: Geological Society of America Abs. with Programs, v. 18, p. 411.

Scott, R.B., 1988, Tectonic setting of Yucca Mountain, southwest Nevada: Geological Society of America, Abstracts with Programs, v. 20, p. 229.

Scott, R.B. and Bonk, J., 1984, Preliminary geologic map of Yucca Mountain, Nye County, Nevada, with geologic sections: U.S. Geological Survey Open-File Report 84-494, scale 1:12,000, plus 10 p.

Scott, R.B. and Castellanos, Mayra, 1984, Stratigraphic and structural relations of volcanic rocks in drill holes USW GU-3 and USW G3, Yucca Mountain, Nye County, Nevada: U.S. Geological Survey Open-File Report 84-491, 121 p.

Scott, R. B., and Whitney, J. W., 1987, The upper crustal detachment system at Yucca Mountain, SW Nevada [abs.]: Geological Society of America Abs. with Programs, v. 19, p. 332-333.

Scott, R.B., Byers, F.M. and Warren, R.G., 1984, Evolution of magma below clustered calderas, Southwest Nevada volcanic field [abstr.], EOS, Transactions of the American Geophysical Union, v.65, p. 1126-1127.

Scott, R.B., Spengler, R.W., Lappin, A.R., and Chornack, M.P., 1982, Structure and intra-cooling unit zonation in welded tuffs of the unsaturated zone, Yucca Mountain, Nevada, a potential nuclear waste repository: EOS, Transactions of the American Geophysical Union, v. 63, no. 18, p. 330.

Scott, R.B., Spengler, R.W., Diehl, S., Lappin, A.R., and Chornack, M.P., 1983, Geologic character of tuffs in the unsaturated zone at Yucca Mountain, southern Nevada: in Mercer,

J.M., Rao, P.C. and Marine, W., eds., Role of the unsaturated zone in radioactive and hazardous waste disposal: Ann Arbor press, Ann Arbor, Michigan, p. 289-335.

Scott, R.B., Bath, G.D., Flanigan, V.J., Hoover, D.B., Rosenbaum, J.G., and Spengler, R.W., 1984, Geological and geophysical evidence of structures in northwest-trending washes, Yucca Mountain, southern Nevada, and their possible significance to a nuclear waste repository in the unsaturated zone: U.S. Geological Survey Open-File Report 84-567, 25 p.

Selner, G.I. and Taylor, R.B., 1988, GSDRAW and GSMAP version 5.0: prototype programs, level 5, for the IBM PC and compatible microcomputers, to assist compilation and publication of geologic maps and illustrations: U.S. Geological Survey Open File Report #88-295A (documentation), 130 p. and #88-295B (executable program disks).

Selner, G.I., Smith, C.L., and Taylor, R.B., 1988, GSDIG: a program to determine latitude/longitude locations using a microcomputer (IBM PC or compatible) and digitizer: U.S. Geological Survey Open File Report #88-014A (documentation) 16 p. and #88-014B (executable program disk).

Smith, C., Ross, H.P., and Edquist, R., 1981, Interpreted resistivity and IP section line W1 Wahmonie area, Nevada Test Site, Nevada: U.S. Geological Survey Open-File Report 81-1350, 14 p.

Smith, R.C., and Bailey, R.A., 1968, Resurgent Cauldrons: Geological Society of America Memoir 116, p. 613-662.

Smith, R.M., 1977, Map showing mineral exploration potential in the Death Valley quadrangle, California and Nevada: U.S. Geological Survey Miscellaneous Field Investigation Map MF-873, 1:250,000 scale.

Snyder, D.B., and Oliver, H.W., 1981, Preliminary results of gravity investigations of the Calico Hills, Nevada Test Site, Nye County, Nevada: U.S. Geological Survey Open-File Report 81-101, 42 p.

Snyder, D.B., and Carr, W.J., 1982, Preliminary results of gravity investigations at Yucca Mountain and vicinity, southern Nye County, Nevada: U.S. Geological Survey Open-File Report 82-701, 36 p.

Snyder, D.B. and Carr, W.J., 1984, Interpretation of gravity data in a complex volcano-tectonic setting, southwestern Nevada: Journal of Geophysical Research. B, v. 89, p. 10,193-10,206.

Spengler, R.W., Byers, F.M., Jr., and Warner, J.B., 1981, Stratigraphy and structure of volcanic rocks in drill hole USW-G1, Yucca Mountain, Nye County, Nevada: U.S. Geological Survey Open-File Report 82-1338, 264 p.

Spengler, R.W. and Chornack, M.P., 1984, Stratigraphic and structural characteristics of volcanic rocks in core hole USW G-4, Yucca Mountain, Nye County, Nevada: U.S. Geological Survey Open-File Report 84-789, 82 p.

Spengler, R.W., Muller, D.C., and Livermore, R.B., 1979, Preliminary report on the geology of drill hole UE25a-1, Yucca Mountain, Nevada Test Site: U.S. Geological Survey Open-File Report 79-1244, 43 p.

Spengler, R.W., and Rosenbaum, J.G., 1980, Preliminary interpretations of geologic results obtained from boreholes UE25a-4, -5, -6, and -7, Yucca Mountain, Nevada Test Site: U.S. Geological Survey Open-File Report 80-929, 35 p.

Spengler, R.W., and Rosenbaum, J.G., 1991, A low-angle breccia zone of hydrologic significance at Yucca Mountain, Nevada: Geological Society of America, Abstracts with Programs, v. 23, p. A119.

Stewart, J. H., 1988, Tectonics of the Walker Lane belt, western Great Basin-Mesozoic and Cenozoic deformation in a zone of shear, *in* Ernst, W. G., ed., Metamorphism and crustal evolution of the western United States, Rubey Vol. VII: Englewood Cliffs, New Jersey, Prentice Hall, p. 683-713.

Stuckless, J. S., Peterman, Z. E. and Muhs, D. R., 1991, U and Sr isotopes in groundwater and calcite, Yucca Mountain, Nevada: evidence against upwelling water: Science, v. 254, p. 551-554.

Sutton, V.D., 1984, Data report for the 1983 seismic-refraction experiment at Yucca Mountain, Beatty, and vicinity, southwestern Nevada: U.S. Geological Survey Open-File Report 84-661, 62 p.

Swadley, W.C., Hoover, D.L. and Rosholt, J.N., 1984, Preliminary report on late Cenozoic faulting and stratigraphy in the vicinity of Yucca Mountain, Nye County, Nevada: U.S. Geological Survey Open-File Report 84-788, 44 p.

Swolfs, H.S. and Savage, W.Z., 1985, Topography, stresses and stability at Yucca Mountain, Nevada, Proceedings - Symposium on Rock Mechanics: Research and engineering applications in rock masses, 26, p. 1121-1129.

Szabo, B.J. and Kyser, T.K., 1985, Uranium, thorium isotopic analyses and uranium-series ages of calcite and opal, and stable isotopic compositions of calcite from drill cores UE25a 1, USW G-2 and USW G-3/GU-3, Yucca Mountain, Nevada: U.S. Geological Survey Open-File 85-224, 30 p.

Szabo, B. J., and Kyser, T. K., 1990, Ages and stable-isotope compositions of secondary calcite and opal in drill cores from Tertiary volcanic rocks of the Yucca Mountain area, Nevada: Geological Society of America Bulletin, v. 102, p. 1714-1719.

Szabo, B.J. and O'Malley, P.A., 1985, Uranium-series dating of secondary carbonate and silica precipitates relating to fault movements in the Nevada Test Site region and of caliche and travertine samples from the Amargosa Desert: U.S. Geological Survey Open-File Report 85-0047, 17 p.

Taylor, E.M., and Huckins, H.E., 1986, Carbonate and opaline silica fault-filling in the Bow Ridge Fault, Yucca Mountain, Nevada -- deposition from pedogenic processes of upwelling ground water: Geological Society of America, Abstracts with Programs, v. 18, no. 5, p. 418.

Thordarson, William, Rush, F.E. , Spengler, R.W. and Waddell, S.J., 1984, Geohydrologic and drill-hole data for test well USW H-3, Yucca Mountain, Nye County, Nevada: U.S. Geological Survey Open-File Report 84-0149, 54 p.

Tingley, J.V., 1984, Trace element associations in mineral deposits, Bare Mountain (Fluorine) mining district, southern Nye County, Nevada: Nevada Bureau of Mines and Geology Report 39, 28 p.

Turrin, B. D., Champion, D., and Fleck, R. J., 1991, $^{40}Ar/^{39}Ar$ age of the Lathrop Wells volcanic center, Yucca Mountain Nevada: Science, v. 253, p. 654-657.

U.S. Department of Energy, 1986, Environmental Assessment Yucca Mountain Site, Nevada Research and Development Area, Nevada, v. 1: Washington, DC, Office of Civilian Radioactive Waste Management.

U.S. Department of Energy, 1988a, Consultation Draft Site Characterization Plan, Yucca Mountain Site, Nevada Research and Development Area, Nevada: Washington, DC,Office of Civilian Radioactive Waste Management, 347 p.

U.S. Department of Energy, 1988b, Site Characterization Plan, Yucca Mountain Site, Nevada Research and Development Area, Nevada: Washington, DC,Office of Civilian Radioactive Waste Management.

U.S. Geologic Survey, 1984, A summary of geologic studies through January 1, 1983 of a potential high-level radioactive waste repository site at Yucca Mountain, southern Nye County, Nevada: U.S. Geological Survey Open-File Report 84-792, 164 p.

Vaniman, D. T., 1991, Calcite, opal, sepiolite, ooids, pellets, and plant/fungal traces in laminar-fabric fault fillings at Yucca Mountain Nevada: Geological Society of America, Abstracts with Programs, v. 23, p. 117.

Vaniman, D.T., and Crowe, B.M., 1981, Geology and petrology of the basalts of Crater Flat: Applications to volcanic risk assessment for the Nevada nuclear waste storage investigations: Los Alamos, New Mexico, Los Alamos National Laboratory Report, LA-8845-MS, 67 p.

Vaniman, D.T., Crowe, B.M., and Gladney, E.S., 1982, Petrology and geochemistry of Hawaiite lavas from Crater Flat, Nevada: Contributions to Mineralogy and Petrology, v. 80, p. 341-357.

Vaniman, D.T., Bish, D.L., and Chipera, S., 1988, A preliminary comparison of mineral deposits in faults near Yucca Mountain, Nevada, with possible analogs: Los Alamos, New Mexico, Los Alamos National Laboratory Report LA-11298-MS, UC-70, 54 p.

Vaniman, D.T., Bish, D., Broxton, D., Byers, F., Heiken, G., Carlos, B., Semarge, E., Caporuscio, F., and Gooley, R., 1984, Variations in authigenic mineralogy and sorptive zeolite abundance at Yucca Mountain, Nevada, based on studies of drill cores USW GU-3 and G-3.

Vogel, T. A., Noble, D. C., and Younker, L. W., 1989, Evolution of a chemically zoned magma body: Black Mountain volcanic center, southwestern Nevada: Journal of Geophysical Research, v. 94, p. 6041-6058.

Vogel, T.A., Ryerson, R.A., Noble, D.C., and Younker, L.W., 1987, Constrains on magma mixing in a silicic magma body: disequilibrium phenocrysts in pumices from a chemically zoned ash-flow sheet: Journal of Geology, v. 95, in press.

Waddell, R.J., 1984, Geohydrologic and drill-hole data for test wells UE-29a#1 and UE-29a#2, Fortymile Canyon, Nevada Test Site: U.S. Geological Survey Open-File Report 84-0142, 25 p.

Wang, J.S.Y., and Narasimhan, T.N., 1985, Hydrologic mechanisms governing fluid flow in partially saturated, fractured, porous tuff at Yucca Mountain: University of California Lawrence Berkeley Laboratory Report SAND84-7202 (LBL-18473), 46 p.

Warren, R.G., and Broxton, D.E., 1986, Mixing of silcic and basaltic magmas in the Wahmonie Formation, southwestern Nevada volcanic field, Nevada: EOS (American Geophysical Union Transactions), v. 67, p. 1261.

Warren, R.G., Byers, F.M., and Caporuscio, F.A., 1984, Petrography and mineral chemistry of units of the Topopah Springs, Calico Hills and Crater Flat Tuffs, and some older volcanic units, with emphasis on samples from drill hole USW G-1, Yucca Mountain, Nevada Test site: Los Alamos, New Mexico, Los alamos National Laboratory Report LA-10003-MS.

Warren, R.G., Nealey, L.D., Byers, F.M., Jr., and Freeman, S.H., 1986, Magmatic components of the Rainier Mesa Member of the Timber Mountain Tuff, Timber Mountain-Oasis Valley Caldera Complex: EOS (American Geophysical Union Transactions), v. 67, p. 1260.

Warren, R. G., Byers, F. M., Jr., Broxton, D. E., Freeman, S. H., and Hagan, R. C., 1989, Phenocryst abundances and glass and phenocryst compositions as indicators of magmatic environments of large-volume ash flow sheets in southwestern Nevada: Journal of Geophysical Research, v. 94, p. 5987-6020.

Warren, R.G., McDowell, F.W., Byers, F.M., Broxton, D.E., Carr, W.J., and Orkild, P.P., 1988, Eposodic leaks from Timber Mountain caldera: new evidence from rhyolite lavas of Fortymile Canyon, southwestern Nevada Volcanic Field: Geological Society of America, Abstracts with Programs, v. 20, p. 241.

Weiss, S.I., 1987, Geologic and Paleomagnetic studies of the Stonewall and Black Mountain volcanic centers, southern Nevada: University of Nevada, Reno-Mackay School of Mines, Reno, Nevada, unpublished MSc Thesis, 67 p.

Weiss, S.I., and Noble, D.C., 1989, Stonewall Mountain volcanic center, southern Nevada: stratigraphic, structural and facies relations of outflow sheets, near-vent tuffs, and intra-caldera units: Journal of Geophysical Research, v. 94, 6059-6074.

Weiss, S.I., Noble, D.C., and Mckee, E.H.,1984, Inclusions of basaltic magma in near-vent facies of the Stonewall Flat Tuff: product of explosive magma mixing: Geological Society of America, Abstracts with Programs, v. 16, p. 689.

Weiss, S. I., Noble, D. C., and McKee, E. H., 1988, Volcanic and tectonic significance of the presence of late Miocene Stonewall Flat Tuff in the vicinity of Beatty, Nevada: Geological Society of America Abs. with Programs, v. 20, p. A399.

Weiss, S. I., Noble, D. C., and McKee, E. H., 1989, Paleomagnetic and cooling constraints on the duration of the Pahute Mesa-Trail Ridge eruptive event and associated magmatic evolution, Black Mountain volcanic center, southwestern Nevada: Journal of Geophysical Research, v. 94, p. 6075-6084.

Weiss, S. I., Noble, D. C., and Larson, L. T., 1989, Task 3: Evaluation of mineral resource potential, caldera geology and volcano-tectonic framework at and near Yucca Mountain; report for July, 1988 - September, 1989: Center for Neotectonic Studies, University of Nevad-Reno, 38 p. plus appendices.

Weiss, S. I., Noble, D. C., and Larson, L. T., 1990, Task 3: Evaluation of mineral resource potential, caldera geology and volcano-tectonic framework at and near Yucca Mountain; report for October, 1989 - September, 1990: Center for Neotectonic Studies, University of Nevad-Reno, 29 p. plus appendices.

Weiss, S. I., Noble, D. C., and Larson, L. T., 1991a, Task 3: Evaluation of mineral resource potential, caldera geology and volcano-tectonic framework at and near Yucca Mountain; report for October, 1990 - September, 1991: Center for Neotectonic Studies, University of Nevad-Reno, 37 p. plus appendices.

Weiss, S. I., Noble, D. C., and Larson, L. T., 1992, Task 3: Evaluation of mineral resource potential, caldera geology and volcano-tectonic framework at and near Yucca Mountain; report for October, 1991 - September, 1992: Center for Neotectonic Studies, University of Nevad-Reno, 44 p. plus appendices.

Weiss, S. I., Noble, D. C., and Larson, L. T., 1993a, Task 3: Evaluation of mineral resource potential, caldera geology and volcano-tectonic framework at and near Yucca Mountain; report for October, 1992 - September, 1993: Center for Neotectonic Studies, University of Nevad-Reno, 41 p. plus appendices.

Weiss, S. I., Ristorcelli, S. J., and Noble, D. C., 1993b, Mother Lode gold deposit, southwestern Nevada: another example of Carlin-type mineralization associated with porphyry magmatism: Geological Society of America Abstracts with Programs, v. 25, p. 161.

Weiss, S. I., Noble, D. C., and Larson, L. T., 1994a, Task 3: Evaluation of mineral resource potential, caldera geology and volcano-tectonic framework at and near Yucca Mountain; report for October, 1993 - September, 1994: Center for Neotectonic Studies, University of Nevad-Reno, 33 p. plus appendices.

Weiss, S. I., Noble, D. C., and Larson, L. T., 1994b, Potential for undiscovered mineral deposits at Yucca Mountain, NV: host rocks, timing and spatial distribution of nearby mineralization [abst]: Geological Society of America Abstracts with Programs, v. 26, p. 311.

Weiss, S. I., Noble, D. C., and Larson, L. T., 1995, Hydrothermal origin and significance of pyrite in ash-flow tuffs at Yucca Mountain, Nevada: Economic Geology (in press).

Weiss, S. I., Connors. K. A., Noble, D. C., and McKee, E. H., 1990, Coeval crustal extension and magmatic activity in the Bullfrog Hills during the latter phases of Timber Mountain volcanism: Geological Society of America Abstracts with Programs, v. 22, p. 92-93.

Weiss, S. I., Noble, D. C., Worthington, J. E., IV., and McKee, E. H., 1993c, Neogene tectonism from the southwestern Nevada volcanic field to the White Mountains, California Part I. Miocene volcanic stratigraphy, paleotopography, extensional faulting and uplift between northern Death Valley and Pahute Mesa: *in* Lahren, M. M., Trexler, J. H., Jr., and Spinosa, C., eds., 1993, Crustal Evolution of the Great Basin and Sierra Nevada: Cordilleran/Rocky Mountain Section, Geological Society of America Guidebook, Department of Geological Sciences, University of Nevada, Reno, p. 353-369.

Weiss, S. I., McKee, E. H., Noble, D. C., Connors, K. A., and Jackson, M. R., 1991b, Multiple episodes of Au-Ag mineralization in the Bullfrog Hills, SW Nevada, and their relation to coeval extension and volcanism: Geological Society of America Abstracts with Programs, v. 23, p. A246.

Weiss, S. I., Noble, D. C., Connors, K. A., Jackson, M. R., and McKee, E. H., 1996, Multiple episodes of hydrothermal activity and epithermal mineralization in the southwestern Nevada volcanic field and their relations to magmatic activity, volcanism and regional extension: (in revision following peer-review by Economic Geology).

Wernicke, B. P., Christiansen, R. L., England, P. C., and Sonder, L. J., 1987, Tectonomagmatic evolution of Cenozoic extension of the North America Cordillera, *in* Coward, M. P., Dewey, J. F., and Hancock, P. L., eds., Continental extensional tectonics: Geol. Soc. London Spec. Pub. 28, p. 203-222.

White, A.F., 1979, Geochemistry of ground water associated with tuffaceous rocks, Oasis valley, Nevada: U.S. Geological Survey Professional Paper 712-E.

Whitney, J. A., and Stormer, J. C., Jr., 1983, Igneous sulfides in the Fish Canyon Tuff and the role of sulfur in calc-alkaline magmas: Geology, v. 11., p. 99-102.

Whitfield, M.S., Eshom, E.P., Thordarson, W., and Schaefer, D.H., 1985, Geohydrology of rocks penetrated in test well USW H-4, Yucca Mountain, Nye County, Nevada: U.S. Geological Survey Water-Resources Investigations Reports, 1985, 33 p.

Whitfield, M.S., Thordarson, W. and Eshom, E.P., 1984, Geohydrologic and drill-hole data for test well USW H-4, Yucca Mountain, Nye County, Nevada: U.S. Geological Survey

Worthington, J. E., IV., 1992, Neogene structural and volcanic geology of the Gold Mountain - Slate Ridge area, Esmeralda County, Nevada, unpublished MSc. thesis, Univ. Nevada, Reno, 76 p.

Worthington, J. E., IV., Noble, D. C., and Weiss, S. I., 1991, Structural geology and Neogene extensional tectonics of the Gold Mountain-Slate Ridge area, southwestern Nevada: Geol. Soc. America Abstr. with Prog., v. 23, p. A247.

Wu, S.S., 1985, Topographic Maps of Yucca Mountain area, Nye County, Nevada, 6 over-size sheets, scale 1:5,000: U.S. Geological Survey Open-File Report 85-0620.

Zartman, R. E., and Kwak, L. M., 1991, Lead isotopes in the carbonate-silica veins of Trench 14, Yucca Mountain, Nevada: Geological Society of America, Abstracts with Programs, v. 23, p. 117.

Table 1. Radiometric Ages of Dikes and Hydrothermal Minerals, Mother Lode - Telluride Mine Area, Northern Bare Mountain, Nevada

Mother Lode mine

K-Ar Age Determinations

No.	Field number	Mineral dated	Rock type	K_2O wt.%	$^{40}Ar^*$ mole/g	$^{40}Ar^*/^{40}Ar$ (%)	Age ±1σ (Ma)
1	3SW-615	illite-smectite*	porphyry dike ore	7.73	1.3597×10^{-10}	40.69	12.2 ±0.4
2	3SW-617	illite-smectite*	porphyry dike ore	7.76	1.4699×10^{-10}	49.79	13.1 ±0.3
3	3SW-665	illite-smectite*	altered limestone	6.13	2.3860×10^{-10}	48.99	26.9 ±0.6

Porphyry Dike Between the Mother Lode and Telluride mines

$^{40}Ar/^{39}Ar$ Single-grain Laser Fusion Determinations

Grain #	$^{40}Ar^*$ (%)	$^{40}Ar/^{39}Ar$	$^{37}Ar/^{39}Ar$	$^{36}Ar/^{39}Ar$	^{39}K(moles) (x 10^{-15})	K/Ca	Apparent Age (Ma) ±1σ
3SW-653 clear sanidine (-30+70 mesh grains); run 2454 (J = 0.000780169 ±0.000001).							
1	79.8	12.98	0.00585	0.00881	8.5	87.2	14.518 ±0.070
2	65.7	10.13	0.879	0.0119	0.065	0.6	9.348 ±1.297
3	74.8	13.65	0.0207	0.0116	5.6	24.7	14.310 ±0.067
4	83.1	12.34	0.0218	0.00698	8.7	23.4	14.384 ±0.045
5	85.9	11.84	0.0223	0.00557	6.0	22.9	14.262 ±0.054
6	83.1	12.41	0.0196	0.00702	5.4	26.1	14.458 ±0.049
7	85.6	12.07	0.0116	0.00583	4.8	44.0	14.475 ±0.051
8	71.7	14.25	0.0113	0.0136	7.7	45.3	14.326 ±0.062
9	88.8	11.61	0.0327	0.00434	6.1	15.6	14.449 ±0.052
10	78.1	13.11	0	0.00965	7.2	ud	14.351 ±0.053
			Preferred age:		mean (n = 9)		14.393 ±0.087

Table 1, continued:

$^{40}Ar/^{39}Ar$ Incremental-heating Determinations

T(°C)	$^{40}Ar^{*}$ (%)	^{39}Ar (%)	$^{40}Ar/^{39}Ar$	$^{37}Ar/^{39}Ar$	$^{36}Ar/^{39}Ar$ (x 10^{-2})	^{39}K(moles) (x 10^{-15})	K/Ca	Apparent Age (Ma) ±1σ
3SW-653 turbid sanidine (-30+70 mesh); run #2088 (J = 0.0007951 ±0.000001).								
501	-0.2	0.02	2140	1.13	7.24	0.055	0.45	-5.362 ±92.803
601	3.7	0.09	1330	bd	4.33	0.19	ud	69.595 ±21.488
700	9.0	0.65	168	0.0480	0.516	1.5	11.0	21.539 ±1.285
800	21.7	2.70	47.8	0.0647	0.127	5.4	7.9	14.821 ±0.311
900	54.3	7.26	18.3	0.0745	0.0283	12.0	6.8	14.200 ±0.087
1000	65.1	14.84	15.4	0.0367	0.0182	20	14.0	14.363 ±0.061
1100	76.5	24.74	13.0	0.0229	0.0103	26	22.0	14.218 ±0.043
1200	79.4	35.13	12.4	0.0205	0.00862	27	25.0	14.121 ±0.041
1300	65.6	49.63	15.1	0.0277	0.0175	38	18.0	14.140 ±0.056
1400	61.9	75.91	16.3	0.0234	0.0210	69	22.0	14.445 ±0.066
1750	69.1	98.75	14.8	0.0175	0.0154	60	29.0	14.606 ±0.054
1750	72.1	100.00	13.5	0.0252	0.0127	3.3	20.0	13.929 ±0.081
Total gas age					(n = 12)	262.5		14.44 ±0.104
Spectrum age calculated from 900-1750 °C fractions:					(n = 7)			14.28 ±0.07
Isochron age (preferred age)					(n = 7)			14.08 ±0.06

Slope ($^{36}tr/^{39}K$) = -0.03230 ± 0.0003763; Intercept ($^{40/36}tr$) = 305.1 ±2.5; Intercept ($^{39}K/^{40}Ar^{*}$) = 0.1015 ±0.0003818
Intercept ($^{36/40}tr$ = 0.003277 ±0.00002637; Intercept ($^{40}Ar^{*}/^{39}K$) = 9.856 ±0.03709

3SW-653 hornblende (-70+140 mesh); run 1864 (J = 0.0008039 ±0.000001).								
800	36.3	0.67	62.7	0.56	13.5	0.089	0.91	32.699 ±1.741
900	75.7	2.09	37.6	0.77	3.10	0.19	0.66	40.825 ±0.737
970	84.7	3.71	34.9	2.50	1.87	0.22	0.20	42.32 ±0.709
1020	88.5	5.13	38.0	1.50	1.51	0.19	0.34	48.142 ±0.732
1061	91.5	6.51	39.9	1.12	1.16	0.18	0.45	52.249 ±0.775
1100	92.7	7.95	33.1	1.60	0.847	0.19	0.32	44.000 ±0.634
1130	79.7	10.11	32.2	3.19	2.28	0.29	0.16	36.891 ±0.511

Table 1, continued:

1160	73.4	13.57	26.3	4.89	2.48	0.46	0.10	27.860 ±0.341
1200	78.6	32.15	17.1	7.36	1.43	2.5	0.069	19.493 ±0.104
1300	86.3	83.98	15.4	6.77	0.883	6.9	0.075	19.227 ±0.052
1650	87.4	100.00	39.0	2.24	1.71	2.1	0.23	48.884 ±0.139
Total gas age:					13.3			26.704 ±0.155
Inferred maximum (saddle) age:								19.20 ±0.12

K-Ar analyses courtesy of Dr. Giday Woldegabriel of the Los Alamos National Laboratory. K-Ar ages were determined in the laboratories of Case Western Reserve University by Dr. Giday Woldegabriel using standard isotope-dilution techniques similar to those described by Dalrympl and Lanphere (1969). Potassium was measured by a lithium metaborate flux fusion-flame photometer method with the lithium serving as an internal standard (Ingamells, 1970).

1 and 2 = porphyry dike ore, north wall of bottom (3950' bench) of open pit, Mother Lode mine (36°54.35'N; 116°39.04'W).

3 = mineralized, thin-bedded limestone of rocks of Joshua Hollow; 10 m east of porphyry dike, south wall of open pit at 4010', Mother Lode mine (36°54.35'N; 116°39.04'W).

4 = propylitically altered silicic porphyry dike between the Mother Lode and Telluride mines (36°54.12'N; 116°39.14'W). Sanidine and hornblende separated by conventional magnetic and heavy liquid techniques; clear and turbid sanidine grains hand-picked from concentrates.

* = < 1 μm size-fraction, interstratified illite-smectite; separated by conventional sedimentation methods.

Constants: $^{40}K\ \kappa_\varepsilon + {}^{40}K\ \kappa_{\varepsilon'} = 0.581 \times 10^{-10}\ yr^{-1}$; $^{40}K_\beta = 4.962 \times 10^{-10}\ yr^{-1}$; atomic abundance $^{40}K/K_{total} = 1.167 \times 10^{-4}$ kmole/kmole.

$^{40}Ar/^{39}Ar$ analyses were carried out in the laboratories of the New Mexico Bureau of Mines and Mineral Resources under the supervision of W.C. McIntosh.

Reactor constants: $(^{36}Ar/^{37}Ar)_{Ca} = 0.00026$; $(^{39}Ar/^{37}Ar)_{Ca} = 0.00070$; $(^{40}Ar/^{39}Ar)_K = 0.01900$; $(^{38}Ar/^{39}Ar)_K = 0.01190$.

bd = below detection; ud = undetermined.

Table 2. Strontium Isotope and Selected Major, Trace- and Immobile-element Concentrations of Porphyry Dikes in Bare Mountain, Nevada

Field #	$^{87}Sr/^{86}Sr_m$	Rb (ppm)	Sr (ppm)	Zr (ppm)	Nb (ppm)	TiO_2 (wt %)	Ba (ppm)	K_2O (wt %)
3DN9-3	0.71007	168	56.5	128	26.5	0.18	704	5.39
3DN9-7	0.71028	170	94.0	150	27.5	0.20	736	5.27
3DN9-11	0.70994	161	132	143	27.5	0.19	788	4.97
3DN9-13	0.70891	128	430	341	13.0	0.54	2026	4.48
3DN9-53	0.71042	165	81.5	119	24.5	0.18	632	5.19
3DN9-61	0.70933	132	526	280	15.5	0.70	1594	5.25

m = measured ratios by thermal-ionization mass spectrometry; all other values are the mean of duplicate analyses by energy-dispersive x-ray fluorescence spectrometry. Analyses carried out in the laboratories of the Branch of Isotope Geology, U.S. Geological Survey, Denver, Colorado, under the supervision of Z.E. Peterman.

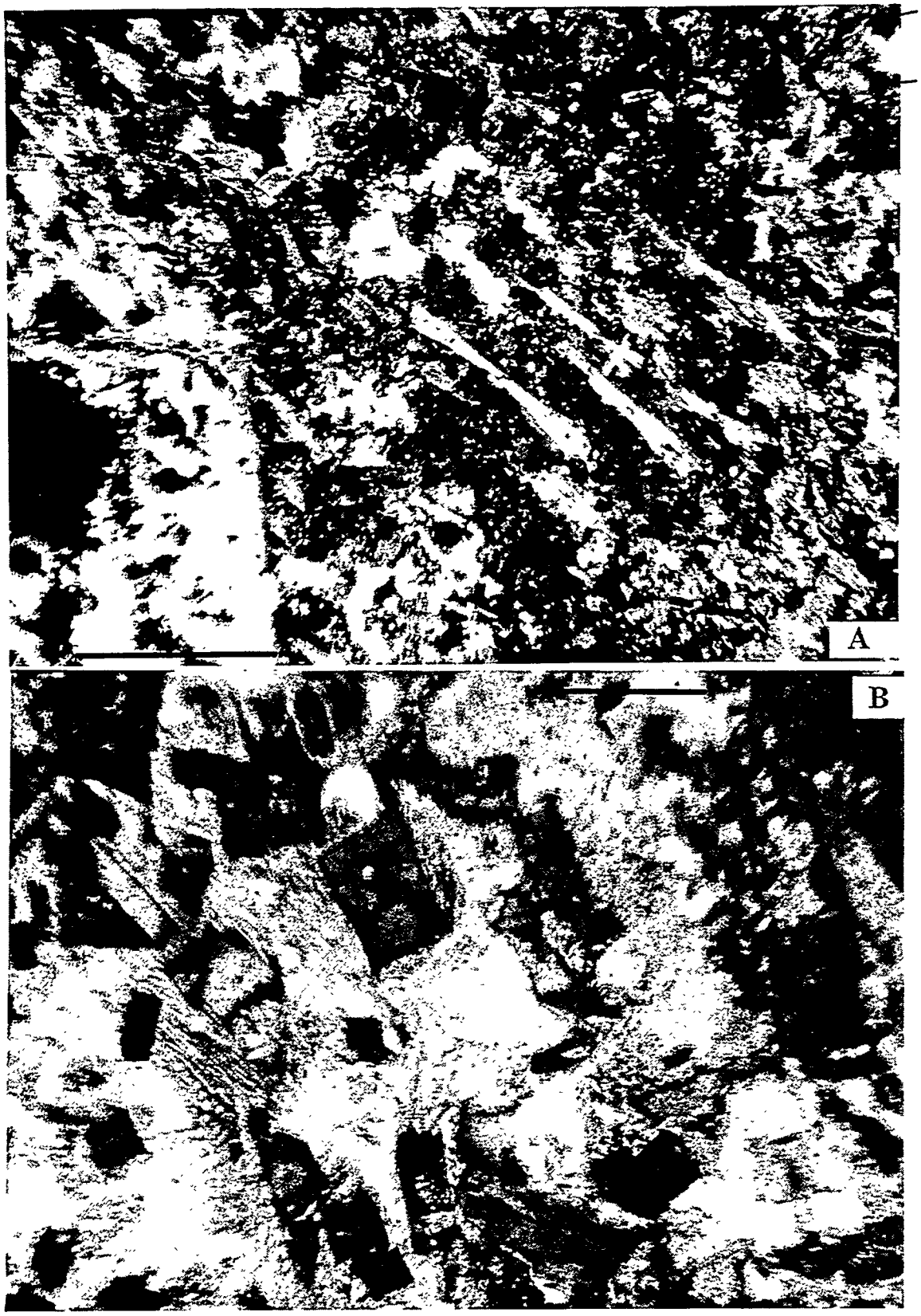

Figure 1. A) Granophyrically crystallized groundmass material in dike at the Sterling mine. Elongate grains are bow-tie feldspar grains that formed on quenching during early stage of crystallization (crossed polars). B) Groundmass material in dike from the Goldspar mine with blockly sanidine and plates of biotite surrounded by a fine granophyric intergrowth of quartz and sanidine (crossed polars). Scale bars are 0.5 mm in length.

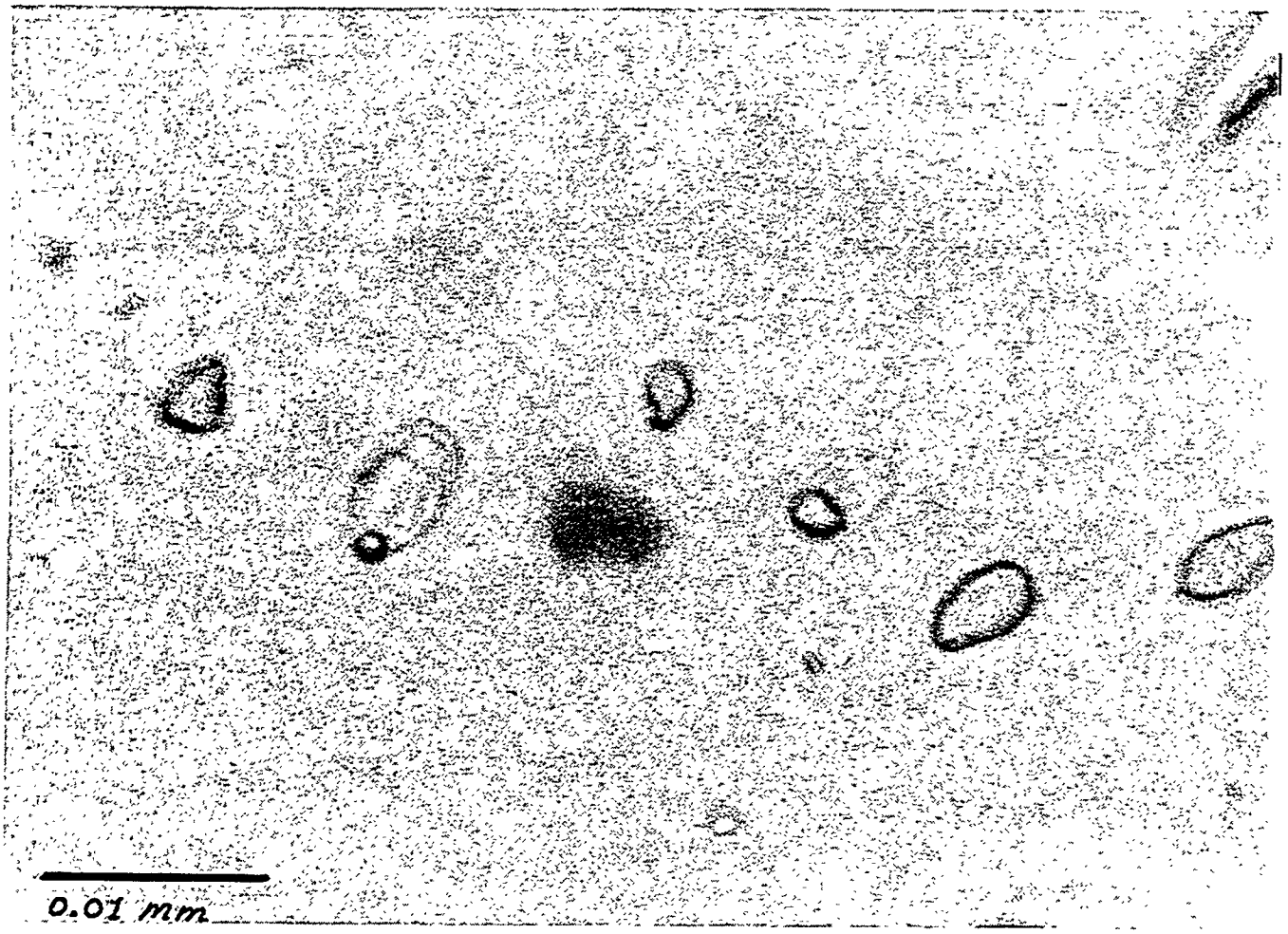

Figure 2. Train of secondary inclusions in quartz phenocryst from dike near the Telluride mine. Note both high-salinity inclusions containing cubes of halite and sylvite(?) and vapor-dominated inclusions, indicating presence of immiscible vapor pahase at the time of trapping.

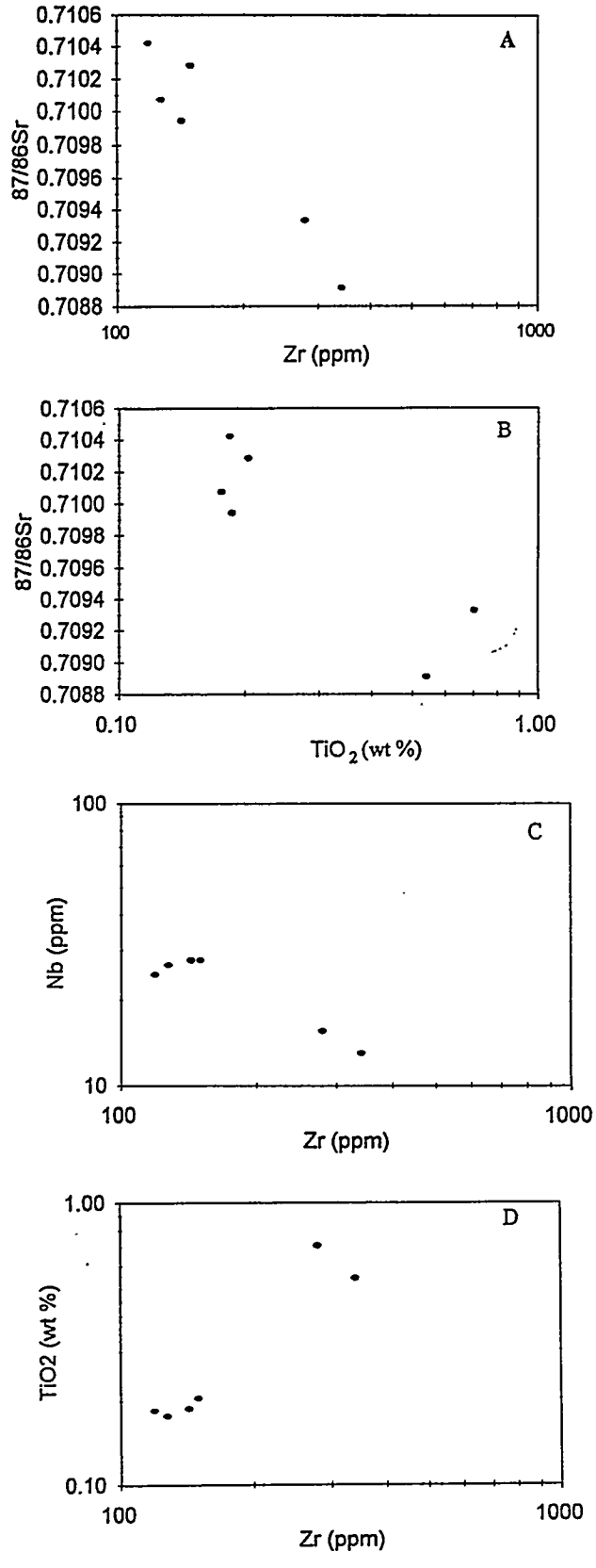

Figure 3. X-Y plots of selected immobile-element and strontium isotopic compositions of silicic porphyry dikes in Bare Mountain. Data from Table 2.

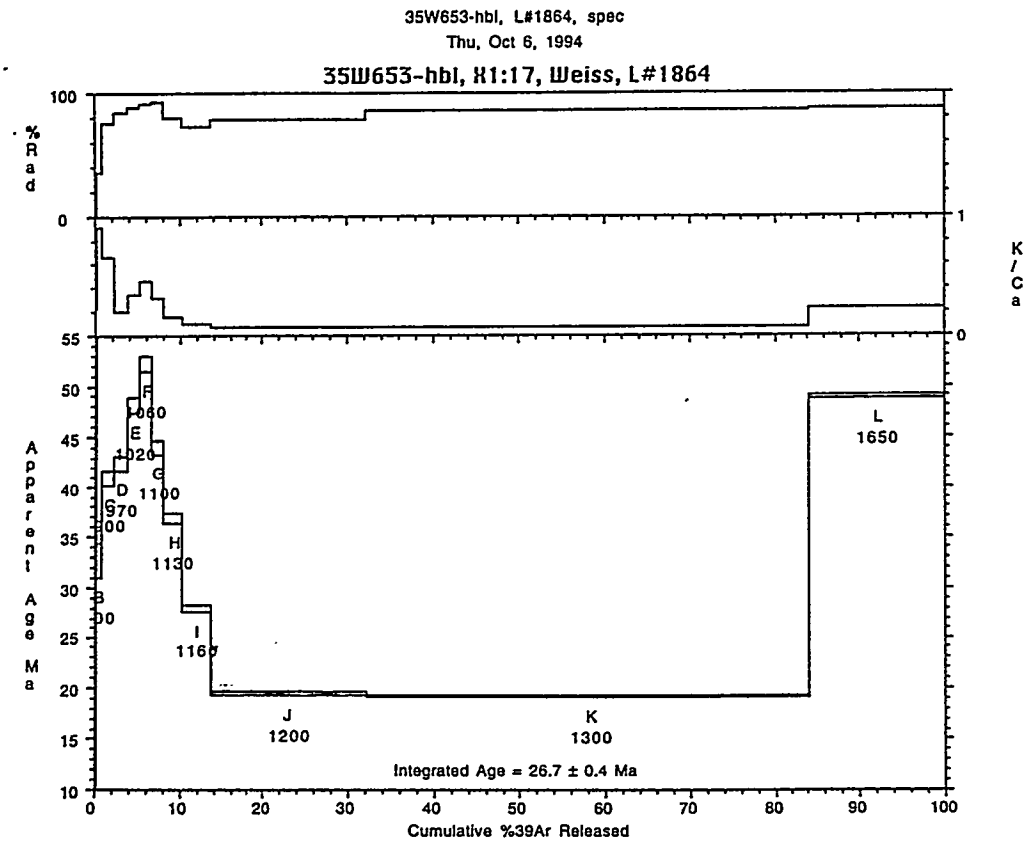

Figure 4. Argon release spectra for incremental heating of hornblende separated from silicic porphyry dike in northern Bare Mountain; field sample number 3SW-653. Sample collected from dike outcrop about 1300 feet south-southwest of the open pit of the Mother Lode mine.

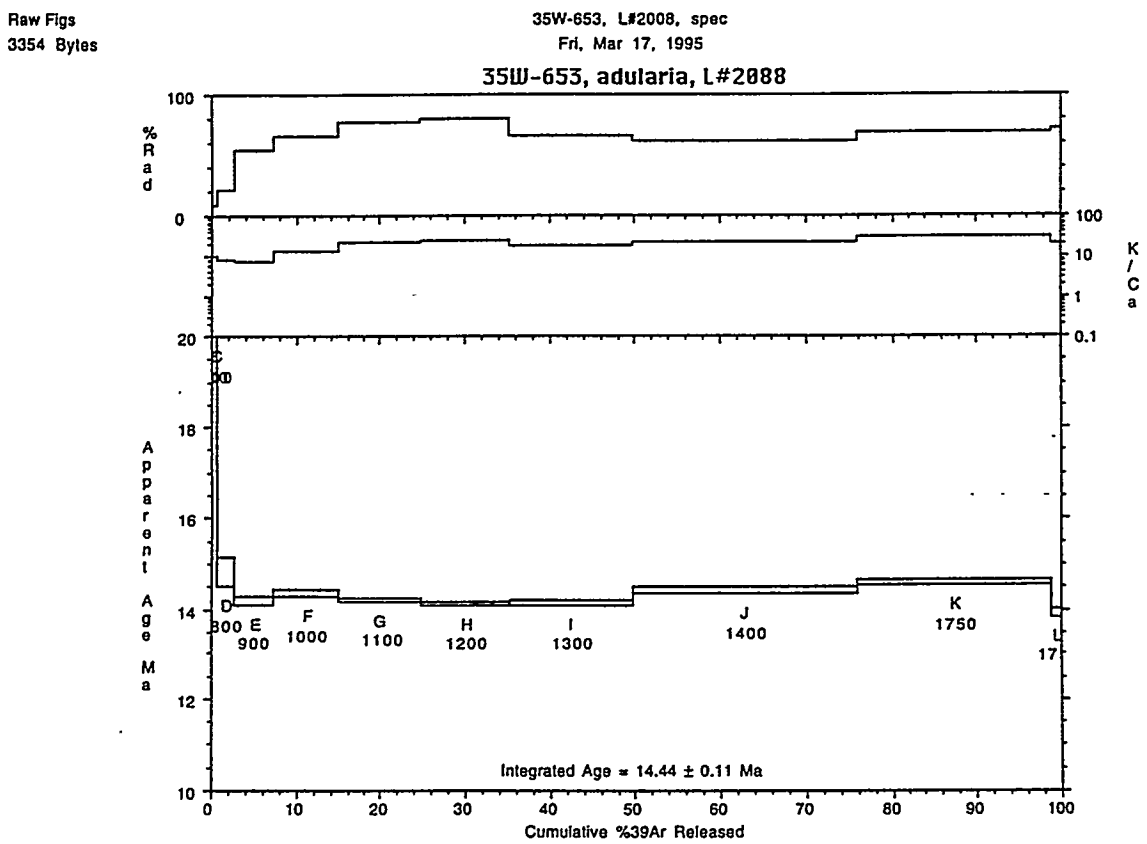

Figure 5. Argon release spectra for incremental heating of turbid sanidine separated from sample 3SW-653.

APPENDIX A

SCIENTIFIC COMMUNICATION

HYDROTHERMAL ORIGIN AND SIGNIFICANCE OF PYRITE IN ASH-FLOW TUFFS AT YUCCA MOUNTAIN, NEVADA

Steven I. Weiss, Donald C. Noble, and Lawrence T. Larson

Department of Geological Sciences, Mackay School of Mines
University of Nevada, Reno, Reno, Nevada, 89557

HYDROTHERMAL ORIGIN AND SIGNIFICANCE OF PYRITE IN ASH-FLOW TUFFS AT YUCCA MOUNTAIN, NEVADA

Steven I. Weiss, Donald C. Noble, and Lawrence T. Larson

Department of Geological Sciences, Mackay School of Mines
University of Nevada, Reno, Reno, Nevada, 89557

Introduction

Yucca Mountain, Nevada, the only site presently being considered for the construction of a national site for the disposal of high-level nuclear waste, is situated between areas of hydrothermally altered rocks peripheral to the Timber Mountain caldera complex of the middle Miocene southwestern Nevada volcanic field (Noble et al., 1991; Castor and Weiss, 1992; Castor et al., 1994; Weiss et al., 1995) (Fig. 1). Areas of altered and mineralized rocks in southwestern Nevada include precious-metal deposits hosted by the same ash-flow units that comprise Yucca Mountain (Weiss et al., 1994; 1995). These areas have been the sites of current and historic mining and mineral exploration. The possible presence of mineral and hydrocarbon resources in the vicinity of Yucca Mountain has raised concerns that exploration in the distant future could disrupt the nuclear waste, resulting in the release of radionuclides to the environment (Johnson and Hummel, 1991). The nature of past fluid flow and water-rock interactions at Yucca Mountain are important factors in assessing the potential for undiscovered mineral resources in the area of the proposed high-level nuclear waste repository. Ample well-documented textural and mineralogic evidence exists for at least one episode of widespread hydrothermal alteration of volcanic rocks deep within Yucca Mountain based on detailed studies of core and cuttings from deep drill holes (e.g., Broxton et al., 1982; Caporusio et al., 1982; Scott and Castellanos, 1984; Vaniman et al., 1984; Warren et al., 1984; Bish, 1987; Bish and Aronson, 1993). The presence of pyrite in major ash-flow units, and, to a lesser extent, in altered silicic lava flows locally present between the ash-flow units was documented.

Based on studies of selected core from 4 of the 13 deep drill holes, Castor et al. (1994) contend that most of the pyrite found in tuffs at Yucca Mountain was introduced as foreign lithic

fragments incorporated during eruption of the tuffs, rather than having been formed in place by hydrothermal activity. This conclusion appears to be based largely on their assertion that most of the pyrite resides in unaltered to variably altered and veined foreign lithic fragments, whereas pyrite-bearing veins are absent in the tuff matrix, titanomagnetite and mafic phenocrysts in the matrix are generally not replaced by pyrite, and feldspar phenocrysts in the pyritic tuffs are generally unaltered. Castor et al. (1994) regarded the much smaller quantities of pyrite disseminated in the tuff matrix, including relatively rare pyritized hornblende and biotite grains, as xenolithic as well.

We have studied core and cuttings from the same drill holes studied by Castor et al. (1994) as well as from 8 additional drill holes in Yucca Mountain. The tuffs that contain pyrite mainly belong to large-volume, subalkaline (metaluminous) rhyolite ash-flow units of middle Miocene age, including the Lithic Ridge Tuff and units of the Crater Flat Group (ca. >150 to 250 km^3 each, Carr et al., 1986; Sawyer et al., 1994), which we have examined in numerous outcrops in surrounding areas of the southwestern Nevada volcanic field. These units lie stratigraphically below the ash-flow sheets of the Paintbrush Group, and underlie the site of the proposed repository. The "lithic" origin of the pyrite of Castor et al. (1994) is not consistent with the temperature, fO_2 and fS_2 of major ash flow eruptions. It is our contention that inconsistent lateral and stratigraphic distribution of the pyrite, textural features of the pyrite, and phase stability considerations are incompatible with the "lithic" origin, and are more reasonably explained by *in-situ* formation from hydrothermal fluids containing low, but geochemically significant, concentrations of reduced sulfur. Such fluids would have been capable of transporting and depositing precious metals and should be a factor considered in assessing the potential for buried mineral resources.

Textural and Stratigraphic Evidence for In-situ Hydrothermal Origin of Pyrite

The disseminated pyrite in lithic fragments and in the groundmass of the ash-flow units in Yucca Mountain consists of anhedral to subhedral, generally pitted and wormy to sieved, or

skeletal(?), individual crystals and granular aggregates of from <5 μm to ~0.5 mm in maximum dimension (Fig. 2). In some grains pits and poikilitic texture appear to result from the presence of numerous inclusions of altered groundmass, whereas other grains, mainly those smaller than about 10 μm in diameter, are commonly subhedral and free of pits and inclusions. Propylitically altered silicic lava in drill hole USW G-2 contains disseminated pyrite grains having textures and morphology indistinguishable from those of the pyrite in the tuffs (Fig. 3). Fractures are occasionally present in pyrite grains in the altered lava, as well as in granular pyrite in the tuffs. The pyrite in the lava is not lithic material, demonstrating that fragmentation and degassing processes of ash-flow eruptions are not neccessarily responsible for the textures and morphology of the pyrite in the tuffs. Instead, as is clearly the case in the altered lavas, the observed textures of pyrite in the tuffs more likely resulted from *in-situ* nucleation and growth from hydrothermal solutions, perhaps followed by partial dissolution.

In Yucca Mountain drill hole USW G-2 (Fig. 4) small amounts of pyrite are disseminated in the altered dacitic lava and associated tuff that lies *between* the Lithic Ridge Tuff and the overlying Tram Tuff of the Crater Flat Group at depths of between 4072 to 4149 ft. Between 3457 and 3544 ft. partially to densely welded ash-flow tuff of the Bullfrog Tuff of the Crater Flat Group contains small amounts (< 1%) of pyrite disseminated in the groundmass, in altered pumice fragments (see below), in sparse lithic fragments and in and near thin quartz and quartz+calcite veinlets (Fig. 5). A steeply dipping, drusy quartz vein cutting the Bullfrog Tuff, although largely oxidized, contains traces of filmy pyrite on and intergrown with quartz at a depth of 3260.8 ft. Although we can not demonstrate fracture control of pyrite throughout the tuff matrix, these veins and numerous additional veins of calcite, ±quartz, ±barite, ±fluorite that are barren of pyrite clearly fill fractures and irregular cavities that cut the host tuffs. The concentration of pyrite within and along the margin of the vein of Figure 5 must be younger than the tuff. This, as well as the pyrite in the pumice fragments, demonstrates that *in-situ* formation of

pyrite *has* occurred, at least locally, *after* the deposition of the Bullfrog Tuff in USW G-2, even though in this drill hole the Lithic Ridge Tuff and the Tram Tuff are largely barren of pyrite.

Pyrite in tuffs at Yucca Mountain is identical within the range of textures and morphologies of pyrite formed during hydrothermal alteration of initially porous ash-flow tuff within and peripheral to precious-metal deposits such as Round Mountain, Divide and Barrick Bullfrog, Nevada (Fig. 6). In these and other districts (e.g., Tonopah, Bonham and Garside, 1979) lithic fragments of intermediate to mafic volcanic rock commonly have been preferentially pyritized, without the formation of pyrite rinds, and/or have greater pyrite contents relative to the surrounding groundmass of hydrothermally altered tuff (Fig. 6B). This is a common observation of geologists working in volcanic terranes and one that is generally attributed to the greater abundance of iron in the fragments. The apparent lack of pyrite veins or fracture control of pyrite in the tuff matrix is not unique to Yucca Mountain. For example, the lower part of the Round Mountain, Nevada, gold deposit (e.g. "type II" ores) consists of large volumes of originally porous, non-welded to slightly welded rhyolite ash-flow tuff containing <1% disseminated pyrite (Sander, 1990; Sander and Einaudi, 1990). Although economic gold grades in the mine are a function of fracture spacing, mine exposures show that the disseminated pyrite in the lower, porous tuffs is unrelated to fractures, which are generally less than a few millimeters in width, widely spaced and are not filled with pyrite. Pervasive hydrothermal alteration and the formation of disseminated pyrite in the lower part of the deposit occurred due to lateral fluid flow controlled by the primary permeability of the tuffs (Sander, 1990; Sander and Einaudi, 1990).

Castor et al. (1994) imply that the pyritic tuffs are eruptive subunits, and apparently consider that the pyritic fragments and disseminated pyrite define distinctive lithic-fragment assemblages that mark time-stratigraphic horizons. Geological relations require that these proposed "subunits", if they exist, must be discontinous on both regional and local scales, being restricted to certain areas of the Bullfrog Hills and certain drill holes in Yucca Mountain (both are areas of

recognized episodes of hydrothermal activity (e.g., Ransome et al., 1910; Carr et al., 1986; Bish, 1987; Castor and Weiss, 1992; Bish and Aronson, 1993). Regionally, pyrite, lithic or otherwise, is not described by Carr et al. (1986) (or observed by our group) in the Lithic Ridge Tuff at its type locality 18 km northeast of Yucca Mountain or in exposures west of the Bullfrog Hills. We have not observed pyrite or limonite pseudomorphs in the thick sections of the Tram Tuff and Bullfrog Tuff exposed in the northwestern part of Yucca Mountain (Fridrich et al., 1994) or in the thinner sections exposed at the south end of Yucca Mountain.

At the local scale, in the subsurface of Yucca Mountain in drill hole USW G-1 (Fig. 4), pyrite is present in the lower part of the Tram Tuff, but is absent in the Lithic Ridge Tuff. Less than 0.5 km to the east in drill hole USW H-1 (Fig. 4) pyrite is present in the Lithic Ridge Tuff, but is absent from the Tram Tuff. Pyrite is present in lower parts of the Bullfrog Tuff and in the *upper* part of the Tram Tuff at 3593 to 3595 ft. in USW G-2, approximately 2.5 km north of USW G-1 and H-1. In UE25B 1H, only 1.9 km southeast of USW H-1, pyrite appears again, but in the *lower* part of the Tram Tuff, and is *absent* from the Lithic Ridge Tuff. Similarly, in USW G-3 (Fig. 4) pyrite is present in both the lower part of the Tram Tuff and in the Lithic Ridge Tuff, but less than one kilometer to the north, only the lower Tram Tuff is pyritic in USW H-3. Less than 4 km east of USW H-3 pyrite is absent from both the Tram Tuff and the Lithic Ridge Tuff in UE25 P1, but is present in argillically altered tuffs below the Lithic Ridge Tuff. In USW H-4 (Fig. 4) we have observed pyrite in welded and devitrified tuffs of the Crater Flat Group, probably within the Bullfrog Tuff, whereas in USW H-5 pyrite is absent.

The laterally discontinuous and stratigraphically inconsistent pyrite distribution, over distances of as little as 0.5 km, would require unrealistically abrupt and fortuitous differences in original deposition, or in subsequent preservation by variations in initial cooling, water-table elevations and/or weathering. Variations in preservation can not account for the absence of pyrite in lithic-rich, clay and zeolite altered, unoxidized, originally glassy tuffs of the lower part of the Tram Tuff in USW G-2. Unoxidized, zeolitic, originally glassy tuffs of the same unit contain

small amounts of pyrite in the groundmass and in lithic fragments in drill holes USW G-1, UE25B 1H and USW G-3. Likewise, unoxidized, originally glassy tuffs of the Lithic Ridge Tuff contain pyrite in USW G-3, but pyrite is absent in unoxidized, originally glassy tuffs of the Lithic Ridge Tuff in USW G-1 and USW G-2. Although pyrite has not been observed in tuffs that underwent primary (cooling) crystallization of the groundmass, we consider the pyrite distribution to have little, if any, relation to genetically meaningful stratigraphic units defined by primary depositional features (e.g., bedded tuff horizons, degree of welding and presence or absence of primary devitrification and vapor phase crystallization) and differences in phenocryst assemblages (Smith, 1960). Such irregular distribution is more reasonably attributable to the channeling of hydrothermal fluids having sufficient activity of reduced sulfur to form pyrite, perhaps near faults, fractures and other zones of enhanced permeability.

Considerations of Phase Stability Relations and Conditions of Ash-flow Eruption and Emplacement

Pyrite disseminated in argillically-altered pumice fragments of the Bullfrog Tuff in USW G-2 and in the Tram Tuff in UE25 B1H (Figs. 5 and 7) must have formed *after* eruption and cooling from magmatic temperatures because pyrite is not a stable phase in magmas of any composition. Even the most sulfur-rich and oxidized magmas do not contain pyrite (e.g., Drexler, 1982; Matthews et al., 1994). Blebs of pyrrhotite crystallized from magmatic sulfide solutions are present in trace amounts in many subalkaline silicic ash-flow tuffs and lavas (Hildreth, 1979; Whitney and Stormer, 1983), but generally survive eruption and cooling only when encapsulation in phenocrysts prevents breakdown by loss of S_2 gas (Keith et al., 1991). Only very rarely are immiscible sulfide solutions contained in quenched silicate melt phase even partly preserved (Keith et al., 1991). A variety of iron-bearing phases commonly form as products of primary, high-temperature devitrification and vapor-phase crystallization (Smith, 1960), but pyrite has never been reported, even in lithophysae or lensoid cavities localized by pumice in which juve-

nile gas was trapped and vapor pressures were sufficient to support the weight of the overlying tuff or lava (Noble, 1968).

Pyrite exposed in vent walls is unlikely to survive the conditions of major ash-flow eruptions. Subalkaline silicic magmas typically erupt at temperatures between about 700 and 900+°C. Iron-titanium oxide temperatures within this range have been reported for tuffs of the Paintbrush and Timber Mountain magmatic stages of the southwestern Nevada volcanic field (Lipman, 1971; Warren et al., 1989). Cooling by admixture of air cannot take place until pyroclastic material leaves the vent. In major ash-flow eruptions such cooling is negligible even during flow outside the vent because of the enormous mass of juvenile magmatic material. Moreover, cooling of the erupted pyroclastic material by adiabatic expansion of the magmatic gas phase must be minor because of the low mass fraction of the gas. The 742°C stability limit of pyrite mentioned by Castor et al. is the *maximum* temperature at which pyrite is stable in the Fe-S system, and is predicated on an activity of S° = 1 (i.e., presence of liquid sulfur) and the *absence* of O_2 (Kullerude and Yoder, 1959; Barton and Skinner, 1979), conditions very unlikely for most subalkaline rhyolite magmas and their exsolved gases (Whitney, 1984). During initial degassing the dominant sulfur specie is SO_2 (Whitney, 1984), but the gases mainly comprise water vapor, CO_2, H_2, HCl, and HF. The calculations of Whitney (1984) show that for typical subalkaline silicic magmas such as the Bishop Tuff and the Fish Canyon Tuff, estimated values of fS_2 at 700°C are 4 and 2 orders of magnitude lower, respectively, than the minimum fS_2 required for pyrite stability at this temperature. At 600°C the estimated fS_2 values are still 4 and 2 orders of magnitude lower, respectively, than the minimum fS_2 needed for pyrite stability (Whitney, 1984). Only the most oxidized and sulfur-rich magmas, such as those of Julcani, Peru (Drexler, 1982), Lascar volcano, Chile, and Pinatubo volcano, Phillipines (Mathews et al., 1994) have estimated fS_2 values near or in the range needed for pyrite stability. The voluminous Paintbrush and Timber Mountain ash-flow units of the southwest Nevada volcanic field would

have had values of fS_2 at 700°C of 5 to 2 orders of magnitude below pryite stability based on calculated fO_2 values in the range of 10^{-18} to 10^{-15} (Warren et al., 1989).

Numerical models suggest that the incorporation of large volumes of lithic fragments in ash-flow tuffs will lower the bulk flow temperatures into the 500 to 650°C range over times on the order of minutes to months and may in some cases inhibit welding (Eichleberger and Koch, 1979; Marti et al., 1991), consistent with the common observation of envelopes of glassy tuff surrounding intracaldera slide blocks and wedges of megabreccia (e.g., Lipman, 1984, Fig. 10b; Fridrich, 1987). More importantly, these calculations demonstrate that lithic fragments less than a few millimeters in diameter are heated to the bulk flow temperature nearly instantaneously, with sub-millimeter sized fragments equilibrating in less than one second, *prior* to significant bulk cooling. The pyrite grains disseminated in the matrix of tuffs at Yucca Mountain are less than 0.5 mm in diameter. Lithic grains of pyrite of this size would have been destroyed by heating to magmatic or near-magmatic temperatures in the presence of magmatic gases during eruption and transport.

Inferring a lithic origin for the pyrite, Castor et al. (1994) cited the lack of welding, low magnetic remanence and high magnetic susceptibility of the pyrite-bearing tuffs as evidence for the emplacement of the tuffs at temperatures below 550 to 580°C. These are, at best, not convincing arguments for the temperature of emplacement. Welding is a function of glass composition, water content and loading, as well as temperature and is thought to occur over minutes to years (Rhiele, 1973; Eichleberger and Koch, 1979). Various pyroclastic deposits of the 1980 eruptions of Mount Saint Helens, all of them unwelded and 2 to 3 orders of magnitude smaller in volume than the pyritic units in Yucca Mountain, were emplaced at temperatures between about 300 to 730°C, with no significant decrease in temperatures along their flow paths (Banks and Hoblitt, 1981).

Detailed rock magnetic and transmission electron microscope studies have shown that the bulk of the magnetic remanence and susceptibility characteristics in glassy ash-flow tuff, includ-

ing that of the Paintbrush Group at Yucca Mountain, are carried by abundant Fe-Ti oxide microcrystals precipitated in the glass during cooling (Schlinger et al., 1988; 1991). In the pyritic units in Yucca Mountain the original quenched glass has largely been altered to clay, zeolites, silica and calcite (Bish, 1987; Broxton, et al., 1982; Caporuscio et al., 1982; Vaniman et al., 1984; Warren, et al., 1984). The low magnetic remanence and high magnetic susceptibility of the altered tuffs are consistent with, and much more plausibly explained by, the destruction of the remanence-carrying microcrystals during hydrothermal alteration of the glass, leaving only the large, high-susceptibility magnetite phenocrysts (± secondary(?) magnetite). We emphasize that unaltered rocks of the Bullfrog and Tram Tuffs exposed elsewhere in the southwestern Nevada volcanic field, including unwelded tuff, do not possess unusually low magnetic remanence, but carry strong, consistent records of the geomagnetic field orientations at the times of their eruptions (Hudson et al., 1994; M. R. Hudson, oral communication, 1994). Unaltered rocks of the Lithic Ridge Tuff record an anomalous geomagnetic field orientation probably associated with a magnetic polarity transition (M. R. Hudson, oral communication, 1994) and may have cooled during a time of low magnetic field intensity.

Trace-element Geochemistry

Trace-element analyses of a number of selected intervals of core and cuttings from drill holes in Yucca Mountain (Table 1) are very similar to the trace-element data for selected intervals given by Castor et al. (1994). Concentrations of As in drill hole samples are in part higher than the concentrations of As in surface samples reported by Castor et al. (1990). The combined data of Castor et al. (1994) and of this report show that concentrations of As, Bi, Hg, Mo, Sb, Se, Te and Zn in some selected samples are as much as one to two orders of magnitude higher than the low levels found in surface samples of unaltered rhyolite ash-flow tuff in the Yucca Mountain area (Castor et al., 1990; Weiss et al., 1991; Castor and Weiss, 1992). Four of our samples contain gold in concentrations of about one order of magnitude greater than are present in fresh, subalkaline rhyolite (typically <0.5 ppb; Connors et al., 1993). Thin veins of breccia

cemented by silica and iron oxides cut oxidized, relatively lithic-poor welded tuffs of the Crater Flat Group in drill holes UE25 C#1, UE25 C#2 and UE25 C#3 and contain as much as 77 ppm As, 2.0 ppm Bi, 15 ppm Sb, and 207 ppm Mo (Table 1). The 142 ppm As and 249 ppm Sb concentrations reported by Castor et al. in USW G-2 are from the largely oxidized vein mentioned previously.

The trace elements that are enriched in selected samples from Yucca Mountain are commonly associated with hydrothermal systems, including those in which precious-metal deposits are formed. The elevated concentrations of trace elements in the selected drill hole samples from Yucca Mountain are within the range of those reported by Castor and Weiss (1992) for altered volcanic rocks in the nearby Bullfrog, Bare Mountain and Wahmonie precious-metal districts when samples of ores and rocks within a few tens of meters of ore zones are excluded, and are comparable to those of altered, but unmineralized rocks in other districts (e.g., Rawhide, Black et al., 1991). We believe the observed enrichments at Yucca Mountain are best explained by deposition from hydrothermal fluids, rather than by derivation from altered lithic fragments as proposed by Castor et al. (1994), even though measured Au and Ag concentrations are low.

Figure 5 of Castor et al. (1994) implies that there are continuous geochemical data for drill holes USW G-3 and GU-3. This is not the case. Most samples represent less than 30 cm of core and are separated by 10 to 70 m of core that was not analysed.

Discussion and Conclusions

The presence of small amounts of fine-grained pyrite disseminated in the matrix of tuffs in Yucca Mountain is an important factor in determining the history of water-rock interactions at and near the repository site. Although pyrite encapsulated *within* lithic rock fragments could perhaps retain sulfur and survive entrainment in major ash-flow eruptions, in all probability unencapsulated grains of millimeter or smaller diameters would be destroyed by the near-instantaneous heating to magmatic and near-magmatic temperatures in magmatic gases, followed by cooling over minimum times of 10's of minutes to days or months. This chemical instability,

together with the textural similarities of the groundmass pyrite to that observed in altered lavas in USW G-2 and in altered porous tuffs in the Divide, Round Mountain, Bullfrog and other districts, the inconsistent lateral and stratigraphic distribution, the presence of pyrite locally in units overlying and underlying the Lithic Ridge Tuff and the Tram Tuff, including propylitically altered silicic lava, the presence of pyrite in altered pumice fragments, and pyrite in and near silica veinlets in the Bullfrog Tuff in USW G-2, leads us to conclude that a much more simple and common process formed the pyrite in the groundmass of the tuffs: sulfidation of iron in the rocks from H_2S- and HS^--bearing hydrothermal fluids. Castor et al. (1994) considered this possibility an "untenable alternative" because of the generally unaltered feldspar phenocrysts, lack of pyritic veins and scarcity of pyritized titanomagnetite, hornblende and biotite phenocrysts in the tuffs. The preservation of unaltered or little-altered magmatic minerals and lack of fracture control of pyrite in the matrix do not indicate that a rock has not been affected by hydrothermal solutions. Under appropriate conditions the common phenocryst minerals present in silicic volcanic rocks can survive relatively intense hydrothermal alteration and even low-grade metamorphism. Unaltered calcium-bearing plagioclase is commonly found in propylitically altered silicic and intermediate volcanic rocks, including rocks containing epidote and/or actinolite. In many cases plagioclase phenocrysts with perfectly preserved progressive and oscillatory zoning are cut by microscopic veinlets of hydrothermal albite or adularia. Sanidine and calcium-bearing plagioclase have been preserved in tuffs that have undergone lower greenschist-facies dynamothermal metamorphism (Noble, 1966). In such cases the very plastic, originally glassy groundmass material has served to protect the phenocrysts from nonhydrostatic stress, which catalyzes the breakdown of the chemically unstable relict high-temperature mineral phases. Biotite phenocrysts likewise are preserved in adularized, pyritic ores and wallrocks at the Barrick Bullfrog mine (Castor and Weiss, 1992), with the high activities of K^+ helping to preserve the relict magmatic biotite. Relict clinopyroxene also is found in some propylitically altered rocks, with low H_2O activities playing a major role in preserving the anhydrous magmatic phase (cf. Schiffman et al., 1984). The partial, or even complete, preservation of phenocryst minerals in

Yucca Mountain rocks therefore in no way indicates that these rocks have escaped the effects of hydrothermal fluids. Although the feldspar and mafic phenocrysts were not thermodynamically stable, the lack of directed stress, combined with fluid compositions buffered to near-neutral pH values and elevated concentrations of Na, K and Si by reaction with highly unstable rhyolitic volcanic glass served to preserve the relict magmatic phases. Such metastability would inhibit sulfidation and explain the scarcity of pyritized biotite and hornblende in the tuffs. Magnetite commonly coexists as a stable phase with pyrite and other sulfides under a range of H_2S, HS^- and O_2 activities and is not necessarily replaced.

As pointed out by Castor et al. (1994), most of the pyrite-bearing lithic fragments consist of volcanic rocks of intermediate compositions. Fluids entering these fragments would have encountered higher iron contents than were present in the tuff matrix and would no longer have been buffered by the composition of the rhyolitic glass. The greater abundance of pyrite in the lithic fragments, relative to the matrix of the tuffs, can be explained by the reaction of the reduced sulfur transported by the fluids with the greater abundance of total iron and of mafic silicate and Fe-Ti oxide phases in the fragments. The uneven lateral and vertical distribution of pyrite can reasonably be attributed to the flow pathways of fluids that contained sufficient reduced sulfur to sulfidize iron-rich phases in the rock mass. Pyrite in the lithic fragments is unlikely to have been dissolved and re-precipitated in the tuff matrix by the infiltration of shallow groundwater.

Oxidation due to primary crystallization of the groundmass during initial cooling of ash-flow tuffs results in greater proportions of ferric to ferrous iron in devitrified tuffs than are present in glassy tuffs (e.g., Weiss et al., 1989). In many cases the iron in primarily crystallized tuffs is entirely in the ferric state. Glassy tuffs in Yucca Mountain, with lower initial Fe^{+2}/Fe^{+3}, may have been more susceptible to sulfidation than the vapor-phase crystallized and devitrified tuffs in which groundmass pyrite has not been recognized.

Castor et al. (1994) state that pyrite in the matrix of the Lithic Ridge and the Tram tuffs is from "pulverized ejecta and is commonly in rounded grains (Fig. 3), probably due to abrasion during pyroclastic transport". We have not observed rounded pyrite grains. In fact, the pyrite (bright) grains shown in their Figure 3 and observed by us in our polished sections are not rounded, but are instead anhedral, have somewhat pitted to embayed margins, and have as many as two poorly developed crystal faces. The small, possibly subspherical voids surrounding two of these grains (dark in their Figure 3) are in the soft, phyllosilicate-rich matrix and may be artifacts of grinding and polishing, particularly if the specimen was not impregnated with epoxy prior to grinding. Moreover, abrasion of these small, relatively hard pyrite grains is difficult to accept when, as shown in their Figure 3, the much more delicate points and cusps of the glass shards have not been destroyed. We note that phenocrysts in ash-flow tuffs are invariably angular and are commonly fractured, but are not rounded by abrasion.

Yucca Mountain is situated in a region containing presently and formerly economic precious-metal deposits of middle and late Miocene age, of which most are about the same age and younger than the rocks of the proposed repository (Fig. 1) (Weiss et al., 1994; 1995). Consequently, the possibility of future mineral exploration in or near Yucca Mountain should be considered in the assessment of possible future human intrusion of the proposed high-level radioactive waste repository. A critical factor is the degree to which future generations perceive mineral potential beneath Yucca Mountain. It therefore seems prudent to correctly determine the origin of the pyrite and the trace-element enrichments, and any other signs of mineralization at Yucca Mountain. The textural, stratigraphic and phase-stability relations discussed above are inconsistent with the interpretation of a "lithic" origin related to major ash-flow eruptions. We believe that the evidence, including the trace-element data, is internally consistent and strongly supports in-situ formation from hydrothermal fluids containing reduced sulfur. Bisulfide-bearing fluids would have been capable of carrying and depositing gold and silver.

It is unlikely that the pyrite is associated with a regional halo of propylitic alteration surrounding the Timber Mountain caldera complex, because such a halo has not been identified. K-Ar ages of illite from drill holes USW G-1 and USW G-2 show that hydrothermal alteration occurred at Yucca Mountain mainly between 10 and 11 million years ago, after the deposition of the Timber Mountain Group and the formation of the caldera complex (Bish and Aronson, 1993). Rocks of the Timber Mountain, Paintbrush and Crater Flat Groups, as well as underlying volcanic units are unaltered around much of the eastern and northeastern margins of the Timber Mountain caldera complex. Local areas of focussed hydrothermal activity south and west of the complex are surrounded by large areas of unaltered rocks (Fig. 1) and vary in age from as old as about 12.9 to 12.6 Ma at Wahmonie and 12.9 to 11.2 Ma in northern Crater Flat and Bare Mountain, to between 8.8 and 7.5 Ma in the Clarkdale-Yellow Gold mine area (Noble et al., 1991; McKee and Bergquist, 1993; Weiss et al, 1995).

Small amounts of pyrite are hardly guides to ore. The pyritic rocks have been found only at depths of greater than 900 m and economically interesting concentrations of Au and Ag have not been observed. Indeed, Yucca Mountain is not attractive for present-day mineral exploration when compared to the nearby Bare Mountain, Calico Hills and Wahmonie areas. Nevertheless, the deep boreholes are situated from about 0.5 to more than 3.0 km apart (Fig. 4), a spacing far too great to rule out the presence of mineral deposits beneath the capping tuffs of the Paintbrush Group.

People of the distant future capable of detecting the pyrite at depths of >900 m would presumably detect the radioactive waste as well. A greater concern should be the possibility that less technologically advanced people would, in all probability, recognize evidence of major mines in the nearby Bare Mountain and Bullfrog districts. Such people could well be attracted to Yucca Mountain because the enormous amount of mined rock from excavation of the repository will indicate the existence of major underground workings, which could both suggest the

possibility of previous mining and suggest relatively easy access to perceived mineral deposits at or below the level of the radioactive waste.

Acknowledgments

This paper draws on studies carried out under contracts with the Nevada Nuclear Waste Project Office. Access to drill core and cuttings from Yucca Mountain was greatly facilitated by the cooperation and assistance of Christopher Lewis, David Merritt and Uel Clanton. Gary Smith alerted us to important references concerning the thermal effects and behavior of lithic fragments in pyroclastic eruptions. We thank Jeffrey D. Keith for kindly reviewing an early version of this paper and Peter W. Lipman, Martin Schoonen and the anonymous person who reviewed the manuscript for *Economic Geology*.

Revised July 24, 1995

REFERENCES

Banks, N. G., and Hoblitt, R., P., 1981, Summary of temperature studies of 1980 deposits: *in* Lipman, P. W., and Mullineaux, D. R., eds., The 1980 eruptions of Mount Saint Helens, Washington, U.S. Geological Survey Professional Paper 1250, p. 295-313.

Barton, P. B., and Skinner, B. J., 1979, Sulfide mineral stabilities: *in* Barnes, H. L., ed., Geochemistry of Hydrothermal Ore Deposits, Wiley and Sons, New York, p. 278-403.

Bish, D.L., 1987, Evaluation of past and future alteration in tuff at Yucca Mountain, Nevada based on clay mineralogy of drill cores USW G-1, G-2, and G-3: Los Alamos National Laboratory Report LA-10667-MS, 41 p.

Bish, D. L., and Aronson, J. L., 1993, Paleogeothermal and paleohydrologic conditions in silicic tuff from Yucca Mountain, Nevada: Clays and Clay Minerals, v. 41, p. 148-161.

Black, J. E., Mancuso, T. K., and Gant, J. L., 1991, Geology and mineralization at the Rawhide Au-Ag deposit, Mineral County, Nevada: *in* Raines, G.L., Lisle, R.E., Shafer, R.W., and

Wilkinson, W.W., eds., Geology and Ore Deposits of the Great Basin, Reno, Geological Society of Nevada, p. 1123-1144.

Bonham, H. F., Jr., and Garside, L. J., 1979, Geology of the Tonopah, Lone Mountain, Klondike and northern Mud Lake Quadrangles, Nevada: Nevada Bureau of Mines and Geology Bulletin 92, 142 p., 1:48,000.

Broxton, D. E., Vaniman, D., Caporuscio, F., Arney, B., and Heiken, G., 1982, Detailed petrographic descriptions and microprobe data from drill holes USW G2 and UE25b-1H, Yucca Mountain, Nevada: Los Alamos, New Mexico, Los Alamos National Laboratory Report LA-10802-MS, 168 p.

Caporuscio, F., Vaniman, D.T., Bish, D.L., Broxton, D.E., Arney, D., Heiken, G., Byers, F.M., and Gooley, R., 1982, Petrologic studies of drill cores USW G2 and UE25b-1H,Yucca Mountain, Nevada: Los Alamos, New Mexico, Los Alamos National Laboratory Report LA-9255-MS, 114 p.

Carr, W.J., Byers, F.M., and Orkild, P.P., 1986, Stratigraphic and volcano-tectonic relations of Crater Flat Tuff and some older volcanic units, Nye County, Nevada: U.S. Geological Survey Professional Paper 1323, 28 p.

Castor, S. B., and Weiss, S. I., 1992, Contrasting styles of epithermal precious-metal mineralization in the southwestern Nevada volcanic field, USA: Ore Geology Reviews, v. 7, p. 193-223.

Castor, S. B., Feldman, S. C., and Tingley, J. V., 1990, Mineral potential report for the U.S. Department of Energy, Serial No. N-50250: Nevada Bureau of Mines and Geology, University of Nevada, Reno, 24 pp.

Castor, S. B., Tingley, J. V., and Bonham, H. F., Jr., 1994, Pyritic ash-flow tuff, Yucca Mountain, Nevada: Economic Geology, v. 89, p. 401-407.

Connors, K., A., Noble, D. C., Bussey, S., D., and Weiss, S. I., 1993, Initial gold contents of silicic volcanic rocks: bearing on the behavior of gold in magmatic systems: Geology, v. 21, p. 937-940.

Drexler, J. W., 1982, Mineralogy and geochemistry of Miocene volcanic rocks genetically associated with the Julcani Ag-Bi-Pb-Cu-Au-W deposit, Peru: Physicochemical conditions of a productive magma body: Unpub. Ph.D. dissertation, Houghton, Michigan Technical University, 259 p.

Eichleberger, J. C., and Koch, F. G., 1979, Lithic fragments in the Bandelier Tuff, Jemez Mountains, New Mexico: Journal of Volcanology and Geothermal Research, v. 5, p. 115-134.

Eng, T., 1991, Geology and mineralization of the Freedom Flats gold deposit, Borealis mine, Mineral County, Nevada: *in* Raines, G.L., Lisle, R.E., Shafer, R.W., and Wilkinson, W.W., eds., Geology and Ore Deposits of the Great Basin, Reno, Geological Society of Nevada, p. 995-1019.

Fridrich, C. J., 1987, The Grizzly Peak cauldron, Colorado: structure and petrology of a deeply dissected resurgent ash-flow caldera: Unpub. PhD dissertion, Stanford, Stanford University, 201 p.

Fridrich, C. J., Orkild, P. P., Murray, M., Price, J. R., Christiansen, R. L., Lipman, P. W., Carr, W. J., Quinlivan, W. D., and Scott, R. B., 1994, Geologic map of the East of Beatty Mountain Quadrangle, Nye County, Nevada: U.S. Geological Survey Open-file Report, 4 sheets, 1:12,000.

Hildreth, W., 1979, The Bishop Tuff: Evidence for the origin of compositional zonation in silicic magma chambers: Geological Society of America Special Paper 180, p. 43-75.

Hudson, M.R., Sawyer, D.A., and Warren, R.G., 1994, Paleomagnetism and rotation constraints for the middle Miocene southwestern Nevada volcanic field: Tectonics, v. 13, no. 258-277.

Johnson, C., and Hummel, P., 1991, Yucca Mountain, Nevada-- nuclear waste or resource rich?: Geotimes, v. 36, p. 14-16.

Keith, J. D., Dallmeyer, R. D., Kim, C., and Kowallis, B. J., 1991, The volcanic history and magmatic sulfide mineralogy of latites of the central East Tintic Mountains, Utah: *in* Raines, G.L., Lisle, R.E., Shafer, R.W., and Wilkinson, W.W., eds., Geology and Ore Deposits of the Great Basin, Reno, Geological Society of Nevada, p. 461-483.

Kullerude, G., and Yoder, H. S., 1959, Pyrite stability relations in the Fe-S system: Economic Geology, v. 54, p. 533-572.

Lipman, P. W., 1971, Iron-titanium oxide phenocrysts in compositionally zoned ash-flow sheets from southern Nevada: Journal of Geology, v. 79, p. 438-456.

Lipman, P. W., 1984, The roots of ash flow calderas in western North America: windows into the tops of granitic batholiths: Journal of Geophysical Research, v. 89, p. 8801-8841.

Marti, J., Diez-Gil, J. L., and Ortiz, R., 1991, Conduction model for the thermal influence of lithic clasts in mixtures of hot gases and ejecta: Journal of Geophysical Research, v. 96, p. 21,879-21,885.

Matthews, S. J., Jones, A. P., and Beard, A. D., 1994, Buffering of melt oxygen fugacity by sulphur redox reactions in calc-alkaline magmas: Journal of the Geological Society, London, v. 151, p. 815-823.

McKee, E.H., and Bergquist, J.R., 1993, New radiometric ages related to alteration and mineralization in the vicinity of Yucca Mountain, Nye County, Nevada: U. S. Geological Survey Open-File Report 93-538, 26 p.

Nash, J. T., Utterback, W. C., and Saunders, J. A., 1991, Geology and geochemistry of the Sleeper gold deposits, Humbolt County, Nevada- an interim report: *in* Raines, G.L., Lisle, R.E., Shafer, R.W., and Wilkinson, W.W., eds., Geology and Ore Deposits of the Great Basin, Reno, Geological Society of Nevada, p. 1063-1084.

Noble, D. C., 1966, Structural state of relict plagioclase from metamorphosed and hydrothermally altered volcanic rocks: Geological Society of America Bulletin, v. 77, p. 495-508.

Noble, D. C., 1968, Laminar viscous flowage structures in ash-flow tuff from Gran Canaria, Canary Island: A discussion: Journal of Geology, v. 76, p. 721-723.

Noble, D. C., Weiss, S. I., and McKee, E. H., 1991, Magmatic and hydrothermal activity, caldera geology, and regional extension in the western part of the southwestern Nevada volcanic field: *in* Raines, G. L., Lisle,R. E., Shafer, R. W., and Wilkinson, W. W., eds., Geology and ore deposits of the Great Basin, Reno, Geological Society of Nevada, p. 913-934.

Ransome, F.L., Emmons, W.H., and Garrey, G.H., 1910, Geology and ore deposits of the Bullfrog district, Nevada: U.S. Geological Survey Bulletin 407, 130 p.

Rhiele, J. R., 1973, Calculated compaction profiles of rhyolitic ash-flow tuffs. Geological Society of America Bulletin, v. 84, p. 2193-2216.

Sander, M. V., 1990, The Round Mountain gold-silver deposit, Nye County, Nevada: *in* Sander, M. V., Black, J. E. and Boden, D. R., Resemblance and contrast among four epithermal gold-silver deposits hosted by volcanic rocks: Round Mountain, Tonopah, Hasbrouck Mountain and Rawhide, Nevada, Field Trip #11 Guidebook, Symposium on the Geology and Ore Deposits of the Great Basin, Reno, Geological Society of Nevada, p. 108-121.

Sander, M. V., and Einaudi, M. T., Epithermal deposition of gold during the transition from propylitic to potassic alteration at Round Mountain, Nevada: Economic Geology, v. 85, p. 285-311.

Sawyer, D. A., Fleck, R. J., Lanphere, M. A., Warren, R. G., Broxton, D. E., and Hudson, M. R., 1994, Episodic caldera volcanism in the Miocene southwestern Nevada volcanic field: revised stratigraphic framework, $^{40}Ar/^{39}Ar$ geochronology, and implications for magmatism and extension: Geological Society of America Bulletin, v. 106, p. 1304-1318.

Scott, R.B. and Castellanos, M., 1984, Stratigraphic and structural relations of volcanic rocks in drill holes USW GU-3 and USW G3, Yucca Mountain, Nye County, Nevada: U.S. Geological Survey Open-file Report 84-491, 121 p.

Schiffman, P. Elders, W. A., Williams, A. E., McDowell, S. D., and Bird, D. K., 1984, Active metasomatism in the Cerro Prieto geothermal system, Baja California, Mexico: A telescoped low pressure, low-temperature metamorphic facies series: Geology, v. 12, p. 12-15.

Schlinger, C. M., Rosenbaum, J. G., and Veblen, D. R., 1988, Fe-oxide microcrystals in welded tuff from southern Nevada: Origin of remanence carriers by precipitation in volcanic glass: Geology, v. 16, p. 556-559.

Schlinger, C. M., Veblen, D. R., and Rosenbaum, J. G., 1991, Magnetism and magnetic mineralogy of ash flow tuffs from Yucca Mountain, Nevada: Journal of Geophysical Research, v. 96, p. 6035-6052.

Smith, R. L., 1960, Zones and zonal variations in welded ash flows: U. S. Geological Survey Professional Paper 354-F, p. 149-159.

Vaniman, D.T., Bish, D., Broxton, D., Byers, F., Heiken, G., Carlos, B., Semarge, E., Caporuscio, F., and Gooley, R., 1984, Variations in authigenic mineralogy and sorptive zeolite abundance at Yucca Mountain, Nevada, based on studies of drill cores USW GU-3 and G-3: Los Alamos, Los Alamos National Laboratory Report LA-9707-MS, 71 p.

Warren, R.G., Byers, F.M., and Caporuscio, F.A., 1984, Petrography and mineral chemistry of units of the Topopah Springs, Calico Hills and Crater Flat Tuffs, and some older volcanic units, with emphasis on samples from drill hole USW G-1, Yucca Mountain, Nevada Test site: Los Alamos, New Mexico, Los Alamos National Laboratory Report LA-10003-MS.

Warren, R. G., Byers, F. M., Jr., Broxton, D. E., Freeman, S. H., and Hagan, R. C., 1989, Phenocryst abundances and glass and phenocryst compositions as indicators of magmatic

Table 1. Trace-element Concentrations of Selected Specimens of Ash-flow Tuff and Lava, Subsurface of Yucca Mountain, Nevada (Ag and Au in ppb, all other values in ppm)

	Hole #	Depth(ft)	Unit	Ag	Au	As	Bi	Hg	Sb	Mo	Zn
1	UE25B-1H	3773.0	Tctp	38.0	0.5	4.2	0.45	0.066	<0.05	0.38	37.4
2	UE25B-1H	3786.0	Tctp	34.5	0.2	4.8	0.55	0.063	0.22	0.47	37.0
3	UE25B-1H	3796.2	Tctp	37.9	<0.2	7.8	0.44	0.068	0.23	0.33	38.4
4	UE25B-1H	3821.8	Tctp	33.7	0.2	5.2	0.45	0.078	<0.05	0.69	38.2
5	UE25B-1H	3825.0	Tctp	34.1	0.6	7.9	0.45	0.080	<0.05	0.27	39.7
6	UE25B-1H	3935.9	Tct?	33.3	0.3	0.7	0.18	0.153	<0.05	0.23	54.1
7	[a]	3935.9	Tct?	40.1	1.1	<0.75	0.17	0.142	<0.15	0.41	53.2
8	UE25B-1H	3959.9	Tlr	28.6	<0.2	0.5	0.18	0.060	0.14	0.23	41.4
9	UE25B-1H	3985.7	Tlr	33.6	0.2	0.3	0.06	<0.020	<0.05	<0.02	36.4
10	UE25 P1	3870.0	Tot	41.1	0.4	5.2	0.16	0.140	<0.07	1.18	30.8
11	UE25 P1	3890.0	Totp	27.1	<0.2	2.7	0.15	0.053	0.42	0.79	125
12	UE25 P1	3920.0	Tot	29.6	<0.2	3.4	0.11	0.039	0.52	0.62	21
13	UE25 P1	4060.0	Totp	54.0	0.5	47.8	0.12	0.092	1.84	2.86	29.4
14	USW G-1	3368.2	Tctp	41.8	<0.2	8.0	0.34	0.073	0.15	0.37	21.2
15	USW G-1	3372.0	Tctp	39.1	2.7	6.8	0.43	0.070	<0.05	0.64	37.9
16	USW G-1	3392.3	Tctp	36.7	0.4	8.4	0.38	0.069	<0.05	0.68	37.4
17	USW G-1	5846.7	Tot	33.3	0.3	2.6	0.07	0.054	<0.05	<0.02	57.3
18	USW G-2	3420.0	Tcb	14.8	1.5	18.0	<0.05	0.649	5.31	0.46	36.8
19	USW G-2	5232.9	Trlp	28.4	0.3	68.8	<0.05	0.192	<0.05	0.59	50.1
20	USW G-2	5254.0	Trl	26.2	<0.2	85.2	0.06	0.220	0.40	1.16	81.9
21	USW G-2	5260.0	Trlp	28.7	0.2	47.1	0.08	0.220	<0.05	2.05	52
22	[b]	5260.0	Trlp	34.9	1.1	50.0	<0.13	0.188	<0.132	2.2	51.8
23	USW G-2	5263.0	Trl	27.9	<0.2	38.6	<0.05	0.081	0.34	0.18	86.8
24	USW G-2	5697.0	Trl	43.0	0.4	1.6	<0.05	0.061	0.17	0.18	76.8
25	USW G-2	5711.9	Trl	38.6	<0.2	0.5	<0.05	0.178	<0.25	<0.02	78.8
26	USW G-3	4754.7	Tlrp	36.7	<0.2	1.5	0.20	0.078	<0.05	0.13	12.7
27	USW G-3	4790.0	Tlrp	36.7	<0.2	1.3	0.15	0.091	0.11	0.30	32.8
28	USW G-3	4805.0	Tlrp	40.2	0.3	1.2	0.27	0.110	<0.05	0.15	31.7
29	USW G-3	4816.7	Tlrp	41.3	0.3	1.1	0.18	0.111	<0.05	0.12	29.8
30	USW G-3	4828.0	Tlr	34.4	<0.2	1.1	0.18	0.053	0.24	0.29	27.7
31	UE25 C#1	2783.0	Tc	8.5	<0.2	18.1	0.11	0.042	15.1	1.25	40.6
32	UE25 C#2	2688.1	Tc	6.5	0.3	5.5	1.11	<0.020	<0.05	<0.02	17.0
33	UE25 C#2	2830.0	Tc	12.4	<0.2	22.4	0.12	0.026	3.72	8.83	9.3
34	UE25 C#2	2900.0	Tc	10.1	0.3	20.4	0.28	0.050	0.47	12.5	27.3
35	UE25 C#3	2900.1	Tc	12.5	0.3	77.4	0.16	0.075	1.49	0.98	39.1
36	UE25 C#3	2902.2	Tc	21.1	0.4	34.3	1.97	0.153	3.37	193	20.8
37	[c]	2902.2	Tc	10.0	<0.2	37.7	1.24	0.113	3.67	207	23.6
38	[d]	2902.2	Tc	9.9	<0.2	23.0	0.67	0.065	2.35	110	19.3
39	[e]	2902.2	Tc	10.4	<0.2	22.7	0.74	0.064	2.3	109	19.1
40	UE25 C#3	2821.3	Tc	4.5	0.3	35.3	<0.05	0.041	4.67	0.29	12.8
Representative rhyolite ash-flow tuff, surface of Yucca Mountain											
41	3SW-58991		Tpc	14.0	0.3	2.41	0.66	0.030	0.126	0.591	47.4

Analyses by U.S. Mineral Laboratories, Inc., using organic-extraction, inductively-coupled plasma-emission spectrography for all elements except Au which was determined by graphite furnace - atomic absorption spectrometry.

Tct= Tram Tuff of the Crater Flat Group; Tlr= Lithic Ridge Tuff; Tot= pre-Lithic Ridge ash-flow tuffs, undivided; Tcb= Bullfrog Tuff of the Crater Flat Group; Trl= rhyolitic lava underlying the Lithic Ridge Tuff; Tc= Crater Flat Group, undivided; Tpc= upper, densely welded, devitrified ash-flow tuff of the Tiva Canyon Tuff of the Paintbrush Group. p following stratigraphic unit signifies pyrite-bearing sample.

[a] Blind duplicate analysis of #6; [b] blind duplicate analysis of #21; [c] replicate analysis of #36; [d] analysis of a separate split of #36; [e] blind duplicate analysis of #38.

Figure Captions

Figure 1 Map showing the distribution of mines and areas of hydrothermally altered rocks in the region of Yucca Mountain, Nevada. Heavy lines show margins of calderas of the southwestern Nevada volcanic field; PPC(?) = proposed Prospector Pass caldera of Carr et al. (1986). CY = Clarkdale-Yellow Gold mine area, TQM = Tolicha-Quartz Mountain area, TH = Transvaal Hills, MM = Mine Mountain, W = Wahmonie-Hornsilver mine area.

Figure 2 A. Pyrite in lithic fragments and the matrix of the Tram Tuff of the Crater Flat Group at a depth of 3773.3 ft., drill-hole UE25 B1H. B. Disseminated pyrite in the matrix of the Lithic Ridge Tuff from drill-hole USW G-3 at depths of 4816.9 ft., and (C) at 4755.0 ft. p = pyrite, goe = goethite, L = lithic fragment, M = matrix.

Figure 3 Small, disseminated subhedral pyrite grains and a larger, embayed, anhedral grain in propylitically altered silicic lava from a depth of 5232.9 ft. in drill hole USW G-2. p = pyrite.

Figure 4 Distribution of drill holes in Yucca Mountain and the areal extent of selected volcanic-hosted Au-Ag deposits in Nevada. Cross-hatch shows sizes, in plan view, of disseminated gold deposits mined at Borealis, Nevada (Eng, 1991). Heavy lines show the high-grade, 10-25 m-wide Sleeper vein zone (Nash et al., 1991). Filled dots show deep drill holes that penetrated units of the Crater Flat Group; open circles indicate planned deep drill holes; outer circles indicate core holes. Open triangles show planned drill holes that will not penetrate the Crater Flat Group.

Figure 5 Pyrite in the Bullfrog Tuff of the Crater Flat Group in drill-hole USW G-2. A. Disseminated and filmy to granular pyrite in groundmass and in clay-altered pumice fragment in unpolished core at 3501.5 ft. Dashed lines show outline of pumice fragment. B. Pyrite along margin and within silica+calcite veinlet at 3459.4 ft. p = pyrite.

Figure 6 Groundmass (A) and lithic fragment (B) of hydrothermally altered Tonopah Summit Member of the Fraction Tuff (Bonham and Garside, 1979) from dump of the Belcher-Divide mine, Divide mining district, Nevada. Note *lack* of pyrite rim or coating on edge of fragment and the anhedral to subhedral, granular to embayed nature of the pyrite grains. p = pyrite, L = lithic fragment, M = tuff matrix.

Figure 7 A. Pyrite along margins and within clay ± zeolite altered pumice fragment partly filled with clear epoxy, Tram Tuff, drill hole UE25 B1H, 3825.5 ft. B. Unpolished slab of Bullfrog Tuff, drill hole USW G-2, 3503.3 ft., with numerous small (<50 μm) pyrite grains in zeolite+clay altered pumice fragment. p = pyrite.

Fig. 1

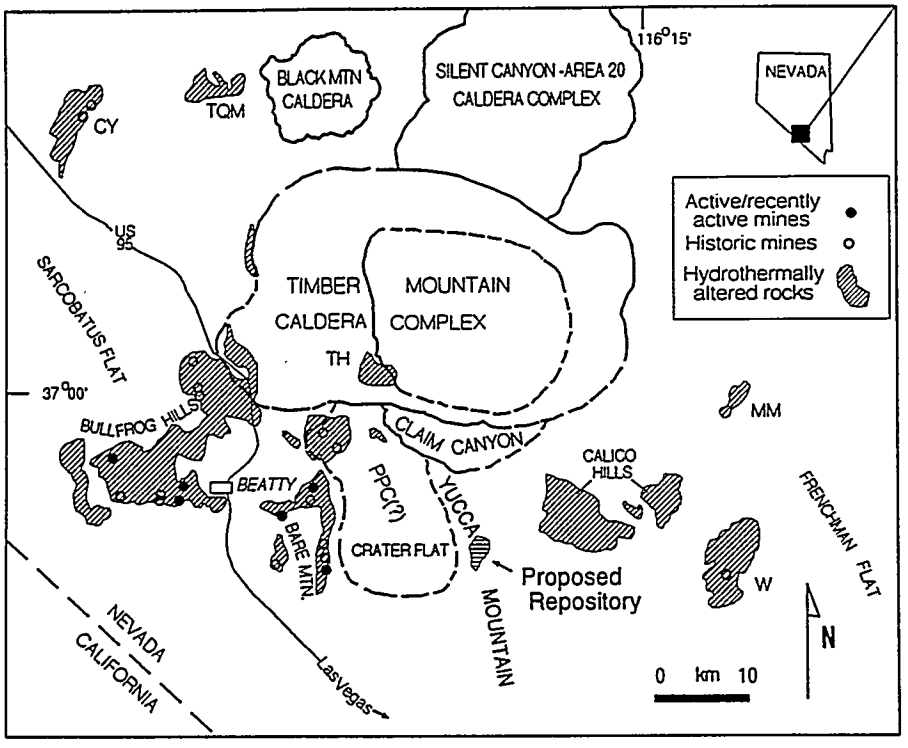
116°15'
NEVADA
BLACK MTN CALDERA
SILENT CANYON - AREA 20 CALDERA COMPLEX
TQM
CY
Active/recently active mines
Historic mines
Hydrothermally altered rocks
US 95
SARCOBATUS FLAT
TIMBER MOUNTAIN CALDERA COMPLEX
TH
37°00'
BULLFROG HILLS
BEATTY
CLAIM CANYON
PPC(?)
YUCCA
CRATER FLAT
BARE MTN.
MM
CALICO HILLS
FRENCHMAN FLAT
Proposed Repository
MOUNTAIN
W
N
NEVADA
CALIFORNIA
Las Vegas
0 km 10

Fig 2
Weiss, Noble
Hanson

Fig. 3

Weiss, Noble + Larson

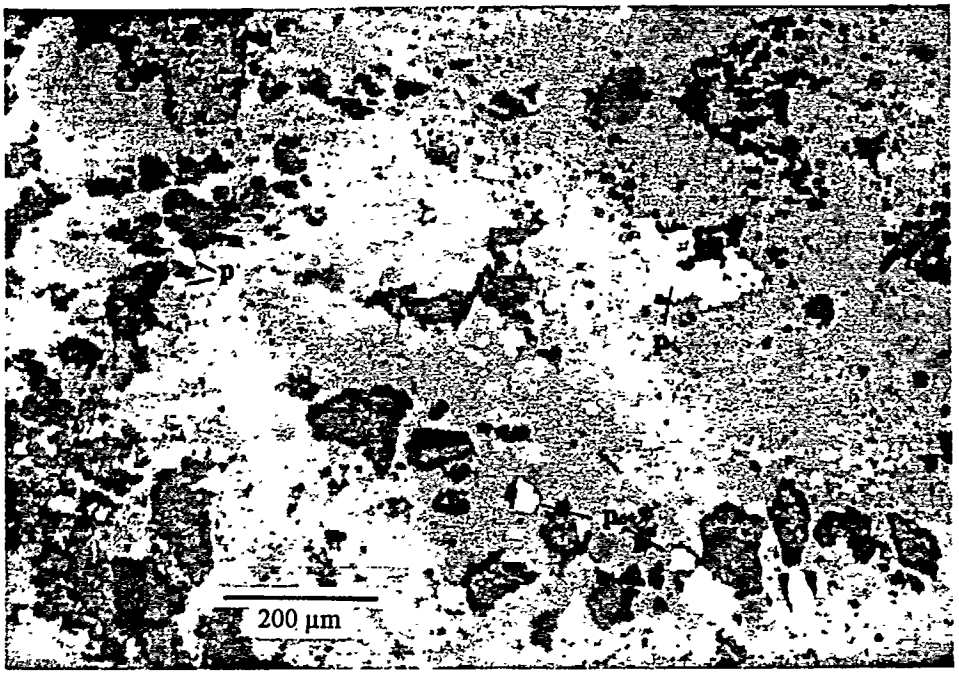

Fig. 4

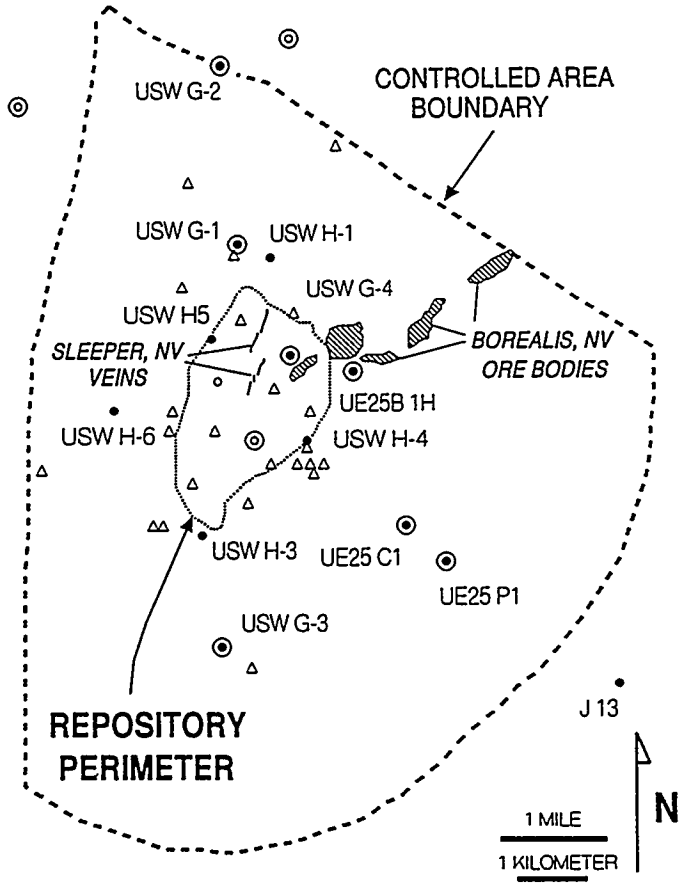
USW G-2
CONTROLLED AREA BOUNDARY
USW G-1
USW H-1
USW G-4
USW H5
SLEEPER, NV VEINS
BOREALIS, NV ORE BODIES
UE25B 1H
USW H-6
USW H-4
USW H-3
UE25 C1
UE25 P1
USW G-3
J 13
REPOSITORY PERIMETER
1 MILE
1 KILOMETER
N

Fig. 5
Weiss, Noble & Larson

Fig. 6
Weiss, Noble & Larson

Fig. 7
Weiss, Wolf et
Lanson

APPENDIX B

revised September 26, 1995 - SIW

Multiple Episodes of Hydrothermal Activity and Epithermal Mineralization in the Southwestern Nevada Volcanic Field and Their Relations to Magmatic Activity, Volcanism and Regional Extension

STEVEN I. WEISS, DONALD C. NOBLE,
Mackay School of Mines, University of Nevada, Reno, Reno, Nevada, 89557
EDWIN H. MCKEE,
U.S. Geological Survey, 345 Middlefield Road, Menlo Park, CA 94025
KATHERINE A. CONNORS AND MAC ROY JACKSON*
Mackay School of Mines, University of Nevada, Reno, Reno, Nevada, 89557

* Present address: Newmont Exploration Ltd., P. O. Box 669, Carlin, NV, 89822-0669.

Abstract

Volcanic rocks of middle Miocene age and underlying pre-Mesozoic sedimentary rocks host epithermal precious metal, fluorite and mercury deposits within and peripheral to major volcanic and intrusive centers of the southwestern Nevada volcanic field (SWNVF) in the southern part of the Great Basin of the western United States. Radiometric ages indicate that episodes of hydrothermal activity mainly coincided with and closely followed major magmatic pulses during the development of the field over a period of more than 4 m.y. Rocks of the SWNVF consist largely of rhyolitic ash-flow sheets, silicic lava domes, and intercalated lava flows and near-vent pyroclastic deposits erupted between 15.2 and 10 Ma from vent areas in the vicinity of the Timber Mountain calderas, and between about 9.4 and 7 Ma from the outlying Black Mountain and Stonewall Mountain centers. In the vicinity of the Timber Mountain calderas, two magmatic stages separated by periods of relative volcanic quiescence can be recognized: the main magmatic stage (15.2 to 12.7 Ma) and the Timber Mountain magmatic stage (11.7 to 10.0 Ma).

During the main magmatic stage most hydrothermal activity coincided with and closely followed ash-flow eruptions of the 12.8- to 12.7-Ma Paintbrush Group. Precious-metal vein deposits of adularia-sericite type of the Wahmonie district formed in the Wahmonie-Salyer volcanic center between about 12.9 and 12.5 Ma, penecontemporaneous with, or at most a few tenths of a million years after, Wahmonie-Salyer volcanism. At about the same time, fluorite and disseminated gold deposits formed in northern and eastern Bare Mountain, 1-2 m.y. after the intrusion of a swarm of silicic porphyry dikes. This timing, together with high Mo, F, Bi and Te, and the spatial association of much of the mineralization with the dikes, suggests a genetic relation to deeper porphyry-type magmatic activity. Continued and/or renewed hydrothermal activity in northern Bare Mountain is suggested by ages of about 12.2 and 11.2 Ma on alunite of probable steam-heated origin near the Telluride mine. Alunite dated at about 12.9 Ma at the Thompson mine indicates that shallow, steam-heated acid-sulfate alteration and Hg mineralization took place at most a few tenths of a million years after eruption of the Paintbrush Group, peripheral to the margin of the related Claim Canyon cauldron.

Hydrothermal activity was more widespread during the Timber Mountain magmatic stage, occurring within a few tenths of a million years after the climactic eruptions of the Timber Mountain Group and coeval with, to as much as 1 m.y. after, the end of post-collapse volcanism of the Timber Mountain caldera cycle. Steam-heated acid-sulfate alteration of units of the Timber Mountain Group and older rocks at the Silicon mine and in the south flank of Mine Mountain took place at about 11.6 and 11.1 Ma, respectively. Identical, aerially extensive alteration in the Calico Hills, dated at about 10.3 Ma, closely preceded the eruptions of nearby and overlying rhyolite domes along the southeast margin of the Timber Mountain I caldera. Acid-sulfate alteration took place at Bailey's hot spring at about 10.2 Ma and in the Transvaal Hills at about 9.9 Ma. Quartz veins and adularia in Oasis Mountain formed at about 10.6 Ma.

Three periods of hydrothermal activity during the Timber Mountain magmatic stage are recognized in the Bullfrog Hills. Gold and silver-bearing, epithermal vein deposits of the low base-metal adularia-sericite type formed in faults cutting ash-flow sheets of the Timber Mountain Group and older units. Quartz-calcite veins at the Yellowjacket mine and north of the Pioneer mine formed within at most a few tenths of a million years after deposition of the 11.45-Ma Ammonia Tanks Tuff of the Timber Mountain Group. Younger and economically more important periods are represented by multistage, Au-Ag bearing fissure veins at the Original Bullfrog, Barrick Bullfrog, Montgomery-Shoshone, Gold Bar, Denver-Tramps and Mayflower mines. Adularia ages show that these deposits formed between about 10.0 to 9.5 Ma, and as recently as about 9.0 Ma, coeval with and as much as about 1 m.y. after, volcanism of the tuffs and lavas of the Bullfrog Hills.

Although hydrothermal activity took place within and adjacent to individual volcanic centers, deposits of economic significance were mainly controlled by normal faults related to regional extensional tectonism, rather than by volcano-tectonic structures such as caldera ring or radial faults, or faults formed by resurgent doming. Two pulses of WNW-ESE directed extension are recognized southeast, south and southwest of the Timber Mountain caldera complex and included the development of the Original Bullfrog-Fluorspar Canyon (OB-FC) fault system, a regional, presently low-angle system of normal faults separating highly faulted and tilted rocks

of the SWNVF from pre-Cenozoic rocks. Fluorite and disseminated gold mineralization in Bare Mountain broadly coincided with the first pulse of faulting, bracketed between 12.8 and 11.7 Ma. Faults and fractures hosting the veins of the Wahmonie district may also represent an early phase of this faulting. The later pulse involved displacement along the Original Bullfrog segment of the OB-FC fault system and imbricate normal faulting and tilting of volcanic rocks to dips as steep as 90°, mainly to the southwest of the Timber Mountain caldera complex. The onset of this deformation took place after 11.45 Ma, but prior to the onset of eruption of the tuffs and lavas of the Bullfrog Hills. Faulting and tilting in the Bullfrog Hills continued synchronously with, and after volcanism of the tuffs and lavas of the Bullfrog Hills, and some of the steeply dipping faults cut the low-angle OB-FC fault, indicating that brittle extension was not rooted in the shallow décollement. Faults formed during this pulse provided the sites of vein deposition in the Bullfrog Hills and continued and/or renewed movement occurred during and after mineralization.

Spatial association and temporal correspondence provide strong evidence for a genetic relation between magmatic and hydrothermal activity in the SWNVF. Faults related to regional extension were critical in localizing precious-metals deposits in the Bullfrog, Bare Mountain and probably the Wahmonie districts, as in other precious-metals districts of late Cenozoic age in the western Great Basin.

Introduction

Volcanic centers of the southwestern Nevada volcanic field (SWNVF) (Fig. 1) record 6 m.y. of intense Miocene igneous activity in the southwestern part of the Great Basin. Epithermal precious-metal, fluorite and mercury deposits are present in widespread zones of hydrothermal alteration within rocks of the field and in underlying pre-Tertiary sedimentary and metasedimentary rocks (Fig. 2). These areas have attracted appreciable exploration and mining activity since the beginning of the 20th century, with total production plus reserves conservatively estimated at about 54 tonnes of gold and 134 tonnes of silver (Castor and Weiss, 1992). Although the volcanic stratigraphic framework, caldera geology and regional hydrology of the SWNVF and younger basaltic activity in the region have been intensively studied (e.g.,

Byers et al., 1989; Noble et al., 1991; Turrin et al., 1991; Sawyer et al., 1994), until recently little attention was directed toward understanding hydrothermal activity in the region either as a process associated with the development of individual volcanic centers or within the context of the development of the entire volcanic field. Initial studies of the timing and stratigraphic settings of hydrothermal alteration and mineralization (Jackson, 1988; Jackson et al., 1988) provided evidence for the broad correspondence of hydrothermal activity to magmatic and volcanic events of the Timber Mountain caldera complex. Noble et al. (1991) pointed out that hydrothermal activity and mineralization were associated with specific magmatic stages in the evolution of the field and Castor and Weiss (1992) emphasized the diverse nature and geologic settings of precious-metal deposits associated with the development of the SWNVF.

In this report we present and interpret geologic information and radiometric age data obtained on hydrothermal minerals from altered and mineralized areas of the SWNVF. We show that multiple, widely distributed hydrothermal systems were broadly coeval with major culminations in magmatic activity of the field, unlike for example, parts of the San Juan volcanic field where hydrothermal mineralization followed caldera formation and major volcanism by 5 to 10 m.y. Although hydrothermal activity took place within and adjacent to individual volcanic centers, faults related to regional extension were a more important element in the control of precious-metal deposits than were volcano-tectonic structures such as caldera ring-fracture systems.

Regional Setting and Volcanic-Stratigraphic Framework

The SWNVF forms part of a broad, discontinuous and compositionally variable belt of volcanic rocks erupted around the periphery of the Great Basin during middle to late Miocene time. This belt is younger than, and in part overprints ignimbrite-dominated Oligocene and early Miocene volcanism. (Armstrong et al., 1969; Stewart and Carlson, 1976; Best et al., 1989). Situated near the southwestern margin of the Great Basin about 150 km NW of Las Vegas, Nevada (Fig. 1), the SWNVF is largely characterized by voluminous silicic ash-flow sheets and intercalated silicic lavas of middle to late Miocene age that were deposited on sedimentary and volcanic rocks of Oligocene to early Miocene age and a complexly deformed and locally meta-

morphosed basement of late Precambrian and Paleozoic sedimentary rocks (Ransome et al., 1910; Cornwall, 1972; Stewart, 1980; Carr, 1984a). The pre-Cenozoic rocks comprise a fairly complete sequence of Late Proterozoic through Mississippian clastic and carbonate continental shelf deposits (Monsen et al., 1990). Most of the volcanic rocks were erupted between about 15.2 Ma and 10 Ma from vents within and peripheral to the central, long-lived complex of collapse-caldera volcanic centers in the Timber Mountain area, and between about 9.5 Ma and 7 Ma from the outlying Black Mountain and Stonewall Mountain centers (Fig. 1; Byers et al., 1989; Noble et al., 1991).

Major stratigraphic units and the volcanic development of the SWNVF are summarized in Table 1. Sawyer et al. (1994) have formally raised most of the regional ash-flow units from the long-used stratigraphic rank of member to the rank of formation, and have raised the formations of previous usage to group rank, resulting in significant changes to the stratigraphic nomenclature that had been in use for more than two decades. Table 1 shows the former nomenclature in parentheses. Numerous radiometric ages constrain the timing of major volcanic events and individual eruptive centers within the field. Radiometric ages have been recalculated, where necessary, using presently accepted abundance and decay constants (Steiger and Jager, 1977; Dalrymple, 1979).

Three distinct periods of magmatic activity may be recognized in the evolution of the SWNVF (Table 1) based on radiometric ages of rocks of the field, together with stratigraphic, petrologic and other geologic data (e.g., Byers et al., 1976a; Noble et al., 1984; Carr et al., 1986; Broxton et al., 1989; Sawyer et al., 1994). These periods have been termed by Noble et al. (1991) the *main magmatic stage*, extending from 15.2 Ma to about 12.7 Ma, the *Timber Mountain magmatic stage* from about 11.7 Ma to about 10 Ma and the *late magmatic stage* from about 9.4 Ma to 7.5 Ma. Within these time intervals, one or more successive ash-flow sheets and cogenetic lava units were erupted from petrologically related magma systems in short, episodic bursts that spanned only 0.1 to 0.4 m.y. (Sawyer et al., 1990, 1994; Noble et al., 1991). Small-volume basaltic cinder cones and lava flows of Pleistocene age in the region (e.g., Turrin et al., 1991) are unrelated to magmatic activity of the SWNVF.

At least nine major ash-flow sheets and many local ash-flow units of rhyolitic composition were erupted during the main magmatic stage, with most of the volcanism occurring between about 14 and 12.7 Ma. Ash-flow units of this stage are commonly zoned from high-silica to low-silica rhyolite and range from subalkaline to peralkaline in composition. Magmatic activity culminated at about 12.8 to 12.7 Ma with the rapid eruption of the four ash-flow sheets of the Paintbrush Group from the Claim Canyon cauldron and the vicinity of Timber Mountain, with a combined original minimum volume of more than 2000 km^3 (Scott et al., 1984).

Eruption of the ash-flow units of the Paintbrush Group was followed by a lull in volcanism of about 1 m.y., during which only relatively small volumes of rhyolitic lava and associated pyroclastic deposits were erupted, mainly near the southern margin of the Claim Canyon cauldron. The Timber Mountain magmatic stage began at about 11.7 to 11.6 Ma with the eruption of rhyolite domes and related pyroclastic aprons (Table 1), remnants of which are preserved within the Claim Canyon cauldron, in the lower part of Beatty Wash and northern Bare Mountain, and in the Bullfrog Hills. This activity was followed closely at 11.6 Ma by the eruption of the voluminous Rainier Mesa Tuff of the Timber Mountain Group and the formation of the Timber Mountain I caldera (Fig. 2) (Byers et al., 1976b; Noble et al., 1991). Eruption of the Ammonia Tanks Tuff of the Timber Mountain Group at 11.45 Ma was accompanied by the formation of the smaller, nested Timber Mountain II caldera. The prominent Timber Mountain resurgent dome formed within, at most, 0.3 m.y. after eruption of the Ammonia Tanks Tuff (Connors et al., 1991). Magmatic activity then continued on a much diminished scale for about 1 m.y. with the emplacement of moat-filling rhyolite tuffs and lavas in the southern part of the caldera (Byers et al., 1976a; 1976b), and the formation of extracaldera rhyolite domes such as those of Shoshone Mountain and in the Bullfrog Hills (Weiss et al., 1990b; Noble et al., 1991). By about 10.5 to 10 Ma, cooling and consolidation of the Timber Mountain magmatic system were sufficient to allow the ascent and eruption of the capping latitic to basaltic lavas in the Bullfrog Hills and the mafic lavas of Dome Mountain within the caldera moat.

Volcanism then shifted to areas northwest of the Timber Mountain caldera complex (Noble et al., 1991). From about 9.4 to about 7 Ma, major magmatic and volcanic activity were

focussed in the outlying Black Mountain and Stonewall Mountain volcanic centers and in the vicinity of Obsidian Butte (Fig. 1). Three extensive and at least three more local units of ash-flow tuff of subalkaline to strongly peralkaline rhyolitic compositions were erupted during this *late magmatic stage*, as well as less voluminous units of silicic to mafic lava. Volcanic rocks of this stage partially filled the moats of the Timber Mountain I and II calderas and distal parts of the Stonewall Flat Tuff reached as far south as Beatty Wash and the southwestern Bullfrog Hills and as far west as the east side of northern Death Valley (Weiss et al., 1988; 1993c).

Relations to Walker Lane structures

The major volcanic centers of the SWNVF are situated near the eastern margins of the Goldfield and Mine Mountain - Spotted Range blocks of the Walker Lane belt (Stewart, 1988). Through-going NW-trending right-lateral strike-slip faults and shear zones of late Cenozoic age, which are characteristic of other parts of the Walker Lane belt, are poorly developed in the SWNVF and, where present, have experienced very little post-midddle Miocene offset. A major, northwest-trending, right-lateral strike slip fault of possible late Cenozoic age between Yucca Mountain and Bare Mountain has been inferred by Schweickert (1989) and northeast- and northwest-trending strike-slip faults have been recognized east of Timber Mountain in the Nevada Test Site (Carr, 1974; 1984a). Most of the movement on these structures appears to have taken place prior to the onset of volcanism of the SWNVF and only locally, as at Mine Mountain (Fig. 2), are rocks of the Timber Mountain Group offset (Orkild, 1968). In places, such as at the north end of Frenchmen Flat (Fig. 2), where faults cutting rocks as young as units of the Timber Mountain Group have been interpreted to define a northwest-trending zone of right-lateral flexural shear (Carr, 1984a), paleomagnetic data show little evidence of vertical-axis rotations and the fault pattern most likely defines an accommodation zone between oppositely tilted extensional domains (Hudson, 1992). Similarly, paleomagnetic data from volcanic strata in other parts of the SWNVF show no evidence for significant rotations about vertical axes that would be expected from major, right-lateral, Walker Lane tectonism during or after development of the SWNVF (Hudson et al., 1994).

Carr (1974; 1984a; 1984b) has proposed that magmatic activity and the development of major volcanic centers of the SWNVF were focussed by deep seated pull-apart structures at right steps between northwest-trending, right-lateral shear zone segments along the eastern margin of the Walker Lane belt. There is little direct evidence to support this idea except, perhaps, for a north-trending gravity low inferred by Carr (1988; 1990) to mark a regional rift zone of middle Miocene age. Most structural features in the SWNVF can be attributed to volcano-tectonic processes, including magmatic tumescence, caldera collapse and resurgent doming (e.g., Christiansen et al., 1977), and to the effects of broadly coeval regional extensional tectonism.

Extensional faulting

Episodes of pre-middle Miocene extension in southwestern Nevada are poorly known from fragmentary evidence (Ekren et al., 1968; Ekren et al., 1971; Schweikert and Caskey 1990; Noble et al., 1991). Basin-and-range style faulting along north-trending normal faults began in the northeastern part of the field between 17 Ma and 14 Ma (Ekren et al., 1968) and continued into Quaternary time (Ekren et al., 1971; Frizzell and Shulters, 1990). Basin-and-range fault displacements are small in much of the field and the large, distinct ranges and valleys of adjacent south-central Nevada pass southwards into the broad volcanic upland of Pahute Mesa. Much of the topography of the SWNVF reflects volcanic and pre-volcanic landforms buried to greater or lesser degrees by successive ash-flow sheets; the exceptionally well-preserved calderas and outflow sheets of the Black Mountain and Timber Mountain centers attest to relatively mild tectonism in the central and northern parts of the field since middle Miocene time.

South and west of the Timber Mountain caldera complex rocks of the SWNVF have been more steeply tilted than in areas to the east and north, locally to dips as steep as 90°, and normal faults are more numerous and more closely spaced (e.g., Carr, 1990). Much of this deformation is associated with the low-angle Original Bullfrog, Amargosa and Fluorspar Canyon normal faults (OB-FC, Fig. 2), which separate highly faulted and tilted rocks of the SWNVF from underlying pre-Cenozoic sedimentary and metamorphic rocks in the southern Bullfrog Hills and northern Bare Mountain (Ransome et al., 1910; Cornwall and Kleinhampl 1961; 1964; Maldon-

ado, 1990a; 1990b; Maldonado and Hausback, 1990; Monsen et al., 1992). Recently some geologists have interpreted these faults as segments of a single, upper crustal, regional detachment fault that accommodated WNW-directed extension of upper-plate rocks, and propose that this fault probably cuts down-section to the southwest through pre-Cenozoic rocks in the Funeral Mountains (Fig. 2), where it is known as the Boundary Canyon fault (Maldonado, 1985; 1990a; 1990b; Carr and Monsen, 1988; Hamilton, 1988; Carr, 1990). Conformable relations between the ash-flow units of the Timber Mountain Group and older, underlying ash-flow sheets in the southern Bullfrog Hills constrain the onset of major faulting and tilting along the Original Bullfrog and Amargosa segments of the OB-FC fault system to after 11.4 Ma (Carr, 1990; Maldonado, 1990a; 1990b; Maldonado and Hausback, 1990). Extensional faulting began earlier above the Fluorspar Canyon segment of the OB-FC fault as shown by angular discordance of as much as 30° between the 12.7-Ma Tiva Canyon Tuff and the 11.6-Ma Rainier Mesa Tuff (Carr and Monsen, 1988; Carr, 1990; Monsen et al., 1992). Extensional deformation between 12.7 Ma and 11.6 Ma also affected areas to the east, such as Yucca Mountain and the Calico Hills where units of the Paintbrush Group and older rocks were offset and tilted prior to deposition of the Rainier Mesa Tuff (McKay and Williams, 1964; Lipman and McKay, 1965; Orkild and O'Connor, 1970; Scott and Bonk, 1984; Carr, 1990).

In the Bullfrog Hills and near the north flank of Bare Mountain the Spearhead Member of the Stonewall Flat Tuff is interbedded with flat-lying conglomeratic deposits that overly and pinch out against the faulted and tilted middle Miocene rocks, indicating that major extension ceased in this area prior to 7.6 Ma (Weiss et al., 1988; 1990b). Most of the deformation associated with the OB-FC fault system and in areas to the east is therefore bracketed between 12.7 and 7.6 Ma. Structural relations in western Pahute Mesa show that extensional faulting in areas to the northwest of the Timber Mountain caldera complex began prior to 13.7 Ma (Minor et al., 1991). Post-7.5-Ma tectonic activity has involved mainly block uplift and faulting with little tilting in areas between northern Death Valley and Pahute Mesa (Noble et al., 1990; Weiss et al., 1993c).

The timing of major WNW-directed extension associated with the OB-FC fault system and in areas to the east corresponds closely to the timing of extension, tilting and basin development elsewhere in the southern Walker Lane belt. Large-magnitude extensional faulting and tilting took place in the Death Valley area between 14 Ma and 8.5 Ma (e.g., Cemen et al., 1985; Wright et al., 1991) and between about 12 and 9 Ma in the Lake Meade-Las Vegas Valley area to the south (Weber and Smith, 1987; Duebendorfer and Smith, 1991; Duebendorfer and Wallin, 1991). To the north in the Silver Peak-Weepah Hills region, detachment-style extension, core complex cooling and development of the Esmeralda basin took place between about 13 Ma and 6 Ma (McKee, 1983; Powers, 1983; Stewart and Diamond, 1990), coeval with much of the faulting and tilting in the Gold Mountain - Slate Ridge area of Esmeralda County (Worthington, 1992; Weiss et al, 1993c).

Timing and Nature of Hydrothermal Activity and Mineralization

Hydrothermal alteration and epithermal mineralization of Neogene age affected volcanic rocks of the SWNVF and underlying basement rocks of pre-Mesozoic age (Fig. 2). Precious-metal and fluorite mines with significant present or past production include the Montgomery-Shoshone, Barrick Bullfrog, Sterling, Mother Lode, Gold Bar and Daisy mines (Fig. 2). The Wahmonie, Mine Mountain, northern Bullfrog Hills, Clarkdale and Tolicha districts have little recorded production, although rich ores are locally present. In addition, dozens of shallow prospect workings are scattered in areas of hydrothermal alteration near Sleeping Butte, Oasis Mountain, north of Bare Mountain and in the Transvaal Hills, the Calico Hills, and northwestern Yucca Mountain (Fig. 2). Various workers have reported on individual mines and prospects (e.g., Ransome et al., 1910; Cornwall and Kleinhampl, 1964; Odt, 1983; Tingley, 1984; Quade and Tingley, 1984; Jorgensen et al., 1989; Greybeck and Wallace, 1991). Castor and Weiss (1992) summarized the general styles of mineralization, alteration and ore mineral assemblages, geochemical characteristics and geologic settings of the Wahmonie, Mine Mountain, Bare Mountain, and Bullfrog districts (Fig. 2). Precious-metal mineralization in these four districts is of the low-sulfidation (adularia-sericite) epithermal type and produced generally base metal-poor disseminated deposits and vein systems. The deposits are hosted by felsic ash-flow tuff, lava,

intercalated sedimentary rocks and intrusive rocks of the SWNVF, and by underlying sedimentary rocks of pre-Mesozoic age. In the case of Wahmonie and Bare Mountain, epithermal precious metal mineralization may be genetically related to deeper porphyry-type igneous activity (Noble et al., 1989; 1991; Castor and Weiss, 1992; Weiss et al, 1993b).

The timing of hydrothermal events is constrained by radiometrically dated rock units (Table 1) and by K-Ar and $^{40}Ar/^{39}Ar$ age determinations on adularia and alunite of hydrothermal origin obtained during this study (Table 2 and McKee and Bergquist, 1993). Alunite and adularia were concentrated using conventional magnetic and heavy liquid techniques. K-Ar and $^{40}Ar/^{39}Ar$ analyses were carried out in the Menlo Park, California, laboratories of the U.S. Geological Survey using standard procedures (Dalrymple and Lanphere, 1969; 1971). The estimated analytical uncertainty at one standard deviation is based on experience with replicate analyses in the Menlo Park laboratories and reflects the uncertainty in the measurement of the argon isotopes, radiogenic ^{40}Ar, and K_2O, and for the $^{40}Ar/^{39}Ar$ analyses, an estimated J-value uncertainty of ±0.5 percent. $^{40}Ar/^{39}Ar$ analyses of samples ~~10~~ 13 and ~~11~~ 14 were carried out on splits of the same concentrates used for the K-Ar analyses. Sample descriptions are given in Appendix 1. Additional information concerning sample collection and analytical procedures is given by McKee and Bergquist (1993).

Hydrothermal Activity Associated with the Main Magmatic Stage

One or more early episodes of hydrothermal activity may have occurred south of the Timber Mountain caldera complex. Approximately 10 km northwest of drill hole USW G-2, in the hills at the north end of Crater Flat (Fig. 2), numerous thin veins of hydrothermal breccia cemented by chalcedonic silica and iron oxides cut the Tram Tuff of the Crater Flat Group, but do not penetrate the overlying 13.3-Ma Bullfrog Tuff of the Crater Flat Group (Weiss et al., 1993a; Fridrich et al., 1994). Above and adjacent to the veins interbedded ash-flow and surge deposits between the Tram and Bullfrog Tuffs have been opalized and contain thin ledges of silica sinter and silicified siltstone.

Wahmonie district: At the Wahmonie district in the southeastern part of the SWNVF (Fig. 2) shallow Ag-Au ores contained in NE-trending quartz-calcite ±adularia veins were worked intermittently on a small scale prior to 1930. The veins are situated within a >30 km^2 area of propylitically and argillically altered andesitic to rhyodacitic lavas, tuffs and breccias of the Wahmonie and Salyer Formations, and dikes and stocks of granodiorite porphyry, andesite and rhyolite (Ball, 1907; Ekren and Sargent, 1965; Castor and Weiss, 1992). These rocks belong to the Wahmonie-Salyer volcanic center (Poole et al., 1965), the eroded remnants of a composite central volcano or dome and flow field of mainly intermediate composition. Volcanism of this center, satellitic to the Timber Mountain caldera complex, is bracketed between the Crater Flat Group and the rhyolite of Calico Hills (Broxton et al., 1989). K-Ar ages of about 13.2 Ma and 12.8 Ma on rocks near the base and top, respectively, of the Wahmonie Formation (Kistler, 1968), are consistent with the stratigraphic constraints (Table 1), as is an age of 13.0 Ma (Sawyer et al., 1994). The undated dikes and stocks have volcanic and subvolcanic groundmass textures and are reasonably interpreted as cogenetic with the surrounding extrusive rocks.

The veins at Wahmonie, as much as 1 to 2 m wide, and quartz-cemented breccia bodies trend northeast and are exposed discontinuously for at least 1 km along strike. These veins contain electrum, hessite and other tellurium-bearing minerals, have bismuth contents as high as 211 ppm, moderately low base-metal contents and are characterized by gangue and selvages containing adularia and sericite (Quade and Tingley, 1984; Castor and Weiss, 1992). K-Ar ages of 12.6 ± 0.4 Ma and 12.9 ± 0.4 Ma (Table 2, samples 2 and 3) have been obtained from adularia separated from intensely adularized and silicified dacitic(?) wall rock containing abundant, closely-spaced veinlets of quartz ± adularia. These ages indicate that hydrothermal activity and mineralization took place in the Wahmonie-Salyer center coeval with, or very shortly after magmatic activity.

As pointed out by Noble et al. (1991) and Castor and Weiss (1992), several lines of evidence suggest the Ag-Au mineralization at Wahmonie may be related to an underlying porphyry system. An altered granodioritic porphyry stock with equigranular to granophyric groundmass texture exposed <1 km north of the veins locally contains abundant quartz veinlets carrying acti-

nolite and pyrite, secondary hypersaline fluid inclusions in quartz phenocrysts and traces of secondary biotite, consistent with the passage of highly saline hydrothermal fluids with a magmatic component. A large felsic pluton beneath and south of the stock is inferred from geophysical data to underlie the district and induced polarization data suggest the presence of ≥2% sulfides below the water table at Wahmonie (Ponce, 1981; 1984; Hoover et al., 1982). In addition, a highly altered body of "intrusive breccia" (Ekren and Sargent, 1965) in the district and the presence of elevated concentrations of tellurium and bismuth in the veins (Castor and Weiss, 1992) are consistent with porphyry-related hydrothermal activity.

Mining activity in the Wahmonie district is believed to have taken place as early as 1853 (Quade and Tingley, 1984), and three shafts to depths of as much as 150 m were sunk following discoveries of high-grade ore in 1928. The stock market crash in 1929 and ensuing depression halted work and little ore was shipped (Cornwall, 1972). In 1940 the district was withdrawn from civilian access for inclusion in the Tonopah Bombing and Gunnery Range and later became part of the Nevada Test Site. The deepest shaft was subsequently used for the disposal of radioactive waste. Consequently, there has been no drilling or systematic geochemical sampling of the veins and workings elsewhere in the district are limited to shallow test pits and a few shallow shafts. Fire assays of selected samples from prospect dumps, vein outcroppings and museum specimens of as much as 31.25 kg silver and 1.03 kg gold per ton (Quade and Tingley, 1984), provide evidence for locally rich Ag-Au mineralization in the district. These data, together with the large lateral extent of the mostly unexplored veins and surrounding alteration zone, suggest a potential for economic Ag-Au mineralization despite the lack of appreciable past production.

Northern and eastern Bare Mountain: To the west, in the northern and eastern parts of Bare Mountain, epithermal fluorite and finely disseminated gold mineralization of approximately the same age as the Ag-Au veins in the Wahmonie district are hosted both by Paleozoic and late Precambrian clastic and carbonate rocks and by rocks of late Cenozoic age (Castor and Weiss, 1992) (Fig. 2). Small amounts of gold and mercury were produced intermittently from the Sterling gold mine and the Telluride gold-mercury camp between 1905 and the late 1970's.

From 1980 through 1993 approximately 150,000 oz of gold were produced from disseminated deposits at the Sterling mine and the Mother Lode mine (Bonham and Hess, 1992; Randol, 1993). Currently subeconomic disseminated gold deposits are present at the Goldspar mine, at and near the Mother Lode mine, at the Secret Pass prospect and in the vicinity of the Daisy mine (Greybeck and Wallace, 1991; Castor and Weiss, 1992). Fluorite was produced from 1918 to 1989, mainly from the Daisy mine, with smaller production from the Goldspar and Mary mines (Papke, 1979; Castor and Weiss, 1992).

Most of Bare Mountain consists of complexly faulted sedimentary and low-grade metasedimentary strata deposited on the North American continental shelf that underwent folding, metamorphism and thrust faulting during Mesozoic time and were exhumed by uplift associated with Cenozoic regional extension (Cornwall and Kleinhampl, 1961; Monsen, 1983; Hamilton, 1988; Monsen et al., 1992). In northern and eastern Bare Mountain the pre-Cenozoic rocks host a swarm of discontinuous, north-trending and steeply dipping, rhyolitic porphyry dikes that are exposed over a north-south distance of 13 km (Fig. 2). The dikes are generally less than 10 meters thick, locally have chilled margins and are variably hydrothermally altered. Dikes between the Sterling and Mary mines contain phenocrystic and primary groundmass feldspar that is partly to completely pseudomorphed by adularia; biotite exhibits little visible alteration. Strong biotite- and potassium feldspar-stable propylitic alteration affects the NNE-trending dike south of the Mother Lode mine. Seemingly unaltered biotite from several of the dikes, all of which are pervasively altered, has given K-Ar ages ranging from about 14.9 Ma to about 13.9 Ma (Marvin et al., 1989; Monsen et al., 1990; Noble et al., 1991), suggesting emplacement during the main magmatic stage. Although the dikes are thin and contain varying amounts of quartz phenocrysts, they have coarsely granophyric groundmass textures and contain secondary, hypersaline fluid inclusions in quartz phenocrysts, consistent with the presence of highly saline fluid. These features and the large lateral extent of the dikes, not typical of other silicic dikes of the SWNVF, and their ages suggest that the dikes are not ring-fracture intrusions related to the postulated Crater Flat-Prospector Pass caldera, as proposed by Carr et al. (1986, p.24). Instead, the silicic dikes probably represent the upper part of a large magmatic system

(Noble et al., 1989; 1991), perhaps with petrochemical similarities to Late Cretaceous, lithophile-element rich stocks and plutons of the Great Basin (Barton and Trim, 1990).

Argillic alteration, bleaching and decarbonatization of the wallrocks accompany the dikes and also are present near the trace of the Fluorspar Canyon fault . Within these zones are areas of fluorite and disseminated gold mineralization at the Sterling, Goldspar, Mary, Mother Lode, Telluride and Daisy mine areas (Fig. 2). A consistent trace element suite including As, Hg, Sb, Ag, Mo, and Tl, and low concentrations of Cu, Pb, and Zn accompany gold and fluorite (Odt, 1983; Tingley, 1984; Greybeck and Wallace, 1991; Castor and Weiss, 1992).

The fluorite deposits at the Goldspar, Mary and Daisy mines consist of banded fluorite veins and small replacement bodies, commonly with cinnabar, in early Paleozoic limestone and dolomite (Cornwall and Kleinhampl, 1964; Papke, 1979; Tingley, 1984). Finely disseminated gold is hosted by clastic and carbonate rocks of latest Precambrian and early Paleozoic age at the Sterling and Goldspar mines, and in the vicinity of the Daisy mine (Odt, 1983; Greybeck and Wallace, 1991). At the Mother Lode mine approximately 35,000 oz of Au were produced from the oxidized cap of a finely disseminated, largely refractory deposit hosted mostly by silicic porphyry dikes and adjacent tuffaceous sandstone, siltstone and interbedded carbonaceous marl and limestone of probable early Miocene age (rocks of Joshua Hollow of Monsen et al., 1990; Weiss et al., 1993b). Underlying Paleozoic sedimentary rocks are mineralized and a smaller, entirely separate deposit has been delineated nearby within quartzite and carbonate rocks probably of the Wood Canyon Formation and other early Paleozoic units (Ristorcelli and Ernst, 1991).

In all of the above deposits alteration is dominantly argillic and quartz veins are not abundant. Silicification is typically absent or weak, although small jasperoid bodies are present near the Mother Lode mine. Base-metal concentrations are low (Cu+Pb+Zn generally < 150 ppm) and Au:Ag ratios are high, generally 1 to 10 for rocks containing 1 ppm or more Au (Odt, 1983; Greybeck and Wallace, 1991; Weiss et al., 1993b). Most sulfides at the Sterling mine are oxidized (Odt, 1983), but at the Mother Lode mine incompletely oxidized rocks contain veinlets and disseminated grains of pyrite, marcasite, arsenian pyrite, arsenopyrite and stibnite (S. I. Weiss and S. J. Ristorcelli, unpub. data, 1993). SEM studies and metallurgical tests on ores of

the Mother Lode deposit show that gold is submicroscopic and resides within sulfide grains (Ristorcelli and Ernst, 1991; S.I. Weiss, unpub. data, 1993). Taken together, the overall style and mineralogy of gold mineralization and associated alteration, elevated As, Sb, Hg, and Tl, and low base metals and Ag contents are typical of the broad class of epithermal, disseminated Au deposits often referred to as "Carlin-type" gold deposits elsewhere in the Great Basin (e.g., Percival et al., 1988; Berger and Bagby, 1990). Unlike most sedimentary-rock hosted disseminated gold deposits, however, Bi and Te concentrations as high as 60 ppm and 5 ppm, respectively, have been found in the Mother Lode deposit (Weiss et al., 1993b), the only deposit for which Bi and Te data are available.

Moderately to steeply dipping faults and fractures structurally below the Fluorspar Canyon fault system provided the principal structural controls and conduits for hydrothermal fluids at the Sterling mine and in the vicinity of the Daisy mine (Odt, 1983; Greybeck and Wallace, 1991). Although much of the Mother Lode deposit is situated adjacent to the northern part of the Fluorspar Canyon fault system, mainly in the hanging wall, exploration drilling has shown that the dikes provided the primary structural control, with relatively high grade ores (0.1 - 0.3 oz/ton Au) comprising a shell along and close to the top of the main dike (Weiss et al., 1993b).

Similar, but generally low grade, disseminated gold mineralization is hosted by the Bullfrog Tuff of the Crater Flat Group above the Fluorspar Canyon fault at the Secret Pass prospect (Fig. 2). Silicification is generally weak and gold is associated with quartz, adularia, calcite, and pyrite (Greybeck and Wallace, 1991). Despite the difference in host-rock lithology, the trace-element assemblage of elevated As, Hg, Sb, Mo, Ag and Tl (Greybeck and Wallace, 1991) is the same as that of the Sterling, Mother Lode and Daisy mine gold deposits (Castor and Weiss, 1992).

Several lines of evidence indicate that hydrothermal activity and gold-fluorite-mercury mineralization in the northern and eastern parts of Bare Mountain took place after emplacement of the porphyry dikes. Bleached rocks, argillic alteration and mineralization of the sedimentary rocks with elevated Mo, F, As, Sb, Hg, ± Tl, Au and Ag in eastern Bare Mountain are spatially closely associated with the dikes. The dikes are largely altered and contain sparse fluorite veins

at the Goldspar and Mother Lode mines. Mineralized dike rocks comprise a large proportion of the Mother Lode gold deposit and altered dikes near the Sterling mine locally contain highly elevated concentrations of Au, Ag, As, Sb, Mo and Hg. K-Ar and $^{40}Ar/^{39}Ar$ ages of about 12.9 Ma have been obtained from adularia that replaces igneous groundmass feldspar and phenocrysts in altered dike rock at the Goldspar mine (Noble et al., 1991), suggesting that alteration and mineralization occurred near the end of the main magmatic stage, 1 to 2 m.y. after emplacement of the dikes. The similar style of fluorite and gold mineralization, alteration, and trace-element signature in the vicinity of the Daisy mine lead us to infer, following Castor and Weiss (1992), a similar timing of hydrothermal acitivity at the Daisy mine area. This also is the case at Secret Pass, where Au-Ag mineralization must be no older than ca. 13.3 Ma, the age of the host rocks of the Bullfrog Tuff. Altered rocks containing adularia and illite can be traced in outcrop into the lower part of the overlying, 12.8-Ma Topopah Spring Tuff of the Paintbrush Group, suggesting an even younger maximum age. A minimum age is provided by the timing of displacement along the Fluorspar Canyon fault which truncated mineralization of the Secret Pass deposit, (Greybeck and Wallace, 1991) and tilted the host rocks and overlying units of the Paintbrush Group as much as about 50° eastward prior to the deposition of onlapping, nearby flat-lying tuffs of the 11.6-Ma Rainier Mesa Tuff. The Secret Pass deposit therefore formed within a few hundred meters of the paleosurface, between 13.3 Ma and 11.6 Ma, and probably after 12.8 Ma.

The formation of gold and fluorite deposits having high Au to Ag ratios 2 m.y. or less after dike emplacement, together with the spatial association with the porphyry dike swarm in eastern Bare Mountain, the high Mo and F contents of altered rocks and the presence of significant Bi and Te at the Mother Lode deposit suggest that Carlin-type (or Carlin-like, cf. Berger and Bagby, 1991, Seedorf, 1991) disseminated gold mineralization in Bare Mountain is related to the porphyry magmatic activity (Noble et al., 1989; 1991; Weiss et al., 1993b).

Interbedded ash-fall, surge and thin ash-flow tuffs associated with the rhyolite domes that predate the Rainier Mesa Tuff are altered to alunite-, kaolinite-, and opal-bearing rocks adjacent to the Mother Lode mine and similar alteration is present southwest of the mine within older rocks along the Tates Wash segment of the Fluorspar Canyon fault. A K-Ar age of 12.2 ± 0.4

Ma (Table 2, sample 6) has been obtained on fine-grained alunite separated from altered tuffaceous conglomerate of the rocks of Joshua Hollow beneath the pre-Rainier Mesa bedded tuffs along the Tates Wash fault. The alunitic conglomerate is part of a poorly exposed section of the (sedimentary) rocks of Joshua Hollow, which elsewhere underlie units of the Crater Flat Group (Monsen et al., 1992) and the 12.2-Ma K-Ar age is therefore not unreasonable. Silurian dolomite along this part of the fault is strongly silicified and subeconomic concentrations of gold and mercury are reportedly present along the fault at depth (D. Fanning, pers. commun., 1987). About 0.5 km to the east, near the Telluride mine, a pipe-like body of hydrothermal breccia in silicified dolomite contains rounded, monomineralic clasts of fine-grained alunite. A K-Ar age of 11.2 ± 0.3 Ma has been obtained on this material (Table 2, sample 4). There is no evidence for the prior existence of significant amounts of sulfide minerals in topographically higher rocks nearby, or in rocks that would have overlain these localities, arguing against a supergene origin for this alunite. Moreover, the carbonate rocks would have buffered fluids associated with the weathering of sulfides. Our interpretation is that alunitic alteration along the Tates Wash segment and in the Telluride mine area reflects shallow hydrothermal activity producing weak Au-Hg mineralization at about 12-11 Ma, with the high sulfate activity required for alunite formation probably produced by the oxidation of condensed H_2S. It is unclear whether this alteration reflects a continuation of the ca. 12.9-Ma activity or a separate, later hydrothermal event. The inferred shallow setting is consistent with the shallow setting of the nearby Secret Pass deposit and requires that considerable uplift and erosion occurred between the time that hypersaline fluid inclusions were trapped in the dikes, and about 12 to 11 Ma.

Base metals, in places accompanied by silver, are found in quartz veins in the western part of Bare Mountain (Cornwall, 1972, Tingley, 1984). These veins postdate folding, cleavage and metamorphic fabrics of inferred Mesozoic age (Monsen, 1983; Monsen et al., 1990) within the Late Proterozoic Stirling Quartzite and the Wood Canyon Formation of Late Proterozoic and Early Cambrian age. The quartz veins, in turn, are truncated by andesite dikes in which the plagioclase and biotite phenocrysts have been thoroughly altered to albite and chlorite, respectively. K-Ar ages of about 26 Ma have been obtained on hornblende from these dikes (Monsen et al.,

1990), suggesting that base-metal mineralization in western Bare Mountain occurred more than 10 m.y. before, and is unrelated to, the emplacement of the silicic dikes and fluorite-Au-Hg mineralization elsewhere in Bare Mountain. At the Gold Ace mine (Fig. 2) coarse, macroscopically visible gold is present along bedding(?) surfaces and compositional layering in marble of lower units of the Stirling Quartzite. Although the age of this deposit is not known, the difference in style of mineralization suggests it is unrelated to the fluorite, Hg and disseminated Au deposits described above.

Thompson mine: Small amounts of mercury were produced during the early 1900's from the Thompson mine located about 5.5 km north of Bare Mountain, near the northern end of Crater Flat (Fig. 2) (Cornwall, 1972; Tingley, 1984). The mine is situated within a large area of argillic and acid-sulfate altered rocks of the Crater Flat Group and Paintbrush Group. (U.S. Geological Survey, 1984; Jackson, 1988). Alteration is structurally controlled by post-Paintbrush, NE- and NNW-trending normal faults, is most intense at intersections between these two fault sets (Ristorcelli and Ernst, 1991), and near the Thompson mine affects rock units as young as the 12.7-Ma Tiva Canyon Tuff. Cinnabar is present as discontinuous stringers within veins composed of fine-grained alunite, halloysite and opaline silica, and as small grains disseminated in ash-flow tuff replaced by porous, fine-grained intergrowths of alunite, opal-CT and kaolinite. We interpret the style and mineral assemblages of alteration and mercury mineralization in and surrounding the Thompson mine to reflect high-level acid alteration and mercury deposition in the vapor-dominated cap above a boiling hydrothermal system. Alunite formed in such an environment is of the steam-heated type of Rye (1993). A K-Ar age of 12.9 ± 0.5 Ma (Table 2, sample 7) has been determined on fine-grained vein alunite from the Thompson mine. This age is indistinguishable, within the limits of the analytical uncertainty, from the age of the host rocks and demonstrates that hydrothermal activity took place within, at most, a few tenths of a million years after deposition of the Tiva Canyon Tuff. In several square kilometers of exposures, mainly to the northeast of the Thompson mine, the alteration does not penetrate the uppermost 30 to 90 m of the Tiva Canyon Tuff, although the lower part of the ash-flow sheet is pervasively

altered, showing that in some areas shallow, syn- to post-Paintbrush hydrothermal fluids did not reach the paleosurface.

Hydrothermal activity associated with the Timber Mountain magmatic stage

Several areas of hydrothermal alteration and epithermal Au-Ag mineralization within and outside the margins of the Timber Mountain caldera complex provide a record of widespread, in part near-surface, hydrothermal activity. This activity was penecontemporaneous with eruption of the 11.6- to 11.45-Ma ash-flow sheets of the Timber Mountain Group, genetically related local units of lava and tuff, and younger units of lava and tuff erupted between 10.5 to 10.0 Ma from vents peripheral to, and west of, the caldera complex.

Silicon mine: Ceramic-grade silica was produced at the Silicon mine (Fig. 2) from steam-heated acid-sulfate altered rocks of the Rainier Mesa Tuff of the Timber Mountain Group (Fig. 3). Alunite separated from alunite and opal-CT bearing tuff at the Silicon mine has given a K-Ar age of 11.6 ± 0.4 Ma (Table 2, sample 5), indicating that hydrothermal activity occurred near the margin of the Timber Mountain I caldera coeval with or, at most, a few tenths of a million years after eruption of the Timber Mountain Group. Near-surface activity occurred at about the same time 7 km to the south at the Telluride mine. Argillic alteration, opalization and pervasive reddish-orange iron-oxide staining surround the alunitic alteration of the Silicon mine and, except where hosted by the Rainier Mesa Tuff, are indistinguishable and have not been separated in Figure 2 from the older argillic and acid-sulfate alteration in the vicinity of the Thompson mine.

Transvaal Hills: North of Beatty Wash in the Transvaal Hills (Fig. 2), argillic and alunitic alteration and silicification affect intracaldera units of the Timber Mountain Group and related, post-collapse lava and tuff within the Timber Mountain I and II calderas (Fig. 2). Quartz veins are present within intracaldera tuffs of the Ammonia Tanks Tuff exposed in the western part of the Timber Mountain resurgent dome. Small amounts of cinnabar are present in acid-leached rocks along the base of the southwest flank of Timber Mountain. The altered rocks are locally overlain by unaltered basaltic lava and ash-flow sheets of the Thirsty Canyon Group (Byers et

al., 1976b), demonstrating that hydrothermal activity ceased prior to about 9.4 Ma. Alunite lining fractures within acid-sulfate altered intracaldera-facies tuffs of the Rainier Mesa Tuff has given a K-Ar age of 9.9 ±0.4 Ma (Table 2, sample 8). This age is consistent with the ages of the host rocks and overlying units and is interpreted to reflect the timing of hydrothermal activity in the Transvaal Hills. Quartz ±pyrite veinlets in cuttings of the Ammonia Tanks Tuff, recovered from depths of between 1050 and 1180 meters in the Coffer #1 oil well in Oasis Valley (Fig. 2), may have formed at about the same time.

Calico Hills: Extensive areas of high-level argillic and advanced argillic alteration are exposed in the Calico Hills, largely within the eroded volcanic dome complex of lavas and near-vent tuffs of the rhyolite of Calico Hills, and overlying units of the Paintbrush Group (McKay, 1963; McKay and Williams, 1964; Jackson, 1988; Simonds, 1989). The volcanic rocks have been altered over wide areas to mixtures of alunite, kaolinite, quartz, opal-CT, and/or chalcedony, locally with sparse pyrite, and to porous acid-leached rock composed mainly of opaline silica. Tabular and irregular replacement bodies of chalcedony and opaline silica are present locally. This style of alteration is interpreted by us to result from high-level, acid-sulfate alteration in a steam-heated, largely vapor-dominated environment. Simonds and Scott (1990) reported the presence of adularia associated with silica and interpreted the alunitic alteration and opaline and chalcedonic silica replacement bodies to reflect areas of paleo hot spring activity. These silica bodies and the presence of adularia within an area of intense alunitic and argillic alteration likely reflect fluctuating water table levels during shallow hydrothermal activity. Argillic and alunitic alteration and silicification can be traced upwards into the Ammonia Tanks Tuff in the eastern part of the Calico Hills, but in the central Calico Hills strongly altered rocks of the Paintbrush Group are directly overlain by unaltered flows of the rhyolite of Shoshone Mountain (Table 1). The rhyolite of Shoshone Mountain consists of rhyolite lava and tuff that represent a thick complex of overlapping and coalesced endogenous domes erupted along the margin of the Timber Mountain caldera complex at and perhaps slightly before about 10.3 Ma, probably from the waning Timber Mountain magmatic system (Noble et al., 1991). These relations bracket hydrothermal activity in the Calico Hills between 11.4 Ma and about 10.3 Ma.

Identical K-Ar ages of 10.4 ± 0.3 Ma, have been determined on alunite from two widely separated localities (Table 2, samples 10 and 11) in the western and eastern parts of the Calico Hills, consistent with hydrothermal activity shortly before eruption of the rhyolite of Shoshone Mountain.

Beneath the altered volcanic rocks in the central part of the Calico Hills, units of Devonian carbonate rocks lie in fault contact above Devonian(?) and Mississippian shale and argillite of the Eleana Formation (McKay and Williams, 1964; Orkild and O'Connor, 1970). Narrow rhyolite dikes intrude the Eleana Formation and a large, shallow stock is inferred from geophysical data to underlie the area (Maldonado et al., 1979; Snyder and Oliver, 1981; Carr, 1984a). The Paleozoic rocks have locally undergone contact metamorphism, presumably associated with the inferred pluton (e.g., Carr, 1984a), and in places contain elevated concentrations of Au, Ag, Sb, As, Cu, Pb, and Zn, scattered base-metal bearing quartz veins, and replacement bodies and veins of brucite, magnesite, fluorite, barite and garnet (Quade and Tingley, 1984; Jackson, 1988; Simonds, 1989; Simonds and Scott, 1990). Although the pluton was considered to be of late Mesozoic age (Carr, 1984a), a middle Miocene age was postulated by Simonds and Scott (1990) based on the fact that alteration and mineralization in both the Paleozoic and Miocene rocks are roughly centered on the geophysically inferred location of the pluton. Further evidence is needed to resolve the relations, if any, between the acid alteration in the volcanic rocks, the contact metamorphism and hydrothermal activity in the underlying sedimentary rocks, and the inferred pluton.

Yucca Mountain: A number of deep drill holes have penetrated rocks of the Crater Flat Group, Lithic Ridge Tuff, intercalated flows of dacitic and rhyolitic lava and older tuffs that have been altered to zeolite- and illite/smectite-dominated assemblages over a lateral extent of at least 20 km^2 beneath Yucca Mountain (e.g. Spengler, 1981; Caporuscio et al., 1982; Maldonado and Koether, 1983; Bish 1987). Veins and irregular cavity fillings of fluorite, barite, quartz and calcite locally are present in these altered rocks and adularia and albite replace feldspar phenocrysts in some intervals (e.g. Warren et al., 1984). The silicic lavas in drill hole USW G-2 are silicified, contain abundant veins of drusy quartz and locally calcite and fluorite, and have

undergone pervasive quartz-albite-calcite, ±chlorite, ±pyrite (propylitic) alteration (Broxton et al., 1982; Caporuscio et al., 1982; Weiss et al., 1992). The Tram and Bullfrog Tuffs and the Lithic Ridge Tuff locally contain small amounts (< 1%) of finely disseminated pyrite in the groundmass, within argillicallly altered pumice fragments and partially replacing biotite, as well as pyrite in veinlets and disseminated in lithic fragments that have been variably silicified, albitized and adularized (Weiss et al., 1990a; 1992; Castor et al., 1992; 1994).. Although veinlets in some of the altered fragments appear to be truncated at the edges of the fragments and may have formed prior to their incorporation in the pyroclastic units (Castor et al., 1994), pyrite disseminated in the altered groundmass and pumice fragments of these tuffs has the same fine-grained, anhedral to subhedral, commonly skeletal and pitted morphology as the pyrite disseminated in propylitically altered silicic lavas beneath Yucca Mountain and is similar to pyrite disseminated in altered ash-flow tuff adjacent to precious-metal deposits in the Round Mountain, Divide, and Bullfrog districts of Nevada (Weiss et al., 1992; 1995). The textural relations, presence of pyrite in pumice fragments, inconsistent lateral and vertical distribution of the pyrite and conditions of temperature, fO_2, and fS_2 far from pyrite stability during major ash-flow eruptions, together provide strong evidence for sulfidation *after* deposition of the ash-flow units (Weiss et al., 1995), in contrast to the interpretation of Castor et al. (1992; 1994), who believe that the pyrite was incorporated from altered wallrocks during the eruption of the tuffs.

The degree of illite-smectite ordering and fluid inclusion homogenization data indicate that alteration temperatures of at least 275°C were reached in the deeper rocks penetrated in drill hole USW G-2 and that maximum temperatures of 200°C and 100°C were reached in rocks of USW G-1 and USW G-3, respectively (Bish, 1987; Bish and Aronson, 1993). K-Ar ages between about 12 and 9 Ma, but mainly of from 11 to 10 Ma, have been obtained from illite (Aronson and Bish, 1987; Bish and Aronson, 1993), consistent with alteration coeval with post-collapse volcanism and magmatic activity of the Timber Mountain II caldera to the north. These ages are 2 to 3 m.y. younger than the youngest altered unit and it is therefore unlikely that they reflect diagenetic or deuteric water-rock interaction during cooling of the host units as suggested by Castor et al. (1992). Following Bish and Aronson (1993), the age data, mineralogy and textural

features are best interpreted as the result of a large, south-flowing hydrothermal system driven by heat from magmatic activity in the nearby Timber Mountain caldera system.

Mine Mountain: Evidence for hydrothermal activity soon after eruption of the Timber Mountain Group is also preserved on the south flank of Mine Mountain, east of the Timber Mountain caldera complex (Figs. 2 and 4). Here argillic and alunitic alteration are present along a northwest-striking normal fault separating the Ammonia Tanks Tuff from tuffs pre-dating the Paintbrush Group (Orkild, 1968). Alunite from this locality has given a K-Ar age of 11.1 ± 0.3 Ma (Table 2, sample 1), providing evidence for alteration within a few tenths of a million years of eruption of the Timber Mountain Group.

On the crest of Mine Mountain, 1.5 km northeast of the area of alunitic alteration, zones of silicification, quartz and quartz-barite veins and hydrothermal breccia mainly within Devonian limestone and dolomite directly above the Mine Mountain thrust fault of Orkild (1968) (Fig. 4) were prospected for silver and mercury during the 1920's (Quade and Tingley, 1984; Castor and Weiss, 1992). This structure, originally considered part of a Mesozoic thrust fault system (Barnes and Poole, 1968), is now thought to have been reactivated with low-angle normal movement of Tertiary age (Carr, 1984a; Caskey and Schweikert, 1992; Hudson and Cole, 1993). Geologic and geochemical data suggest similarities to the Candelaria, Nevada, silver district or, alternatively, overprinting of a Pb and Zn-rich base-metal system by later precious metals and mercury (Castor and Weiss, 1992).

Structural relations suggest that some or all of this mineralization may be younger than the 11.4-Ma Ammonia Tanks Tuff. The veins and hydrothermal breccia cut the Mine Mountain low-angle fault, supporting a Tertiary age for hydrothermal activity. Quartz-barite veins both fill and are cut by moderately to steeply dipping minor faults and fractures that commonly have subhorizontal slickensides (S.I. Weiss and L.T. Larson, unpub. data, 1989). These relations most likely reflect strike-slip movement coeval with vein formation. On the south flank of Mine Mountain, units of the Timber Mountain Group and northwest-striking faults that cut them, are offset with apparent left-lateral displacement of about 1 km by closely spaced northeast-striking faults (Orkild, 1968) referred to by Carr (1984a) as the Mine Mountain fault (Fig. 4). The area

of most numerous veins and intense silicification along the crest of Mine Mountain trends northeast, parallel to the Mine Mountain fault. Synmineralization strike-slip movements of faults and fractures in the zone of veins and silicification may have been kinematically related to the post-Ammonia Tanks displacement on the Mine Mountain fault. If this is the case, hydrothermal activity along the crest of Mine Mountain may be, at least in part, younger than 11.4 Ma, consistent with the 11.1 ± 0.3-Ma age obtained on the nearby alunite-bearing tuff.

Bullfrog Hills - Oasis Mountain area: Multiple episodes of Au-Ag mineralization during the Timber Mountain magmatic stage

The most important production of gold and silver in the SWNVF has been from vein deposits in the Bullfrog Hills, west of the Timber Mountain caldera complex, situated within large areas affected by hydrothermal alteration that post-dated deposition of the Timber Mountain Group (Fig. 2). Following the initial discovery of gold at the Original Bullfrog mine in 1904, gold and silver production from the Bullfrog district totalled at least $3 million by 1940 (Couch and Carpenter, 1943). Most production was from the Montgomery-Shoshone mine, with much smaller production from the Original Bullfrog and Gold Bar mines, several small mines near Rhyolite, and the Mayflower and Pioneer mines about 12 km to the north (Fig. 2). Exploration since the mid-1970's led to the delineation of bulk-mineable reserves at the Montgomery-Shoshone mine, open-pit production for three years at the Gold Bar mine, and the discovery and development of an entirely new deposit, now known as the Barrick Bullfrog mine, that is expected to produce at least 1.8 million ounces of gold (Jorgenson et al., 1989; Castor and Weiss, 1992).

The Bullfrog Hills largely consist of an upper structural plate of highly faulted and tilted Miocene volcanic and minor intercalated sedimentary rocks that are separated from underlying sedimentary and metamorphic rocks of Proterozoic and Paleozoic age by normal faults, including the low-angle Original Bullfrog segment of the OB-FC fault system (Ransome et al., 1910; Cornwall and Kleinhampl, 1964; Maldonado, 1985; 1990a). The volcanic units are mainly silicic ash-flow sheets erupted from volcanic centers of the SWNVF, including the Lithic Ridge Tuff, ash-flow sheets of the Crater Flat, Paintbrush, and Timber Mountain Groups, and interca-

lated lavas of silicic to mafic composition. A local sequence of dominantly rhyolitic lava flows, domes and related near-vent pyroclastic deposits, in many places underlain by olivine basalt and capped by flows of latitic to basaltic lava, overlies the Timber Mountain Group and older ash-flow sheets with apparent angular unconformity of as much as about 35° (Fig. 5) (cf. Maldonado, 1990a; Ahern and Corn, 1981; Weiss et al., 1990b; S.I. Weiss and K.A. Connors, unpub. mapping 1989-1991). This sequence includes the rhyolite of Rainbow Mountain, the latite of Donovan Mountain and the rhyolite of Sober-up Gulch (Maldonado, 1990b; Maldonado and Hausback, 1990; Minor et al., 1993; Sawyer et al., 1994), as well as the underlying olivine basalt, intercalated sedimentary rocks and tectonic megabreccia deposits, and other rhyolite tuffs and flows that overlie the latites in the Bullfrog Hills and Springdale Mountain. For simplicity, the entire assemblage is informally termed the tuffs and lavas of the Bullfrog Hills (Table 1); radiometric ages show that this sequence, was erupted prior to about 10 Ma (Marvin et al., 1989; Noble et al., 1991).

Upper-plate rocks are cut and tilted, mainly to the east, as much as 90° by numerous north- to northeast-striking, generally west-dipping normal faults (Ransome et al., 1910; Cornwall and Kleinhampl, 1964; Maldonado, 1990b; Maldonado and Hausback, 1990; S.I. Weiss and K.A. Connors, unpub. mapping 1989-1991). Fault patterns and structural relations reflect numerous imbricated faults and suggest the presence of both planar-rotational and listric faults. This deformation has long been recognized as the result of strong WNW-ESE directed upper crustal extension estimated at about 25 percent (Ransome et al., 1910) to more than 100 percent (Maldonado, 1988; 1990a). Landslide and debris-flow deposits containing blocks of various volcanic units and pre-Tertiary rocks as much as 700 m in length interfinger with the tuffs and lavas of the Bullfrog Hills and provide evidence for crustal instability and steep topography during this major pulse of extension (Weiss et al., 1990b).

All of the Au-Ag production has come from fissure veins hosted by the Original Bullfrog segment of the OB-FC fault and, more importantly, by portions of moderately- to steeply-dipping normal faults within the upper plate (Fig. 5). The veins consist primarily of banded, crustiform and drusy quartz, bladed calcite, and quartz-calcite cemented breccia of vein fragments and

highly altered wallrock fragments. Throughout the district the veins contain trace amounts of adularia, illite, pyrite (now largely oxidized), and show textural evidence for multiple stages of fracturing, crustiform and banded vein filling, and brecciation (Ransome et al, 1910; Jorgenson et al., 1989; Castor and Weiss, 1992). Principal ore minerals are electrum and acanthite; concentrations of Hg, As, Sb and base metals are generally low in the veins and altered wall-rocks (Hg <0.25 ppm; As <50 ppm; Sb <4.0 ppm; Cu <50 ppm; Pb <25 ppm; Zn <50 ppm), although Cu concentrations as high as several thousand ppm and Sb as high as a few hundred ppm have been reported for high-grade ores of the Original Bullfrog and Barrick Bullfrog mines (Castor and Weiss, 1992). Copper contents are generally greater than Pb or Zn (S. B. Castor and S. I. Weiss, unpub. data, 1990). Silver to gold ratios are low (8:1 at the Montgomery-Shoshone mine and 1:1 to 2:1 at the Barrick Bullfrog mine; Jorgenson et al., 1989). Wallrocks are mainly rhyolitic ash-flow tuffs of the SWNVF and near-vein alteration is characterized by replacement of igneous alkali and plagioclase feldspar by adularia, silica flooding, and the presence of numerous quartz veinlets, disseminated pyrite and small amounts of illite. This rock grades out initially into zones of adularia ±albite replacement of feldspar phenocrysts, thin discontinuous quartz veinlets and minor illite, and at greater distances into large areas of illitic alteration, where plagioclase phenocrysts and groundmass are partly to completely replaced by illite and calcite ±albite, ±adularia (Castor and Weiss, 1992). X-ray fluorescence analyses of a small number of samples from the Barrick Bullfrog and Montgomery-Shoshone mines show that potassium and rubidium concentrations are high with respect to unaltered host rocks and have a clear positive correlation, providing evidence for locally intense potassium and rubidium metasomatism within and near major veins (Fig. 6a). This metasomatism is particularly apparent considering that silicification has not reduced potassium contents through dilution (Fig. 6b). Metasomatized rocks are strongly depleted in sodium (0.07 to 1.68 wt%) and calcium (0.02 to 0.89 wt%). Homogenization temperatures of about 200°C to 150°C and salinities of <1.5 wt% NaCl equivalent have been reported by Jorgenson et al. (1989) for fluid inclusions in samples from the Barrick Bullfrog and Montgomery-Shoshone mines. The above features are characteristic of the low base metal type of the adularia-sericite (low-sulfidation) class of volcanic-hosted

epithermal precious metal deposits, which include Oatman, Arizona, Aurora, California, and Round Mountain, Sleeper and National, Nevada.

Southern Bullfrog Hills: The principal fissure vein at the Barrick Bullfrog mine (Fig. 2) follows a normal fault (Middle Plate fault of Jorgenson et al., 1989) dipping approximately 45° westward that brings an east-dipping hanging-wall section of tuffs belonging to the Crater Flat Group, Paintbrush Group and Timber Mountain Group, against ash-flow tuffs of the Crater Flat Group and an underlying unit of silicic lava that is widely exposed beneath the Crater Flat and Lithic Ridge Tuffs elsewhere in the Bullfrog Hills (cf. Maldonado and Hausback, 1990). The main vein (Fig. 7a) varies from about 10 to 40 m in width and consists of multiple generations of complexly cross-cutting and closely spaced veins and sheeted veins, and altered wallrock fragments and brecciated vein fragments surrounded by later stages of quartz and/or calcite. Some of the quartz is amethystine. These features provide strong evidence for multiple stages of vein deposition concurrent with multiple episodes of fracturing and brecciation and demonstrate repeated fault movements during mineralization. Fragments of pre-Cenozoic sedimentary rocks are not uncommon locally, requiring upward transport by explosively boiling hydrothermal fluids. Ore minerals include Ag-poor and Ag-rich electrum, acanthite and uytenbogaardtite (Ag_3AuS_2) in close paragenetic association, commonly accompanied by chrysocolla, suggesting final Au-Ag-S equilibration at temperatures near 113°C (Barton, 1980; Castor and Weiss, 1992; Castor and Sjoberg, 1993). Traces of tetrahedrite, chalcopyrite and galena have also been reported (Jorgenson et al., 1989). In higher levels of the mine well-developed subparallel fault surfaces form the upper and lower boundaries of the main vein, much of which is highly shattered (Fig. 7b); at deeper levels these fault surfaces become anastomosing and transect the main vein, indicating that movement of the host fault continued after the final stages of vein deposition (Weiss et al., 1991; Castor and Weiss, 1992). Adjacent hanging-wall rocks, largely of the Rainier Mesa Tuff, contain disseminated pyrite and abundant adularia as intergrowths with fine-grained, secondary quartz in the groundmass and abundant thin veins of quartz and calcite, locally with traces of adularia. Adularia, less commonly albite, and locally quartz replace the sanidine and plagioclase phenocrysts. Footwall lavas adjacent to the main vein are albitized,

contain disseminated pyrite, and are cut by ore-grade stockwork zones consisting of two types of Au-bearing veins: quartz-calcite-adularia veins and veins containing mixtures of hydrothermal breccia, solid black hydrocarbon, pyrite, quartz, chlorite and calcite (Fig. 7c).

Gold and silver were produced at the Montgomery-Shoshone mine 2 km to the north (Fig. 2) from quartz-calcite veins and vein-cemented fault breccia texturally, chemically and mineralogically similar to mineralization at the Lac Bullfrog deposit (Jorgenson, et al., 1989; Castor and Weiss, 1992). Veins at the Montgomery-Shoshone mine are hosted by steeply-dipping faults and fractures in the upper plate, largely within the Ammonia Tanks Tuff (Maldonado and Hausback, 1990). Alteration, including strong adularization and silica flooding within and adjacent to the veins, is identical to that observed at the Barrick Bullfrog mine and elsewhere in the southern Bullfrog Hills, such as at the Denver-Tramps and Gibraltar mines near Rhyolite (Fig. 2 and Fig. 5). At the Denver-Tramps and Gibraltar mines Au-Ag bearing quartz-calcite veins are also hosted by high-angle faults within units of the Paintbrush and Timber Mountain Groups, and are texturally, mineralogically and geochemically similar, if not identical, to those of the Montgomery-Shoshone and Barrick Bullfrog mines (Castor and Weiss, 1992).

At the Original Bullfrog mine in the western part of the district Au-Ag ore was mined along the shallowly north-dipping Original Bullfrog segment (Ransome et al., 1910) of the OB-FC fault within a shattered, tabular mass of complexly cross-cutting open-space quartz and calcite veins, brecciated veins and vein-encrusted and silicified wallrock fragments. Cross-cutting and textural relations reflect repeated episodes of fracturing, brecciation and open-space filling, consistent with fault movements during vein formation. Sheeted veins and quartz-calcite cemented breccia extend upward into adjacent adularized and silicified rocks of the moderately east dipping Lithic Ridge Tuff and underlying silicic lava, but the main body of vein material appears to be truncated against underlying, highly sheared Paleozoic clastic and carbonate rocks (Carr et al., 1986; Maldonado, 1990a). This truncation, along with the shattered nature of the vein, provides evidence for late movement along the Original Bullfrog fault after the final stages of vein deposition (Ransome et al., 1910). Ore and gangue mineralogy and textures, initially described by Ransome et al. (1910), and minor element signatures are remarkably similar to that

of the Barrick Bullfrog mine, including the presence and close paragenetic association of uytenbogaardite replacing gold-poor electrum and intergrown with gold-rich electrum, acanthite and chrysocolla. (Castor and Weiss, 1992; Castor and Sjoberg, 1993).

Adularia separated from ore composed of a mixture of quartz-calcite veins and adularized wallrock fragments at the Barrick Bullfrog mine has given an $^{40}Ar/^{39}Ar$ age of 9.8 ± 0.3 Ma (Table 2, sample 18), in agreement with a more precise, $^{40}Ar/^{39}Ar$ incremental-heating age of 9.99 ± 0.04 Ma reported by Eng et al. (1995). Based on these two ages, an average age for mineralization at the Barrick Bullfrog mine is *ca.* 9.9 Ma. Two kilometers to the northeast at the Montgomery-Shoshone mine, adularia separated from vein and altered wallrock material has given a K-Ar age of 9.5 ± 0.2 Ma (Morton et al., 1977), which is a minimum of 0.2-0.3 m.y. younger than the incremental-heating age of the Barrick Bullfrog deposit. These data, together with the similarities in style of alteration and mineralization, and structural and stratigraphic settings, provide evidence that closely similar mineralization may have been episodic and related to separate hydrothermal systems, rather than a single large system. Veins and Au-Ag deposits at the nearby Denver-Tramps and Gibraltar mines, 1.5-2 km west of the Barrick Bullfrog mine, also share the above similarities, and may have formed during the *ca.* 9.9 Ma pulse of hydrothermal activity.

K-Ar and $^{40}Ar/^{39}Ar$ ages of 8.7 ± 0.3 Ma and 9.2 ± 0.3 Ma, respectively, have been obtained on two splits of adularia separated from a single specimen of thoroughly adularized and silicified Lithic Ridge Tuff at the Original Bullfrog mine (Table 2, sample 13). These ages are indistinguishable within the limits of the analytical uncertainty. Although $^{40}Ar/^{39}Ar$ age determinations of sanidine are in some cases considered to be more reliable than K-Ar ages (e.g. Hausback et al., 1990), on the basis of the analytical data alone it is difficult to assign greater weight to one determination over the other; a reasonable estimate of the age of hydrothermal activity and mineralization at the Original Bullfrog mine is about 9 Ma. This estimate and the $^{40}Ar/^{39}Ar$ age are distinctly younger than the ages determined from adularia from the Barrick Bullfrog mine. The presence of the rare mineral uytenbogaardtite with similar paragenetic association in high-grade ores at both the Original Bullfrog and the Barrick Bullfrog mines provides

evidence for nearly identical hydrothermal activity and mineralization at the Original Bullfrog mine as much as 1 m.y. after that of the Barrick Bullfrog area.

Multi-stage quartz-calcite veins and vein-cemented breccia along normal faults in the upper plate were also mined for gold and silver at the Gold Bar mine, located about 4 km to the northwest of the Original Bullfrog mine (Fig. 2 and Fig. 5). Wallrocks include ash-flow tuffs of the Crater Flat Group and the Paintbrush Group, demonstrating that hydrothermal activity is younger than about 12.8 Ma. The veins occupy faults that formed during the same pulse of extensional faulting, bracketed between 11.4 Ma and 7.6 Ma, and gangue mineralogy and textures, wallrock alteration style and assemblages, and trace-element geochemistry are essentially identical to those at the Original Bullfrog, Barrick Bullfrog, and Montgomery-Shoshone mines. As pointed out by Ransome et al. (1910), slickensided fault surfaces and thin seams of gouge present within the veins and locally separating the veins from adjacent wallrocks indicate that faulting continued after deposition of the veins. Although not dated radiometrically, mineralization at the Gold Bar mine is inferred to have taken place at the same time as, and to be genetically related to, ore formation elsewhere in the southern part of the Bullfrog Hills.

Northern Bullfrog Hills and Oasis Mountain: The coarse landslide and debris-flow deposits that interfinger with the tuffs and lavas of the Bullfrog Hills host gold- and silver-bearing quartz-calcite veins along fractures and normal faults at the Mayflower mine in the northern Bullfrog Hills (Fig. 2 and Fig. 5). These veins are texturally, mineralogically and geochemically similar to veins in the southern Bullfrog Hills (Castor and Weiss, 1992). North of the Mayflower mine, rocks of the Crater Flat and Paintbrush Groups are silicified and adularized in the vicinity of quartz, quartz-calcite and calcite veins occupying normal faults and fractures. Silicified and adularia-bearing rocks are surrounded by areas in which sanidine has been preserved and plagioclase has been replaced by illite and/or kaolinite. Similar alteration is present at Oasis Mountain (Fig. 2) where quartz and quartz-calcite veins containing subeconomic concentrations of Au and Ag are present along a steeply dipping fault within a thick section of the Ammonia Tanks Tuff. Alteration to the south and southwest, between Oasis Mountain and Bailey's hot spring, is largely argillic, but includes areas of opal-alunite-kaolinite alteration, locally

with pyrite, interpreted as the result of shallow, steam-heated acid-sulfate alteration above a fluctuating water table. This zone includes the area of intense alunitic alteration and silica-rich leached rock, locally with native sulfur, within the Ammonia Tanks Tuff at Bailey's hot spring (Fig. 2).

Two splits of adularia from the same sample of adularized and silicified wallrock fragments incorporated in vein material from the Mayflower mine give K-Ar and $^{40}Ar/^{39}Ar$ ages of 10.0 ± 0.3 and 9.9 ± 0.3 Ma, respectively (Table 2, sample 14). These ages are identical to those of the Montgomery-Shoshone and Barrick Bullfrog mines, within the limits of the analytical uncertainty, and are about 0.7 m.y. older than the $^{40}Ar/^{39}Ar$ age from the Original Bullfrog mine.

An earlier episode of hydrothermal activity is evident north of the Mayflower mine. A K-Ar age of 11.0 ±0.4 Ma has been obtained on adularia separated from metasomatized tuff of the Crater Flat Group along a quartz vein about 1.5 km south of the Yellowjacket mine (Table 2, sample 15). At the Yellowjacket mine (Fig. 2) adularia separated from quartz-calcite-pyrite vein material containing fragments of adularized tuff has given an $^{40}Ar/^{39}Ar$ age of 11.3 ±0.3 Ma (Table 2, sample 17). These ages reflect hydrothermal activity in the northern part of the Bullfrog Hills within at most a few tenths of a million years after deposition of the Ammonia Tanks Tuff and volcanism of the local tuffs and lava of Fleur de Lis Ranch and tuff of Cut-off Road in the nearby, western part of the Timber Mountain I caldera.

A K-Ar age of 10.6 ±0.3 Ma (Table 2, sample 12) determined on adularia separated from potassium metasomatized and silicified tuff of the Ammonia Tanks Tuff adjacent to the veins in Oasis Mountain falls between, and overlaps within the limits of analytical uncertainty, both the K-Ar age from the Mayflower mine and the K-Ar age from the northern Bullfrog Hills. Hypogene alunite replacing phenocrysts and groundmass in the Ammonia Tanks Tuff at Bailey's hot spring has given a K-Ar age of 10.2 ±0.3 Ma (Table 2, sample 9). This age is identical, within the limits of the analytical uncertainty, to the age from Oasis Mountain and the ages from the Mayflower and Barrick Bullfrog mines. In contrast to the water-saturated conditions reflected by the veins and adularia-stable alteration within the Ammonia Tanks Tuff at Oasis Mountain,

vapor-dominated conditions south of Oasis Mountain between about 10 to 10.5 Ma are implied by the high-level acid-sulfate alteration within the same unit at Bailey's hot spring, and within overlying megabreccia deposits (presumably deposited in topographically low areas) that are widely exposed west and northwest of Bailey's hot spring (Fig. 5). Stratigraphically equivalent megabreccia and conglomerate at the Mayflower mine apparently were below the water table at about 10 Ma.

Hydrothermal activity poorly constrained in time

Areas of argillic alteration, quartz veins, opaline silicification, and/or locally abundant iron oxides after pyrite are present near the structural margin of the Claim Canyon cauldron in northern Yucca Mountain (Fig. 2). Units of the Crater Flat Group, Paintbrush Group, and Paintbrush-related lava and caldera-margin breccia (Byers et al., 1976b) are affected by this alteration. Accordingly, hydrothermal activity in these areas must at least in part be younger than 12.7 Ma, although earlier alteration of the Crater Flat Group can not be ruled out. These areas may represent stratigraphically and topographically higher parts of the large, *ca.* 11- to 10-Ma hydrothermal system recognized within Yucca Mountain, where hydrothermal fluids perhaps ascended to higher stratigraphic and topographic levels along numerous faults and fractures near the structural margin of the Claim Canyon cauldron, and/or may reflect closer proximity to Timber Mountain magmatic activity.

Northwest of the Timber Mountain caldera complex, areas of hydrothermal alteration and precious-metal mineralization are present in Quartz Mountain and in the Clarkdale-Yellow Gold area (Fig. 2; Cornwall, 1972; Quade and Tingley, 1984). Gold- and silver-bearing epithermal quartz veins are hosted by north- to northeast-trending faults and fractures (Quade and Tingley, 1984). Veins and silicification in the Quartz Mountain area are present in silicic lavas stratigraphically below the 13.7-Ma Grouse Canyon Tuff of the Belted Range Group (Noble and Christiansen, 1968) and possibly older than the tuff of Tolicha Peak. A K-Ar age of 13.9 ±0.4 Ma (Table 2, sample 16) has been obtained on devitrified groundmass of the tuff of Tolicha Peak from an exposure on the south flank of Gold Mountain (Fig.1). The Grouse Canyon Tuff

is not present in the mineralized areas and it is not altered in exposures 1 to 2 km to the east; it is therefore impossible to place a lower limit on the age of mineralization.

Alteration and Au-Ag mineralization in the Clarkdale-Yellow Gold mining area is bracketed between about 11.4 and 7.5 Ma. Examination of aerial photographs and brief field reconnaissance indicate that quartz-calcite veins of the district are hosted by tuffs of the Timber Mountain Group, overlying units of coarse volcanic conglomerate and sandstone, and lava assigned by Minor et al. (1993) to the 8.8 ±0.3 Ma rhyolite of Obsidian Butte (Noble et al., 1991). Adularia- and illite-bearing altered rocks, similar to those of the Bullfrog district, are present along faults and fractures within the Rainier Mesa and Ammonia Tanks Tuffs along faults and fractures. The overlying sedimentary rocks and small plugs and a dome of the rhyolite of Obsidian Butte have been locally replaced by nearly monomineralic bodies of alunite and chalcedonic quartz, as well as by mixtures of kaolinite, alunite, opal and chalcedonic quartz. Unaltered tuffs of the Spearhead Member of the Stonewall Flat Tuff directly overlie intensely altered conglomerate near the Yellow Gold mine, demonstrating that hydrothermal activity in the district ceased prior to about 7.5 Ma.

Evidence for hydrothermal activity early in the development of the SWNVF is found east and south of Sleeping Butte, near the western margin of the Timber Mountain I caldera (Fig. 2), where the tuff of Sleeping Butte and tuffs of a thick, unnamed ash-flow unit have undergone variable degrees of silicification and adularization. Nearby tuffs of the Ammonia Tanks Tuff are unaltered, indicating that hydrothermal activity ocurred prior to about 11.45 Ma.

Interrelations of Mineralization, Magmatic Activity, and Extensional Faulting

Epithermal mineralization is found in areas of hydrothermal alteration within and marginal to volcanic and intrusive centers of the SWNVF (Fig. 2), as has been observed in other intracontinental volcanic fields of Cenozoic age, such as the Mogollon-Datil (Elston et al., 1973), San Juan (e.g., Lipman et al., 1976), and Jemez (Gardiner et al., 1986; Woldegabriel and Goff, 1989) volcanic fields. This distribution around and within the Timber Mountain caldera complex, and initial K-Ar age determinations and stratigraphic information, led Jackson et al.

(1988) and Jackson (1988) to propose that, with the exception of Wahmonie, the Thompson mine and possibly eastern Bare Mountain, most areas of hydrothermal activity and epithermal mineralization in the southern part of the field were related to the intense, widespread magmatic and volcanic activity of the Timber Mountain magmatic system. Further work led Noble et al. (1991) to emphasize the temporal and spatial association of hydrothermal activity and mineralization with magmatic events of *both* the main and Timber Mountain magmatic stages in the development of the SWNVF.

Radiometric ages for hydrothermal activity in the southern part of the field (Fig. 8) overlap and closely follow the culminations of the main and Timber Mountain magmatic stages at about 12.7 Ma and 11.45 Ma, respectively. During the main magmatic stage, silicic porphyry dikes in Bare Mountain and calc-alkaline, intermediate-composition lavas, tuffs and intrusions at Wahmonie were derived from magma systems peripheral to the central caldera complex. Most fluorite and gold mineralization in the eastern part of Bare Mountain was associated with hydrothermal activity between about 13 Ma and 12.5 Ma that followed the emplacement of the silicic porphyry dikes by about 1 to 2 m.y. This time lag probably reflects continued and/or renewed magmatic activity of the deeper porphyry system. Shallow acid-sulfate alteration and epithermal mercury mineralization took place at the Thompson mine, near the southwestern margin of the Claim Canyon cauldron, within a few tenths of a million years after eruption of the Tiva Canyon Tuff, which marked the culmination of the main magmatic stage (Broxton et al., 1989; Noble et al., 1991; Sawyer et al., 1994). Epithermal Ag-Au vein deposits formed in the Wahmonie district at about the same time, during the latter stages of, or shortly following igneous activity of the Wahmonie-Salyer volcanic center.

During the Timber Mountain magmatic stage, alunitic alteration formed at the Silicon mine, near the Telluride mine and at Mine Mountain, probably as the result of oxidation of H_2S and acid leaching in shallow, steam-heated portions of hydrothermal systems peripheral to the Timber Mountain caldera complex. The earliest episode of adularia-stable alteration and associated quartz-calcite vein formation in the northern Bullfrog Hills occurred at about 11.3 to 11 Ma, coeval with or at most a few tenths of a million years after eruption of the Ammonia Tanks Tuff,

tuffs and lavas of Fleur de Lis Ranch, and the 11.4-Ma tuff of Cut-off Road. South of the central caldera complex, ages of from 11 to 10 Ma on illite from tuffs of pre-Paintbrush age in the subsurface of Yucca Mountain suggest that a hydrothermal system of large lateral extent was associated with the waning Timber Mountain magmatic system centered not far to the north. Alteration in northern and northwestern Yucca Mountain affected rocks as young the Paintbrush Group, and, although not radiometrically dated, may be of the same age. Hydrothermal fluids may have ascended to higher stratigraphic and topographic levels in northern Yucca Mountain along faults and fractures related to the margin of the Claim Canyon cauldron, possibly because of the close proximity to the Timber Mountain magma system.

Following collapse of the Timber Mountain II caldera and eruption of the tuffs and lava of Fleur de Lis Ranch and tuff of Cut-off Road in the western part of the caldera complex, magmatic activity and volcanism continued until about 10 Ma with the eruption of mainly rhyolitic domes and related pyroclastic deposits, and smaller volumes of latitic and basaltic lavas in the Bullfrog Hills (see below) and within and adjacent to the southern margins of the complex. Shallow, steam-heated alunitic and argillic alteration in the Calico Hills, Transvaal Hills and at Bailey's hot spring, and adularization and quartz vein formation at Oasis Mountain were penecontemporaneous with this volcanism. In the southern Bullfrog Hills and at the Mayflower mine adularia ages of about 10 to 9 Ma indicate that alteration and epithermal Au-Ag mineralization were penecontemporaneous with, and continued for about 1 m.y. after, the end of volcanism in the Bullfrog Hills.

Coeval extension, magmatic activity and volcanism, and precious-metal mineralization in the Bullfrog Hills-Oasis Mountain area

A simplified stratigraphic diagram showing major units, radiometric ages and structural relations of the tuffs and lavas of the Bullfrog Hills to older and younger rocks in the Bullfrog Hills is given in Figure 9. Two principal units of interbedded ash-flow tuff and pyroclastic surge deposits of high-silica rhyolite are each overlain and intruded by rhyolite plugs, domes and flows (Fig. 9). These two pyroclastic units and a number of the rhyolite plugs, domes and flows are petrographically and lithologically similar to tuffs of the Rainier Mesa Tuff, containing abundant

large phenocrysts of quartz and alkali feldspar, with lesser amounts of sodic plagioclase, accessory biotite and only traces of hornblende in some rocks. The pyroclastic rocks have abundant small- and large-scale cross bedding, scour-and-fill structures and discontinuous, extremely lithic-rich layers, and are reasonably interpreted as near-vent pyroclastic deposits associated with the eruption of certain of the rhyolite domes and flows (Maldonado and Hausback, 1990; Weiss et al., 1990b; Noble et al., 1991). Radiometric ages from rocks of the tuffs and lavas of the Bullfrog Hills (Fig. 9), including thin flows of olivine basalt locally present at the base of the sequence, suggest that the entire sequence was erupted rapidly between about 10.5 to 10 Ma. The rhyolitic domes, flows and related tuffs of the sequence are reasonably interpreted as products of the latter stages of the Timber Mountain caldera cycle, based on their ages, proximity to the western margin of the Timber Mountain caldera complex and similarities to the Rainier Mesa Tuff (Noble et al., 1991).

Several lines of evidence indicate that extensional faulting and tilting in the Bullfrog Hills were coeval with the eruption of the tuffs and lavas of the Bullfrog Hills. No obvious angular discordance is present between the ash-flow sheets of the Timber Mountain Group or underlying ash-flow sheets in the Bullfrog Hills, constraining major faulting to be younger than 11.45 Ma. However, throughout the Bullfrog Hills the Ammonia Tanks Tuff and older units dip more steeply than do nearby younger rocks of the tuffs and lavas of the Bullfrog Hills (Cornwall and Kleinhampl, 1964; Maldonado, 1990b; Maldonado and Hausback, 1990) and in widely separated locations, an angular discordance of as much as 35° is present between units of the tuffs and lavas of the Bullfrog Hills and the underlying rocks (Fig. 5) (Ahern and Corn, 1981; Connors, Weiss and Noble, Plate 1 *in* Connors, 1995). This discordance most likely represents a district-wide angular unconformity (Fig. 9) and demonstrates that faulting and substantial tilting began prior to volcanism of the tuffs and lavas of the Bullfrog Hills, contrary to the interpretation of Maldonado (1990a). Layers of coarse breccia that locally contain enormous blocks of pre-Cenozoic and Cenozoic units, including the Rainier Mesa Tuff, Ammonia Tanks Tuff, tuffs and lava of Fleur de Lis Ranch and the tuff of Cut-off Road, interfinger with units of the tuffs and lavas of the Bullfrog Hills (Fig. 5 and Fig. 9). The unequivocal presence of blocks of the post-

Ammonia Tanks units rules out an origin associated with collapse of the Timber Mountain I or II calderas. These breccia layers are interpreted as tectonic megabreccia, consisting of landslide and debris-flow deposits shed from steep topography, such as fault scarps, during deposition of the tuffs and lavas of the Bullfrog Hills (Weiss et al., 1990b). One or more major, west-facing scarps probably formed along the Oasis Valley fault zone (Fig. 5) where the Ammonia Tanks Tuff has been displaced at least 600 to 900 meters by down-to-the-west movement (Connors et al., 1995).

Further evidence for synvolcanic tectonism comes from the latitic lavas near the top of the tuffs and lavas of the Bullfrog Hills (Fig. 9). Locally there is an upwards decrease in the dip of successive latite flows, and in the northern Bullfrog Hills the latites drape fault scarps and irregular topography cut in underlying rhyolite flows and tuffs (Cornwall and Kleinhampl, 1964; Connors, Weiss and Noble, Plate 1 *in* Connors, 1995). Rhyolite plugs and dikes of the sequence, which in some cases can be traced upwards into domes and flows, both intrude and are also cut by normal faults, providing evidence for the interaction of silicic magmas that fed eruptions of the tuffs and lavas of the Bullfrog Hills with faults at shallow levels in the upper plate. Basaltic dikes also intrude and are cut by faults in the upper plate in the southern Bullfrog Hills (Ransome et al., 1910) and at the 916 m level in the Barrick Bullfrog mine a thin, hydrothermally altered and brecciated basaltic dike can be seen to intrude and pinch out within the main fault and vein system.

Throughout the Bullfrog Hills numerous, generally west-dipping normal faults cut tilted sections of the tuffs and lavas of the Bullfrog Hills, indicating that faulting and tilting continued or resumed after deposition of these rocks. Map patterns and exposed fault surfaces indicate that some of these faults are steeply dipping and in all probability cut the Original Bullfrog segment of the OB-FC fault system. Exploratory drilling in the southern Bullfrog Hills near Rhyolite and in the vicinity of the Barrick Bullfrog mine has demonstrated offsets of the OB-FC fault system of on the order of several hundreds of feet by faults such as the Barrick Bullfrog mine fault (middle plate fault of Jorgenson et al., 1989) and the Montgomery-Shoshone fault, which have dips of 45 to 80°, respectively (Jorgenson et al., 1989; J. Marr, pers. commun., 1990; T.

Osmondson, pers. commun., 1992). A similar relationship is exposed 3 km east of the Mayflower mine (Figs. 5 and 10) where low-angle normal faults cut an east-facing, vertical to slightly overturned section of the Lithic Ridge Tuff, Crater Flat Group, and Paintbrush Group and separate these units from underlying strata of Early Cambrian age. Although this situation is analogous to the truncation of the same sequence of east-dipping ash-flow units against pre-Cenozoic rocks near the Original Bullfrog mine by the gently north-dipping Original Bullfrog fault, east of the Mayflower mine the low-angle faults are offset as much as several hundred meters by younger, steeply-dipping faults (Fig. 10). However, much of the rotation of the gently west-dipping to approximately 25° east-dipping low-angle faults shown in Figure 10 is inferred to result from the cumulative displacement of relatively late, down-to-the-west faults farther to the east (such as the Oasis Valley fault zone), perhaps following, or penecontemporanous with, isostatic rebound and flexure of the lower plate (e.g., Spencer, 1984; Buck, 1988). The offsets indicated by drilling in the southern Bullfrog Hills and the relations observed east of the Mayflower mine reflect extension at least in part accommodated by faults that cut the OB-FC fault system. Such offsets and brittle deformation in the lower plate contradict the model of Maldonado (1990a, 1990b) and Maldonado and Hausback (1990), and argue for revisions to their cross sections that show that all faults in the upper plate merge with, and/or are truncated by, the Original Bullfrog segment of the OB-FC fault system. The presence of dikes and plugs intruding some of these faults is consistent with a connection to deep structures, presumably also of extensional nature, that channeled magmas upward to, and/or above, the level of the OB-FC detachment fault system (Weiss et al., 1990).

The Au-Ag vein deposits in the Bullfrog Hills are hosted by shallowly to steeply-dipping faults and fractures that formed near the base of, and within, the upper plate during the pulse of post-Ammonia Tanks extensional faulting. Vein textures at the Original Bullfrog, Barrick Bullfrog, Montgomery-Shoshone and Gold Bar mines reflect episodic brecciation and are best explained as a result of movements along the host faults during mineralization, although breccia of probable hydrothermal origin is present as well. The K-Ar and $^{40}Ar/^{39}Ar$ ages therefore provide evidence that the faults at the Barrick Bullfrog and Montgomery-Shoshone mines were

active at about 9.9 and 9.5 Ma, and for faulting at the Original Bullfrog mine at about 9.0 Ma. The well-developed post-mineral fault surfaces and shattered nature of the vein at the Barrick Bullfrog mine indicate that fault movements in the upper plate continued after about 9.9 Ma. Veins at the Montgomery-Shoshone mine are both hosted within and truncated by the northeast-trending Montgomery-Shoshone fault that juxtaposes essentially unaltered units of the tuffs and lavas of the Bullfrog Hills against altered and mineralized rocks of the Timber Mountain Group (Ransome et al., 1910; Maldonado and Hausback, 1990), indicating substantial fault displacement after about 9.5 Ma. Likewise, the shattered nature of the Original Bullfrog vein and its truncation against unmineralized rocks below the Original Bullfrog fault show that movement of the Original Bullfrog segment of the OB-FC fault system continued after about 9.0 Ma. These relations are consistent with the fact that entire sections of the *ca.* 10- to 10.5-Ma tuffs and lavas of the Bullfrog Hills are commonly tilted as much as 35° and cut by numerous faults. Mineralization in the Bullfrog Hills was, therefore, penecontemporaneous with, as well as structurally controlled by, extensional faulting that continued after mineralization. The older ages of about 11.3 and 11.0 Ma for veins in the northern Bullfrog Hills are consistent with faulting and hydrothermal activity in the vicinity of the Yellow Jacket mine early during this interval of deformation.

Discussion and Summary

Since the advent of radiometric dating, numerous workers have demonstrated close space-time associations of hydrothermal activity and mineralization with volcanic and shallow igneous activity. In many cases, such as at Bodie, California, (Silberman et al., 1972), various deposits of the Maricunga belt, Chile (Sillitoe et al., 1991), Tavua caldera in Viti Levu, Fiji (Setterfield et al., 1992), Sleeper, Nevada (Conrad et al. 1993), Arcata, Peru (Candiotti et al., 1990), Orocopampa, Peru (McKee et al., 1994) and Round Mountain, Nevada (Henry et al., 1994), it has been shown that hydrothermal activity took place toward the end of, or shortly after, volcanism and was presumably related to the emplacement and cooling of subjacent, late-stage magma bodies. Few studies of the duration of epithermal mineralization have been carried out using $^{40}Ar/^{39}Ar$ dating techniques and cross-cutting relations, but it has generally been accepted that individual

hydrothermal systems responsible for volcanic-related epithermal precious-metal deposits have lifespans on the order of 0.5 m.y. or less, to about 1.5 m.y. (e.g., Silberman, 1985). K-Ar and $^{40}Ar/^{39}Ar$ ages suggest that hydrothermal activity may have taken place over a period of as long as 2 m.y. at the volcanic dome-hosted Sleeper gold-silver deposit in northwestern Nevada (Conrad et al., 1993). Hydrothermal activity at Steamboat Springs, Nevada, has occurred episodically over a period of about 3 m.y. (Silberman et al., 1979). The dome-hosted Ag-Sn deposits of Cerro Rico de Potosi, Bolivia, apparently formed during two of three recognized episodes of hydrothermal activity that took place at about 12.4 Ma, 11.1 to 10.5 Ma and 8 to 6 Ma (Cunningham et al., 1994). Evidence for long-lasting, episodic and/or more complex hydrothermal activity, in some cases involving multiple hydrothermal centers, comes mainly from porphyry systems and large volcanic centers and intracontinental volcanic fields (e.g., Butte, Montana, Meyer et al., 1968; western San Juan caldera complex, Lipman et al., 1976; Julcani, Peru, Noble and Silberman, 1984; Jemez, New Mexico, Woldegabriel and Goff, 1989; Woldegabriel, 1990; Chila Cordillera, Peru, Swanson et al., 1993) where hydrothermal activity overlapped multiple periods of magmatic and volcanic activity.

In the SWNVF multiple hydrothermal systems were active over a period of at least 4 m.y. that included portions of the main and Timber Mountain magmatic stages. Hydrothermal activity may have occurred in the Sleeping Butte area prior to the eruption of the 13.7-Ma Grouse Canyon Tuff, and possibly prior to 14.0 Ma in the vent area of the Lithic Ridge Tuff. Radiometric ages and stratigraphic relations indicate that presently known episodes of hydrothermal activity were in large part coeval with, and continued for 1 to 2 m.y. after, the climactic eruptions of the Paintbrush Group and Timber Mountain Group at about 12. 7 Ma and 11.45 Ma, respectively, and the magmatic activity in Bare Mountain and the Wahmonie-Salyer center. In the southern Bullfrog Hills hydrothermal activity and mineralization may have taken place as late as about 9 Ma. No evidence has been recognized for hydrothermal activity 5 to 10 m.y. *after* the caldera cycles, related to later magmatic systems, as is the case, for example, with the Silverton and Summitville calderas of the San Juan volcanic field (Lipman et al., 1976; Bar-

tos, 1993), and the Alunite Ridge-Deer Trail Mountain area of the Marysvale volcanic field (Cunningham et al., 1984; Beaty et al., 1986).

A broad spatial association between hydrothermal and magmatic activity in the SWNVF is shown by the distribution of alteration and mineralization within and peripheral to the southern and western margins of the Timber Mountain caldera complex and the older Claim Canyon caldron, and in outlying centers of igneous and volcanic activity at Bare Mountain and Wahmonie. Alteration is widespread in the Bullfrog Hills and the Calico Hills in and adjacent to areas of extracaldera domes and flows erupted late in the Timber Mountain magmatic stage. The spatial association, in combination with the close temporal correspondence between magmatic-volcanic activity and hydrothermal activity, provides strong evidence in support of a genetic relation between pulses of magmatic activity and multiple episodes of hydrothermal alteration and mineralization.

Altered and mineralized areas of the SWNVF are diverse in style, mineralogy, alteration and trace-element signatures, suggesting that in addition to differences in their geologic settings, the hydrothermal systems varied significantly in their composition. Silver-rich precious metal-bearing quartz and quartz-calcite veins with abundant Te, and locally Bi, but modest base-metal contents, were deposited at the Wahmonie-Salyer center between about 13 to 12.5 Ma, possibly above a porphyry-type magmatic system near the end of, or shortly following, local volcanism. At about the same time, fluorite and disseminated Au mineralization formed in the northern and eastern parts of Bare Mountain in and near silicic porphyry dikes emplaced about 1 to 2 m.y. earlier. The disseminated style of mineralization, abundant As, Sb, Hg, and Tl, low base metal concentrations and high Au:Ag ratios are features typical of sedimentary rock-hosted disseminated Au deposits commonly referred to as Carlin-type deposts elsewhere. At Bare Mountain the presence of hypersaline fluid inclusions in the altered dikes, abundant Mo, F and, locally, Bi and Te, and the timing of mineralization 1 to 2 m.y. after dike emplacement, are consistent with a magmatic affinity, perhaps as distal products of deeper porphyry-type magmatic-hydrothermal activity (Noble et al., 1989; 1991; Weiss et al., 1993b). Silicification and deposition of steeply dipping quartz and quartz-barite veins containing high concentrations of base

metals, Ag and Hg in Paleozoic rocks at Mine Mountain may have taken place at about 11.1 Ma. Excellent examples of adularia-sericite deposits of the low base-metal type formed in the Bullfrog Hills during at least three periods of hydrothermal activity between 11.3 and about 9 Ma. A similar style of alteration and mineralization is inferred for the little-studied Au-Ag bearing veins in the Clarkdale and Tolicha-Quartz Mountain districts. Zones of alunitic and argillic alteration in the Clarkdale area, on the south flank of Mine Mountain, in the Calico Hills, Transvaal Hills, Silicon and Thompson mine area, near the Mother Lode and Telluride mines, and in areas of the Bullfrog Hills and Oasis Valley, including Bailey's hot spring, are interpreted as the result of steam-heated acid-sulfate processes near and/or above paleo-watertables, implying relatively shallow hydrothermal environments.

Two pulses of E-W to ESE-WNW regional extension of Miocene age are recognized in the southern and southwestern parts of the SWNVF. Based on the strikes of the silicic dikes in Bare Mountain, the least principal stress direction was oriented in a E-W to WNW-ESE direction at about 14 Ma, prior to the beginning of the first pulse. The first pulse coincided with the 1 m.y. hiatus in volcanism between the main and Timber Mountain magmatic stages and involved tilting along N-S to NE-trending faults, mainly in areas south of the Timber Mountain caldera complex, including the area of Yucca Mountain and in the northern part of Bare Mountain. Extension was in part accommodated by movement on the Fluorspar Canyon segment of the OB-FC fault system. The contrast between relatively shallow alunitic alteration and mercury mineralization in the Telluride - Mother Lode mine area and porphyry-type groundmass crystallization and hypersaline inclusions in the dikes suggests that considerable uplift, on the order of 1 km, took place in the northern part of Bare Mountain between about 14 and 12.2 Ma. This uplift may have, in large part, resulted from tectonic denudation associated with the early pulse of extension and faulting along the Fluorspar Canyon segment, although some uplift prior to deposition of the 13.2-Ma Crater Flat Group is possible as well.

Major displacements along the Original Bullfrog segment of the OB-FC fault system, and the major tilting and imbricate normal faulting in the Bullfrog Hills took place during the younger pulse of extension between 11.4 Ma and 7.6 Ma. This younger deformation overlapped

in time and space with magmatic activity and volcanism of the waning Timber Mountain stage west of the Timber Mountain caldera complex. Precious-metal deposits at the Barrick Bullfrog, Montgomery-Shoshone, Rhyolite, Original Bullfrog, Gold Bar, Mayflower and Yellowjacket mines were structurally controlled by the Original Bullfrog fault and more steeply dipping faults in the upper plate that formed during the younger pulse of extension. Vein and breccia textures and structural relations show that mineralization took place concurrently with extensional faulting, and that faulting continued after mineralization. Radiometric ages indicate at least three periods of hydrothermal activity and vein deposition: one at about 11.3 to 11 Ma in the northern part of the Bullfrog Hills, the second at about 10 to 9.9 Ma in the southern part of the Bullfrog Hills and at the Mayflower mine in the northern Bullfrog Hills, and the third at about 9 Ma at the Original Bullfrog mine. The oldest period closely followed eruption of the Ammonia Tanks Tuff and the tuffs and lava of Fleur de Lis Ranch. The middle period, possibly consisting of two sub-episodes if the 9.5 ± 0.2 Ma age at the Montgomery-Shoshone mine is correct, began at about the end of volcanism of the tuffs and lavas of the Bullfrog Hills and perhaps extended for about 0.5 m.y. The ages are consistent with mineralization at the Original Bullfrog mine at about 9 Ma, as much as 1 m.y. after formation of nearly identical deposits at the Barrick Bullfrog mine and elsewhere in the Bullfrog Hills. This suggests that mineralization in the southern Bullfrog Hills was episodic and may have been produced by similar, but separate, perhaps spatially overlapping hydrothermal systems. Nevertheless, the identical styles of alteration and mineralization, similar mineralogy and trace-element signatures, and the presence of uytenbogaardtite at both the Barrick Bullfrog and Original Bullfrog mines can be used to argue that widely separated, productive veins in the southern Bullfrog Hills were deposited in a single, areally extensive hydrothermal system active between about 10 to 9 Ma. Such a large, long-lived system may have developed in response to heating over a wide area, resulting from some combination of the rise of synextensional magmas that fed eruptions of the tuffs and lavas of the Bullfrog Hills, extensional thinning of the crust, and the high fracture permeability created by the numerous, closely spaced faults in the upper plate. As extensional faulting and tectonic denudation of the heated middle to upper crust continued, high permeability may have allowed

heating of deeply circulating meteoric water long after the end of local magmatic activity, providing a potential mechanism for hydrothermal activity as late as about 9 Ma at the Original Bullfrog mine. The fact that productive veins are widely scattered in a large area of altered rocks suggests that gold and reduced sulfur were not evenly distributed through the hydrothermal fluids. For this reason, and considering the extremely low initial gold contents of the subalkaline rhyolitic rocks in the upper plate (~0.2 to 0.4 ppb Au, Connors et al., 1993), we speculate that ores in the district may reflect very localized inputs of gold to the hydrothermal system from magmatic fluids (e.g., Bartos, 1993; Gibson et al., 1993).

The economically most important producers of precious metals in the SWNVF, the Bullfrog and Bare Mountain districts, are, along with the Wahmonie district, spatially and temporally associated with centers of igneous and volcanic activity. Nevertheless, in all three areas faults and fractures related to regional extension provided the most important structural controls for mineralization, rather than volcano-tectonic features such as ring fractures, caldera-margin faults, or faults associated with resurgent doming. Veins in the Bullfrog Hills are hosted by, and were deposited during movements of, upper crustal extensional faults that were active during and after the waning stages of local magmatic and volcanic activity. At Wahmonie the veins formed within northeast-trending high-angle faults and fractures associated with horst-and-graben structures that developed shortly after volcanism of the Wahmonie-Salyer center. The gold and fluorite deposits of similar age in Bare Mountain were structurally controlled largely by north-south to northeast-trending, moderately to steeply dipping faults and fractures mainly below the Fluorspar Canyon fault, as well as by the porphyry dikes, consistent with regional east-west to WNW-ESE extension. The importance of regional extension as a major factor in the genesis of precious metals deposits of early Miocene age in the southern Walker Lane belt, including Paradise Peak, Tonopah and Goldfield, Nevada, has been pointed out by John et al. (1989) and Seedorf (1991). We believe that this is also the case with the Bullfrog, Wahmonie and Bare Mountain districts in the SWNVF, where multiple episodes of magmatic activity, volcanism, extension and mineralization were, moreover, closely interrelated during middle and late Miocene time.

Acknowledgments

This paper draws on studies carried out by K. A. Connors, M.R. Jackson, D.C. Noble, and S. I. Weiss under contracts from the Nevada Nuclear Waste Project Office (through the Center for Neotectonic Studies) and Cordex Exploration Company (through the Department of Geological Science) at the Mackay School of Mines, University of Nevada, Reno. Additional support by a research grant to K. A. Connors from the Geological Society of America and a grant to S. I. Weiss from the Mackay Mineral Research Institute is gratefully acknowledged. The authors benefited from the insights of the many people who have contributed to understanding the volcano-tectonic framework of the SWNVF, and from lively discussions with M. D. Carr, W. J. Carr, S. B. Castor, B. Claybourne, D. Fanning, S. M. Green, J. D. Greybeck, L. T. Larson, T. Osmondson, J. M. Proffett, Jr., S. J. Ristorcelli, D. A. Sawyer and A. B. Wallace. We are particularly grateful for the interest and support for detailed mapping and stratigraphic studies provided by A.B. Wallace and Cordex Exploration. We thank D and H Mining Inc., Gexa Gold Corp., Lac Minerals USA Inc., Saga Exploration Co., and U.S. Precious Metals Inc., for access to their properties. Field work in restricted areas of the Nevada Test Site was made possible by the cooperation of the staff at Operations Control and the Yucca Mountain Project Office at the Nevada Test Site. R. P. Ashley, G. B. Dalrympl, J. D. Keith and D. A. Sawyer provided useful and constructive reviews of the manuscript.

REFERENCES

Ahern, R., and Corn, R.M., 1981, Mineralization related to the volcanic center at Beatty, Nevada: Arizona Geological Society Digest, v. XIV, p. 283-286.

Armstrong, R.L., Ekren, E.B., McKee, E.H., and Noble, D.C., 1969, Space-time relations of Cenozoic silicic volcanism in the Great Basin of the western United States: American Journal of Science, v. 267, p. 478-490.

Aronson, J.L., and Bish, D.L., 1987, Distribution, K/Ar dates, and origin of illite/smectite in tuffs from cores USW G-1 and G-2, Yucca Mountain, Nevada, a potential high-level radioactive waste repository [abs.]: Program with Abstracts, 24th Annual Meeting, Clay Minerals Soc., Socorro, New Mexico, v. 25.

Ball, S.H., 1907, A geologic reconnaissance in southwestern Nevada and eastern California: U. S. Geological Survey Bulletin 308, 218 p.

Barnes, H., and Poole, F.G., 1968, Regional thrust-fault system in Nevada Test Site and vicinity, *in* Eckel, E.G., ed., Nevada Test Site: Geological Society of America Memoir 110, p. 233-238.

Barton, M.D., 1980, The Ag-Au-S system: Economic Geology, v. 75, p. 306-316.

Barton, M.D., and Trim, H.E., 1990, Late Cretaceous two-mica granites and lithophile-element mineralization in the Great Basin [abs.]: Geology and Ore Deposits of the Great Basin, Reno/Sparks, Nevada, 1990, Program with Abstracts, p. 76.

Bartos, P.J., 1993, Comparison of gold-rich and gold-poor quartz-base metal veins, western San Juan Mountains, Colorado: the Mineral Point area as an example: Society of Economic Geologists Newsletter, no. 15.

Beaty, D.W., Cunningham, C.G., Rye, R.O., Steven, T.A., and Gonzalez-Urien, E., 1986, Geology and geochemistry of the Deer Trail Pb-Zn-Ag-Cu manto deposits, Marysvale district, west-central Utah: Economic Geology, v. 81, p. 1932-1952.

Berger, B.R., and Bagby, W.C., 1991, The geology and origin of Carlin-type gold deposits: *in* Foster, R.P., ed., Gold Metallogeny and Exploration, Blackie, Glasgow, p. 210-248.

Best, M.G., Christiansen, E.H., Deino, A.L., Grommé, C.S., McKee, E.H., and Noble, D.C., 1989, Eocene through Miocene volcanism in the Great Basin of the western United States: New Mexico Bureau of Mines Mineral Resources Memoir 47, p. 91-133.

Bish, D.L., 1987, Evaluation of past and future alteration in tuff at Yucca Mountain, Nevada based on clay mineralogy of drill cores USW G-1, G-2, and G-3: Los Alamos National Laboratory Report LA-10667-MS, 41 p.

Bish, D.L., and Aronson, J.L., 1993, Paleogeothermal and paleohydrologic conditions in silicic tuff from Yucca Mountain, Nevada: Clays and Clay Minerals, v. 41, p. 148-161.

Bonham, H.F., Jr., and Hess, R.H., 1992, The Nevada mineral industry, 1992: Nevada Bureau of Mines and Geology Special Publication MI-1992, 52 p.

Broxton, D.E., Vaniman, D., Caporuscio, F., Arney, B., and Heiken, G., 1982, Detailed petrographic descriptions and microprobe data fro drill holes USW-G2 and UE25b-1H, Yucca Mountain, Nevada: Los Alamos, New Mexico, Los Alamos National Laboratory Report LA-10802-MS, 168 p.

Broxton, D.E., Warren, R.G., and Byers, F.M., Jr., 1989, Chemical and mineralogic trends within the Timber Mountain-Oasis Valley caldera complex, Nevada: Evidence for multiple cycles of chemical evolution in a long-lived silicic magma system: Journal of Geophysical Research, v. 94, p. 5961-5985.

Buck, W.R., 1988, Flexural rotation of normal faults: Tectonics, v. 7, p. 959-973.

Byers, F.M., Jr., Carr, W.J., and Orkild, P.P., 1989, Volcanic centers of southwestern Nevada: evolution of understanding, 1960-1988: Journal of Geophysical Research, v. 94, p. 5908-5924.

Byers, F.M., Jr., Carr, W.J., Orkild, P.P., Quinlivan, W.D. and Sargent, K.A., 1976a, Volcanic Suites and related cauldrons of Timber Mountain-Oasis Valley caldera complex: U.S. Geological Survey Professional Paper 919, 70 p.

Byers, F.M., Jr., Carr, W.J., Christiansen, R.L., Lipman, P.W., Orkild, P.P., and Quinlivan, W.D., 1976b, Geologic map of the Timber Mountain Caldera area, Nye County, Nevada: U.S. Geological Survey Miscellaneous Investigation Map I-891, 1:48,000 scale.

Candiotti de los Rios, H., Noble, D.C., and McKee, E.H., 1990, Geologic setting and epithermal silver veins of the Arcata district, southern Peru: Economic Geology, v. 85, p. 1473-1490.

Caporuscio, F., Vaniman, D.T., Bish, D.L., Broxton, D.E., Arney, D., Heiken, G., Byers, F.M., and Gooley, R., 1982, Petrologic studies of drill cores USW-G2 and UE25b-1H, Yucca Mountain, Nevada: Los Alamos National Laboratory Report LA-9255-MS, 114 p.

Carr, W.J., 1974, Summary of tectonic and structural evidence for stress orientation at the Nevada Test Site: U. S. Geological Survey Open-file Report 74-176, 83 p.

Carr, W.J., 1984a, Regional structural setting of Yucca Mountain, southwestern Nevada, and late Cenozoic rates of tectonic activity in part of the southwestern Great Basin, Nevada and California: U.S. Geological Survey Open-File Report 84-0854, 114 p.

Carr, W.J., 1984b, Timing and style of tectonism and localization of volcanism in the Walker Lane belt of southwestern Nevada [abs.]: Geological Society of America, Abstracts with Programs, v. 16, p. 464.

Carr, W.J., 1988, Volcano-tectonic setting of Yucca Mountain and Crater Flat, *in* Carr, M.D., and Yount, J.C., eds., Geologic and hydrologic investigations of a potential nuclear waste disposal site at Yucca Mountain, southern Nevada: U.S. Geological Survey Bulletin 1790, p. 35-49.

Carr, W.J., 1990, Style of extension in the Nevada Test Site region, southern Walker Lane belt; and integration of volcano-tectonic and detachment fault models, *in* Wernicke, B.P., ed., Basin and Range extensional tectonics near the latitude of Las Vegas, Nevada: Geological Society of America Memoir 176, Boulder, Colorado, p. 283-303.

Carr, W.J., Byers, F.M., and Orkild, P.P., 1986, Stratigraphic and volcano-tectonic relations of Crater Flat Tuff and some older volcanic units, Nye County, Nevada: U.S. Geological Survey Professional Paper 1323, 28 p.

Carr, M.D., and Monsen, S.E., 1988, A field trip guide to the geology of Bare Mountain, *in* Weide, D.L., and Faber, M.L., eds., This Extended Land: Geological Society of America Field Trip Guidebook, Cordilleran Section Meeting, Las Vegas, Nevada, p. 50-57.

Caskey, S.J., and Schweikert, R.A., 1992, Mesozoic deformation in the Nevada Test Site and vicinity: implications for the structural framework of the Cordilleran fold and thrust belt and Tertiary extension north of Las Vegas Valley: Tectonics, v. 11, p. 1314-1331.

Castor, S.B., and Weiss, S.I., 1992, Contrasting styles of epithermal precious-metal mineralization in the southwestern Nevada volcanic field, USA: Ore Geology Reviews, v. 7, p. 193-223.

Castor, S.B., and Sjoberg, J.J., 1993, Uytenbogaardtite, Ag_3AuS_2, in the Bullfrog mining district, Nevada: Canadian Mineralogist, v. 31, p. 89-98.

Castor, S.B., Tingley, J.V., and Bonham, H.F., Jr., 1992, Subsurface mineral resource analysis, Yucca Mountain, Nevada, Preliminary Report 1: Lithologic logs: Nevada Bureau of Mines and Geology Open-file Report 92-4, 11 p. plus appendices.

Castor, S.B., Tingley, J.V., and Bonham, H.F., Jr., 1994, Pyritic ash-flow tuff, Yucca Mountain, Nevada: Economic Geology, v. 89, p. 401-407.

Cemen, I., Wright, L.A., Drake, R.E., and Johnson, F.C., 1985, Cenozoic sedimentation and sequence of deformational events at the southeastern end of the Furnace Creek strike-slip fault zone, Death Valley region, California, *in* Biddle, K.T., and Christie-Blick, N., eds., Strike-slip deformation, basin formation, and sedimentation: Society of Economic Paleontologists and Mineralogists Special Publication No. 37., p. 127-141.

Christiansen, R.L., Lipman, P.W., Carr, W.J., Byers, F.M., Jr., Orkild, P.P., and Sargent, K.A., 1977: Timber Mountain-Oasis Valley caldera complex of southern Nevada: Geological Society of America Bulletin, v. 88, p. 943-959.

Connors, K.A., 1995, Studies in silicic volcanic geology in the Great Basin of western North America: Unpublished Ph.D dissertation, Reno, Mackay School of Mines, University of Nevada, Reno, XX p., (in review).

Connors, K.A., Weiss, S.I., and Noble, D.C., 1995, The Oasis Valley fault: the principal break-away structure and eastern limit of Late Miocene extensional faulting in the Bullfrog Hills, southwestern Nevada [abs.]: EOS, Transactions of the American Geophysical Union,., v. 76, p. 284.

Connors, K.A., McKee, E.H., Noble, D.C., and Weiss, S.I., 1991, Ash-flow volcanism of Ammonia Tanks age in the Oasis Valley area, SW Nevada: bearing on the evolution of the Timber Mountain calderas and the timing of formation of the Timber Mountain II resurgent dome [abs.]: EOS, Transactions of the American Geophysical Union,., v. 72, p. 570.

Connors, K.A., Noble, D.C., Bussey, S.D., and Weiss, S.I., 1993, The initial gold contents of silicic volcanic rocks: bearing on the behavior of gold in magmatic systems, Geology, v. 21, p. 937-940.

Conrad, J.E., McKee, E.H., Rytuba, J.J., Nash, T.J., and Utterback, W.C., 1993, Geochronology of the Sleeper deposit, Humboldt County, Nevada: epithermal gold-silver mineralization following emplacement of a silicic flow-dome complex: Economic Geology, v. 88, p. 317-327.

Cornwall, H.R., 1972, Geology and mineral deposits of southern Nye County, Nevada: Nevada Bureau of Mines Geological Bulletin 77, p. 49.

Cornwall, H.R., and Kleinhampl, F.J., 1961, Geology of the Bare Mountain quadrangle, Nevada: U.S. Geological Survey Map GQ-157, 1:62,500 scale.

Cornwall, H.R., and Kleinhampl, F.J., 1964, Geology of the Bullfrog quadrangle and ore deposits related to the Bullfrog Hills caldera, Nye County, Nevada, and Inyo County, California: U.S. Geological Survey Professional Paper 454-J, 25 p.

Couch, B.F., and Carpenter, J.A., 1943, Nevada's metal and mineral production: Nevada Bureau of Mines Geol. Bulletin 38, 159 p.

Cunningham, C.G., Rye, R.O., Steven, T.A., and Mehnert, H.H., 1984, Origins and exploration significance of replacement and vein-type alunite deposits in the Marysvale volcanic field, west central Utah: Economic Geology, v. 79, p. 50-71.

Cunningham, C.G., Zartman, E.E., McKee, E.H., Rye, R.O., Naeser, C.W., and Ericksen, G.E., 1994, Timing and origin of ore deposition at the Cerro Rico de Potosi Ag-Sn and Porco Ag-Zn-Pb-Sn deposits, Bolivia [extended abs.]: U. S. Geological Survey Circular 1103A, p. 23-26.

Dalrymple, G.B., 1979, Critical tables for conversion of K-Ar ages from old to new constants: Geology, v. 7., p. 558-560.

Dalrymple, G.B., and Lanphere, M.A., 1969, Potassium-argon dating-- principals, techniques and applications to geochronology: San Francisco, W.H. Freeman Co., 258 p.

Dalrymple, G.B., and Lanphere, M.A., 1971, $^{40}Ar/^{39}Ar$ technique of K-Ar dating: A comparison with the conventional technique: Earth and Planetary Science Letters, v. 12,p. 300-308.

Duebendorfer, E.M., Feuerbach, D.L., and Smith, E.I., 1990, Syntectonic sedimentation, volcanism, and kinematics along the inferred eastern extension of the Las Vegas shear zone, Nevada [abs.]: Geological Society of America Abstracts with Programs, v. 22, p. 20.

Duebendorfer, E.M., and Smith, E.I., 1991, Tertiary structure, magmatism, and sedimentation in the Lake Mead region, southern Nevada: *in* Seedorf, E., ed., 1991 Spring Field Trip Guide Book, Geological Society Nevada Spec. Pub. 13, Reno, Nevada, p. 66-95.

Deubendorfer, E.M., and Wallin, E.T., 1991, Basin Development and syntectonic sedimentation associated with kinematically coupled strike-slip and detachment faulting, southern Nevada: Geology, v. 19, p. 87-90.

Ekren, E.B., Anderson, R.E., Rogers, C.L., and Noble, D.C., 1971, Geology of northern Nellis Air Force Base Bombing and Gunnery Range, Nye County, Nevada: U.S. Geological Survey Professional Paper 651, 91 p.

Ekren, E.B., Rodgers, C.L., Anderson, R.E., and Orkild, P.P., 1968, Age of Basin and Range faults in the Nevada Test Site and Nellis Air Force Range, *in* Eckel, E.B., ed., Nevada Test Site: Geological Society of America Memoir 110, Boulder, Colorado, p. 247-250.

Ekren, E.B., and Sargent, K.A., 1965, Geologic map of Skull Mountain quadrangle at the Nevada Test Site, Nye County, Nevada: U.S. Geological Survey Geologic Quadrangle Map GQ-387, 1:24,000.

Elston, W.E., Damon, P.E., Coney, P.E., Rhodes, R.C., Smith, E.I., and Bikerman, M., 1973, Tertiary volcanic rock, Mogollon-Datil province, and surrounding region: K-Ar dates, patterns of eruption and periods of mineralization: Geological Society of America Bulletin, v. 84, p. 2259-2274.

Eng, T., Boden, D. R., and Biggs, J. O., 1995, Geology and mineralization of the Bullfrog mine and vicinity, Nye County, Nevada: *in* Callicrate, T. E., ed., Gold Deposits of the Walker Lane, 1995 Symposium Field Trip I Giudebook, Reno, Geological Society of Nevada.

Fleck, R. J., Lanphere, M. A., Turrin, B., and Sawyer, D. A., 1991, Chronology of late Miocene to Quaternary volcanism and tectonism in the southwest Nevada volcanic field [abs.]: Geological Society of America Abstracts with Programs, v. 23, p. 25.

Fridrich, C.A., Orkild, P.P., Murray, M., Price, J.R., Christiansen, R.L., Lipman, P.W., Carr, W.J., Quinlivin, W.D., and Scott, R.B., 1994, Geologic map of the East Of Beatty Mountain 7.5' Quadrangle, Nye County, Nevada: U. S. Geological Survey Open-file Report, 1:12,000 scale, 4 sheets.

Frizzell, V.A., Jr., and Shulters, J., 1990, Geologic map of the Nevada Test Site: U.S. Geological Survey Miscellaneous Investigation Map I-2046, 1:100,000.

Gardiner, J.N., Goff, F., Garcia, S., and Hagan, R.C., 1986, Stratigraphic relations and lithologic variations in the Jemez volcanic field, New Mexico: Jour. Geophys. Research, v. 91, p. 1763-1778.

Gibson, P.C., Tosdal, R.M., and Noble, D.C., 1993, Magmatic source for metals in and adularia-sericite type Ag-Au vein system: Lead isotopic compositions at the Orcopampa district, Peru [abs.]: Geological Society of America Abstracts with Programs, v. 25, p. A42.

Greybeck, J.D., and Wallace, A.B., 1991, Gold mineralization at Fluorspar Canyon near Beatty, Nye County, Nevada: *in* Raines, G.L., Lisle, R.E., Shafer, R.W., and Wilkinson, W.W., eds., Geology and ore deposits of the Great Basin: Symposium Proceedings, Geological Society of Nevada, Reno, Nevada, p. 935-946.

Hamilton, W.B., 1988, Detachment faulting in the Death Valley region, California and Nevada, *in* Carr, M.D., and Yount, J.C., eds., Geologic and hydrologic investigations of a potential nuclear waste disposal site at Yucca Mountain, southern Nevada: U.S. Geological Survey Bulletin 1790, p. 51-86.

Hausback, B.P., Deino, A.L., Turrin, B.T., McKee, E.H., Frizzell, V.A., Noble, D.C., and Weiss, S.I., 1990, New $^{40}Ar/^{39}Ar$ ages for the Spearhead and Civet Cat Canyon Members of the Stonewall Flat Tuff, Nye County, Nevada: Evidence for systematic errors in standard K-Ar age determinations on sanidine: Isochron/West, No. 56, p. 3-7.

Henry, C.D., Castor, S.B., and Elson, H.B., 1994, $^{40}Ar/^{39}Ar$ geochronology and geologic setting of volcanism and gold mineralization at Round Mountain, Nevada [abs.]: Geological Society of America Abstracts with Programs, v. 26, p. A141.

Hoover, D.B., Chornack, M.P., Nervick, K.H., and Broker, M.M., 1982, Electrical studies at the proposed Wahmonie and Calico Hills Nuclear Waste Sites, Nye County, Nevada: U.S. Geological Survey Open-File Report 82-466, 45 p.

Hudson, M.R., 1992, Paleomagnetic data bearing on the origin of arcuate structures in the Frenchman Peak - Massachusetts Mountain area of southern Nevada: Geological Society Am. Bulletin, v. 104, p. 581-594.

Hudson, M.R., and Cole, J.C., 1993, Kinematics of faulting in the Mine Mountain area of southern Nevada: evidence for pre-Middle Miocene extension [abs.]: Geological Society of America Abstracts with Programs, v. 25, p. 55.

Hudson, M.R., Sawyer, D.A., and Warren, R.G., 1994, Paleomagnetism and rotation constraints for the middle Miocene southwestern Nevada volcanic field: Tectonics, v. 13, no. 258-277.

Jackson, M.R., 1988, The Timber Mountain magmato-thermal event: an intense widespread culmination of magmatic and hydrothermal activity at the southwestern Nevada volcanic field: Unpublished M.S. thesis, Mackay School of Mines, Univ. Nevada, Reno, 46 p.

Jackson, M.R., Noble, D.C., Weiss, S.I., Larson, L.T., and McKee, E.H., 1988, Timber Mountain magmato-thermal event: an intense widespread culmination of magmatic and hydrothermal activity at the SW Nevada volcanic field [abs.]: Geological Society of America Abstracts with Programs, v. 20, p. 171.

John, D.A., Thomason, R.E., and McKee, E.H., 1989, Geology and K-Ar geochronology of the Paradise Peak mine and the relationship of pre-Basin and Range extension to Early Miocene precious metal mineralization in west-central Nevada: Economic Geology, v. 84, p. 631-649.

Jorgensen, D.K., Rankin, J.W., and Wilkins, J., Jr., 1989, The geology, alteration and mineralogy of the Bullfrog gold deposit, Nye County, Nevada: Society Mining Eng. Preprint 89-135, 13 p.

Kistler, R.W., 1968, Potassium-argon ages of volcanic rocks in Nye and Esmeralda Counties, Nevada: Geological Society of America Memoir 110, p. 251-263.

Lipman, P.W., and McKay, E.J., 1965, Geologic map of the Topopah Spring SW quadrangle, Nevada: U.S. Geological Survey Geologic Quadrangle Map GQ-439, 1:24,000 scale.

Lipman, P.W., Fisher, S.S., Mehnert, H.H., Naeser, C.W., Luedke, R.G., and Steven, T.A., 1976, Multiple ages of mid-Tertiary mineralization and alteration in the western San Juan Mountains, Colorado: Economic Geology, v. 71, p. 571-588.

McKay, E.J., 1963, Hydrothermal alteration in the Calico Hills, Jackass Flats quadrangle, Nevada Test Site: U.S. Geological Survey Technical Letter NTS-43, 6 p.

McKay, E.J., and Williams, W.P., 1964, Geology of Jackass Flats quadrangle, Nevada Test Site, Nevada: U.S. Geological Survey Geologic Quadrangle Map GQ-368, 1:24,000 scale.

McKee, E.H., 1983, Reset K-Ar ages: evidence for three metamorphic core complexes, western Nevada: Isochron/West, no. 38, p 17-20.

McKee, E.H., and Bergquist, J.R., 1993, New radiometric ages related to alteration and mineralization in the vicinity of Yucca Mountain, Nye County, Nevada: U. S. Geological Survey Open-File Report 93-538, 26 p.

McKee, E.H., Gibson, P.C., Noble, D.C., and Swanson, K.E., 1994, Timing of igneous activity, alteration and mineralization at the Orcopampa Ag-Au district, southern Peru [extended abs.]: U. S. Geological Survey Circular 1103A, p. 65-66.

Maldonado, F., 1985, Late Tertiary detachment faults in the Bullfrog Hills, southwestern Nevada [abs.]: Geological Society of America Abstracts with Programs, v. 17, p. 651.

Maldnado, F., 1988, Geometry of normal faults in the upper plate of a detachment fault zone, Bullfrog Hills, southern Nevada [abs.]: Geological Society of America, Abstracts with Programs, v. 20, p. 178.

Maldonado, F., 1990a, Structural geology of the upper plate of the Bullfrog Hills detachment fault system, southern Nevada: Geological Society of America Bulletin, v. 102, p. 992-1006.

Maldonado, F., 1990b, Geologic map of the northwest quarter of the Bullfrog 15-minute quadrangle, Nye County, Nevada: U.S. Geological Survey Miscellaneous Investigation Map I-1985, 1:24,000.

Maldonado, F, and Hausback, B.P., 1990, Geologic map of the northeast quarter of the Bullfrog 15-minute quadrangle, Nye County, Nevada: U.S. Geological Survey Miscellaneous Investigation Map I-2049, 1:24,000.

Maldonado, F., and Koether, S.L., 1983, Stratigraphy, structure, and some petrographic features of Tertiary volcanic rocks at the USW G-2 drill hole, Yucca Mountain, Nye County, Nevada: U.S. Geological Survey Open-File Report 83-732, 83 p.

Maldonado, F., Muller, D.C., and Morrison, J.N., 1979, Preliminary geologic and geophysical data of the UE25a-3 exploratory drill hole, Nevada Test Site, Nevada: U.S. Geological Survey Open-File Report 81-522.

Marvin, R. F., and Cole, J. C., 1978, Radiometric ages: compilation A, U. S. Geological Survey: Isochron/West, no. 22, p. 3-14.

Marvin, R.F., Mehnert, H.H., and Naeser, C.W., 1989, U.S. Geologic Survey radiometric ages - compilation "C", part 3: California and Nevada: Isochron/West, no. 52, p. 3-11.

Marvin, R.F., Byers, F.M., Mehnert, H.H., Orkild, P.P, and Stern, T.W., 1970, Radiometric ages and stratigraphic sequence of volcanic and plutonic rocks, southern Nye and western Lincoln Counties, Nevada: Geological Society of America, Bulletin, v. 81, p. 2657-2676.

Meyer, C., Shea, E.P., Goddard, C.C., Jr., and staff, 1968, Ore deposits at Butte, Montana: *in* Ridge, J.D., ed., Ore deposits of the United States, 1933-1967; American Institute of Mining, Metallurgy, and Petroleum Engineering., New York, v. 2, p. 1363-1416.

Minor, S.A., Sawyer, D.A., Orkild, P.P., Coe, J.A., Wahl, R.R., and Frizzell, V.A., Jr., 1991, Neogene migratory extensional deformation revealed on new map of the Pahute Mesa 1:100,000-scale quadrangle, southern Nevada [abs.]: EOS, Transactions of the American Geophysical Union,, v. 72, p. 469.

Minor, S.A., Sawyer, D.A., Wahl, R.R., Frizzell, V.A., Jr., Schilling, S.P., Warren, R.G., Orkild, P.P., Coe, J.A., Hudson, M.R., Fleck, R.J., Lanphere, M.A., Swadley, W.C., and Cole, J.C., 1993, Preliminary geologic map of the Pahute Mesa 30' x 60' quadrangle, Nevada: U.S. Geological Survey Open-file Report 93-299, 1:100,000.

Monsen, S.A., 1983, Structural evolution and metamorphic petrology of the Precambrian-Cambrian strata, northwestern Bare Mountain, Nevada: Unpublished M.S. thesis, Davis, University of California, 66 p.

Monsen, S.A., Carr, M.D., Reheis, M.C., and Orkild, P.P., 1990, Geologic map of Bare Mountain, Nye County Nevada: U.S. Geological Survey Open-file Report 90-25, 1:24,000.

Monsen, S.A., Carr, M.D., Reheis, M.C., and Orkild, P.P., 1992, Geologic map of Bare Mountain, Nye County Nevada: U.S. Geological Survey Miscellaneous Investigation Map I-2201, 1:24,000.

Morton, J.L., Silberman, M.L., Bonham, H.F., Garside, L.J., and Noble, D.C., 1977, K-Ar ages of volcanic rocks, plutonic rocks, and ore deposits in Nevada and eastern California - Determinations run under the USGS-NBMG cooperative program: Isochron/West, n. 20, p. 19-29.

Noble, D.C., and Christiansen, R.L., 1968, Geologic map of the southwest quarter of the Black Mountain quadrangle, Nye County, Nevada: U.S. Geological Survey Miscellaneous Investigation Map I-562, 1:24,000.

Noble, D.C., Sargent, K.A., Ekren, E.B., Mehnert, H.H., and Byers, F.M., Jr., 1968, Silent Canyon volcanic center, Nye County, Nevada: Geological Society of America Special Paper 101, p. 412-413.

Noble, D.C., and Silberman, M.L., 1984, Evolucíon volcanica y hidrotermal y chronología de K/Ar del Distrito Minero del Julcani: Geological Society of Peru, Vol. Jubilar, 60 Aniv., Fasc. 5, 35 p.

Noble, D.C., Weiss, S.I., and Green, S.M., 1989, High-salinity fluid inclusions suggest that Miocene gold deposits of the Bare Mtn. district, NV, are related to a large buried rare-metal rich magmatic system [abs.]: Geological Society of America Abstracts with Programs, v. 21, p. 123.

Noble, D.C., Weiss, S.I., and McKee, E.H., 1990, Style, timing, distribution, and direction of Neogene extension within and adjacent to the Goldfield section of the Walker Lane structural belt: EOS, Trans. American Geophysical Union, v. 71, p. 618-619.

Noble, D.C., Weiss, S.I., and McKee, E.H., 1991, Magmatic and hydrothermal activity, caldera geology, and regional extension in the western part of the southwestern Nevada volcanic field, *in* Raines, G.L., Lisle, R.E., Shafer, R.W., and Wilkinson, W.W., eds., Geology and Ore Deposits of the Great Basin, Reno, Geological Society of Nevada, p. 913-934.

Noble, D.C., Vogel, T.A., Weiss, S.I., Erwin, J.W., McKee, E.H., and Younker, L.W., 1984, Stratigraphic relations and source areas of ash-flow sheets of the Black Mountain and Stonewall Mountain volcanic centers, Nevada: Journal of Geophysical Research, v. 89, p. 8593-8602.

Odt, D.A., 1983, Geology and geochemistry of the Sterling gold deposit, Nye County, Nevada: Unpublished M.S. thesis, Reno, Univ. Nevada, Reno, 91 p.

Orkild, P.P., 1968, Geologic map of the Mine Mountain quadrangle, Nye County, Nevada: U.S. Geological Survey Geologic Quadrangle Map GQ-746, 1:24,000 scale.

Orkild, P.P., and O'Connor, J.T., 1970, Geologic map of the Topopah Spring quadrangle, Nye County, Nevada: U.S. Geological Survey Geologic Quadrangle Map GQ-849, 1:24,000 scale.

Papke, K.G., 1979, Fluorspar in Nevada: Nevada Bureau of Mines and Geology Bulletin 93, 77 p.

Percival, T.J., Bagby, W.C., and Radtke, A.S., 1988, Physical and chemical features of precious metal deposits hosted by sedimentary rocks in the western United States: *in* Schafer, R.W., Cooper, J.J., and Vikre, P.G., eds., Bulk Mineable Precious Metal Deposits of the Western United States, Geological Society of Nevada, Reno, p. 11-34.

Ponce, D.A., 1981, Preliminary gravity investigations of the Wahmonie site, Nevada Test Site, Nye County, Nevada: U.S. Geological Survey Open-file Report 81-522, 64 p.

Ponce, D.A., 1984, Gravity and magnetic evidence for a granitic intrusion near Wahmonie, Nevada Test Site, Nevada: Journal of Geophysical Research, v. 89, p. 9401-9413.

Poole, F.G., Carr, W.J., and Elston, D.P., 1965, Salyer and Wahmonie Formations of south-eastern Nye County, Nevada: U.S. Geological Survey Bulletin 1224-A, p. A44-A51.

Powers, S.L., 1988, Two lineation directions in the Mineral Ridge core complex, Esmeralda County, Nevada [abs.]: Geological Society of America Abstracts with Programs, v. 20, p. 222.

Quade, J., and Tingley, J.V., 1984, A mineral inventory of the Nevada Test Site, and portions of Nellis Bombing and Gunnery Range, southern Nye County, Nevada: Nevada Bureau of Mines and Geology Open-file Report 82-2, 40 p. plus appendices.

RANDOL, 1993, Randol Mining Directory 1993/1994, U.S. mines and mining companies, Randol International, Ltd., Golden, Colorado, 734 p.

Ransome, F.L., Emmons, W.H., and Garrey, G.H., 1910, Geology and ore deposits of the Bullfrog district, Nevada: U.S. Geological Survey Bulletin 407, 130 p.

Ristorcelli, S.J., and Ernst, D.R., 1991, Summary report: USNGS exploration 1990-1991, Nye County, Nevada, unpublished company report, U.S. Nevada Gold Search Joint Venture, Carson City, 104 p.

Rye, R.O., 1993, The evolution of magmatic fluids in the epithermal environment: the stable isotope perspective: Economic Geology, v. 88, p. 733-753.

Sawyer, D.A., and Sargent, K.A., 1989, Petrologic evolution of divergent peralkaline magmas from the Silent Canyon caldera complex: Journal of Geophysical Research, v. 94, p. 6021-6040.

Sawyer, D.A., Fleck, R.J., Lanphere, M.A., Warren, R.G., and Broxton, D.E., 1990, Episodic volcanism in the southwest Nevada volcanic field: new $^{40}Ar/^{39}Ar$ geochronologic results [abs.]: EOS, Transactions of the American Geophysical Union, v. 71, p. 1296.

Sawyer, D. A., Fleck, R. J., Lanphere, M. A., Warren, R. G., Broxton, D. E., and Hudson, M. R., 1994, Episodic caldera volcanism in the Miocene southwestern Nevada volcanic field: revised stratigraphic framework, $^{40}Ar/^{39}Ar$ geochronology, and implications for magmatism and extension: Geological Society of America Bulletin, v. 106, p. 1304-1318.

Schweikert, R.A., 1989, Evidence for a concealed dextral strike-slip fault beneath Crater Flat, Nevada [abs.]: Geological Society of America Abstracts with Programs, v. 21, p. A90.

Schweikert, R.A., and Caskey, S.J., 1990, Pre-Middle Miocene extensional history of the Nevada Test Site (NTS) region, southern Nevada [abs.]: Geological Society of America Abstracts with Programs, v. 22, p. 81.

Scott, R.B. and Bonk, J., 1984, Preliminary geologic map of Yucca Mountain, Nye County, Nevada, with geologic sections: U.S. Geological Survey Open-file Report 84-494, scale 1:12,000, plus 10 p.

Scott, R.B., Byers, F.M. and Warren, R.G., 1984, Evolution of magma below clustered calderas, Southwest Nevada volcanic field [abs.], EOS, Transactions of the American Geophysical Union, v. 65, p. 1126-1127.

Seedorf, E.A., 1991, Magmatism, extension and ore deposits of Eocene to Holocene age in the Great Basin -mutual effects and preliminary proposed genetic relationships: in Raines, G.L., Lisle, R.E., Shafer, R.W., and Wilkinson, W.W., eds., Geology and Ore Deposits of the Great Basin, Reno, Geological Society of Nevada, p. 133-178.

Setterfield, T.N., Mussett, A.E., and Oglethorpe, R.D.J., 1992, Magmatism and associated hydrothermal activity during the evolution of the Tavua caldera: ^{40}Ar-^{39}Ar dating of the volcanic, intrusive, and hydrothermal events: Economic Geology, v. 87, p. 1130-1140.

Silberman, M.L., White, D.E., Keith, T.E.C., and Dockter, R.D., 1979, Duration of hydrothermal activity at Steamboat Springs, Nevada, from ages of associated volcanic rocks: U.S. Geological Survey Professional Paper 458-D, 14 p.

Silberman, M.L., Chesterman, C.W., Kleinhampl, F.J., and Gray, C.H., Jr., 1972, K-Ar ages of volcanic rocks and gold-bearing quartz-adularia veins in the Bodie mining district, Mono County, California: Economic Geology, v. 67, p. 597-604.

Silberman, M.L., 1985, Geochronology of hydrothermal alteration and mineralization: Tertiary epithermal precious-metal deposits in the Great Basin: U. S. Geological Survey Bulletin 1646, p. 55-70.

Sillitoe, R.H., McKee, E.H., and Vila, T., 1991, Reconnaissance K-Ar geochronology of the Maricunga gold-silver belt, northern Chile: Economic Geology, v. 86, p. 1261-1270.

Simonds, F.W., 1989, Geology and hydrothermal alteration in the Calico Hills, southern Nevada: Unpublished M.S. thesis, Boulder, Univ. Colorado, 136 p.

Simonds, F.W., and Scott, R.B., 1990, Hydrothermal alteration at the Calico Hills, Nye County, Nevada [abs.]: Geology and Ore Deposits of the Great Basin Program with Abstracts, Geological Society of Nevada, Reno, p. 126.

Snyder, D.B., and Oliver, H.W., 1981, Preliminary results of gravity investigations of the Calico Hills, Nevada Test Site, Nye County, Nevada: U.S. Geological Survey Open-File Report 81-101, 42 p.

Spencer, J., 1984, Role of tectonic denudation in warping and uplift of low-angle normal faults: Geology, v. 12, p. 95-98.

Spengler, R.W., Byers, F.M., Jr., and Warner, J.B., 1981, Stratigraphy and structure of volcanic rocks in drill hole USW-G1, Yucca Mountain, Nye County, Nevada: U.S. Geological Survey Open-File Report 82-1338, 264 p.

Steiger, R.H., and Jäger, 1977, Subcommission on geochronology- convention on the use of decay constants in geo- and cosmochronology: Earth and Planetary Science Letters, v. 36, p. 359-362.

Stewart, J.H., 1980, Geology of Nevada: Nevada Bureau of Mines and Geology Special Publication 4, 136 p.

Stewart, J.H., 1988, Tectonics of the Walker Lane belt, western Great Basin-Mesozoic and Cenozoic deformation in a zone of shear, *in* Ernst, W.G., ed., Metamorphism and crustal evolution of the western United States, Rubey Vol. VII: Prentice Hall, Englewood Cliffs, p. 683-713.

Stewart, J.H., and Carlson, J.E., 1976, Cenozoic rocks of Nevada: Nevada Bureau of Mines and Geology Map 52, 1:1,000,000.

Stewart, J.H., and Diamond, D.S., 1990, Changing patterns of extensional tectonics; Overprinting of the basin of the middle and upper Miocene Esmeralda Formation in western Nevada by younger structural basins: Geological Society of America Memoir 176, p. 447-476.

Swanson, K.E., Noble, D.C., McKee, E.H., and Gibson, P.C., 1993, Collapse calderas and other Neogene volcanic and hydrothermal features of the Chila Cordillera and adjacent areas, southern Peru [abs.]: Geological Society of America Abstracts with Programs, v. 25, p. 153.

Tingley, J.V., 1984, Trace element associations in mineral deposits, Bare Mountain (Fluorine) mining district, southern Nye County, Nevada: Nevada Bureau of Mines and Geology Report 39, 28 p.

Turrin, B.D., Champion, D.E., and Fleck, R.J., 1991, $^{40}Ar/^{39}Ar$ age of the Lathrop Wells volcanic center, Yucca Mountain, Nevada: Science, v. 253, p. 654-657.

U.S. Geologic Survey, 1984, A summary of geologic studies through January 1, 1983 of a potential high-level radioactive waste repository site at Yucca Mountain, southern Nye County, Nevada: U.S. Geological Survey Open-File Report 84-792, 164 p.

Warren, R.G., Byers, F.M., and Caporuscio, F.A., 1984, Petrography and mineral chemistry of units of the Topopah Springs, Calico Hills and Crater Flat Tuffs, and some older volcanic units, with emphasis on samples from drill hole USW G-1, Yucca Mountain, Nevada Test site: Los Alamos, New Mexico, Los Alamos National Laboratory Report LA-10003-MS, 78 p.

Weber, M.E., and Smith, E.I., 1987 Structural and geochemical constraints on the reassembly of mid-Tertiary volcanoes in the Lake Mead area of southern Nevada: Geology, v. 15, p. 553-556.

Weiss, S.I., and Noble, D.C., 1989, Stonewall Mountain volcanic center, southern Nevada: stratigraphic, structural and facies relations of outflow sheets, near-vent tuffs, and intracaldera units: Journal of Geophysical Research, v. 94, 6059-6074.

Weiss, S.I., Noble, D.C., and McKee, E.H., 1988, Volcanic and tectonic significance of the presence of late Miocene Stonewall Flat Tuff in the vicinity of Beatty, Nevada [abs.]: Geological Society of America Abstracts with Programs, v. 20, p. A399.

Weiss, S.I., Noble, D.C., and Larson, L.T., 1990a, Task 3: Evaluation of mineral resource potential, caldera geology and volcano-tectonic framework at and near Yucca Mountain; report for October, 1989 - September, 1990: Center for Neotectonic Studies, University of Nevada, Reno, 29 p. plus appendices.

Weiss, S.I., Noble, D.C., and Larson, L.T., 1992, Task 3: Evaluation of mineral resource potential, caldera geology and volcano-tectonic framework at and near Yucca Mountain; report for October, 1990 - September, 1991: Center for Neotectonic Studies, University of Nevada, Reno, 44 p. plus appendices.

Weiss, S.I., Noble, D.C., and Larson, L.T., 1993a, Task 3: Evaluation of mineral resource potential, caldera geology and volcano-tectonic framework at and near Yucca Mountain; report for October, 1991 - September, 1992: Center for Neotectonic Studies, University of Nevada, Reno, 41 p. plus appendices.

Weiss, S.I., Ristorcelli, S.J., and Noble, D.C., 1993b, Mother Lode gold deposit, southwestern Nevada: another example of Carlin-type mineralization associated with porphyry magmatism [abs.]: Geological Society of America Abstracts with Programs, v. 25, p. 161.

Weiss, S.I., Noble, D.C., and Larson, L.T., 1995, Pyritic ash-flow tuff, Yucca Mountain, Nevada- A discussion: Economic Geology (in review).

Weiss, S.I., Connors. K.A., Noble, D.C., and McKee, E.H., 1990b, Coeval crustal extension and magmatic activity in the Bullfrog Hills during the latter phases of Timber Mountain volcanism [abs.]: Geological Society of America Abstracts with Programs, v. 22, p. 92-93.

Weiss, S.I., McKee, E.H., Noble, D.C., Connors, K.A., and Jackson, M.R., 1991, Multiple episodes of Au-Ag mineralization in the Bullfrog Hills, SW Nevada, and their relation to coeval extension and volcanism [abs.]: Geological Society of America Abstracts with Programs, v. 23, p. A246.

Weiss, S.I., Noble, D.C., Worthington, J.E., IV, and McKee, E.H., 1993c, Neogene tectonism from the southern Nevada volcanic field to the White Mountains, California, Part I. Miocene volcanic stratigraphy, paleotopography, extensional faulting and uplift between northern Death Valley and Pahute Mesa: *in* Lahren, M.M., Trexler, J.H. Jr., and Spinosa, C., eds., Crustal Evolution of the Great Basin and Sierra Nevada: Cordilleran/Rocky Mountain Section, Geological Society of America Guidebook, Dept. Geological Science, University of Nevada, Reno, p. 353-382.

Woldegabriel, G., 1990, Hydrothermal alteration in the Valles caldera ring fracture zone and core hole VC-1: evidence for multiple hydrothermal systems: Journal of Volcanology and Geothermal Research, v. 40, p. 105-122.

Woldegabriel, G., and Goff, F., 1989, Temporal relations of volcanism and hydrothermal systems in two areas of the Jemez volcanic field, New Mexico: Geology, v. 17, p. 986-989.

Wright, L.A., Thompson, R.A., Troxel, B.W., Pavlis, T.L., DeWitt, E.H., Otton, J.K., Ellis, M.A., Miller, M.G., and Serpa, L.F., 1991, Cenozoic magmatic and tectonic evolution of the east-central Death Valley region, California: *in* Walawender, M.J., and Hanan, B.B., eds., Geologic excursions in southern California and Mexico, Geological Society of America Field Trip Guidebook, San Diego, California, p. 93-127.

Worthington, J.E., IV, 1992, Neogene structural and volcanic geology of the Gold Mountain - Slate Ridge area, Esmeralda County, Nevada: Unpublished M.S. thesis, Reno, University of Nevada, Reno, 78 p.

Figure Captions:

Fig. 1 Map showing calderas and major volcanic centers of the southwestern Nevada volcanic field. Modified from Noble et al. (1991). SM = Stonewall Mountain; OB = Obsidian Butte; BM = Black Mountain; SC = Silent Canyon center; WS = Wahmonie-Salyer center; PP(?) = proposed Prospector Pass caldera of Carr et al. (1986). FLV-DV-FC FZ = Fish Lake Valley-Death Valley-Furnace Creek fault zone.

Fig. 2 Locations of mineral deposits, areas of hydrothermally altered rocks, caldera margins, and other structural and physiographic features of the southern part of the southwestern Nevada volcanic field. Porphyry dikes in Bare Mountain shown by dotted lines. OB-FC = the Original Bullfrog-Fluorspar Canyon fault system; BC = Boundary Canyon fault (modified from Carr and Monsen, 1988). B = Bailey's hot spring, BW = Beatty Wash, CH = Calico Hills, CY = Clarkdale-Yellow Gold mine area, D = Daisy mine, G = Gold Bar mine, GA = Gold Ace mine, GD = Goldspar/Diamond Queen mine, BGB = Barrick Bullfrog mine, M = Mary mine, ML = Mother Lode mine, MM = Mine Mountain, MS = Montgomery-Shoshone mine, My = Mayflower mine, OB = Original Bullfrog mine, OM = Oasis Mountain, P = Pioneer mine, R = Denver-Tramps and Gibralter mines near Rhyolite, S = Sterling mine, Si = Silicon mine, SP = Secret Pass prospect, T = Telluride mine, Th = Thompson mine, TH = Transvaal Hills, TO = Tolicha-Quartz Mountain district, W = Wahmonie, YJ = Yellowjacket mine. O = Obsidian Butte, SB = Sleeping Butte. Small open dots labeled G1, G2 and G3 refer to deep drill holes USW G-1, USW G-2 and USW G-3. TM-I caldera associated with the eruption of the 11.6-Ma Rainier Mesa Tuff; TM-II caldera associated with the eruption of the 11.45-Ma Ammonia Tanks Tuff. Hammer and pick = active and recently producing mines, o = historic mines, x = prospect, + = Coffer #1 exploratory well.

Fig. 3 Residual silica and acid-leached rocks of the Rainier Mesa Tuff of the Timber Mountain Group near the Silicon mine, interpreted as the result of shallow, steam-heated acid-sulfate alteration.

Fig. 4 Geologic map of Mine Mountain showing structural features and the principal areas of alteration and mineralization. Modified from Orkild (1968) and Frizzell and Schulters (1990).

Fig. 5 Generalized geologic map of the Bullfrog Hills. Modified from Ransome et al. (1910), unpublished mapping of S. I. Weiss and K. A. Connors (1989-1991), Maldonado (1990b), Maldonado and Hausback (1990), and Monsen et al. (1992). Section A - A' shown in Figure 10. OBF = Original Bullfrog fault, AF = Amargosa fault, FC = Fluorspar Canyon fault and OVFZ = Oasis Valley fault zone. Mines and other features labeled as in Fig. 2. Zpu = Late Proterozoic and early Paleozoic sedimentary and metamorphic rocks, undivided; Tmo = Timber Mountain and older ash-flow sheets and units of lava and tuffaceous sedimentary rocks, Tpi = silicic, coarse-grained porphyritic dike of undetermined age; Tbh = tuffs and lavas of the Bullfrog Hills, m denotes landslide (megabreccia) deposits; Tri = rhyolitic plugs, dikes and domes of the tuffs and lavas of the Bullfrog Hills, includes post-Crater Flat Group phenocryst-poor rhyolitic plugs and dikes in the Pioneer - Yellowjacket area.

Fig. 6 Plot of A) K_2O vs. Rb and B) K_2O vs. SiO_2/Al_2O_3 for samples of altered wallrocks at the Barrick Bullfrog and Montgomery-Shoshone mines. Dashed boxes show approximate range of values for unaltered high- and low-silica rhyolite ash-flow tuff of the Timber Mountain Group (Broxton et al., 1989). X's and +'s show rocks from the Montgomery-Shoshone and Barrick Bullfrog mines, respectively. Triangle shows banded quartz-calcite vein with about 25% wallrock fragments from the Polaris vein at the Montgomery-Shoshone mine. Analyses by X-ray fluorescence methods in the analytical laboratory of the Nevada Bureau of Mines and Geology under the supervision of P.J. Lechler.

Fig. 7 A) North wall of the open-pit, Phase I, at the Barrick Bullfrog mine showing the main vein (between arrows); view is to the northwest. B) West-dipping fault in northwest wall, Phase I, of open pit at the Barrick Bullfrog mine. Fault separates east-dipping, strongly silicified and potassium metasomatized ash-flow tuff of the Rainier Mesa Tuff, above, from underlying ore composed of brecciated quartz-calcite veins and altered wallrock fragments. C) Altered footwall lava cut by gold-bearing stockwork of dark colored veins and veinlets containing mixtures of quartz, black hydrocarbon, calcite, pyrite, chlorite and wallrock fragments. Carbonaceous veins are cut by light colored veins containing quartz, calcite, adularia and locally pyrite.

Fig. 8 Timing of hydrothermal activity in the southwestern Nevada volcanic field. Dots show radiometric age determinations, error bars at ±1 σ. ** signifies $^{40}Ar/^{39}Ar$ ages. Open symbol shows timing constrained by stratigraphic relations.  age recalculated from Morton et al. (1977);  ages from Noble et al. (1991).

Fig. 9 Diagrammatic summary of volcanism, extensional faulting and hydrothermal activity of the Bullfrog Hills. Open diamonds show radiometric ages of volcanic rocks from Marvin and Cole (1978), Marvin et al. (1989), Hausback et al. (1990), Maldonado and Hausback (1990), and Noble et al. (1991); solid diamonds show $^{40}Ar/^{39}Ar$ ages of adularia, x's show K-Ar ages of adularia; solid dots show weighted averages of K-Ar and $^{40}Ar/^{39}Ar$ ages from the same samples; error bars at ±1 σ. [1] = rhyolite of the Tracking Station (Marvin et al., 1989) and tuff of Sober-up Gulch (Maldonado and Hausback, 1990). [2] = latite of Donovan Mountain (Minor et al., 1993). [3] includes the rhyolite of Burton Mountain (Marvin and Cole,1978; Carr 1984a). SFT = Stonewall Flat Tuff, AT = Ammonia Tanks Tuff. NBH = northern Bullfrog Hills; SBH = southern Bullfrog Hills.

Fig. 10 Simplified cross section (A - A') in the northern Bullfrog Hills showing early, presently low-angle normal faults displaced and rotated by younger, higher-angle normal faults. Megabreccia deposits within the tuffs and lavas of the Bullfrog Hills near the east end of A - A' dip approximately 18° to 20° to the east. Cwu, Cz and Cc refer, respectively, to the Cambrian upper part of the Wood Canyon Formation, Zabriskie Quartzite, and the Carrara Formation, most recently described by Monsen et al. (1992) from more complete exposures at Bare Mountain. Tot = older tuffs; Tlr = Lithic Ridge Tuff; Tc = single cooling unit of the Crater Flat Group; Tpi = silicic porphyry intrusion containing sanidine phenocrysts as large as 1.5 cm in maximum dimension. Tp = single cooling unit of the Paintbrush Group; M = coarse landslide (megabreccia) deposits within the tuffs and lavas of the Bullfrog Hills; Tht_2 = unwelded, pumice-rich rhyolite ash-flow tuff and surge unit #2 of the tuffs and lavas of the Bullfrog Hills (Fig. 9); Thri = rhyolite plug of the tuffs and lavas of the Bullfrog Hills; Qac = Quaternary alluvium and colluvium.

APPENDIX

Descriptions of samples used in K-Ar and $^{40}Ar/^{39}Ar$ dating. Field numbers correspond to Table 2. Additional information concerning sample collection and sample localities is given by McKee and Bergquist (1993).

3MJ-224B: Mixture of quartz-adularia-calcite ± pyrite veins and altered wallrock fragments of aphyric andesite or dacite lava flow of the Wahmonie Formation, from outcrop about 800' NNW of the Hornsilver mine. Wallrock fragments are composed of fine-grained intergrowths of quartz, adularia and illite.

3SW-147: Altered porphyritic hornblende-biotite andesite or dacite lava flow of the Wahmonie Formation containing quartz ±adularia veinlets from outcrop about 650' NW of the Hornsilver mine. Biotite and hornblende phenocrysts are completely replaced by illite, plagioclase is pseudomorphed by adularia, and groundmass is composed of fine-grained intergrowths of quartz, illite and adularia.

3MJ-118: Alunitized, poorly sorted, matrix-supported tuffaceous conglomerate adjacent to the Tate's Wash segment of the Fluorspar Canyon fault, north flank of Bare Mountain. Volcanic clasts and matrix replaced by mixtures of fine-grained quartz, alunite and halloysite. Alunite comprises anhedral to blocky crystals of about 0.005 mm in maximum dimension. Conglomerate *underlies* pre-Rainier Mesa Tuff bedded ash-fall and ash-flow tuffs (cf. Jackson, 1988; Bergquist and McKee, 1993).

3MJ-130a: Angular to subrounded clasts composed of pure, very fine-grained alunite in matrix-supported breccia body cutting carbonate rocks of the Roberts Mountains Formation. Matrix consists of partially to completely alunitized porous tuff, including originally glassy pumice fragments. Alunite comprises anhedral to blocky crystals of about 0.010 mm in maximum dimension.

Thompson mine: Vein composed of 85% fine-grained alunite and 15% halloysite cutting tuffs of the Paintbrush Group. Wallrocks altered to porous mixtures of opal-CT, kaolinite and alunite.

Silicon mine: Dense, alunitized and silicified rhyolitic ash-flow tuff containing small phenocrysts and phenocryst fragments of quartz and relict feldspar; sample is composed of about 35% alunite (≤0.2 mm in maximum dimension) intergrown with about 65% fine-grained quartz and opal.

3MJ-216A: Vein containing about 95% fine-grained alunite and about 5% quartz within argillically altered ash-flow tuff of the Rainier Mesa Tuff, eastern Calico Hills. Alunite comprises aggregates of anhedral to blocky crystals ≤0.010 mm in maximum dimension.

3SW-137A: Alunitized tuff of the rhyolite of Calico Hills; sample consists of a porous mixture of 50% fine-grained alunite, nearly 50% opal-CT, and traces of kaolinite. Alunite comprises anhedral to blocky crystals ≤0.010 mm in maximum dimension.

3SW-303: Alunitized, previously vitric, partially welded ash-flow tuff of the Ammonia Tanks Tuff, south flank of Mine Mountain. Feldspar and mafic accessory phenocrysts and pumice fragments completely replaced by granular mosaics of blocky to bladed alunite (crystals ≤0.2 mm in maximum dimension), ± small amounts of kaolinite. Many large shards and pumice fragments replaced by finer-grained granular alunite; most of the groundmass glass is altered to kaolinite.

3MJ-176: Silicified lithic-rich ash-flow tuff of the Lithic Ridge Tuff adjacent to the main vein at the Original Bullfrog mine; contains numerous thin quartz and quartz-adularia veinlets. Groundmass replaced by fine-grained quartz, adularia and illite/smectite. Feldspar phenocrysts replaced by adularia, albite, illite and quartz.

Mayflower mine: Adularized nonwelded, crystal-rich, rhyolitic ash-flow tuff from dump at the Mayflower mine. Adularia crystals are present as coatings on fracture surfaces and feldspar phenocrysts are pseudomorphed by non-turbid adularia having mottled extinction; groundmass composed of fine-grained polygonal to granophyric intergrowths of quartz with anhedral to euhedral adularia.

Bullfrog Hills: Silicified and adularized rhyolitic ash-flow tuff of the Crater Flat Group adjacent to thin quartz vein along NE-striking fault between the Yellowjacket and Pioneer mines. Contains quartz veinlets and is composed of approximately 75% quartz, 20% adularia and 5% illite.

3MJ-74a: Silicified and adularized rhyolitic ash-flow tuff of the Ammonia Tanks Tuff, adjacent to north-trending quartz vein in Oasis Mountain. Contains numerous veinlets of quartz. Feldspar phenocrysts pseudomorphed by adularia, albite and quartz, and mafic accessory phenocrysts replaced by illite. Groundmass consists of fine-grained intergrowths of quartz with sparse adularia and illite.

BAILEY'S: Alunitized rock of the Ammonia Tanks Tuff near active, presently near-neutral hot spring. Feldspar and accessory phenocrysts replaced by granular mosaics of blocky to bladed alunite (≤0.4 mm in maximum dimension). Groundmass altered to mixtures of fine-grained alunite, opal-CT, chalcedony, and kaolinite.

3MJ-6: Drusy veinlets of clear alunite crystals, as much as 0.5 mm in maximum dimension, along fractures in altered, originally glassy, densely welded, ash-flow tuff (vitrophyre) of the Rainier Mesa Tuff, Transvaal Hills. Vitrophyre is altered to a fine-grained mixture of alunite, kaolinite and opal.

Ttp: Devitrified groundmass of densely welded, shard-rich, nearly aphyric ash-flow tuff of the tuff of Tolicha Peak. Sample collected by D.C. Noble from hogback at the base of the south side of Gold Mountain, Esmeralda County, Nevada.

BBSF-2: Silicified and adularized wallrock fragment composed of ash-flow tuff cut by chalcedonic quartz veinlets, within vein ore of the upper silica-flooded zone, "middle-plate fault", west wall at 1018m level, Barrick Bullfrog mine. Feldspar phenocrysts pseudomorphed by adularia and quartz, and small amounts of illite and albite. Groundmass composed of granophyric intergrowths of secondary quartz with anhedral to euhedral, very fine-grained adularia and traces of illite.

3SW-357: Pyritic quartz vein containing silicified and adularized fragments of welded, rhyolitic ash-flow tuff of the Crater Flat Group, dump of the Yellowjacket mine. Feldspar phenocrysts pseudomorphed by adularia, quartz and illite; groundmass composed of quartz, anhedral adularia, illite/smectite and disseminated pyrite partly replaced by jarosite.

Table 1. Volcanic-Stratigraphic Framework and Geochronology of the Southwestern Nevada Volcanic Field

Major Ash-flow Units and Lavas		Radiometric	Volcanic Center/location
Unit	Subunit	Age (Ma)	
	Late Magmatic Stage		
Stonewall Flat Tuff	Civet Cat Canyon Member	7.5	Stonewall Mountain caldera complex
	Spearhead Member	7.6	
Rhyolite of Obsidian Butte		8.8	Obsidian Butte
Thirsty Canyon Group *(Tuff)*	Gold Flat Tuff (*Member*)	9.2	Black Mountain caldera complex
	Trail Ridge Tuff (*Member*)		
	Pahute Mesa Tuff (*Member*)		
	Rocket Wash Tuff (*Member*)	9.4	
	Timber Mountain Magmatic Stage		
Mafic lavas			Timber Mountain caldera II; moat and periphery
Tuffs and lavas of the Bullfrog Hills, rhyolite of Shoshone Mountain		10.5-10.0	Periphery and west of Timber Mountain caldera II
Tuff of Cut-off Road, rhyolite lavas of Beatty Wash, tuffs and lava of Fleur de Lis Ranch, tuff of Buttonhook Wash		11.4	Western part of Timber Mountain caldera complex
Timber Mountain Group (*Tuff*)	Ammonia Tanks Tuff (*Member*)	11.45	Timber Mountain caldera II
	Rainier Mesa Tuff (*Member*)	11.6	Timber Mountain caldera I
Pre-Rainier Mesa rhyolite lavas, domes		11.7-11.6	Periphery and west of Timber Mountain caldera I
	Main Magmatic Stage		
Post-collapse rhyolite lavas, domes		12.7-12.5	South margin of Claim Canyon cauldron
Paintbrush Group (*Tuff*)	Tiva Canyon Tuff (*Member*)	12.7	Claim Canyon cauldron
	Yucca Mountain Tuff (*Member*)		All others from area of Timber Mountain caldera complex
	Pah Canyon Tuff (*Member*)		
	Topopah Spring Tuff (*Member*)	12.8	
Calico Hills Formation		12.9	Flow-dome complexes southeast of Claim Canyon cauldron and Area 20 caldera
Wahmonie and Salyer Formations		13.2-12.8	Wahmonie
Crater Flat Group (*Tuff*)	Prow Pass Tuff (*Member*)		Uncertain; likely sources include area of Timber Mountain, Silent Canyon-Area 20 caldera complex, NW Yucca Mountain, and/or proposed Prospector Pass caldera complex
	Bullfrog Tuff (*Member*)	13.25	
	Tram Tuff (*Member*)		
Belted Range Group (*Tuff*)	Grouse Canyon Tuff (*Member*)	13.7	Silent Canyon caldera complex
Tuff of Tolicha Peak		13.9	Uncertain; likely source area in the vicinity of Mount Helen
Dacitic lavas and breccias			Bullfrog Hills, periphery of Crater Flat
Lithic Ridge Tuff		14.0	Uncertain
Rhyolitic lavas and dikes, Silicic dikes of Bare Mountain		14 - 15?	Bullfrog Hills, periphery of Crater Flat, eastern Bare Mountain
Tub Spring Tuff (*Member of Belted Range Tuff*)		14.9	Silent Canyon caldera complex
Older tuffs			Unknown
Sanidine-rich tuff			Unknown
Tuff of Yucca Flat		15.1	Unknown
Redrock Valley Tuff		15.2	Unknown

Table 1, continued.

Nomenclature in use prior to the changes of Sawyer et al. (1994) shown with italics in parentheses after major unit names. Compiled from discussions given by Byers et al. (1976a, 1989), Christiansen et al. (1977), Noble et al. (1984, 1991), Carr et al. (1986), Sawyer and Sargent (1989), Weiss and Noble (1989) and radiometric age data of Kistler (1968), Noble et al. (1968), Marvin et al. (1970; 1989), Hausback et al. (1990), Fleck et al. (1991), Sawyer et al. (1990; 1994), Noble et al. (1991), Monsen et al. (1992) and Weiss et al. (1993c). Ages corrected using modern constants.

[1] Includes the rhyolite lava flows and tuffs of Rainbow Mountain (Maldonado, 1990a; Maldonado and Hausback, 1990), as well as overlying latitic to basaltic lavas.

Table 2. Radiometric Age Data for Specimens from the Southern Portion of the Southwestern Nevada Volcanic Field

Conventional K-Ar Age Determinations

No.	Field number	Mineral dated	District/Area of Mineralization	Latitude N.	Longitude W.	K_2O wt.%	$^{40}Ar^*$ mole/g	$^{40}Ar^*/^{40}Ar$ (%)	Age $\pm 1\sigma$ (Ma)
	Wahmonie and Mine Mountain								
1	3SW-303	Al	Mine Mountain	36°58.46'	116°9.83'	9.04	1.4483×10^{-10}	55.6	11.1 ± 0.3
2	3SW-147	Ad	Wahmonie	36°49.21'	116°10.07'	12.96	2.3657×10^{-10}	59.5	12.6 ± 0.4
3	3MJ-224B	Ad	Wahmonie	36°49.25'	116°10.03'	14.0	2.6018×10^{-10}	66.5	12.9 ± 0.4
	Bare Mountain and northern Crater Flat								
4	3MJ-130a	Al	Telluride mine area	36°53.66'	116°39.5'	10.65	1.7212×10^{-10}	71.3	11.2 ± 0.3
5	Silicon mine	Al	Tram Ridge	36°57.51'	116°38.6'	6.89	1.1560×10^{-10}	52.3	11.6 ± 0.4
6	3MJ-118	Al	West of Telluride mine	36°53.86'	116°39.5'	2.25	3.9508×10^{-11}	26.6	12.2 ± 0.4
7	Thompson mine	Al	Northern Crater Flat	38°56.94'	116°38.0'	6.48	1.2085×10^{-10}	19.6	12.9 ± 0.5
	Transvaal Hills, Oasis Valley and Calico Hills								
8	3MJ-6	Al	Transvaal Hills	37°1.07'	116°34.52'	9.05	1.2940×10^{-10}	37.0	9.9 ± 0.4
9	BAILEY'S	Al	Bailey's hot spring	36°58.58'	116°43.08'	7.89	1.1572×10^{-10}	60.2	10.2 ± 0.3
10	3MJ-216A	Al	Eastern Calico Hills	36°54.20'	116°14.28'	11.02	1.6491×10^{-10}	87.3	10.4 ± 0.3
11	3SW-137A	Al	Western Calico Hills	36°52.78'	116°21.47'	8.38	1.4028×10^{-10}	19.4	10.4 ± 0.3
12	3MJ-74a	Ad	Oasis Mountain	37°2.6'	116°44.93'	5.32	8.1468×10^{-11}	43.4	10.6 ± 0.3
	Bullfrog Hills								
13	3MJ-176	Ad	Original Bullfrog mine	36°54.06'	116°53.1'	12.4	1.5497×10^{-10}	49.5	8.7 ± 0.3
14	Mayflower	Ad	Mayflower mine	36°59.73'	116°47.30'	13.71	1.9745×10^{-10}	78.7	10.0 ± 0.3
15	Bullfrog Hills	Ad	North of Pioneer mine	37°0.80'	116°45.53'	11.19	1.7741×10^{-10}	65.7	11.0 ± 0.4
	Tuff of Tolicha Peak								
16	Ttp	wr	Gold Mountain	37°14.6'	117°15.2	4.85	9.7235×10^{-11}	71.2	13.9 ± 0.4

Table 2, continued.

$^{40}Ar/^{39}Ar$ Multigrain Resistance-furnace Fusion Determinations

No.	Field number	Mineral dated	District/Area of Mineralization	Latitude	Longitude	$^{40}Ar/^{39}Ar$	$^{36}Ar/^{39}Ar$	$^{37}Ar/^{39}Ar$	$^{40}Ar^{*}$ (%)	J	Age ±1σ (Ma)
	Northern Bullfrog Hills										
14	Mayflower*	Ad	Mayflower mine	36°59.73'	116°47.30'	1.9522	3.0617×10^{-3}	1.9447×10^{-3}	50.3	0.00560	9.9± 0.3
17	3SW-357*	Ad	Yellowjacket mine	37°1.92'	116°47.64'	3.1573	6.7614×10^{-3}	2.3506×10^{-3}	34.7	0.00574	11.3± 0.3
	Southern Bullfrog Hills										
13	3MJ-176**	Ad	Original Bullfrog mine	36°54.06'	116°53.1'	2.7466	5.0852×10^{-2}	1.4295×10^{-3}	45.3	0.00041	9.2± 0.3
18	BBSF-2*	Ad	Barrick Bullfrog mine	36°53.73'	116°48.84'	1.7893	2.6974×10^{-3}	3.3729×10^{-3}	51.8	0.00587	9.8± 0.3

Ad = adularia; Al = alunite; wr = whole-rock (devitrified groundmass).

Constants: $^{40}K\ \kappa_{\varepsilon} + {}^{40}K\ \kappa_{\varepsilon'} = 0.581 \times 10^{-10}\ yr^{-1}$; $^{40}K_{\beta} = 4.962 \times 10^{-10}\ yr^{-1}$; atomic abundance $^{40}K/K_{total} = 1.167 \times 10^{-4}$ kmole/kmole.

* Reactor constants: $(^{36}Ar/^{37}Ar)_{Ca} = 0.000264$; $(^{39}Ar/^{37}Ar)_{Ca} = 0.000673$; $(^{40}Ar/^{39}Ar)_{K} = 0.065$.

** Reactor constants: $(^{36}Ar/^{37}Ar)_{Ca} = 0.000275$; $(^{39}Ar/^{37}Ar)_{Ca} = 0.000729$; $(^{40}Ar/^{39}Ar)_{K} = 0.002$.

Additional descriptive information on sample locations and sample mineralogy is given in the Appendix and in McKee and Bergquist (1993).

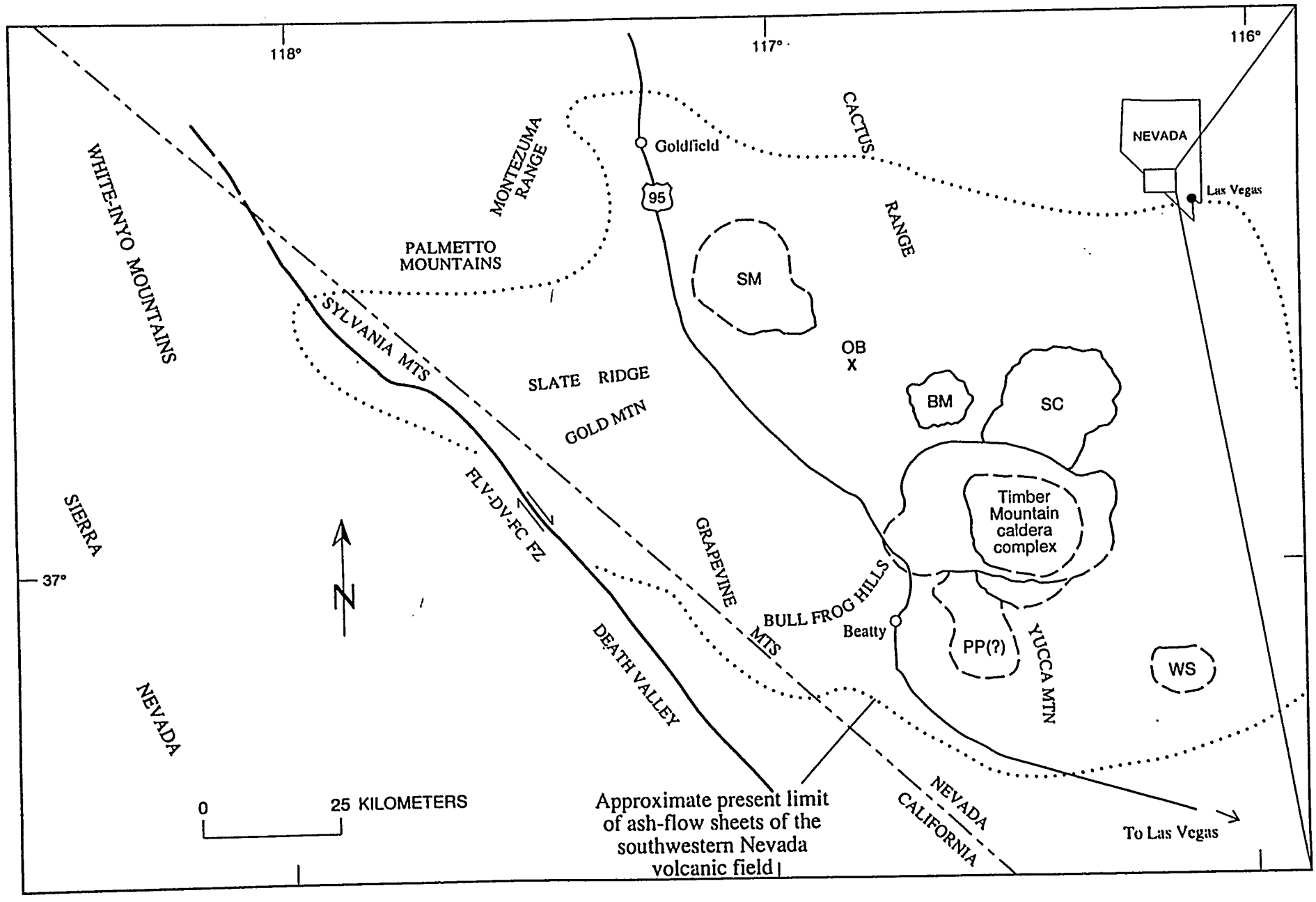
118°
117°
116°
37°
WHITE-INYO MOUNTAINS
SIERRA NEVADA
MONTEZUMA RANGE
PALMETTO MOUNTAINS
SYLVANIA MTS
SLATE RIDGE
GOLD MTN
FLV-DV-FC FZ
DEATH VALLEY
GRAPEVINE MTS
BULL FROG HILLS
Beatty
Goldfield
95
CACTUS RANGE
NEVADA
Las Vegas
SM
OB
BM
SC
Timber Mountain caldera complex
PP(?)
YUCCA MTN
WS
N
0
25 KILOMETERS
Approximate present limit of ash-flow sheets of the southwestern Nevada volcanic field
NEVADA
CALIFORNIA
To Las Vegas

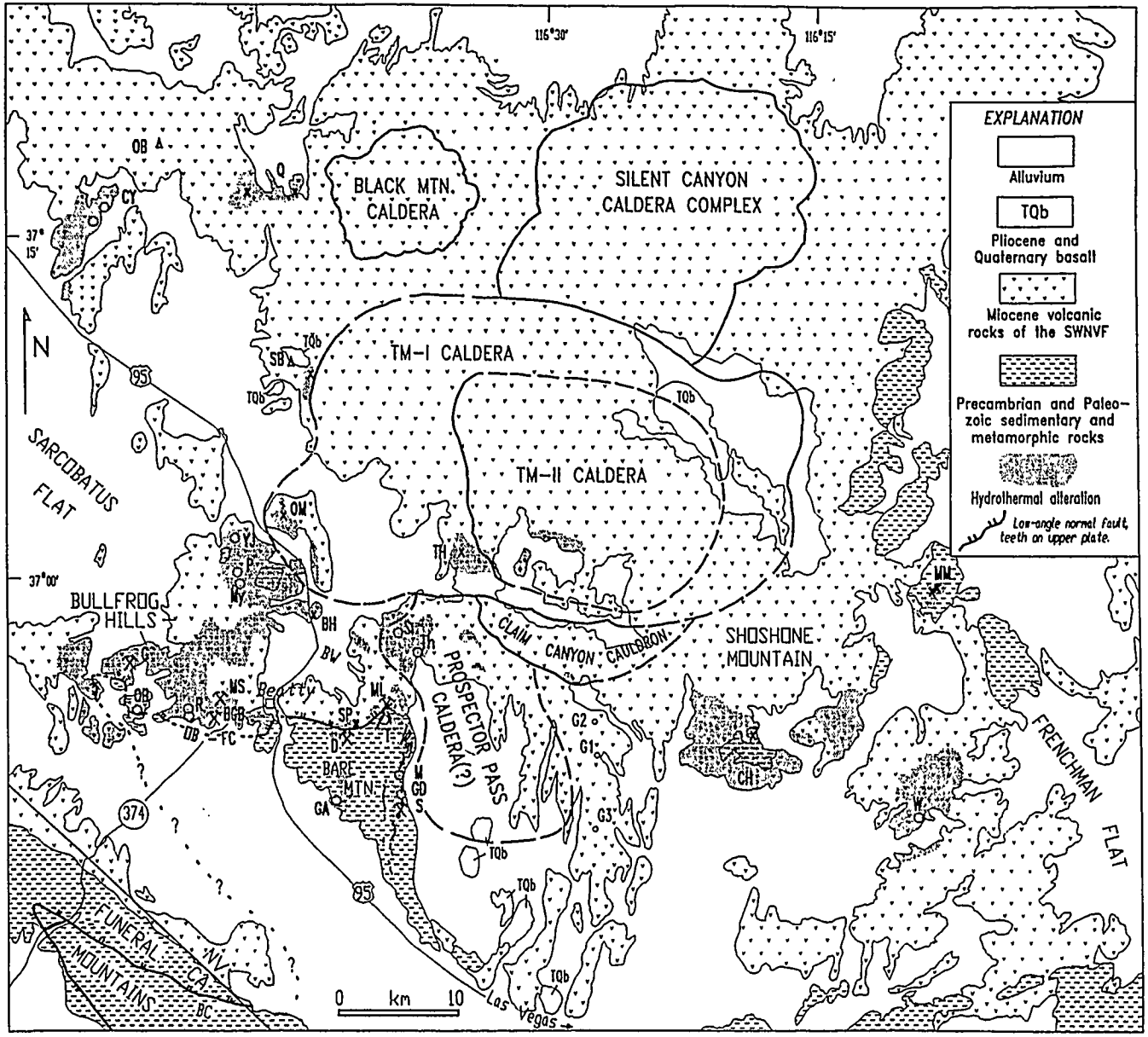
116°30'
116°15'
37° 15'
37°00'
N
BLACK MTN. CALDERA
SILENT CANYON CALDERA COMPLEX
TM–I CALDERA
TM–II CALDERA
SARCOBATUS FLAT
BULLFROG HILLS
CLAIM CANYON CAULDRON
PROSPECTOR PASS CALDERA(?)
SHOSHONE MOUNTAIN
FRENCHMAN FLAT
BARE MTN.
FUNERAL MOUNTAINS
CA
NV
Las Vegas
0 km 10
95
374
85
EXPLANATION
Alluvium
TQb
Pliocene and Quaternary basalt
Miocene volcanic rocks of the SWNVF
Precambrian and Paleozoic sedimentary and metamorphic rocks
Hydrothermal alteration
Low-angle normal fault, teeth on upper plate.

Fig. 2

Fig. 2

Fig. 3

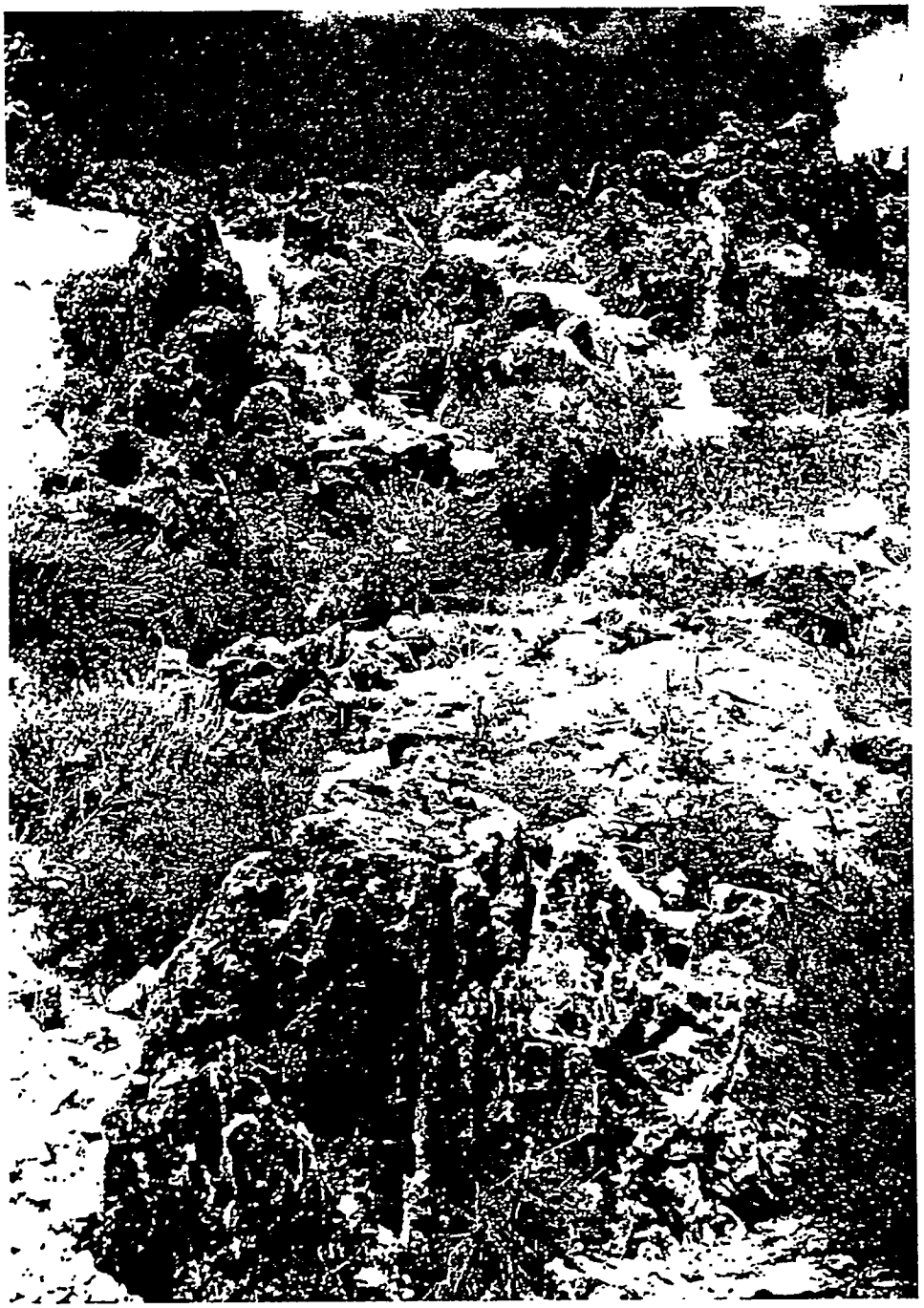

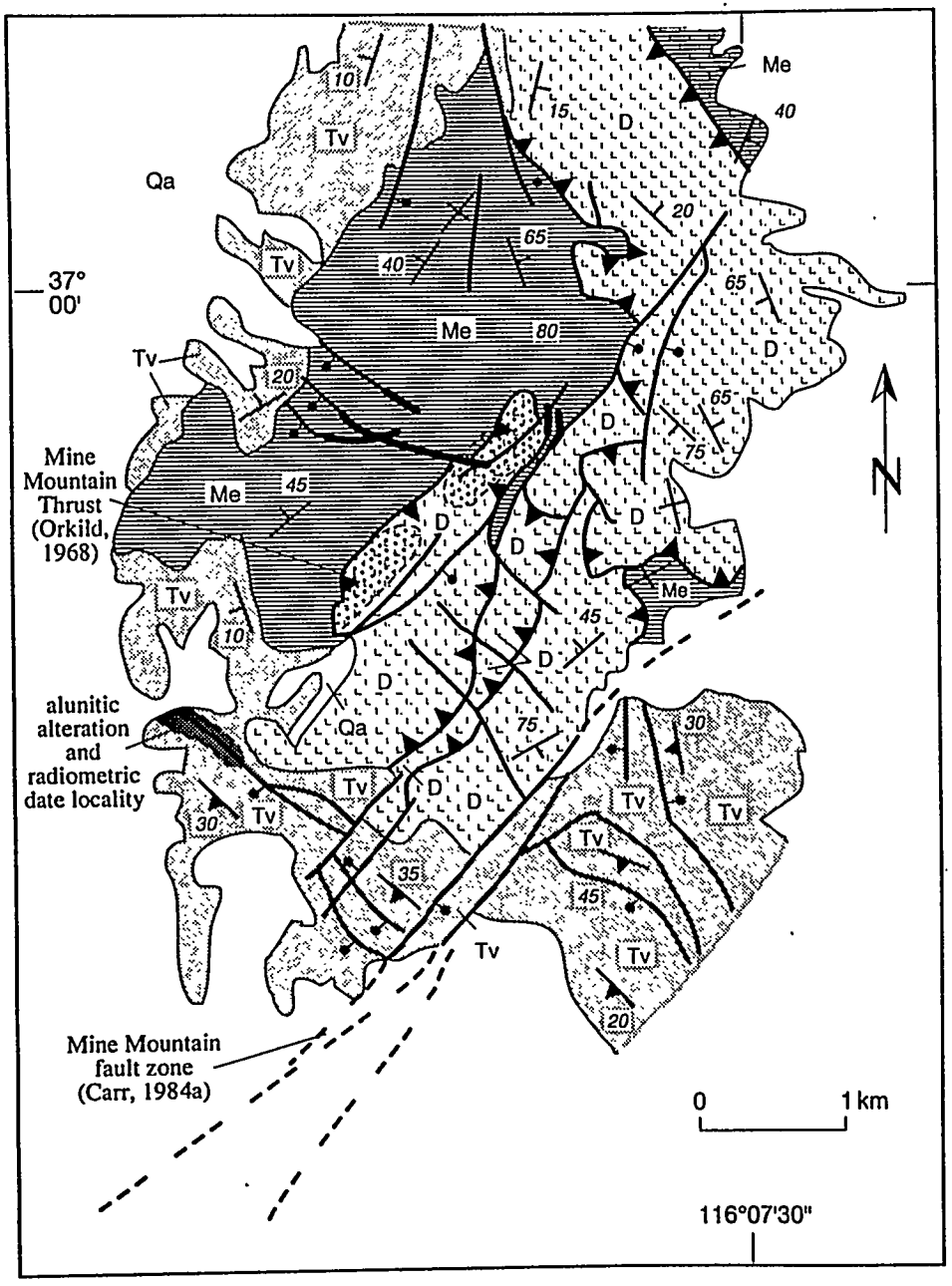

EXPLANATION

- Quaternary alluvium
- Miocene volcanic and sedimentary rocks
- Mississippian Eleana Formation
- Devonian limestone and dolostone
- Stipple shows principal areas of silicification, veins and hydrothermal and tectonic breccia along the crest of Mine Mountain
- Quartz and quartz-barite veins
- Strike and dip direction of beds
- 30 Strike and dip direction of foliation in ash-flow and bedded tuffs
- Mine Mountain "thrust." Teeth on upper plate

Fig.5

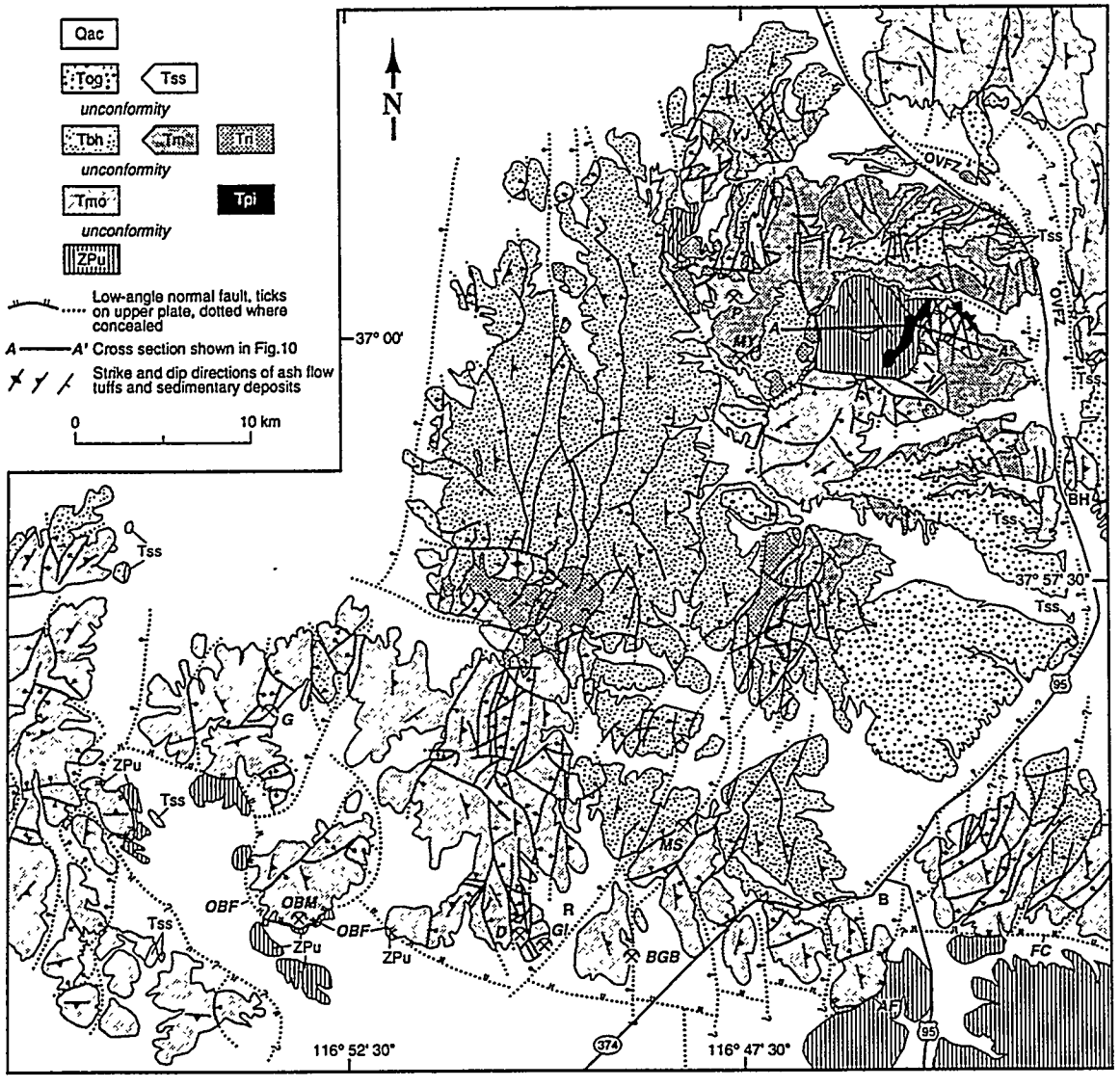
Qac
Tog
Tss
unconformity
Tbh
Tm
Tr
unconformity
Tmo
Tpi
unconformity
ZPu
Low-angle normal fault, ticks on upper plate, dotted where concealed
A —— A' Cross section shown in Fig.10
Strike and dip directions of ash flow tuffs and sedimentary deposits
0
10 km
N
37° 00'
116° 52' 30"
116° 47' 30"
37° 57' 30"
OVFZ
Tss
BH
MY
G
ZPu
OBF
OBM
D
Gl
R
MS
BGB
B
FC
F
95
374

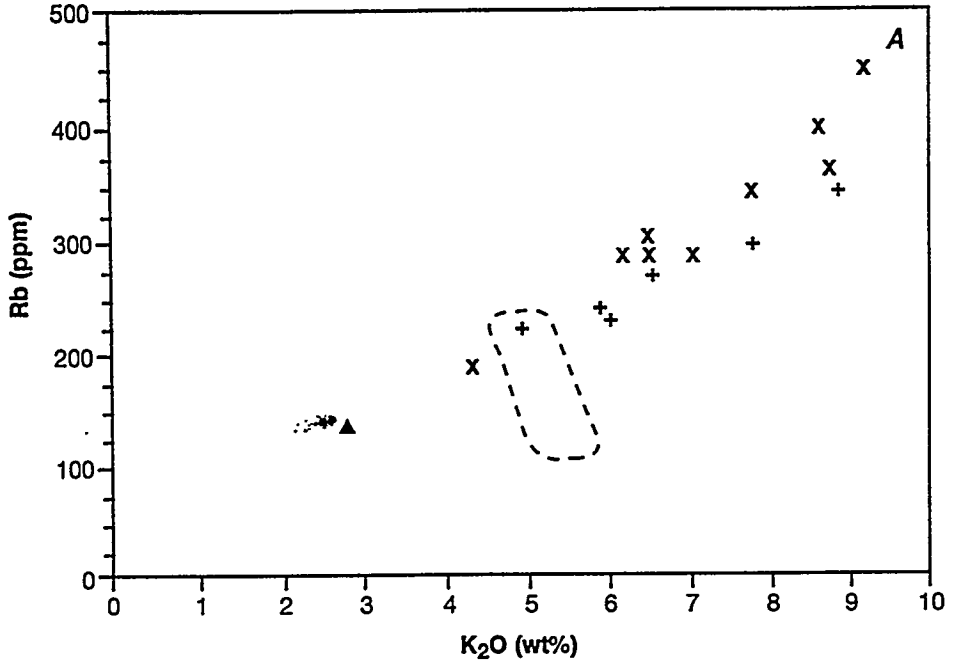
A
Rb (ppm)
500
400
300
200
100
0
0 1 2 3 4 5 6 7 8 9 10
K2O (wt%)

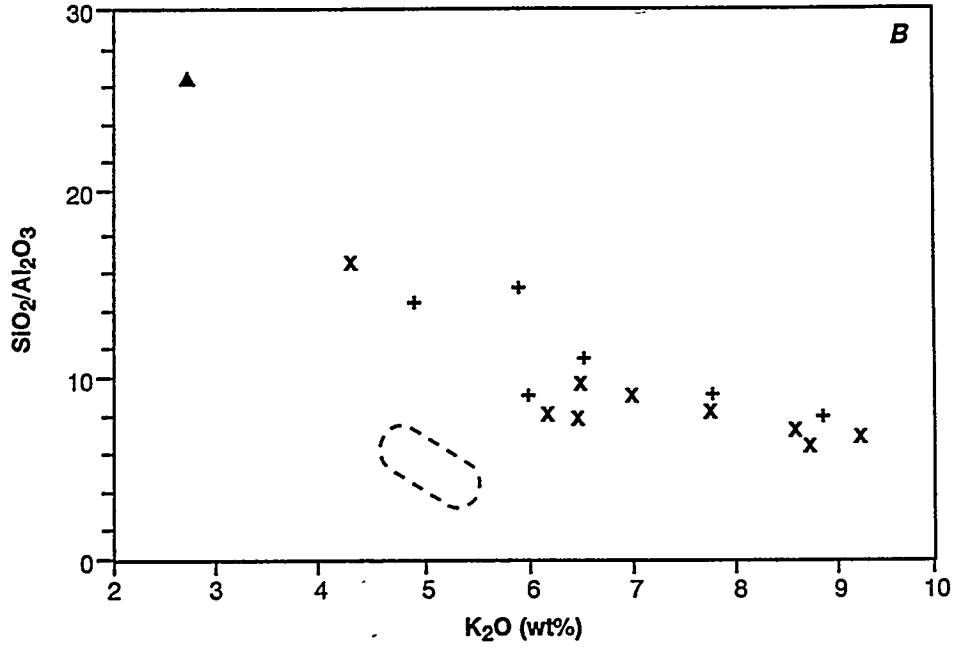
B
SiO2/Al2O3
30
20
10
0
2 3 4 5 6 7 8 9 10
K2O (wt%)

Fig. 8

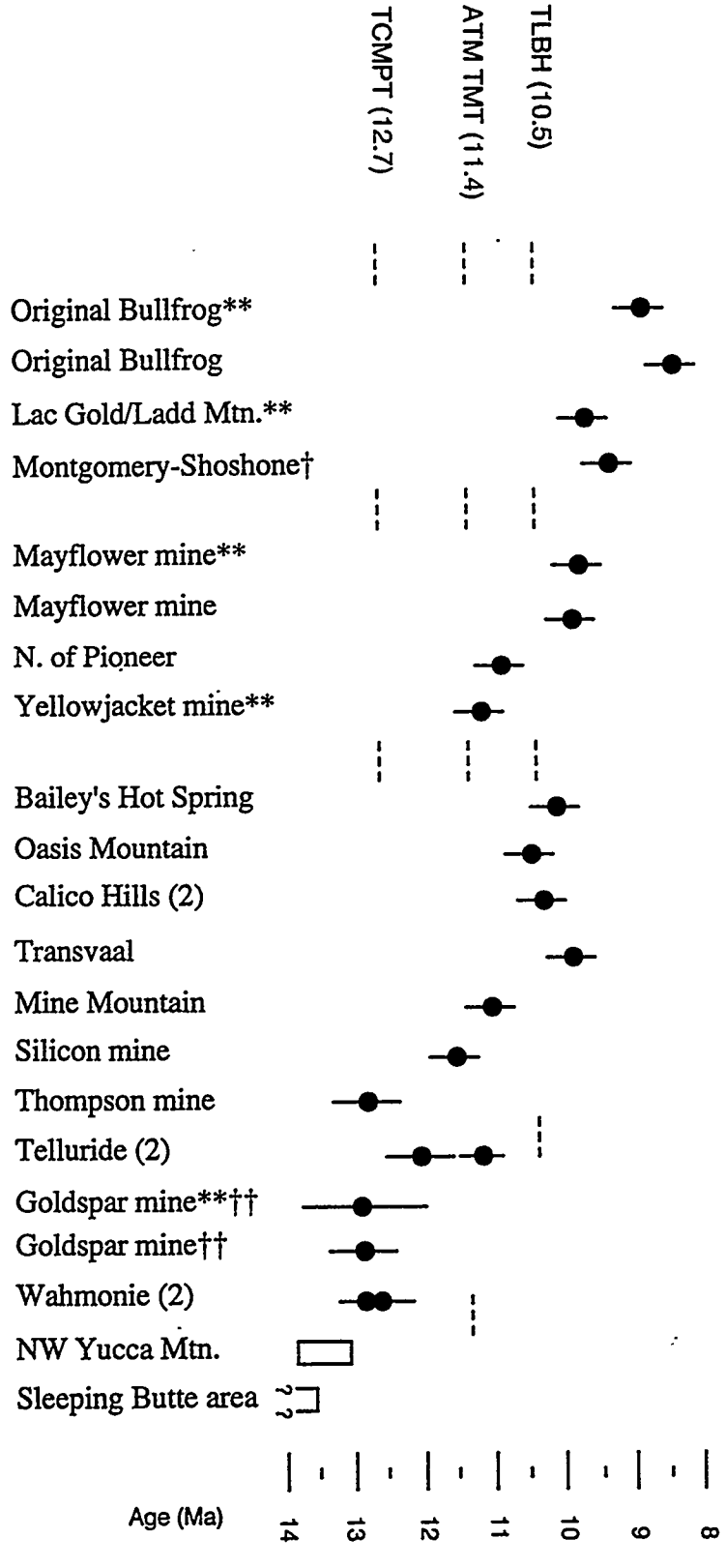
TCMPT (12.7)
ATM TMT (11.4)
TLBH (10.5)
Original Bullfrog**
Original Bullfrog
Lac Gold/Ladd Mtn.**
Montgomery-Shoshone†
Mayflower mine**
Mayflower mine
N. of Pioneer
Yellowjacket mine**
Bailey's Hot Spring
Oasis Mountain
Calico Hills (2)
Transvaal
Mine Mountain
Silicon mine
Thompson mine
Telluride (2)
Goldspar mine**††
Goldspar mine††
Wahmonie (2)
NW Yucca Mtn.
Sleeping Butte area
?
?
Age (Ma)
14
13
12
11
10
9
8

Fig. 9

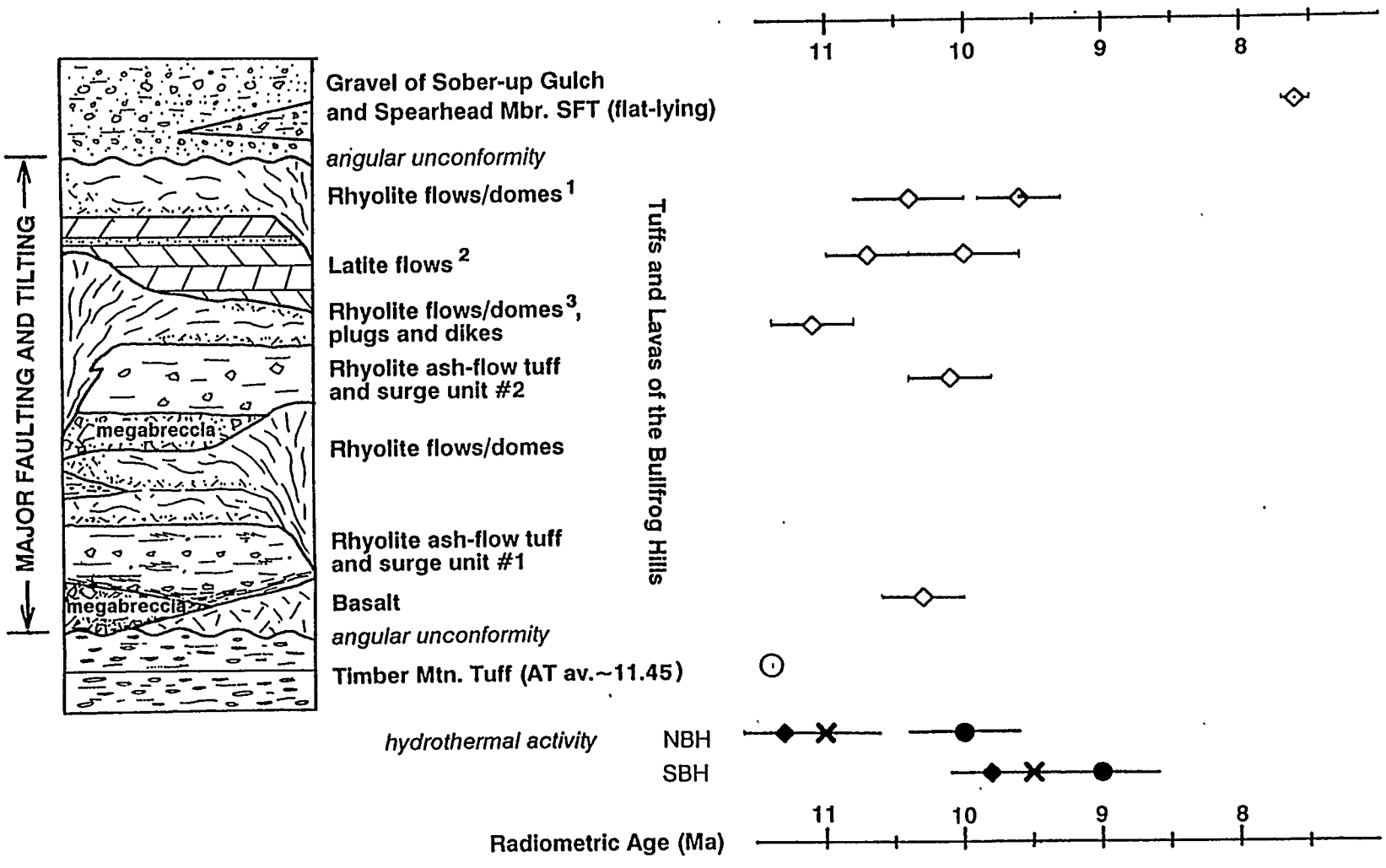
11
10
9
8
Gravel of Sober-up Gulch
and Spearhead Mbr. SFT (flat-lying)
angular unconformity
Rhyolite flows/domes 1
Latite flows 2
Rhyolite flows/domes 3,
plugs and dikes
Rhyolite ash-flow tuff
and surge unit #2
megabreccia
Rhyolite flows/domes
Rhyolite ash-flow tuff
and surge unit #1
Basalt
megabreccia
angular unconformity
Timber Mtn. Tuff (AT av.~11.45)
MAJOR FAULTING AND TILTING
Tuffs and Lavas of the Bullfrog Hills
hydrothermal activity
NBH
SBH
11
10
9
8
Radiometric Age (Ma)

Fig. 10

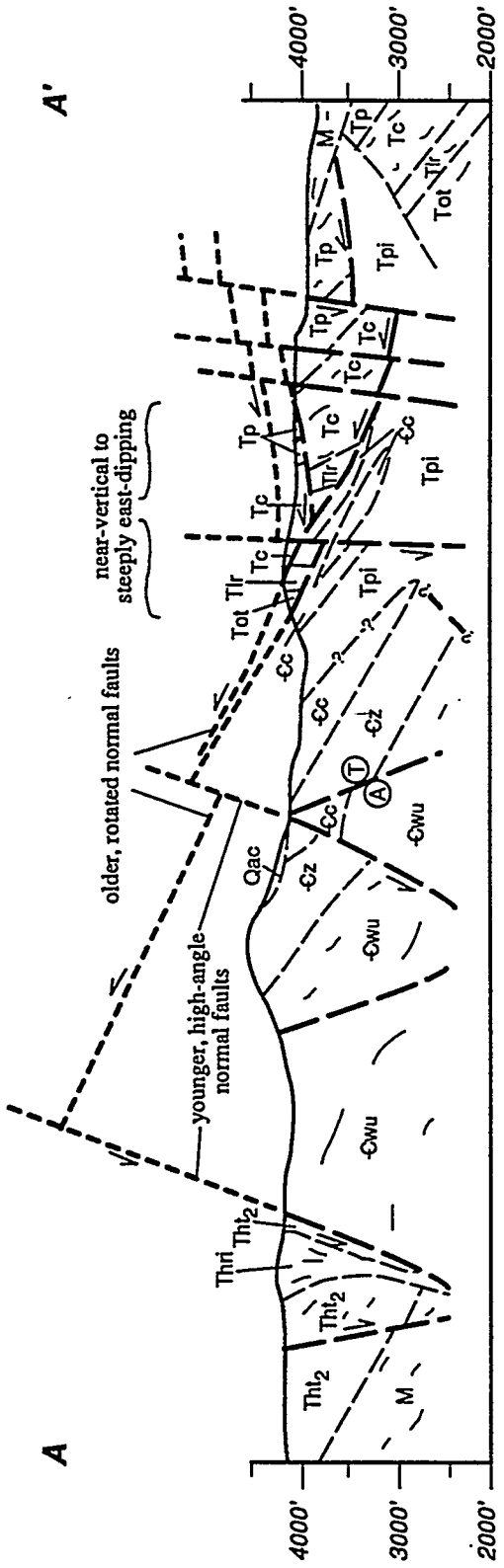
A
A'
4000'
3000'
2000'
older, rotated normal faults
younger, high-angle normal faults
near-vertical to steeply east-dipping
Tht2
Thr1
Tot
Tlr
Tc
Tp
Tpi
Qac
Cc
Cz
Cwu
M

APPENDIX C

THE PROBLEMS WITH FORMING GOLD DEPOSITS BY LEACHING OF SILICIC VOLCANIC SEQUENCES AND THE SIGNIFICANCE OF LOW-LEVEL GOLD ANOMALIES IN SILICIC VOLCANIC TERRANES

K.A. Connors, S.I. Weiss, and *D.C. Noble*, Mackay School of Mines, University of Nevada, Reno, NV 89557

Silicic volcanic rocks have markedly lower initial gold contents than previously thought, generally in the range of ≤0.1 to 1.0 ppb, with many containing only ≤0.1 to 0.3 ppb Au (Connors, et al., *Geology*, 1993). In particular, subalkaline rhyolite tuffs and lavas of the type that host gold deposits in such districts as Rawhide, Round Mountain and Bullfrog, Nevada, have gold contents between 0.1 and 0.7 ppb, with a mean of about 0.2 ppb. Primary controls on gold contents of silicic volcanic rocks appear to be bulk composition, melt structure, and the amount and timing of separation of vapor, mineral, and sulfide and/or metal melt phases. The very low gold content of glassy, subalkaline silicic rocks may largely reflect the removal of gold by vapor separation from the magma prior to and during eruption.

Leaching of silicic and intermediate volcanic rocks, particularly high-silica, non-peralkaline rhyolites, does not appear to be a viable mechanism for obtaining the gold found in volcanic-hosted gold deposits. Enormous volumes of volcanic rock with ≤0.2 ppb gold would have to be leached by extremely large hydrothermal cells to form economic deposits. The close temporal link between many gold deposits and their volcanic host rocks, the demonstrated mobility of gold in magmatic volatiles, and the probable leaching of gold primarily in the higher-temperature cores of convective cells, suggests that gold is largely derived from magmatic systems. Moreover, altered volcanic rocks in the vicinity of volcanic-hosted gold deposits commonly have gold contents in the range of 5 to 50 ppb, indicating that these rocks have been enriched in gold by one to two orders of magnitude, rather than being depleted. This does not exclude the possibility of a contribution of gold from leaching at depth of other, more gold-rich, sources such as certain carbonaceous sedimentary sequences or mafic rocks.

The extremely low *initial* gold content of most rhyolites suggests that gold concentrations of 1 to 10+ ppb in rocks and alluvium in silicic volcanic terranes represent real, and potentially significant anomalies. In non-lateritic, arid weathering environments such in the Basin and Range province, low-level gold enrichments in silicic volcanic rocks cannot be attributed to leaching and concentration by descending surface water, which is oxic and of moderate to high pH. These conditions, and the effective absence of reduced sulfur, rule out the dissolution and transport of gold by the formation of bisulfide and chloride complexes. Scavenging of gold by thiosulfate complexes is also unlikely in the absence of nearby sulfide bodies in contact with oxygenated water. Although gold-organic ligand complexes and the gold-hydroxyl complex $AuOH(H_2O)^0$ are believed to be stable under surface conditions, complexation reactions would compete with strong sorbing of gold by abundant iron, and lesser manganese oxides. Low-level gold anomalies in silicic volcanic terranes must, therefore, largely reflect addition of gold either from ascending hydrothermal fluids, or perhaps from anoxic groundwater that has reacted with gold-enriched rocks at depth. These anomalies can be used to delineate structural or other hydrologic controls potentially responsible for localizing gold mineralization.

At Yucca Mountain, Nevada, rhyolitic ash-flow tuffs and lavas have aggregate thicknesses of 1.5 to >2 km. Low-detection level gold analyses obtained on surface rock samples show that seemingly unaltered, devitrified Tiva Canyon Tuff near the Bow Ridge fault contains 0.5 to 0.7 ppb Au, more than twice the concentration found in dense glassy rocks of the unit. Fault breccia and carbonate±silica deposits in faults and fractures cutting the Tiva Canyon Tuff commonly contain as much as 10 ppb Au, nearly two orders of magnitude more than initial concentrations (0.1-0.2 ppb) in the host tuffs. Median arsenic concentrations increase from 1.6 ppm for samples with <0.5 ppb Au (expected values for unaltered, devitrified rhyolitic ash-flow tuff), to 6 ppm As for samples with 3 ppb Au. A variety of isotopic, textural and petrographic data have led some workers to conclude that secondary carbonate±silica deposits at Yucca Mountain formed at ambient temperatures from surficial processes under oxidizing, high-pH conditions. Unless gold has been added to the surficial environment by eolian or other, even more unlikely, processes, the addition of gold from hydrothermal or other deeply circulating fluids remains the only reasonable explanation for the enrichments of Au and As observed at Yucca Mountain.

Because of their low initial gold content, silicic volcanic rocks are extremely sensitive indicators of the passage of gold-bearing fluids. Given the surface conditions prevailing in the Great Basin, these gold-bearing fluids must have a hydrothermal component, with the contained gold derived either from magmatic systems or from gold-rich rocks through which the hydrothermal fluids passed. In either case, low-level gold anomalies in silicic volcanic rocks merit serious attention in efforts to evaluate potential for gold mineralization.

HIGH PRECISION $^{40}AR/^{39}AR$ AGES OF RHYOLITIC HOST ROCK AT THE SLEEPER DEPOSIT, HUMBOLDT COUNTY, NEVADA

J.E. Conrad and *E.H. McKee*, U.S. Geological Survey, 345 Middlefield Rd., Menlo Park, CA 94025

New high precision $^{40}Ar/^{39}Ar$ laser fusion ages have been obtained for the rhyolite porphyry host rock at the Sleeper deposit and nearby rhyolite flows in the Slumbering Hills. The use of high-precision laser-fusion $^{40}Ar/^{39}Ar$ techniques resolves several problems encountered in previous geochronologic studies of the Sleeper deposit. Previous estimates of the age of the rhyolite host were limited in accuracy by a high proportion of atmospheric argon contamination in some samples and by incomplete extraction of radiogenic argon in K-Ar analyses. This led to analytical uncertainty (±) of as much as 18 percent of the age for certain key samples. Laser fusion $^{40}Ar/^{39}Ar$ ages for two drill core samples of unaltered rhyolite several hundred meters west of the mine are 16.44±0.09 and 16.47±0.07 Ma, and two exposures of rhyolite in the Slumbering Hills give ages of 16.35±0.05 and 16.31±0.06 Ma. These new ages indicate that: 1) emplacement of the rhyolite host took place over a relatively brief period, probably no more than about 200,000 years; 2) rocks of the same age as the rhyolite host and presumably related to the host are more widespread than previous dating suggested. Flows correlative to the ore host in the Sleeper pit are exposed about 3 kilometers east in the Slumbering Hills. In total, this igneous complex was at least 5 kilometers across; 3) a very close temporal relationship exists between volcanism and mineralization at the Sleeper deposit. Adularia from the oldest gold-bearing veins at Sleeper is 16.2±0.3 Ma (Conrad and others, 1993), indicating a relatively short period between eruption of the host rhyolite (as young as 16.31±0.06 Ma) and the development of the high-grade gold-bearing quartz-adularia veins. This period was probably no more than about 600,000 years and may have been less than 100,000 years; and 4) the rhyolite was emplaced just prior to eruption of peralkaline volcanic rocks from the McDermitt volcanic field 20 to 50 km to the north, which include the 16.1 Ma tuff of Oregon Canyon and the 15.6 Ma tuff of Long Ridge that are exposed about 5 km northwest of the Sleeper deposit (Rytuba and McKee, 1984). These tuffs may have covered the rhyolite porphyry during mineralization at Sleeper, although they are not presently in contact.

The Sleeper deposit serves as a typical example of a low sulfidation, quartz-adularia Au-Ag deposit. These data provide additional insight into the evolutionary history of this type of deposit, wherein hydrothermal activity starts at or near the end of volcanic activity as part of the same magmatic hydrothermal system and continues for a short period after local volcanism ends.

REFERENCES

Conrad, J.E., McKee, E.H., Rytuba, J.J., Nash, J.T., and Utterback, W.C., 1993, Geochronology of the Sleeper deposit, Humboldt County, Nevada: Epithermal gold-silver mineralization following emplacement of a silicic flow-dome complex: Economic Geology, v. 88, no. 2, p. 81-91.

Symposium Program with Abstracts, Geology and Ore Deposits of the American Cordillera, Geological Society of Nevada, 1995

APPENDIX D

1995, EOS, Trans. AGU, V.76, p.284

The Oasis Valley Fault: The Principal Breakaway Structure and Eastern Limit of Late Miocene Synvolcanic Extension in the Bullfrog Hills, Southwestern Nevada

K A Connors, S I Weiss and D C Noble (All at: Department of Geological Sciences, Mackay School of Mines, Univ. of Nevada-Reno, Reno, NV 89557)

The Oasis Valley fault (OVF) is the principal breakaway for W to WNW directed extension in the northern Bullfrog Hills. The fault generally follows US Highway 95, trending nearly N-S north of Beatty, NV. This fault, or fault zone, is the structural boundary between the highly faulted Bullfrog Hills and the much less faulted western part of the Timber Mountain I caldera in the Oasis Valley area of the southwestern Nevada volcanic field. The OVF marks the effective eastern limit of Late Miocene synvolcanic faulting of the highly extended Bullfrog Hills structural domain. It is the easternmost and best documented of several subparallel, approximately N-S trending 'first-order' structures in an area where geologic mapping demonstrates a pattern of major down-to-the-west normal faults, with smaller, interspersed faults of varying offset.

The Bullfrog Hills and Oasis Valley areas, separated by the OVF, have different stratigraphic sections and volcano-tectonic styles. In the Oasis Valley area, an unusually thick section of the Ammonia Tanks Member (ATM) of the Timber Mountain Tuff is overlain by the tuffs and lava of Fleur de Lis Ranch (TFDL) and the tuff of Cutoff Road (TCR), deposited within the western part of the Timber Mountain I caldera. Here the location of the OVF fault closely coincides with the topographic margin of the caldera. The entire exposed section, with a composite thickness of more than 1500 m, is generally concordant and was deposited between about 11.45 and 11.40 Ma. In contrast, in the Bullfrog Hills the ATM is thinner, the TFDL is absent, and the exposed section includes units that range from Paleozoic to Late Miocene in age. The section in the Bullfrog Hills includes a conformable sequence of ash-flow sheets of the *main* and *Timber Mountain magmatic stages* that is unconformably overlain by the 10 to 10.5 Ma tuffs and lavas of the Bullfrog Hills (TLBH), which includes complexly intercalated and lithologically variable synvolcanic and syntectonic debris-flow deposits. Block lithology and distribution within the debris-flow unit show that the main source for these deposits was in the Oasis Valley area. Therefore, volcanic rocks in the area east of Oasis Valley, dated at 11.45 to 11.40 Ma, were exposed and being eroded by 10-10.5 Ma. The very large size of some of the blocks in the debris flow unit, as much as 500 m long, indicates that there was pronounced topographic relief--probably steep, west-dipping scarps of the active Oasis Valley fault.

Extensional deformation of the Bullfrog Hills-Oasis Valley area began after deposition of the ATM and the TCR at about 11.4 Ma. Widespread eastward tilting occurred prior to deposition of the TLBH, probably along numerous down-to-the-west faults, synchronous with and possibly before formation of the OVF. One or more buried normal faults must be present east of Oasis Valley to produce the 20 to 30° eastward tilting of tuffs and lavas found in the Oasis Valley area. As evolution of the area progressed, faulting ceased east of the OVF, but significant movement along the OVF brought about additional tilting of *Timber Mountain stage* and older units, and rotation of earlier down-to-the-west faults in the northern Bullfrog Hills. The development of the OVF 'breakaway' created a topographic high in the Oasis Valley area, resulting in the westward shedding of blocks and debris-flow deposits synchronous with volcanism in the Bullfrog Hills and deposition of the TLBH. Continued movement on the OVF and sub-parallel faults to the west resulted in tilting of the debris-flow deposits and the TLBH to dips of as much as 20-35° E. The OVF probably represents the northern extension of the Beatty Fault of Ransome et al., 1910, for which a throw of some 1500 m was estimated. Conservative reconstructions along the OVF suggest a minimum of 600 to 900 m of offset; total offset could be considerably greater. West of the OVF one, or possibly two, additional major normal faults, subparallel to and probably initiated slightly later than the OVF, account for most of the stratigraphic offset in the Bullfrog Hills.

The Oasis Valley fault was an important element in the later volcano-tectonic evolution of the Bullfrog Hills structural domain, and Oasis Valley marks a persistent boundary between distinct volcano-tectonic zones. This boundary was first expressed as a caldera-related topographic barrier that restricted deposition of ATM and overlying units and, later, as the edge of a topographic high that provided blocks present within the debris-flow sequence of the Bullfrog Hills.

Submittal Information

1. 1995 Spring Meeting
2. [redacted]GU Member #
3. (a) Katherine A. Connors
   Mackay School of Mines
   MS 176
   University of Nevada-Reno
   89557

   (b) Tel: 702-784-5803

   (c) Fax: 702-784-5079

   (d) email: kathy@usgs.unr.edu
4. T
5. (a) –
   (b) 8165 Structural geology
   (b) 8199 General or misc.
   (b) 8404 Ash Deposits
6. Title Only
7. 0 %
8. $40.00 enclosed (student rate)
9. (C)
10.
11. Yes

SECTION IV

Task 4 Annual Report

October 1994–September 1995

James N. Brune and Abdolrasool Anooshehpoor

Objectives

In the past year our objectives have been to: (1) Operate, upgrade, and make preliminary analysis of data from the Yucca Mountain Microearthquake Network (YMMN). (2) Maintain the three broad-band downhole digital seismograph stations at Nelson, Nevada, Troy Canyon, Nevada and Deep Springs, California. (3) Establish the rate, or upper limit on the rate, and magnitude threshold of background microearthquake activity in the immediate vicinity of the proposed repository. (4) Monitor any changes in the activity, *e.g.*, microearthquake activity or rockbursts, induced by the Tunnel Boring Machine (TBM) tunneling operations. (5) Study implications of background seismic activity for the conclusion Stock *et al.*, (1985) that the rocks in the proposed repository block are near a state of incipient normal faulting. (6) Proceed with design plans and proposal to DOE for installation of laser strainmeter in the ESF tunnel, originally proposed as part of Task 4.

Activities

We continued monitoring microearthquakes in the vicinity of the proposed nuclear waste repository near Yucca Mountain. We have been recording continuous digital data from the four high-frequency stations (fig. 1) in Solitario Canyon (YNB, 70ft deep), on Yucca Crest (YYM, 417ft deep), Crater flat (YFC), and Black Cone (YBC) since July 1994. In September 1994, we rerouted the data stream to a stand-alone SUN workstation (Platinum) for a more dependable uninterrupted data collection. The daily data was routinely monitored by a student and the seismic events with S-P time less than 3s were identified and hard copies were made. Weekly data from YMMN was compressed and stored on Digital Audio Tapes (DAT) along with the computer code for uncompressing the data. Fig. 2 shows the recorded data from a small earthquake near Alice Ridge ($M_L = 0.6$; May 5, 1995) on YYM, YNB, and YCF stations. The Black Cone station (YBC) was not functioning at that time. In September 1994, we examined the digital data at the high-frequency stations recorded during the Tunnel Boring Machine (TBM) activities. There was no evidence that the background noise at our recording stations had increased.

In order to increase the network sensitivity and lower the microearthquake magnitude detection threshold, we submitted a proposal to DOE to install geophones in the existing boreholes on the Nevada Test Site near the proposed repository. We were given permission to install

high-frequency geophones in a number of boreholes (fig 3) that were to be instrumented with Dr. Joseph Rousseau's Downhole Instrumentation Station Apparatuses (DISA).

In July 1995, two geophone packages were installed in boreholes UE-25 UZ#4 and UE-25 UZ#5 at the depths of 235 ft and 250 ft (figs. 4 and 5), respectively. Each package contained two vertical *L-10B*, 4.5 Hz geophones (manufactured by Mark Products) potted with epoxy in a clear PVC pipe. A four-conductor cable brings the signal to the surface station. The two geophones in each package may be connected in series (to reduce the random noise in the geophones) or used independently (to reduce the chance of losing signal in a given hole in case one geophone fails). For about two weeks, a RefTek data acquisition system recorded continuous digital data from geophones at boreholes UZ#4 and UZ#5 at a rate of 100 and 200 samples per second, respectively. Figs. 6 and 7 show the time histories and spectra of the background noise for these two boreholes, respectively. The peaks in the spectra correspond to about 15Hz and its higher harmonics at about 30 and 60Hz. The harmonic noise is due to a generator supplying power to the nearby field facility unit. In future, if the signals from these two boreholes are to be used, the background noise has to be reduced. This can be achieved by relocating the generator a few hundred meters away from the site.

Recently, we prepared two more identical packages; one is being installed in USW UZ#7a at a depth of 425 ft and the other is scheduled to be installed in borehole SD#12 at a depth of 1550 ft in November 1995. Unfortunately, due to the lack of fundings, we are unable to bring signals from these new downhole stations as well as the VSP sensor strings in borehole UZ#16 to the University of Nevada-Reno Seismological Laboratory (UNRSL).

We continued monitoring the Nevada Nuclear Waste Projects Office (NWPO) broad band stations at Troy Canyon, Nelson, and Deep Springs (fig. 8).

References

Stock, J.M., J.H. Healy, S.H. Hickman and M.D. Zoback, 1985. Hydraulic fracturing stress measurement at Yucca Mountain,, Nevada, and relationship to the regional stress field, J. Geophys. Res., vol. 90, pp 8691-8706.

List of Figures

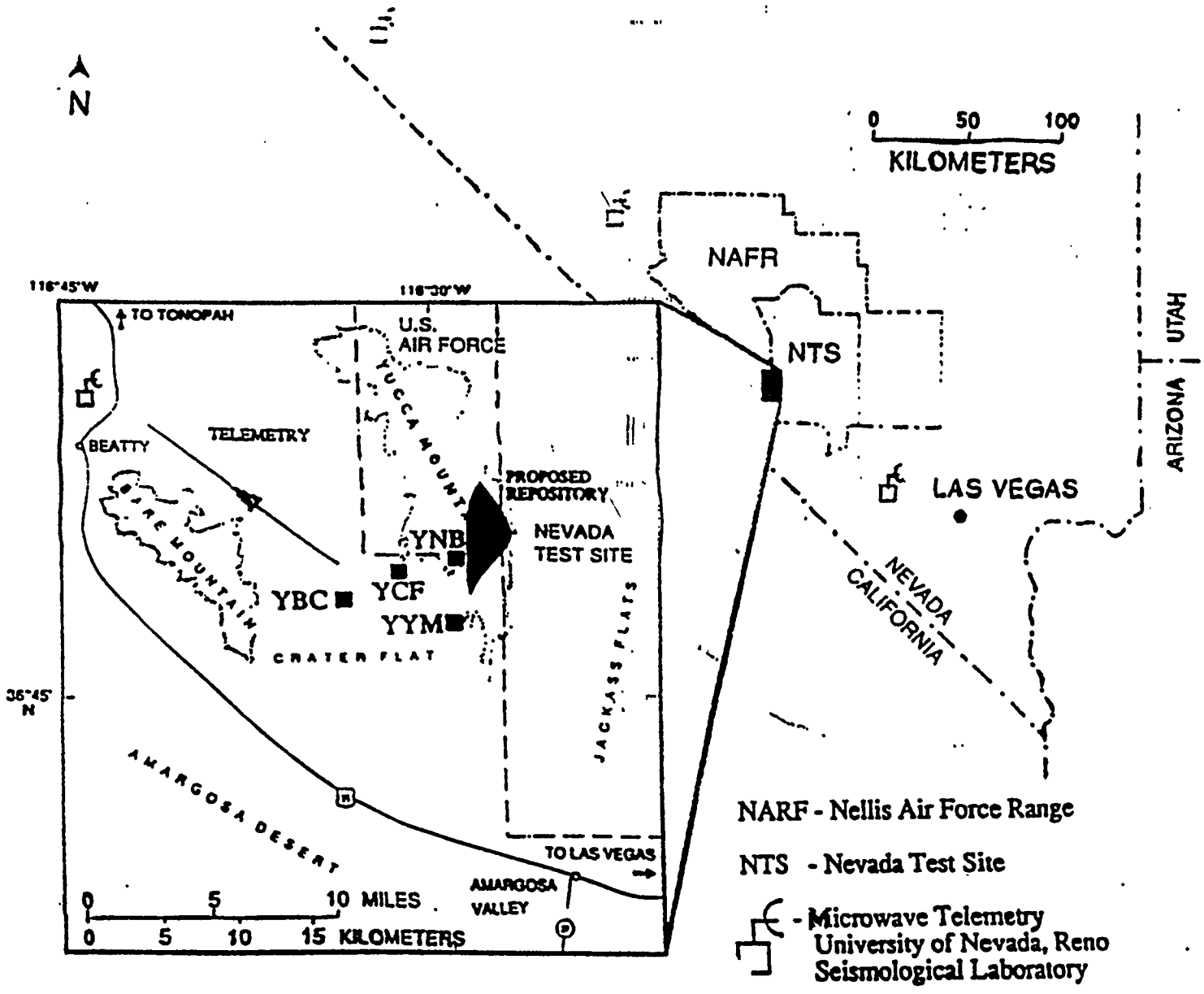

Figure 1. Location Map for Yucca Mountain Microearthquake Net (YMMN)

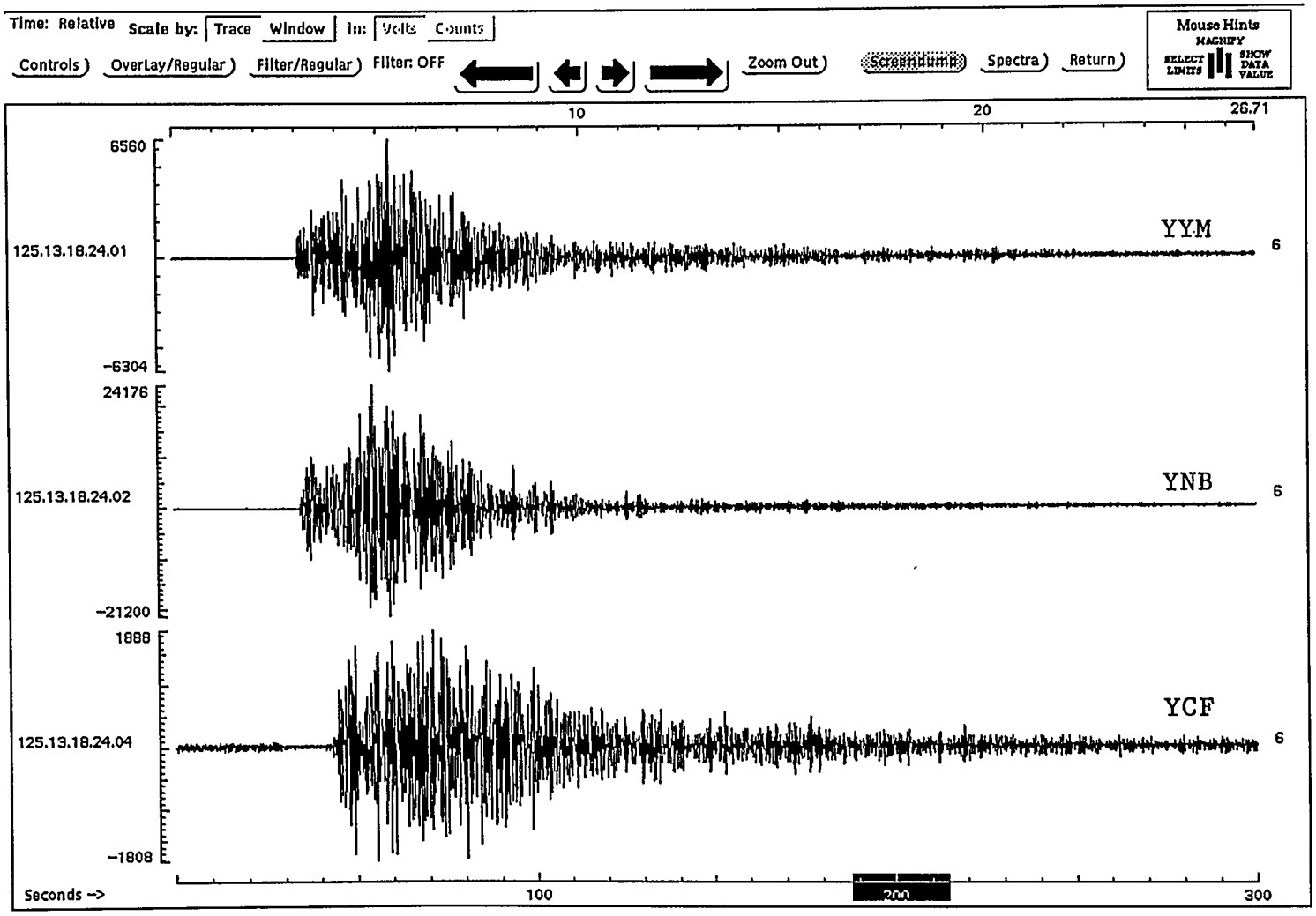
Time: Relative
Scale by:
Trace
Window
In:
Volts
Counts
Controls
OverLay/Regular
Filter/Regular
Filter: OFF
Zoom Out
Screendump
Spectra
Return
Mouse Hints
MAGNIFY
SELECT LIMITS
SHOW DATA VALUE
10
20
26.71
6560
125.13.18.24.01
-6304
YYM
6
24176
125.13.18.24.02
-21200
YNB
6
1888
125.13.18.24.04
-1808
YCF
6
Seconds ->
100
200
300

Figure 2

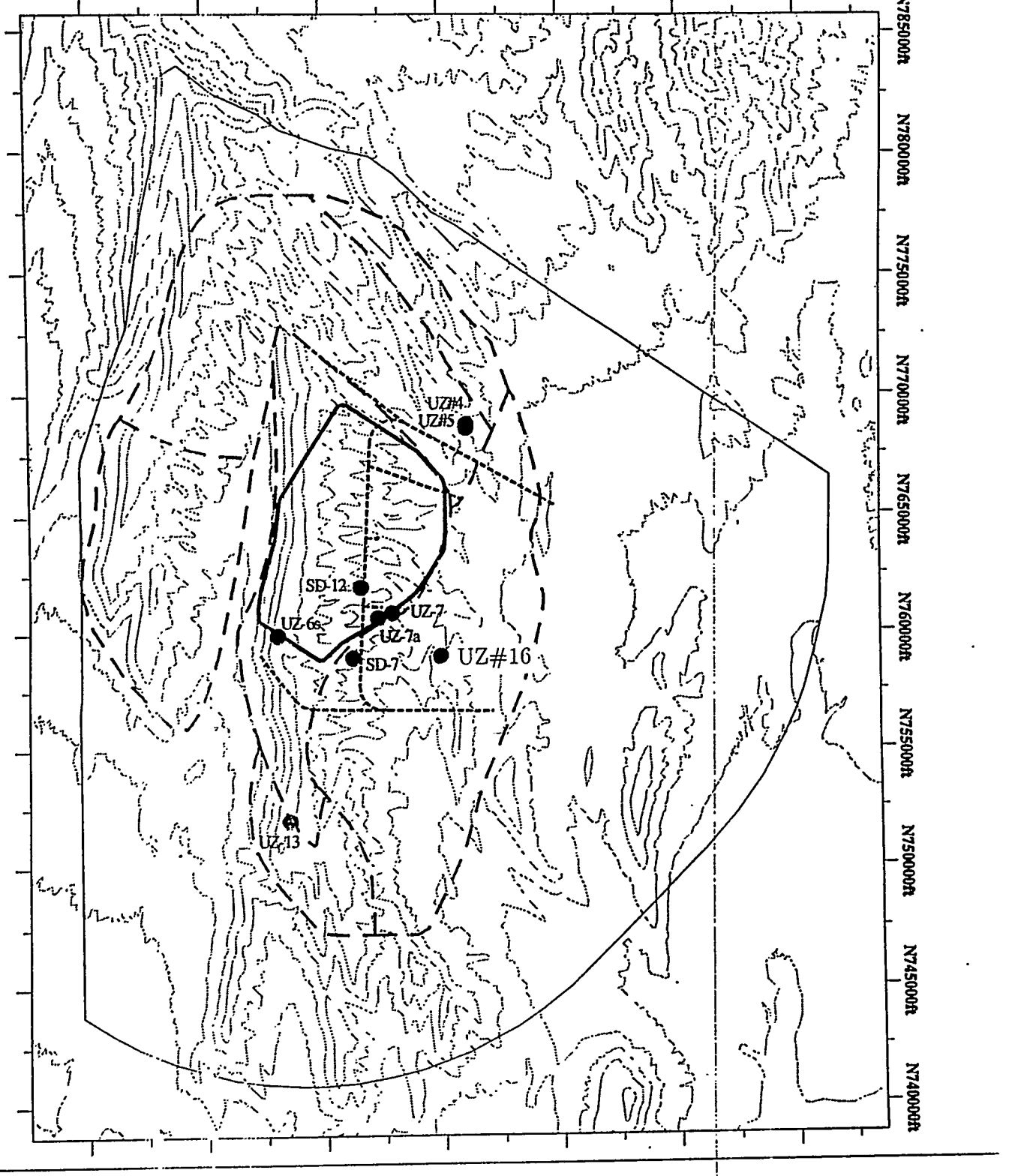

Legend:

- Borehole
- Possible Usable Area for Repository Expansion
- ESF Ramp
- Potential Repository Outline
- Conceptual Controlled Area Boundary
- Elevation Contour 200 ft Interval

N

1 0 1 2 MILES

1 0 1 2 KM

YUCCA MOUNTAIN

SITE CHARACTERIZATION PROJECT

Figure 13

Location Map of Evaluated Boreholes

YMP-95-035.0

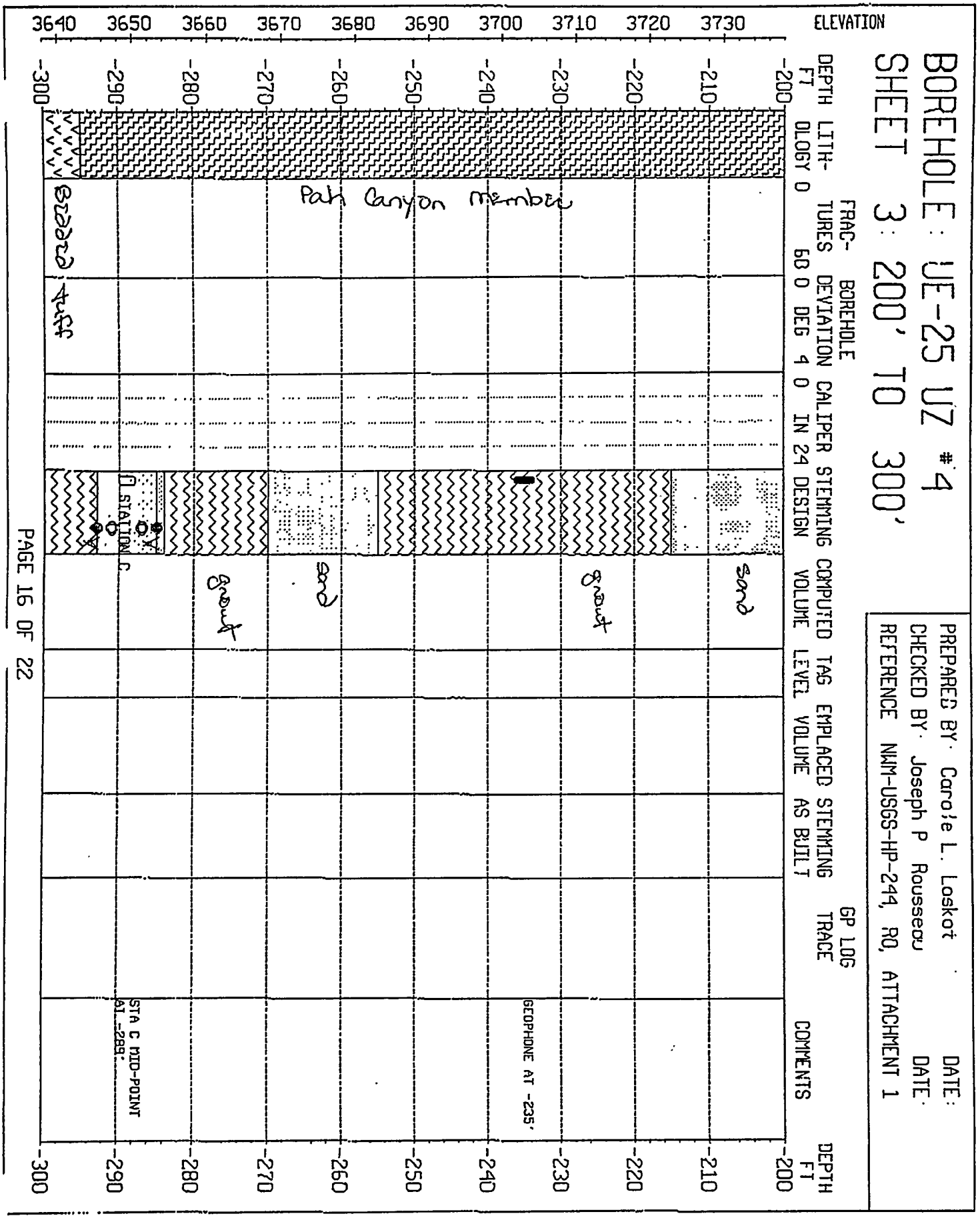
BOREHOLE: UE-25 UZ #4
SHEET 3: 200' TO 300'
PREPARED BY: Carole L. Laskot
CHECKED BY: Joseph P Rousseau
REFERENCE NWM-USGS-HP-244, RQ, ATTACHMENT 1
DATE:
DATE:
ELEVATION
DEPTH FT
LITHOLOGY
FRACTURES
BOREHOLE DEVIATION
CALIPER
STEMMING
COMPUTED TAG
EMPLACED STEMMING
GP LOG TRACE
COMMENTS
Bedded tuff
Pah Canyon Member
sand
grout
sand
grout
STATION C
GEOPHONE AT -235'
STA C MID-POINT AT -288'
PAGE 16 OF 22

Figure 4

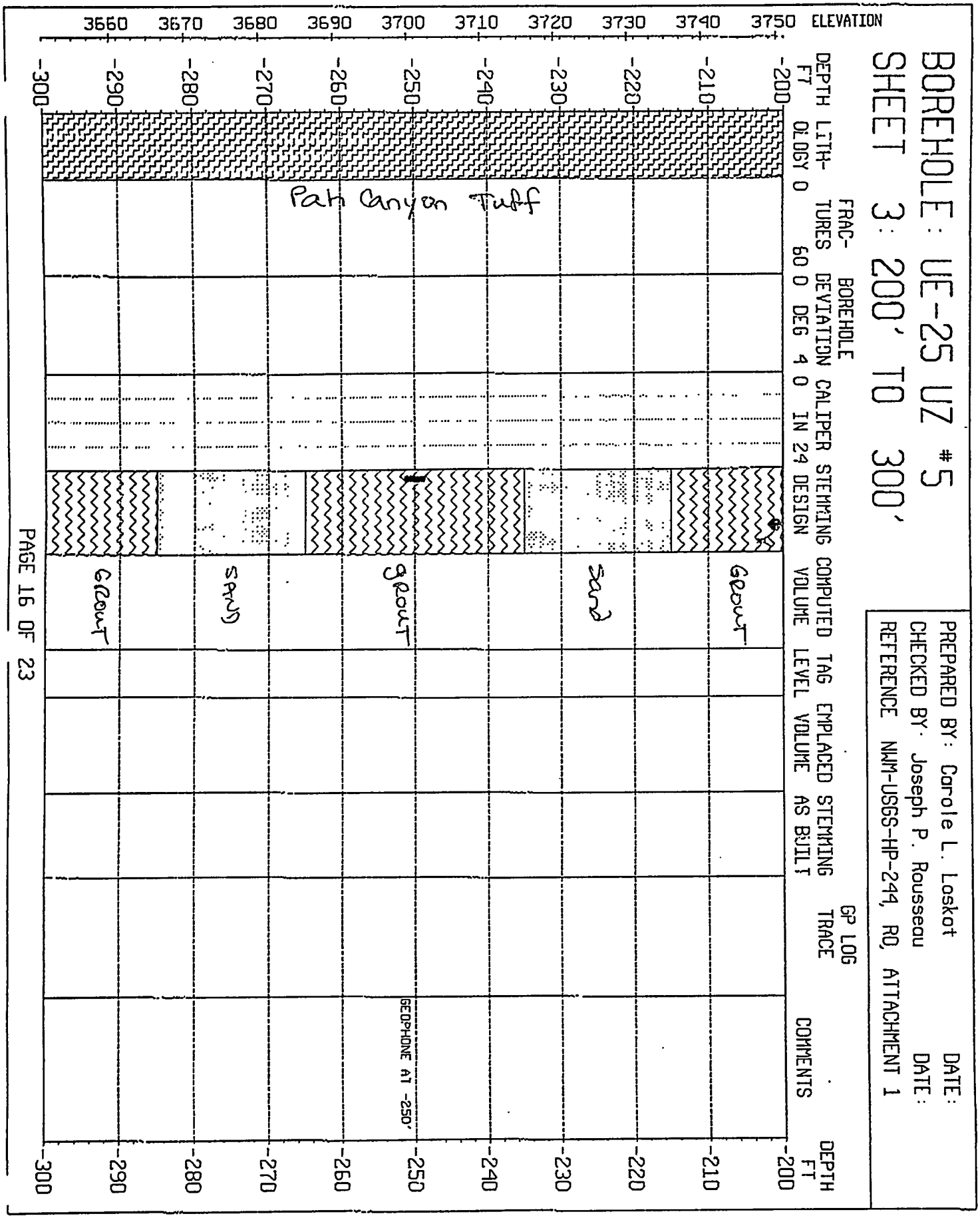
BOREHOLE: UE-25 UZ #5
SHEET 3: 200' TO 300'
PREPARED BY: Carole L. Loskot
DATE:
CHECKED BY: Joseph P. Rousseau
DATE:
REFERENCE NWM-USGS-HP-244, RQ, ATTACHMENT 1
ELEVATION
DEPTH FT
LITHOLOGY
FRACTURES
BOREHOLE DEVIATION
CALIPER
STEMMING
COMPUTED TAG
EMPLACED STEMMING VOLUME
GP LOG TRACE
COMMENTS
Pah Canyon Tuff
Grout
Sand
Grout
Sand
Grout
GEOPHONE AT -250'
PAGE 16 OF 23

Figure 5

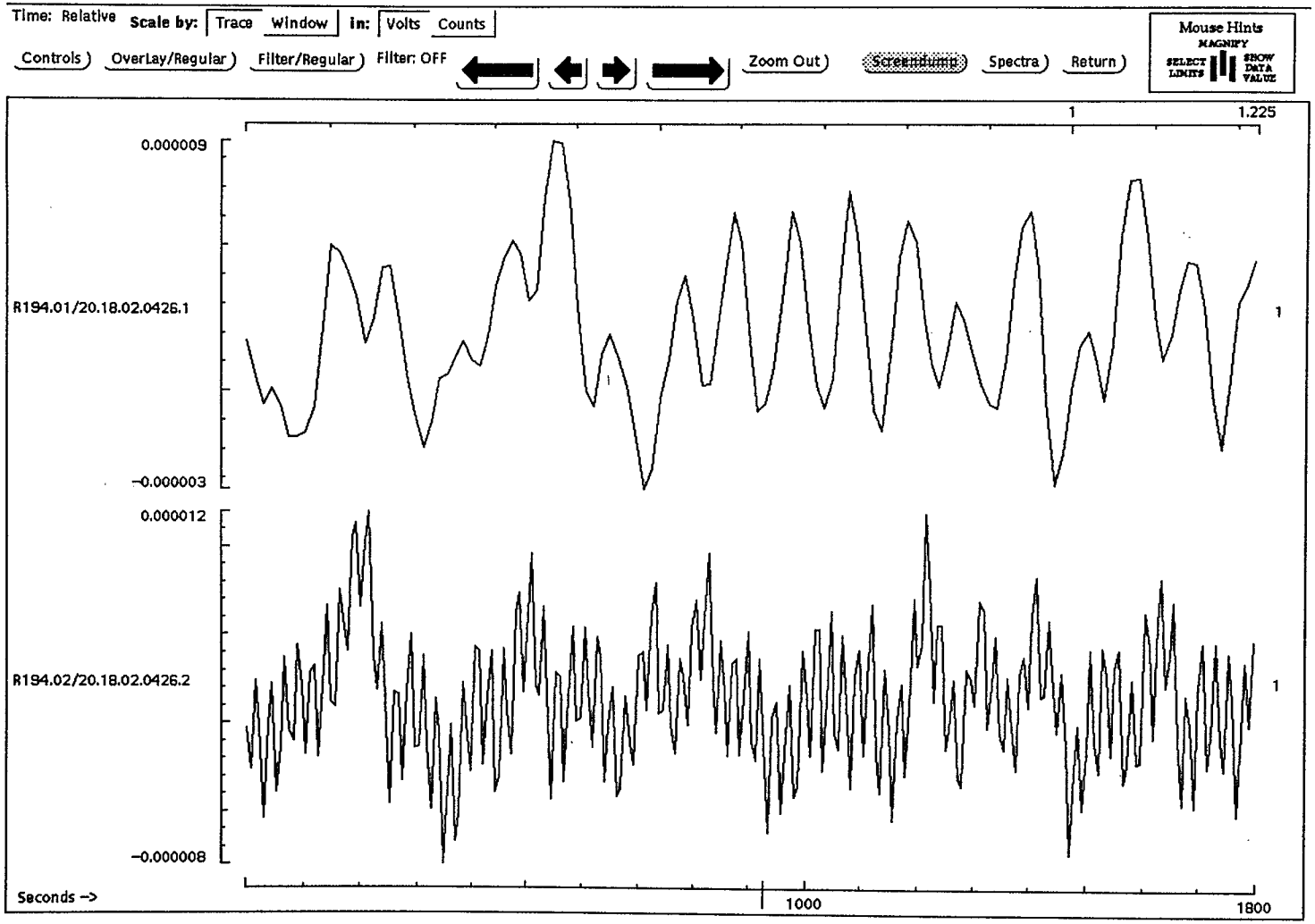
Time: Relative
Scale by: Trace Window
In: Volts Counts
Controls
Overlay/Regular
Filter/Regular
Filter: OFF
Zoom Out
Screendump
Spectra
Return
Mouse Hints
MAGNIFY
SELECT LIMITS
SHOW DATA VALUE
1
1.225
0.000009
R194.01/20.18.02.0426.1
-0.000003
1
UZ#4
0.000012
R194.02/20.18.02.0426.2
-0.000008
1
UZ#5
Seconds ->
1000
1800

Figure 6

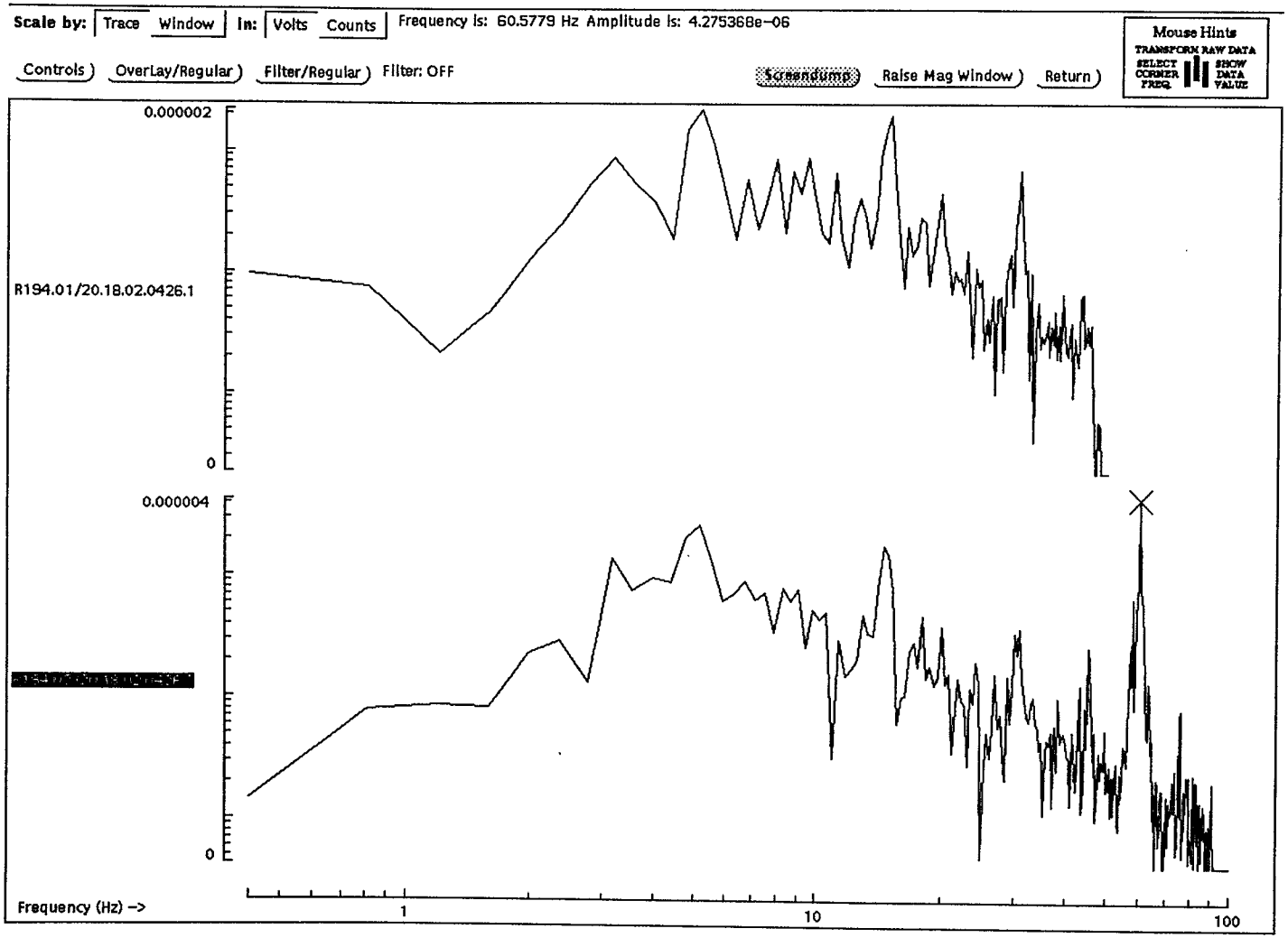
Scale by: Trace Window In: Volts Counts Frequency is: 60.5779 Hz Amplitude is: 4.275368e-06
Mouse Hints
TRANSFORM RAW DATA
SELECT CORNER FREQ.
SHOW DATA VALUE
Controls
OverLay/Regular
Filter/Regular
Filter: OFF
Screendump
Raise Mag Window
Return
0.000002
R194.01/20.18.02.0426.1
0
0.000004
0
Frequency (Hz) ->
1
10
100
UZ#4
UZ#5

Figure 7

UNIVERSITY OF NEVADA, RENO
DIGITAL SEISMIC NETWORK

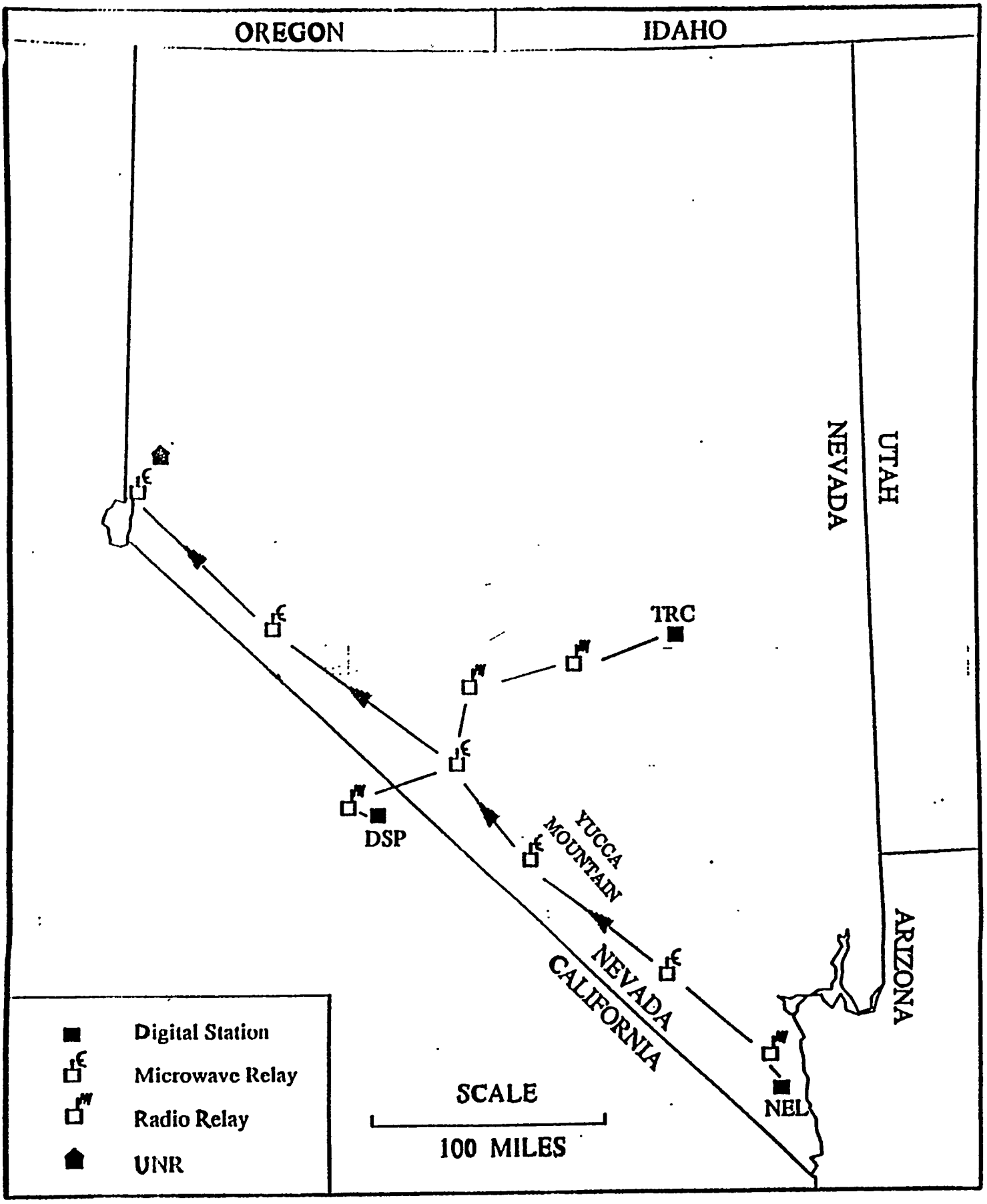

Figure 8

SECTION V

PROGRESS REPORT--OCTOBER 1, 1994 TO SEPTEMBER 30, 1995

TASK 5--Tectonic and Neotectonic framework of the Yucca Mountain Region

Personnel

Principal Investigator: Richard A. Schweickert

Research Associate Professor: Mary M. Lahren, July 1, 1995 to August 31, 1995

Graduate Research Assistants:

a. **Zhang, Y.--October, 1993-September, 1994**
b. **Wellman, E.--October, 1994-May, 1995**
c. **Plank, G.--October, 1994-May, 1995**

Part I. *Highlights of research accomplishments*

a. Revision and submission of new manuscript on the Amargosa fault system

b. Structural studies at Bare Mountain, immediately west of Crater Flat

c. Invited lecture on "Faulting near Yucca Mountain and implications for storage of Nuclear Waste", March 29, 1995

Part II. *Research projects*

This section highlights ongoing research projects that have been conducted by Task 5 personnel.

1. *Regional overview of structure and geometry of Mesozoic thrust faults and folds in the area around Yucca Mountain*; R. A. Schweickert and M. M. Lahren.

This study will provide important information about the deep structural geometry of Paleozoic units and their bounding faults, which is necessary both for understanding of Tertiary faults at Yucca Mountain and for the correct formulation of regional hydrologic models. This study has led to the recognition of a previously unknown strike-slip fault beneath

Crater Flat, and of major pre-Middle Miocene extension in the NTS region.

2. *Kinematic analysis of low and high angle normal faults and strike-slip faults in the Bare Mountain area, study of metamorphic rocks, and comparison of structures with the Grapevine Mountains* Y. Zhang and R. Schweickert

Bare Mountain is a direct analog of the deep structure beneath Cenozoic ash flow tuffs at Yucca Mountain. This study is designed to determine the structural evolution of Bare Mountain by field analysis of the timing and slip directions of high and low-angle normal faults exposed there, and by integrating field data into structural cross-sections. This work has continued to provide better constraints on the displacement histories of the faults. A number of deep cross-sections have been constructed through Bare Mountain to build up a model of the structural evolution of the area. The development of these structures will be compared with possible analogs in the Grapevine Mountains and the CP Hills to develop firm constraints on the deep structure beneath the Yucca Mountain area.

3. *Evaluation of pre-Middle Miocene structure of Grapevine Mountains and its relation to Bare Mountain.* R. Schweickert and M.M. Lahren

This study is to clarify the significance of pre-Middle Miocene and possibly pre-Tertiary extension and detachment faulting on crustal structure in the area between the NTS and Death Valley, and beneath Yucca Mountain.

4. *Evaluation of paleomagnetic character of Tertiary and pre-Tertiary units in the Yucca Mountain region, as tests of the Crater Flat shear zone hypothesis and the concept of oroclinal bending.* S. Gillett, R. Karlin, Y. Zhang, and R. A. Schweickert.

Published paleomagnetic data from various volcanic units at Yucca Mountain show that up to 30° of progressive north-to-south clockwise rotation has occurred since mid-Miocene. This study has expanded the data base to various Paleozoic, Mesozoic, and Cenozoic units near Bare

Mountain to understand the regional variations of magnitude and timing of rotations.

5. *Late Quaternary fault patterns in southern Amargosa Valley, Stewart Valley, and Pahrump Valley.* M.M. Lahren and R.S. Schweickert.

This project has involved the compilation of all available data on the distribution and style of late Quaternary faults in the region, primarily from mapping by Donovan and Hoffard (M.S. Theses completed under Task 5) and USGS mapping. This compilation has clarified the late Quaternary structural setting of Yucca Mountain, and strongly suggests linkage exists between Yucca Mountain/Crater Flat and the Pahrump-Stateline faults.

Part III.

Brief summaries of research results during FY 1994-95

This section presents a summary of progress to date. Because these projects are long-term and field-intensive, the results are still preliminary, and should not be quoted without permission. Many of our interpretations are speculative.

1. Regional overview of structure and geometry of Mesozoic thrust faults and folds in the area around Yucca Mountain. and ***Quaternary fault patterns and basin history of Pahrump and Stewart Valleys, Nevada and California.***

R. A. Schweickert and M. M. Lahren.

Gravity, seismic, paleomagnetic, structural, stratigraphic, volcanic, spring, and stratigraphic data suggest that a major N24W-trending dextral strike-slip system passes beneath Crater Flat and Yucca Mountain. It represents the principal zone of late Quaternary fault movements in the area east of Death Valley, because Quaternary faults in southern Amargosa Valley provide a connection from the Pahrump-Stateline fault zones to Crater Flat. Both normal faults and late Cenozoic volcanic cones in Crater Flat appear to be manifestations of this strike-slip fault system.

A shortened version of a manuscript on this topic was submitted to Science in June, 1995, and received unfavorable reviews due to its brevity. A longer version is being prepared for submission to GSA Bulletin.

3. *Evaluation of pre-Middle Miocene structure of Grapevine Mountains and its relation to Bare Mountain.* R. Schweickert and M.M. Lahren.

No new field work was done in 1994-95.

4. *Kinematic analysis of low and high angle normal faults in the Bare Mountain area, and comparison of structures with the Grapevine Mountains* Y. Zhang has continued, part time, during 1994-95, to work on a new structural model for Bare Mountain.

Bare Mountain provides evidence that the deep structures of Paleozoic rocks that lie beneath Yucca Mountain include major top to the southeast low angle normal faults and pre-14 Ma N-S striking dextral strike-slip faults.

Geologic map compilations are now complete. Work continues on detailed structural cross-sections. These maps and sections show the structural patterns and Mesozoic and Cenozoic geologic history of Bare Mountain.

Y. Zhang is expected to have this work complete by December, 1995.

5. *Evaluation of paleomagnetic character of Tertiary and pre-Tertiary units in the Yucca Mountain region, as tests of the Crater Flat shear zone hypothesis and the concept of oroclinal bending.* S. Gillett, R. Karlin, Y. Zhang, and R. A. Schweickert.

(See 1993 progress report; no new work on this phase of the study was done in 1994 or 1995; the work already completed will form a major part of Y. Zhang's Ph. D. dissertation)

Part IV. *Other activities of Task 5 personnel*

1. Technical review of reports for the Center

None formally assigned; reviewed a number of new publications, including:

Reheis, M. C., and others, 1995, Quaternary soils and dust deposition in southern Nevada and California: Geol. Soc. America Bull., v. 107, p. 1003-1022;

Applegate, J. D. R., and Hodges, K. V., 1995, Mesozoic and Cenozoic extension recorded by metamorphic rocks in the Funeral Mountains,

California: Geol. Soc. America Bull., v. 107, p. 1063-1076;
Rogers, N. ., and others, 1995, Late Cenozoic basaltic magmatism in the western Great Basin, California and Nevada: Jour. Geophys. Res., v. 100, p. 10287-10302;
Scott, R., and others, 1995, Relation of peralkaline magmatism to heterogeneous extension during the Middle Miocene, southeastern Nevada: Jour. Geophys. Res., v. 100, p. 10381-10402;
Brook, W. E., and others, 1995, The 40Ar/39Ar ages and tectonic setting of the middle Eocene northeast Nevada volcanic field: Jour. Geophys. Res., v. 100, p. 10403-10416;
Walker, J. D., and others, 1995, Connection between igneous activity and extension in the central Mojave metamorphic core complex, California: Jour. Geophys. Res., v. 100, p. 10477-10494;
Holm, D. K., 1995, Relation of deformation and multiple intrusion in the death Valley extended region, California, with implications for magma entrapment mechanism: Jour. Geophys. Res., v. 100, p. 10495-10507;
Minor, S. A., 1995, Superposed local and regional paleostresses: Fault-slip analysis of Neogene extensional faulting near coeval caldera complexes, Yucca Flat, Nevada: Jour. Geophys. Res., v. 100, p. 10507-10529;
Zandt, G., and others, 1995, Crust and mantle structure across the Basin and Range-Colorado Plateau boundary at 37 degrees N latitude and implications for Cenozoic extensional mechanism: Jour. Geophys. Res., v. 100, p. 10529-10548;
Ozalaybey, S., and Savage, M., 1995, Shear-wave splitting beneath western United States in relation to plate tectonics: Jour. Geophys. Res., v. 100, p. 18135-18150.

2. *Meetings attended in relation to the Yucca Mountain Project and the Center for Neotectonic Studies*

a. UNR Environmental Sciences Seminar, March 29, 1995, RAS gave invoted lecture on "Faulting near Yucca Mountain and Implications for storage of Nuclear Waste."

4. *Professional reports provided to NWPO*

a. None

5. *Abstracts published*

a. None

6. *Papers submitted for publication in peer-reviewed literature*

a. Strike-slip fault system in Amargosa Valley and Yucca Mountain, Nevada: Schweickert, R. A., and Lahren, M.M. (appendix 1); Submitted 6/16; rejected July 20, 1995; longer version will be resubmitted to GSA Bulletin.

7. *Graduate theses supported by NWPO*

a. Zhang, Y., in progress, Structural and kinematic analysis of Mesozoic and Cenozoic structures at Bare Mountain, Nye County, Nevada

b. Two graduate students supported during this year, E. Wellman and G. Plank, transferred to other projects, Wellman due to poor performance in classes, Plank to begin a new funded project in Dixie Valley, Nevada.

Appendix I.

Preprint

version of 6/15/95

STRIKE-SLIP FAULT SYSTEM IN AMARGOSA VALLEY AND YUCCA MOUNTAIN, NEVADA

Richard A. Schweickert and Mary M. Lahren

Department of Geological Sciences and Center for Neotectonic Studies

University of Nevada, Reno, Nevada 89557

ABSTRACT

The Amargosa Desert fault system, part of a 250-km-long system of dextral strike-slip faults east of the Death Valley region, extends beneath Crater Flat and Yucca Mountain, Nevada. Total dextral displacement on the fault system exceeds 40 km, and ~25 km may have occurred since about 11.5 Ma. The system has

Quaternary and possibly Holocene displacement.

Both normal faults and basaltic volcanic cones near Yucca Mountain may be controlled by this regional strike-slip fault system. This fault system has important implications for assessment of future volcanic and seismic hazards at the proposed high-level nuclear waste repository at Yucca Mountain.

INTRODUCTION

Yucca Mountain, Nevada, the site of a proposed high-level nuclear waste repository, lies at the southern edge of the Southwest Nevada Volcanic Field (SWNVF) within the Walker Lane belt (Fig. 1), a region noted for dextral and sinistral strike-slip faults, large extension, and irregular topographic grain.[1] This paper presents evidence that a NW-striking, dextral strike-slip shear system exists beneath Yucca Mountain and adjacent Crater Flat. We refer to the proposed fault system as the Amargosa Desert fault system (ADFS).

STRUCTURAL SETTING

Within the region around Yucca Mountain (Fig. 1), a Mesozoic fold and thrust belt involving Paleozoic miogeoclinal strata has been disrupted by Cenozoic extension. Large extension affected the area between the Spotted Range and the Eleana Range [2], the Death Valley-Nopah Range region [3,4], and the area north and west of Bare Mountain (Fig. 1).[5,6,7]

Strike-slip faults and related deformation are also of major importance (Fig. 1)[1], as indicated by the Las Vegas Valley shear zone, the Pahrump-Stateline fault, and the Death Valley-Furnace Creek fault zone, together with other strike-slip faults

farther west.

GEOPHYSICAL AND STRUCTURAL EVIDENCE FOR EXISTENCE OF A NW-STRIKING FAULT SYSTEM IN AMARGOSA VALLEY

Dextral strike-slip faults southeast of the Yucca Mountain area (Fig. 1, inset B) form a 150-km-long-system and include the Ivanpah and Stateline faults, Mesquite Valley-Pahrump fault, the Stewart Valley fault, and faults in southern Amargosa Valley (also known as Amargosa Desert).[8,9,10,11]

Evidence that the strike-slip fault system continues northwestward through southern Amargosa Desert, Crater Flat, and the SWNVF is summarized in Table 1 and presented below. Other lines of evidence that may conflict with the hypothesis are discussed later.

Evidence For The ADFS

Gravity data. A continuous series of elongate Bouguer gravity lows [12,13,14] define a narrow structural depression extending from Pahrump, Stewart, and southern Amargosa valleys northward through the Yucca Mountain-Crater Flat area and into the Timber Mountain caldera (Figs. 1, 2).[12,13,14] Because deep basins and linear Bouguer lows characterize most strike-slip faults in the region[14], and here coincide in part with known strike-slip faults, we suggest that this structural depression is related to a strike-slip fault system, the ADFS (Fig. 1, 2).

The Gravity fault (Fig. 2), a major buried fault that strikes N24W for 30 km from the north end of Stewart Valley, lies along the trend of our inferred ADFS. It has over 1 km of down-to-the-west normal displacement.[15] Ten kilometers south of Lathrop Wells, the Gravity fault bends to a north-northeast strike, whereas we

project the ADFS northwestward toward Crater Flat and Yucca Mountain.

Distribution of springs. A major N24W-trending alignment of over 30 springs (Fig. 2), one of the largest spring concentrations in the southern Great Basin, also lies along the Gravity fault, indicating important structural control of groundwater flow.

Seismic data. The Gravity fault and another possible fault of the ADFS both were imaged with seismic data (Fig. 2).[16] The western end of seismic profile AV-1 shows two faults about 2 km apart. Both faults may be west-dipping normal faults related to the Gravity fault[16]; alternatively, we interpret the western fault as a subvertical strike-slip fault forming a segment of the ADFS.

Faults at Bare Mountain. A set of north-striking, right-oblique faults with up to 10 km of dextral displacement occurs within Bare Mountain (Fig. 1), at the west edge of Crater Flat.[7,17] These faults predate a set of 14 Ma dacitic dikes.[17] We interpret them as marking pre-Middle Miocene dextral displacement within the ADFS.

Distribution of volcanic centers. Four major Quaternary and Pliocene basaltic centers or cone clusters aligned with the ADFS (Figs. 1-3), include: (1) a buried Pliocene(?) center 1 km south of Lathrop Wells, (2) the Big Dune Cone (about 20 ka), (3) several 1.2 Ma cones in Crater Flat, and (4) Sleeping Butte (about 240-320 ka), a few kilometers southwest of Pahute Mesa.[12,18,19,20] Several of the clusters have northeast-trending fissures and alignments of cones.[21] The lavas are transitional alkalic-tholeiitic basalts or hawaiites, and were derived from a high $^{87}Sr/^{86}Sr$ mantle source.[20,22]

Late Quaternary basaltic cinder cones in the southern part of the Walker Lane belt commonly are aligned along strike-slip faults.[23] Other examples include the Owens Valley fault zone, the Southern Death Valley fault zone, and the Death Valley-Furnace Creek fault zone (Fig. 3).

Vertical-axis rotations. Clockwise vertical-axis rotations of ash-flow tuffs documented at Yucca Mountain and at Sleeping Butte, contrast with a lack of vertical-axis rotation in areas both east and west[24,25](Fig. 3) and coincide exactly with the projected trace of the ADFS. This data, discussed in more detail later, is consistent with 22-24 km dextral slip.[26]

Quaternary faults. During late Quaternary to Holocene times, dextral and normal displacements east of Death Valley have been concentrated in the ADFS between Pahrump Valley and Yucca Mountain (Fig. 4). A northwest-trending zone of late Quaternary scarps extends from southern Pahrump Valley through Stewart and southern Amargosa valleys, and this zone lies directly on trend with late Quaternary faults in Crater Flat and Yucca Mountain.[21,27,28,29,30]

Some Quaternary faults in southern Amargosa Valley may have dextral displacements.[27] Scarps aligned with the Gravity fault have west-side-down normal separation, and individual scarps strike more northerly than the overall zone, suggesting the scarps may have formed as R-shears or extension fractures in a zone of right-lateral shear.[27,31] Quaternary faults with dextral strike-slip have also been documented in Stewart Valley and along the eastern edge of the Nopah Range.[28]

The youngest deposits cut by these faults are poorly dated, but the faults are inferred to have been active in late Quaternary to Holocene times.[27,28,29]

We suggest that the displacement zone in Pahrump, Stewart, and southern Amargosa Valleys continues north-northwest into the Crater Flat area, because no significant faults or scarps have been found in northern Amargosa Valley between the Funeral Mountains and Bare Mountain and no faults connect this zone to Death Valley.[29] No surface ruptures are apparent near Fortymile Wash, possibly suggesting that displacement predates late Holocene alluvial deposits.[32,33]

MAGNITUDE AND TIMING OF DISPLACEMENT

About 35-45 km of dextral displacement has probably occurred along the proposed ADFS and related faults to the south (Table 2).

Several Paleozoic facies boundaries (Table 2, Fig. 1) that may have been offset 25-35 km dextrally across the proposed ADFS[34,35] are poorly constrained because of sparse outcrop.

The most distinctive displaced features include folds with anomalous vergence and thrust faults. The Striped Hills anticline (Fig. 1) extends from the Striped Hills to the Spotted Range, and is characterized by a steeply dipping to overturned north limb. This fold forms part of the upper plate of the northwest-vergent CP thrust.[2] A comparable large anticlinal fold at Bare Mountain lies in the upper plate of the north-vergent Panama thrust and includes a major northward vergent, overturned limb (Fig. 1).[7] These folds both have vergence opposite that of most folds in the fold-thrust system[36] and are of similar, very large amplitude, involving about 4.5 km of stratigraphic thickness.[26]

Our studies support correlation of the folds, because both folds show similar fabric relations and structural styles. In both areas the large folds are D_2 structures

that have been superimposed upon older south-vergent folds and cleavage.

The Montgomery thrust may match the Clery thrust (Fig. 1).[35] Both thrusts are southeast-vergent, mark the same facies boundary, and have similar stratigraphic throw.

Twenty-five to thirty kilometer offsets of the folds and thrusts are consistent with dextral separations of other thrusts 150 km to the southeast, which suggest over 20 km of dextral displacement on the Ivanpah and Stateline faults (Fig. 1, Inset B).[11,37]

Paleomagnetic data may provide an independent estimate of displacement. Assuming that vertical axis rotations of 11.45 Ma-ash-flow tuffs at Yucca Mountain[24,38] were caused by heterogeneous simple shear, displacement of about 22-24 km since 11.45 Ma can be estimated by shear strain integration. This analysis utilizes a N24W-striking, parallel-sided shear zone ~16 km wide, with the western boundary the eastern edge of Bare Mountain and the eastern boundary at the northeastern edge of Yucca Mountain.[24,38] The resulting estimate is very approximate because of non-parallel shear zone boundaries, uncertainties in location of the boundaries, and small rotations in areas to the east.

ARGUMENTS AGAINST THE ADFS

The strongest objections to the hypothesized ADFS are: 1) the lack of a throughgoing surface trace north of Stewart Valley and within the SWNVF, 2) Mississippian strata may form a continuous belt between Bare Mountain and the Calico Hills, precluding dextral displacements, and 3) some stratigraphic units brought together by restoring 25-30 km of slip on the fault zone have markedly

different thicknesses.

The lack of a throughgoing surface trace suggests to us that the ADFS is a basement fault system which is partially detached from faults in the overlying Cenozoic volcanic section, as observed along strike-slip faults in other parts of the Walker Lane belt[39]. The part of the volcanic section in the SWNVF overlying the basement fault system has deformed principally by top-to-the-west normal faulting and rotational shear. The northern continuation of the ADFS beyond the SWNVF is unknown, but possibilities include a gradual transfer of dextral displacement to extensional faulting.

There is no evidence for a continuous belt of Mississippian strata between Bare Mountain and the Calico Hills. An aeromagnetic high extending west from Mississippian strata in the Calico Hills (Fig. 1) continues only to the northern part of Yucca Mountain, where it curves toward the northwest[40]; it does not extend across the north end of Crater Flat and therefore does not join Mississippian rocks at the north end of Bare Mountain.

Stratigraphic thickness data do not preclude 25-35 km displacement on the ADFS. The Zabriskie Quartzite at Bare Mtn is 345-m-thick, while in the Striped Hills it is 120-m-thick.[41] It is important to note, however, that the two measured sections (open circles, Fig. 1) are not in the same structural position relative to the Panama-CP thrust . The section in the Striped Hills is in the upper plate, while the section at Bare Mountain lies in the lower plate; no complete sections of the Zabriskie are preserved in the same plate in both areas. Other units in the two areas appear to have similar thicknesses, regardless of structural position.

We conclude that lack of a throughgoing surface trace and data on aeromagnetic highs and stratigraphic thicknesses do not preclude large dextral displacement on the ADFS and related faults.

TECTONIC MODEL

The existence of the ADFS is supported by a wide range of geological and geophysical evidence, as much evidence, in fact, as most of the other strike-slip faults in the southern Great Basin. We interpret the ADFS as a deep-seated, NW-striking, dextral, transtensional, strike-slip shear zone (Fig. 1), one of several such fault systems in the southern part of the Walker Lane belt. The combined length of the ADFS and the Pahrump-Mesquite-Stateline-Ivanpah faults (Fig. 1) is at least 250 km, and the total amount of displacement could in places exceed 40 km.

We suggest that, within the SWNVF, dextral slip in pre-Cenozoic basement is partially detached from the overlying Cenozoic volcanic section, which has deformed by top-to-the-west normal faulting and rotational shear.

Alignments of basaltic cones along the ADFS probably mark conduits controlled by extension fissures deep within the crust and/or by shallow Riedel shears or extension fractures. This accounts for the observation that slip events on some faults at Yucca Mountain have been accompanied by basaltic eruptions.[42,43]

An extensional right stepover may occur in the Yucca Mountain-Crater Flat area, as suggested by the northeast strike of normal faults. Probable pullapart structures in the fault system (Fig. 1) include northern Pahrump Valley, Stewart Valley, and possibly Crater Flat, where Cenozoic fill is 3-4 km thick.[14,28,44,45] Exposed faults at Crater Flat and Yucca Mountain (Fig. 4) therefore may be viewed as

rotational normal faults within a pullapart zone at a right step in the dextral transtensional system.[24,42]

The ADFS probably initiated prior to middle Miocene time. Others have suggested that middle Miocene calderas of the SWNVF (Fig. 1) were localized along a major right stepover in a dextral shear system.[12] If so, the ADFS may originally have been part of a more complex zone of strike-slip and extensional faulting, and evolved gradually into a more linear zone.

Late Quaternary surface faults at Yucca Mountain, Crater Flat, and in southern Amargosa Valley, together with the clustered Quaternary to Holocene basaltic cinder cones (Fig. 4), probably indicate that the ADFS is presently active, albeit at relatively low rates.

Modern seismicity in the Yucca Mountain region characteristically occurs at 2 to 11 km depths. Focal mechanisms, although not well constrained, suggest N-striking focal planes with strike-slip mechanisms.[46] As in much of the Great Basin, they do not correlate well with surface faults. Many of these events may be occurring along fractures or shears along the ADFS.

IMPLICATIONS

Further study of the evolution and nature of this 250-km-long strike-slip system (e.g., its timing and rates of motion, and whether it represents plate boundary motion, is an extension-related transfer zone, or represents motion along the edge of a large crustal block) is needed to understand and model the timing, recurrence, and displacements of surface faults at Yucca Mountain, and their relation to volcanic events. Nevertheless, both fault slip events and volcanism in

the vicinity of Yucca Mountain, the proposed high-level nuclear waste repository, may be driven by displacements along this regional strike-slip fault system. Consideration of the ADFS will impact assessments of future volcanic and seismic hazards at Yucca Mountain.

FIGURE CAPTIONS

Figure 1. Sketchmap of a part of southern Nevada and southeastern California near the Yucca Mountain region showing selected Mesozoic and Cenozoic structural features. Shading indicates mountain ranges exposing pre-Tertiary rocks. Localities: BC = Black Cone, BD = Big Dune Cone, L = Lathrop Wells Cone, M = localities exposing Mississippian clastic rocks, PV=Pahrump Valley, RC=Red Cone, SB=Sleeping Butte Cone, SV=Stewart Valley, SWNVF= Southwestern Nevada volcanic field, Y=Yucca Mountain. Faults: DV-FCFZ=Death Valley-Furnace Creek fault zone, LVVSZ=Las Vegas Valley shear zone. Light dashed line shows limit of SWNVF; calderas are shown with ticked lines. Short dashed line west of Calico Hills shows position of aeromagnetic high.[40] Open circles at Bare Mountain and Striped Hills are locations of published stratigraphic sections. Ruled areas are pullapart basins. Light, double-ticked lines north of Yucca Mountain delineate a possible older pullapart structure. Quaternary and Holocene basaltic cinder cones are shown in black. Inset A: Walker Lane belt and area of Inset B. Inset B: Area of Fig. 1 and mapped strike-slip faults southeast of Amargosa Desert. Abbreviations - inset B: Y=Yucca Mountain, SV=Stewart Valley fault, P=Pahrump fault, M=Mesquite Valley fault, ST=Stateline fault, IV=Ivanpah fault.

Figure 2. Map of southern Amargosa Valley, showing the Gravity fault, aligned springs, and the approximate trace of the proposed Amargosa fault system. USGS AV-1--USGS seismic line.[16] Buried cone is identified on Figure 3 as Lathrop Wells cone.

Figure 3. Map of the southern Great Basin in Nevada and southeastern California

showing major Quaternary and older basaltic volcanic centers and their association with Cenozoic strike-slip faults (modified from ref. 12). Circles with ticks near Sleeping Butte and Crater Flat show location and amount of rotated domains documented by paleomagnetic studies.[24,38] Areas east and west show no evidence for vertical-axis rotations. Shaded dashed fault is trace of proposed Amargosa fault system.

Figure 4. Map of Quaternary faults in the Amargosa Valley-Pahrump Valley region (compiled from refs. 27,28,29,30,31, and 47). Quaternary and Pliocene volcanic centers are shown in black. Outline of the proposed Yucca Mountain high-level nuclear waste repository is shown. RVFZ--Rock Valley fault zone, YM--Yucca Mountain, DV--Death Valley.

REFERENCES CITED

1. J. H. Stewart, in *Metamorphism and Crustal Evolution of the Western United States*, W. G. Ernst, Ed. (Prentice-Hall, Inc., Englewood Cliffs, N.J., 1988), p. 683.

2. S. J. Caskey and R. A. Schweickert, *Tectonics* **11**, 1314 (1992).

3. J. H. Stewart, *Geology* **11**, 153 (1983).

4. B. Wernicke, G. J. Axen, J. K. Snow, *Bull. Geol Soc. America* **100**, 1738 (1988).

5. M. D. Carr and S. A. Monsen, in *This Extended Land, Geological Journeys in the Southern Great Basin*, D. L. Weide and M. L. Faber, Eds. (Geol. Soc. America, Boulder, Colo.), p.50 (1988).

6. F. Maldonado, *Bull. Geol Soc. America* , **102**, 992 (1990).

7. S. A. Monsen, M. D. Carr, M. C. Reheis, P. P. Orkild, *Geologic Map of Bare Mountain, Nye County, Nevada* (U. S. Geol. Survey Misc. Investigations Map I-2201) (1993).

8. M. A. Liggett and J. F. Childs, *NASA Technical Report*, p.1, (1978).

9. D. F. Hewett, *U. S. Geol. Survey Prof. Paper* **275**, p. 1 (1956).

10. G. T. Malmberg, *U. S. Geol. Survey Water Supply Paper* **1832**, p. 1 (1967).

11. R. J. Fleck, *Bull. Geol Soc. America* **82**, 1437 (1971).

12. W. J. Carr, *U. S. Geol. Survey Open-File Report* , **OF 84-854**, p. 1 (1984).

13. W. J. Carr, in *Basin and Range Tectonics Near the Latitude of Las Vegas, Nevada*, B. P. Wernicke, Ed., (Mem. Geol. Soc. America, **176**), p. 283 (1990).

14. L. A. Wright, in *Late Cenozoic Evolution of the Southern Great Basin*, M. A. Ellis, Ed. (Nev. Bur. Mines and Geol., Open-File Report **89-1**), p. 1 (1989).

15. I. J. Winograd and W. Thordarsson, *U. S. Geol. Survey Prof. Paper*, **712-C**, p. 1 (1975).

16. T. M. Brocher, M. D. Carr, K. F. Fox, P. E. Hart, *Bull. Geol Soc. America* **105**, 30 (1993).

17. Y. Zhang and R. A. Schweickert, *Geol. Soc. America Abs. with Programs* **23**, p. A185 (1991), and work in progress, 1994.

18. B. Crowe and W. J. Carr, *U. S. Geol. Survey Open-File Report*, **80-375**, p. 1 (1980).

19. S. G. Wells, L. D. McFadden, C. E. Renault, B. M. Crowe, *Geology* **18**, 549 (1990).

20. B. Crowe, S. Self, D. Vaniman, R. Amos, F. Perry, *Jour. Geol.*, **91**, 259 (1983).

21. J. E. Faulds, J. W. Bell, D. L. Feuerbach, and A. Ramelli, *Nevada Bureau of Mines and Geology*, **Map 101** (1994).

22. D. T. Vaniman, B. A. Crowe, E. S. Gladney, *Contr. Min. and Pet.*, **80**, 341 (1982).

23. A. Aydin, R. A. Schultz, D. Campagna, *Annales Tectonicae* **IV**, 45 (1990); A. Aydin and A. Nur, *Tectonics*, **1**, 95 (1982).

24. M. R. Hudson, D. A. Sawyer, R. G. Warren, *Tectonics* **13**, 258 (1993).

25. Y. Zhang, S. L. Gillett, R. E. Karlin, R. A. Schweickert, *Geol. Soc. America Abstracts with Programs* , **25**, 169 (1993).

26. R. A. Schweickert, *Geol. Soc. America Abstracts with Programs* **21**, p. A90 (1989).

27. D. E. Donovan, thesis, Univ. Nevada, Reno (1991).

28. J. L. Hoffard, thesis, Univ. Nevada, Reno (1991).

29. M. C. Reheis and J. S. Noller, *U. S. Geol. Survey Open-File Report* **OF-90-41**, p. 1(1990).

30. M. C. Reheis, *U. S. Geol. Survey Open-File Report* **OF-92-193**, p. 1 (1992).

31. This NNW-trending zone of Quaternary scarps appears to be crossed at its northern end by a NE-trending zone of Quaternary scarps that may be related to the left-lateral Rock Valley fault zone (Fig. 4). Ref. 27 and J. C. Yount, R. R. Shroba, C. R. McMasters, H. E. Huckins, and E. A. Rodriguez, *U.S.Geological Survey Miscellaneous Field Studies Map,*

MF-1824 (1987).

32. W. C. Swadley, *U. S. Geol. Survey Misc. Inv. Map* **I-1361** (1983).

33. V. Frizzell and J. Shulter, *U. S. Geol. Survey Misc. Inv. Map* **I-2046** (1990).

34. J. D. Cooper, R. H. Miller, F. A. Sundberg, in *Geology of Selected Areas in the San Bernardino Mountains, Western Mojave Desert, and Southern Great Basin, California*, J. D. Cooper, B. W. Troxel, and L. A. Wright, Eds. (Geol. Soc. America, Cordilleran Sec., Anaheim, Ca), p. 97 (1982).

35. C. H. Stevens, P. Stone, P. Belasky, *Bull. Geol. Soc. America* **103,** 876 (1991).

36. J. K. Snow and B. P. Wernicke, *Bull. Geol. Soc. America* **101,** 1351 (1989).

37. B. C. Burchfiel, oral comm. to RAS, 1990.

38. J. G. Rosenbaum, M. R. Hudson, and R. B. Scott, *Jour. Geophys. Res* **96,** 1963 (1991).

39. R. F. Hardyman and J. S. Oldow, *in Geology and Ore Deposits of the Great Basin,* Geol. Soc. Nevada, p. 279 (1991).

40. G. D. Bath and C. E. Jahren, *U. S. Geol. Survey Open-File Report* **OF-84-120,** p.1 (1984).

41. J. H. Stewart, *U. S. Geol. Survey Prof. Paper* **620,** p. 1 (1970).

42. K. F. Fox and M. D. Carr, *Radioactive Waste Management and the Nuclear Fuel Cycle* **13,** 37 (1989).

43. R. R. Shroba, J. W. Whitney, E. M. Taylor, K. F. Fox, Jr., *Geol. Soc. America Abs. with Programs* **22,** 83 (1990).

44. D. B. Snyder and W. J. Carr, *Jour. Geophysical Research* **89,** 10,193 (1984).

45. H. D. Ackermann, W. D. Mooney, D. B. Snyder, V. D. Sutton, *U. S. Geol. Survey Bull* **1790,** 23 (1988).

46. A. M. Rogers, S. C. Harmsen, and M. E. Meramonte, *U. S. Geol. Survey Open-File*

Report OF-87-408, 1 (1987).

47. M. A. McKittrick, *U. S. Geological Survey Miscellaneous Field Studies Map* MF-1941(1988).

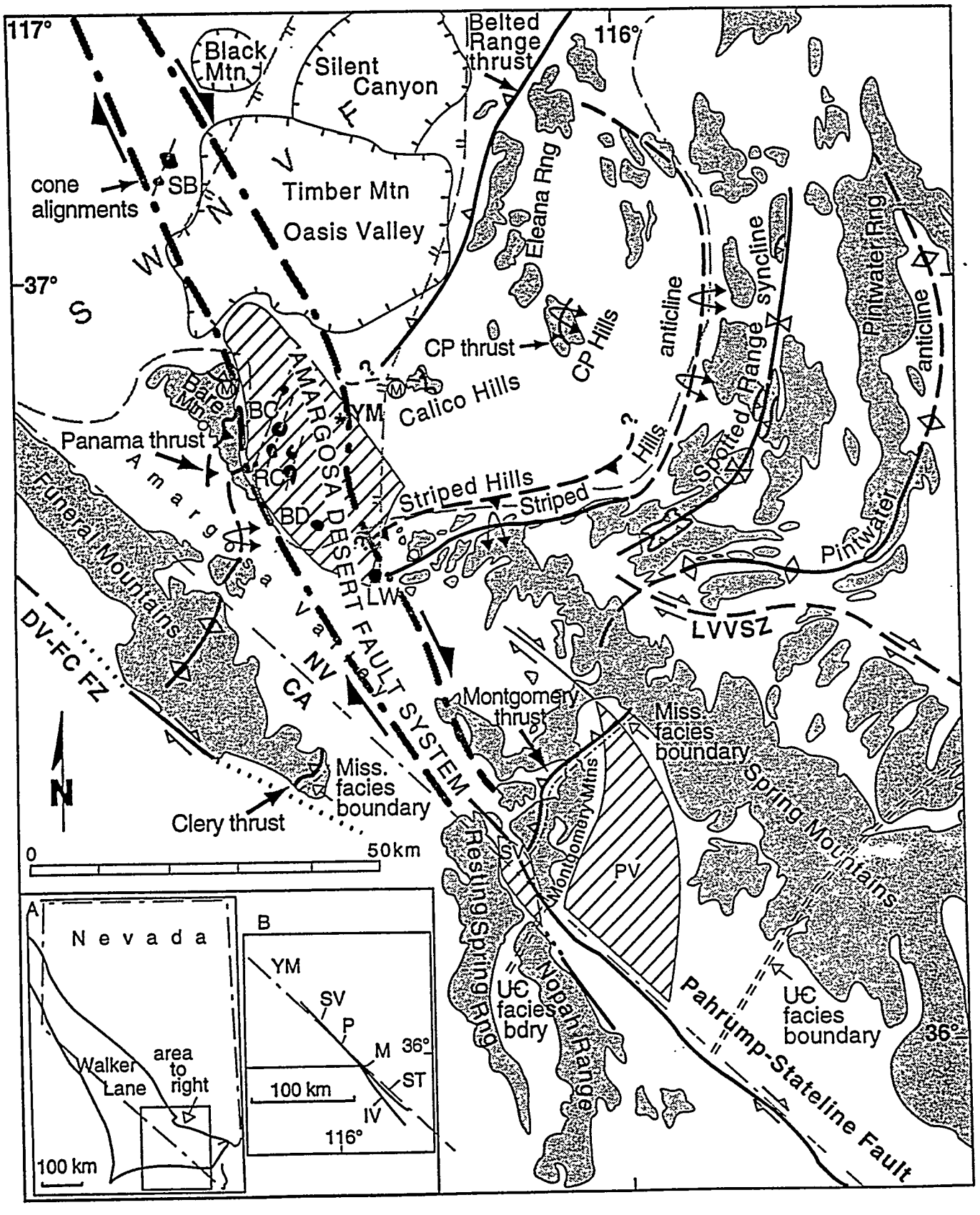
117°
116°
37°
Black Mtn
Silent Canyon
Belted Range thrust
cone alignments
SB
Timber Mtn
Oasis Valley
Eleana Rng
CP thrust
CP Hills
anticline
syncline
Spotted Range
Pintwater Rng
anticline
Bare Mtn
BC
YM
Calico Hills
Panama thrust
RC
BD
AMARGOSA DESERT FAULT SYSTEM
Striped Hills
Striped
Hills
Pintwater
Amargosa Valley
Funeral Mountains
DV-FC FZ
LW
LVVSZ
NV
CA
Montgomery thrust
Miss facies boundary
Spring Mountains
Miss. facies boundary
Clery thrust
N
0
50km
Resting Spring Rng
SV
Montgomery Mtns
PV
Nopah Range
UC facies bdry
UC facies boundary
Pahrump-Stateline Fault
36°
A
Nevada
B
YM
SV
P
M
36°
ST
IV
100 km
116°
Walker Lane
area to right
100 km

Fig 1

Fig 2

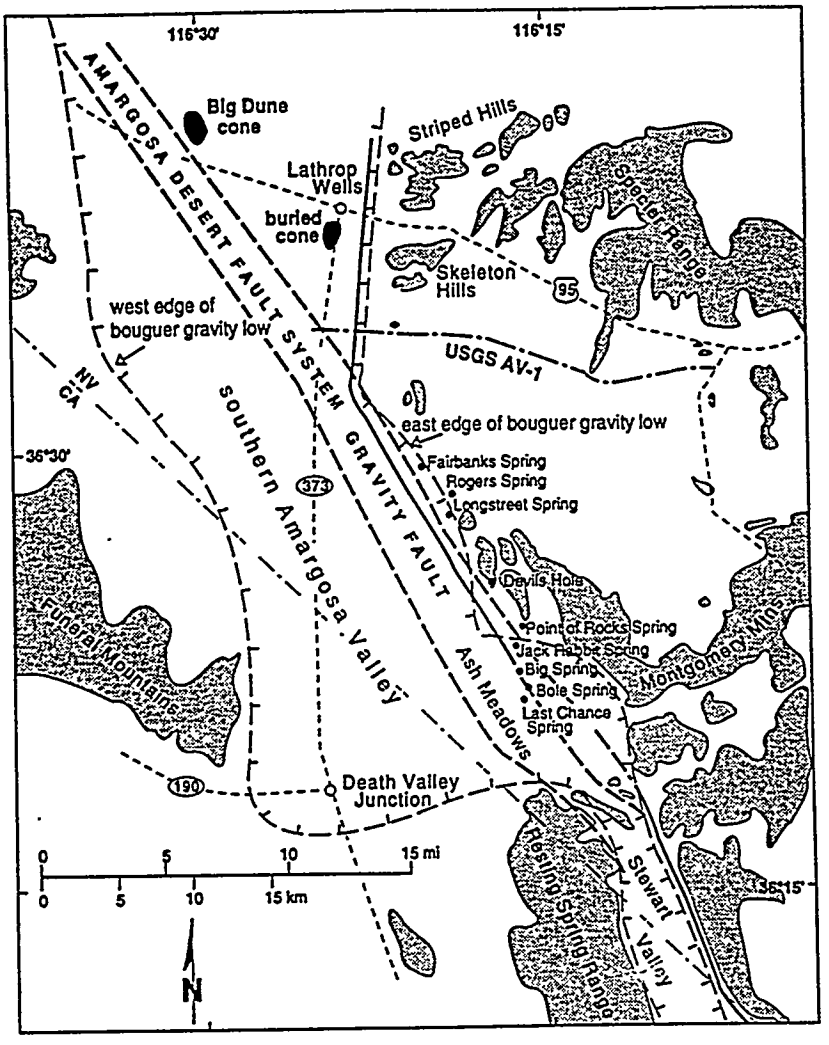
116°30'
116°15'
AMARGOSA DESERT FAULT SYSTEM
GRAVITY FAULT
Big Dune cone
Striped Hills
Lathrop Wells
buried cone
Skeleton Hills
95
west edge of bouguer gravity low
USGS AV-1
NV 373
Southern Amargosa Valley
east edge of bouguer gravity low
36°30'
373
Fairbanks Spring
Rogers Spring
Longstreet Spring
Devils Hole
Point of Rocks Spring
Jack Rabbit Spring
Big Spring
Bole Spring
Last Chance Spring
Ash Meadows
Funeral Mountains
190
Death Valley Junction
0 5 10 15 mi
0 5 10 15 km
N
Resting Spring Range
Stewart Valley
36°15'

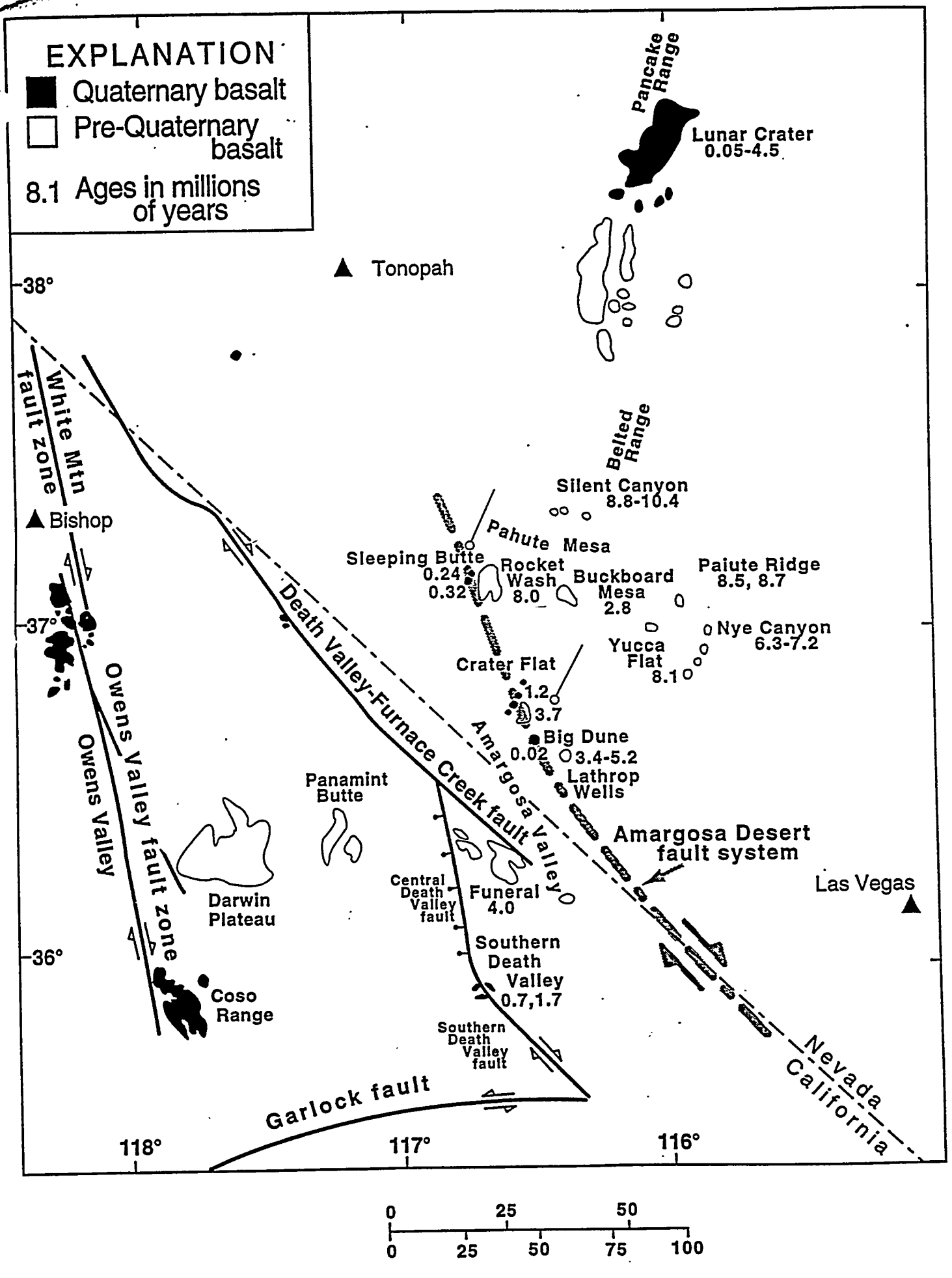
EXPLANATION
Quaternary basalt
Pre-Quaternary basalt
8.1 Ages in millions of years
Pancake Range
Lunar Crater
0.05-4.5
Tonopah
38°
White Mtn fault zone
Bishop
Belted Range
Silent Canyon
8.8-10.4
Pahute Mesa
Sleeping Butte
0.24
0.32
Rocket Wash
8.0
Buckboard Mesa
2.8
Paiute Ridge
8.5, 8.7
Nye Canyon
6.3-7.2
Yucca Flat
8.1
Crater Flat
1.2
3.7
Death Valley-Furnace Creek fault
Amargosa Valley
Big Dune
0.02
3.4-5.2
Lathrop Wells
Panamint Butte
Amargosa Desert fault system
Las Vegas
37°
Owens Valley
Owens Valley fault zone
Darwin Plateau
Central Death Valley fault
Funeral
4.0
Southern Death Valley
0.7,1.7
36°
Coso Range
Southern Death Valley fault
Garlock fault
Nevada
California
118°
117°
116°
0
25
50
0
25
50
75
100

Fig 4

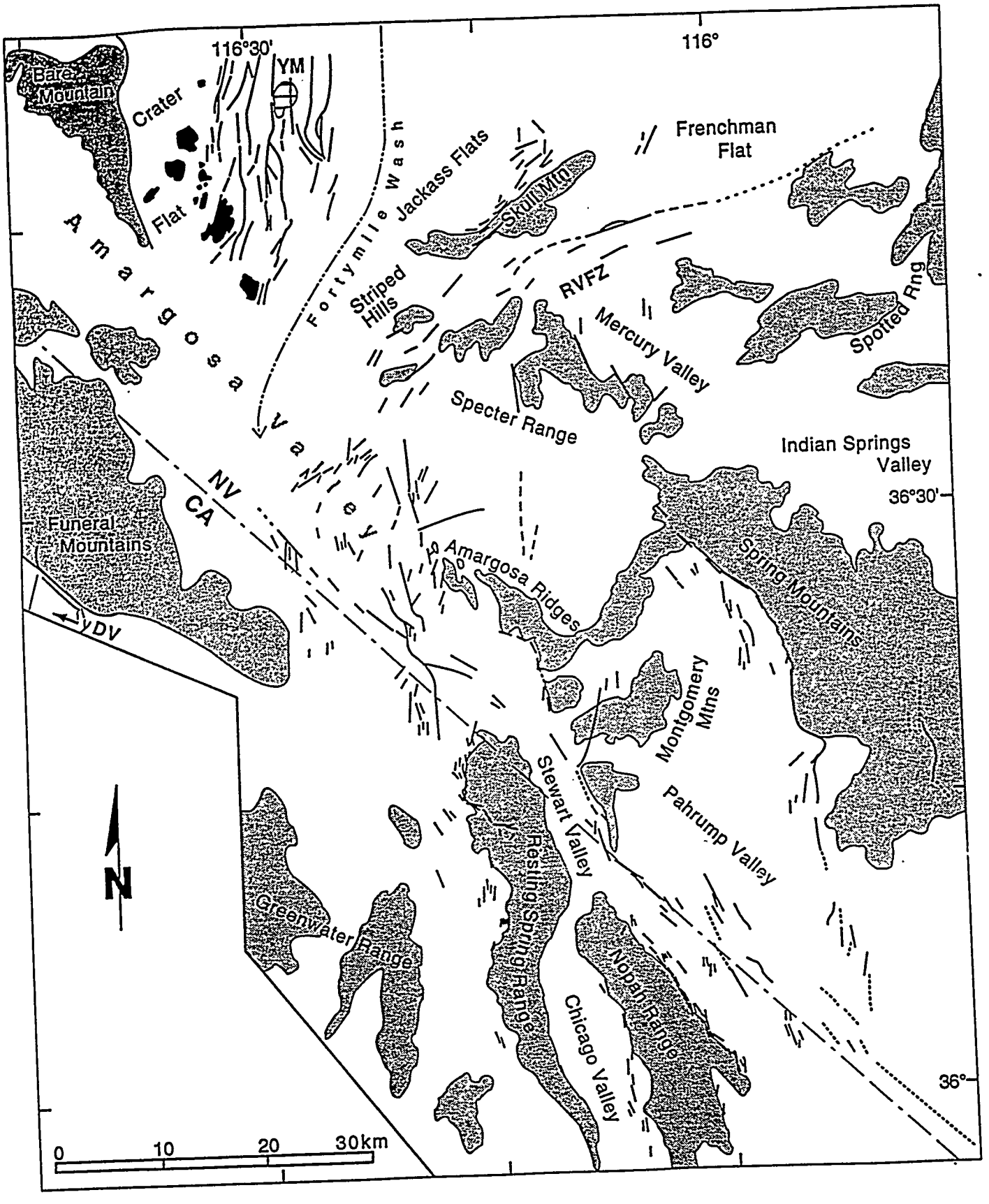
116°30'
116°
YM
Bare Mountain
Crater
Flat
Fortymile Wash
Jackass Flats
Skull Mtn
Frenchman Flat
Amargosa Valley
Striped Hills
RVFZ
Mercury Valley
Spotted Rng
Specter Range
Indian Springs Valley
36°30'
NV
CA
Funeral Mountains
Amargosa Ridges
Spring Mountains
yDV
Montgomery Mtns
Stewart Valley
Pahrump Valley
Resting Spring Range
Nopah Range
Chicago Valley
Greenwater Range
N
36°
0
10
20
30km

Table 1. Evidence for and against a throughgoing strike-slip fault system between Crater Flat and Stewart and Pahrump Valleys

For	Against
1. Bouguer gravity lows - indicate structural continuity. 2. These coincide with known dextral faults to south (Stewart Valley, Pahrump, Stateline, Ivanpah faults. 3. Gravity fault and 30 major springs form prominent N24W alignment in Southern Amargosa Valley. 4. Fault imaged at west end of seismic line AV-1. 5. N-striking dextral faults in Bare Mountain. 6. Alignment of Quaternary and Pliocene basaltic centers and volcanic cone clusters. 7. Miocene ash-flow tuffs show clockwise vertical axis rotations only along ADFS. 8. Zone of Quaternary normal and strike-slip faults coincides with ADFS.	1. Lack of mappable throughgoing surface fault. 2. Possibility of a continuous E-W belt of Mississippian strata between Bare Mountain and Calico Hills. 3. Mismatch of stratigraphic thicknesses when 25-30 km slip is restored.

Table 2. Evidence for magnitude and timing of displacement

Displaced feature	Dextral slip
1. Upper Cambrian facies boundary[34]	35 km
2. Mississippian facies boundary[35]	25-35 km
3. Regional north-vergent anticline[2,7,26]	26-30 km
4. Montgomery-Clery thrusts[35]	25 km
5. 11.45 Ma ash-flow tuffs--rotational strain[24,38]	22-24 km
6. Stratigraphic and structural units at Bare Mountain[7]	10 km*
Summary: Up to 45 km maximum dextral displacement. Up to 24 km dextral displacement since 11.45 Ma. Quaternary faults suggest continued activity.	

*additive to offsets of other features

THE GLOBAL WEEKLY OF RESEARCH
SCIENCE

20 July, 1995

Dr. Richard A. Schweickert
Department of Geological Sciences
University of Nevada
Reno, NV 89557

Dear Rich and Mary:

Our review of your manuscript entitled "Strike-slip fault system in Armargosa Valley..." is now complete, and I regret to say that we have decided against publishing the work in SCIENCE. Unfortunately, as you can see, both referees made extensive comments that, while not refuting your hypothesis, clearly indicate that addition discussion and clarification are needed on many points. While I anticipate that you might be able to address many of these comments, overall the reviews are not sufficiently enthusiastic regarding publication to allow the paper to compete for our very limited space. I hope that you find the extensive comments helpful, however, in preparing the manuscript for submission to another journal.

Sincerely and best regards,

R. Brooks Hanson
Senior Editor
(202) 326-6506
bhanson@aaas.org

Headquarters
1333 H Street NW, Washington, DC 20005 USA • Telephone: (+1) 202-326-6500 • Fax: (+1) 202-289-7562
Europe Office
Thomas House, George IV Street, Cambridge, UK CB2 1HH • Telephone: (+44) 0223 302067 • Fax: (+44) 0223 302068
Published by the American Association for the Advancement of Science

SECTION VI

University of Nevada, Reno
Center for Neotectonic Studies

Task 8: Evaluation of Hydrocarbon Potential

Report of Investigations
October, 1994 through September, 1995

Principal Investigators:
Patricia H. Cashman
James H. Trexler, Jr.

INTRODUCTION

Task 8 is responsible for assessing the hydrocarbon potential of the Yucca Mountain vicinity. Our main focus is the upper Paleozoic source rock stratigraphy in the NTS area. Regional structural geology is the next priority -- it controls distribution and extent of source rocks, as well as their burial history and thermal maturation.

STRATIGRAPHY

During the 1994-1995 funding period, we measured three new sections (at Bare Mountain, Carbonate Wash, and the Spotted Range, see Fig.s 1 - 5) and made detailed stratigraphic descriptions in three additional new localities where a measured section was not possible (the upper plate in the Calico Hills, the lower plate in the Calico Hills -- on the surface and in the UE25a-3 drillhole -- and the lower plate of the CP thrust -- in the ER 6-2 drillhole). All of these sections, as well as our existing measured section at Mine Mountain, were sampled for conodonts. These new stratigraphic descriptions are widely distributed geographically, including localities just outside the western, northern and southeastern boundaries of the NTS, and are evenly divided between the Eleana Formation and the Chainman Shale. Notably, all of these sections include the depositional base of the clastic section, where it overlies Devonian carbonates. We have been successful in obtaining conodonts from many of these sections, both below and above the clastic/carbonate transition. The combination of lithostratigraphic descriptions and biostratigraphic control have dramatically improved our understanding of regional stratigraphic correlations and paleogeography. New biostratigraphic control has also required us to re-examine the sections at Mine Mountain and Shoshone Mountain. All of these sections are described briefly below.

(1) Measured section, base of the **Eleana Fm at Carbonate Wash** (Fig.s 1, 2, 3)**:** The section starts in slope facies carbonates and extends up into the chert-litharenite submarine fan. The first clastic signal is quartz sand. A thin but distinctive black bedded-chert interval occurs within the quartz sand section and signals a relatively brief period of hemipelagic deposition (we believe this interval can be seen in other sections, and may be used with caution for regional correlation). The chert litharenite and conglomerate of the Eleana submarine fan overlies the quartz sand section; higher parts of the section are not preserved at Carbonate Wash. Biostratigraphic results: Limestone samples from immediately below the first arrival of clastic sediment and within the quartz sand section are barren of conodonts. The remaining splits from these samples are being processed, and one additional sample (from lower in the carbonate section) remains to be processed.

(2) Measured section, base of the **Eleana Fm at Bare Mountain** (Fig.1,2, 4)**:** The section starts in slope facies, silty carbonates and extends up through siltstones and a chert-litharenite submarine fan section into bioclastic grainstones of

the upper Eleana Fm. The first clastic signal is quartzose siltstone, which is overlain by siliceous argillite and chert. These are overlain by chert litharenite and conglomerate, and by bioclastic grainstone, of the Eleana submarine fan. Biostratigraphic results: The lowest chert litharenite occurs interbedded with grainstones that contain conodonts; our new conodont biostratigraphy indicates that this occurred in Osagean time. **Note**: this important new locality is the only direct biostratigraphic control on the age of the base of the Eleana submarine fan system.

(3) Described section, **Eleana Fm in the Calico Hills** (upper structural plate): The section starts in Devonian slope facies carbonate, and extends up through clastic rocks and bedded chert into a limestone and siltstone section. Again, the first clastic signal is quartz sandstone and siltstone. This is followed by a significant thickness of black bedded chert. The chert is overlain by an anomalous siltstone, silty limestone and limestone section which contains a thin pebbly mudstone horizon with radiolarian chert pebbles. Biostratigraphic results: Limestone immediately below the first arrival of quartz sand contains Middle Devonian conodonts. Limestones both below and above the siltstone and pebbly mudstone are Kinderhookian. **Note:** The pebbly mudstone is anomalous sedimentologically, and, if this age control is correct , it is also anomalous chronologically -- it appears to be older than the first arrival of recycled chert we see elsewhere.

(4) Re-evaluation and reinterpretation of the **"transitional Eleana" at Mine Mountain and Shoshone Mountain**, incorporating new biostratigraphic results: The base of both of these sections is a sandy, karsted limestone (Guilmette?), unconformably overlain by siltstone which contains two or three bioclastic limestone beds. Based on these similarities in lithostratigraphy and in biostratigraphy (see below), we now correlate the short clastic section at Shoshone Mountain with the Mine Mountain ("transitional Eleana") section. (Our previous interpretation was that the rocks at Shoshone Mountain might represent the depositional base of the Chainman Shale). At Shoshone Mountain, only 225m of section is preserved. In the thick (1040m) section preserved at Mine Mountain, the middle and upper parts of the siltstone contain relatively thin and fine-grained chert litharenites of the Eleana submarine fan, overlain by bioclastic grainstones. The highest part of the section contains anomalous quartz sands contaminated by chert lithic fragments. These appear to have been deposited between the Eleana basin (with its chert lithic source) and the Chainman shelf-slope (with its quartz sand source). Biostratigraphic results: Limestones low in the clastic section at both localities contain a combination of recycled Devonian conodonts and Kinderhookian conodonts; the latter include juveniles, and do not appear to be recycled. These limestones are interpreted to be Kinderhookian in age. Bioclastic grainstone beds high in the Mine Mountain section are Chesterian, the same age as similar bioclastic grainstones in the Eleana Formation in the Eleana Range and at Bare Mountain. As mentioned in earlier reports, we have established the base of Chesterian grainstones as a regional biostratigraphic marker that can be used for correlation throughout the NTS area.

(5) Described section, base of the **Chainman Shale in the ER 6-2 core from CP Hills:** This section is overturned, and underlies the upper plate of the CP thrust; it starts in sandy limestones (Guilmette?), which are depositionally overlain by interbedded shale, siltstone and quartz sandstone of the Chainman Shale. Although the underlying limestone was probably deposited in shallow water, there is no evidence of subaerial exposure, as there is in the karsted limestones at Mine Mountain and Shoshone Mountain. Biostratigraphic results: None yet -- this is a new core obtained for the D.O.E.'s Environmental Restoration Program, and sampling will not be permitted until logging is complete and a sampling procedure is approved; we anticipate being able to sample it in October, 1995.

(6) Described section, **Chainman Shale in the Calico Hills:** We re-examined parts of the UE25a-3 core (from the Calico Hills) that includes the depositional base of the Chainman Shale. Here, Chainman is deposited on laminated (relatively deep water?) carbonates. Chainman Shale exposed in the Calico Hills contains quartz sand beds and local bioclastic limestones, and is thought to represent the upper part of the Chainman section. Biostratigraphic results: The carbonates at the base of the UE25a-3 section are barren of conodonts. The bioclastic limestones are Chesterian (or maybe even lowermost Pennsylvanian?) in age, based on new conodont and foraminifera identifications.

(7) Measured section, base of **Chainman Shale in the Spotted Range** (Fig.s 1, 5): The Late Devonian Narrow Canyon Limestone is overlain by a Mississippian section comprising the Mercury and Timpi Canyon limestones and the Chainman Shale; the Chainman is structurally truncated. The Mercury Limestone is an open-marine grainstone with abundant macrofossils. The Timpi Canyon Limestone is micrite and wackestone. The contact with the overlying Chainman Shale is a silicified horizon. The Chainman here consists of interbedded micrite and calcareous siltstone, with uncommon allodapic grainstone beds. Exposure is fairly good, and no carbonaceous shale is preserved. Biostratigraphic results: The first clastic influx low in the section is quartz sand, and is interbedded with Famennian (uppermost Devonian) carbonates. The top of the Timpi Canyon Fm. is no older than late Kinderhookian, based on conodonts. The Chainman Shale here yields foraminifera that range in age from Meramecian to lower Chesterian. Interpretation: The Narrow Canyon - Mercury - Timpi Canyon section is correlative with lower Mississippian strata seen elsewhere in the area, especially the lower section at Mine Mountain. Here it is much thicker, and represents a paleogeographic position much nearer the craton edge, possibly an open shelf setting. The top of the Kinderhookian Timpi Canyon Limestone is capped by an interval of silicification and oxidation that may represent a hiatus in deposition, and possibly subareal exposure. The Chainman Shale here appears to be a relatively shallow marine carbonate unit with affinities to upper Mississippian limestones to the east. The carbonaceous Chainman shales were deposited entirely to the west of the position of this section.

STRUCTURAL GEOLOGY

During the 1994-1995 funding period, we completed mapping and structural interpretation in the southern Eleana Range, worked with Jim Cole of the USGS to completely reinterpret and remap the Paleozoic rocks in the Calico Hills, and collected structural data in selected other areas (e.g., northern Syncline Ridge, southern Quartzite Ridge). Significant results include:

(1) Most of the Paleozoic rocks that are exposed in the Calico Hills are part of a multiply-deformed but structurally coherent thrust plate that was emplaced eastward over the Chainman Shale along a sub-horizontal thrust fault. The thrust plate contains a Devonian slope carbonate section and the lower Mississippian clastics (basal Eleana Formation) that overlie it. The east-verging folding and thrusting are interpreted to be footwall deformation related to the Belted Range thrust.

(2) The Eleana Formation and underlying dolomites are NOT present in the 2500' core from drillhole UE25a-3 in the Calico Hills. The drill pad is topographically low on the south side of the Calico Hills, and is located in the Chainman Shale, structurally below the thrust. The UE25a-3 core goes through the Chainman and into the laminated carbonate that is its depositional base.

(3) Both units in the Calico Hills, and the intervening thrust fault, were later deformed by northwest- to north-vergent folding. This penetrative deformation is concentrated in kink-like bands across the Calico Hills, leaving bands where the earlier deformation does not appear to be reoriented. This later deformation is interpreted to be footwall deformation under the westward extension of the CP thrust system. The upper plate of the CP thrust does not crop out in the Calico Hills, but the style and orientation of this second folding event document its proximity and suggest that its orientation changes westward across the Calico Hills from NE-SW to E-W.

(4) Two thrust plates of Eleana Formation were emplaced eastward over the Chainman Shale along a sub-horizontal contact in the Eleana Range. The internally imbricated, structurally higher, Castle plate was emplaced <u>after</u> the structurally lower, internally coherent, Tongue Wash plate, demonstrating "out-of-sequence" thrusting. Non-cylindrical deformation at the northern edge of the Castle plate probably reflects a lateral ramp and suggests that the Castle plate did not extend farther north than it now occurs.

(5) The unnamed thrust separating the Eleana Formation from the Chainman Shale ramps upsection in the upper plate between the Calico Hills and the Eleana Range, supporting the interpretation that the Eleana Formation was emplaced eastward over the Chainman Shale.

(6) A NNW-striking left-lateral fault forms the eastern boundary of West Ridge in the southern Eleana Range. It has displaced part of a hanging-wall anticline in the Castle plate southward several km. It has a similar orientation and sense of motion to a fault exposed in Tongue Wash, to the north; these two faults may be genetically related.

(7) West-vergent folding in the Tippipah Limestone at the northeasternmost end of Syncline Ridge is thought to be footwall deformation under the CP thrust, and to suggest its proximity. Here, the west-verging deformation strikes almost due north, suggesting that the CP thrust too strikes north here, and underlies the west side of Yucca Flat.

(8) Chainman Shale and Tippipah Limestone underlie the west-verging CP thrust in the CP Hills (also at Syncline Ridge -- see above), indicating that they were originally deposited west of the rocks in the upper plate of this thrust. The upper plate is Cambrian rocks in the CP Hills; progressively younger Paleozoic rocks crop out in intermittent exposures to the northwest, ending in the Devonian carbonates and Mississippian ("transitional" Eleana) clastics at Mine Mountain. If these Paleozoic rocks are structurally continuous, the "transitional" Eleana of Mine Mountain and Shoshone Mountain would appear to be emplaced westward over the Chainman and Tippipah of the CP Hills and Syncline Ridge... and thus to have been formed to the east of them. This restoration is at odds with the apparent paleogeography based on sedimentary facies and lithology, in which the Mine Mountain section appears to have been deposited between the Eleana basin and the Chainman shelf/slope.

SOURCE ROCK COMPOSITION -- CHAINMAN SHALE FROM UE17e

During the 1994-1995 funding period, consultant Donna Herring completed a study of mudrock samples from the Chainman Shale in the UE17e core. Since only the mudrocks of the cored interval have source-rock potential, 58 mudrock samples were selected from the total of 170 samples collected; they were chosen to represent significant changes in mudrock lithology, and to sample thick zones of similar lithology at 40'-60' intervals. The UE17e drillhole is at the northwestern end of Syncline Ridge, a few tens of meters from the contact of the Chainman with the overlying Tippipah Limestone. The drillhole therefore starts in the uppermost part of the Chainman. Herring's conclusions are presented in full in Appendix 2, and are summarized briefly here:

(1) The majority of samples above 1500' depth are silt-free, while the majority of samples below are silty. Herring interprets this to be a primary depositional feature, representing a change in provenance or other sedimentologic condition.

(2) The entire section is characterized by gypsum and/or anhydrite, which Herring thinks is primary. As such, it indicates restricted circulation in the Chainman depositional basin.

(3) Dolomitic zones are thought to be primary depositional features, and may be useful for correlation.

(4) Smectite or interlayered illite/smectite is present in minor amounts throughout the core, and is concentrated in erratically occurring high-smectite zones that do not have any obvious relationship to other compositional variations. These observations are consistent with the source of the smectite being airborne volcanic ash.

(5) In spite of the presence of several compositional variables (silt, anhydrite, dolomite, smectite), no systematic repetitions were noted. This suggests that there is not large-scale structural repetition throughout the drillhole, and therefore that the Chainman mudstone section is at least 2000' thick in the vicinity of Syncline Ridge.

IMPLICATIONS FOR HYDROCARBON POTENTIAL

In this section, we briefly review our current understanding of source rock potential, maturation, reservoirs and traps. We conclude with a summary of areas of remaining uncertainty. We are beginning to know enough to take an "exploration" view of the problem: we now have some fairly good control on: (1) the presence and distribution of potential source rocks, and (2) the regional-scale structural control on thermal maturity. To a lesser extent, we have some ideas about the distribution of potential reservoir rocks, and the locations and styles of structures that could create traps. It is a very complex problem, but tractable.

Source

The Chainman Shale represents the most important potential source rock in the Paleozoic section. In the most complete Chainman section -- the UE17e core -- the Chainman contains organic-rich shales throughout the section. Gypsum, anhydrite and, locally, dolomite occur throughout the section, indicating restricted circulation in the Chainman basin -- conditions favorable to the preservation of organic material.

Our organic geochemical results from the Chainman are restricted to scattered surface samples plus the UE17e core from northern Syncline Ridge and the UE 25a-3 core from the Calico Hills. Unweathered core samples are preferable to surface samples for this purpose. TOC content in 27 samples from the UE17e core range from 0.8% to 1.8%, with only one sample below 1%. The original TOC content of these

rocks was almost certainly higher (see "Maturation", below). TOC content of 12 samples from the UE25a-3 core are in the same range (0.6% to 1.9%, with only one sample below 1%). (Note: All these data are presented in the 1994 annual report; we have no new TOC results this year.)

Our new mapping (particularly in the Calico Hills) has clarified the regional extent of the Chainman Shale -- it occurs across the width of the NTS, and extends an unknown distance farther to the west. The greatest thickness of carbonaceous shales (potential source rocks) occurs within the NTS; the Chainman appears to be thinning westward and to be changing composition eastward. At its westernmost surface exposure, an intact Chainman section underlies the Calico Hills. Here, it is deposited on slope facies carbonates and is structurally truncated above by an east-verging thrust fault. The UE25a-3 core from the Calico Hills contains a structural thickness of 700m of moderately-dipping Chainman section. The additional thickness represented by surface exposures is probably relatively small. Uppermost Mississippian dates from surface samples of the Chainman here indicate that we are seeing an almost complete Chainman section. At its easternmost surface exposure, in the Spotted Range, the Chainman is micrite and calcareous siltstone, with no carbonaceous shale, suggesting that most carbonaceous rock was deposited west of there. However, the upper part of the Chainman is structurally truncated in the Spotted Range, and upper Mississippian Chainman is carbonaceous shale in east-central Nevada. The depositional base of the Chainman spans the shelf-slope transition in the underlying Devonian carbonates between the western exposures in the Calico Hills and the eastern exposures in the Spotted Range.

Maturation

The thermal history of Paleozoic rocks at the NTS area is tied to their position in the thrust stack. Rocks in the upper plates of the major east- and west-verging thrusts are overmature, as are the rocks immediately underlying these thrusts. The lower plate to both thrust systems --cropping out between the east-verging thrusts under the Belted Range thrust and the west-verging CP thrust -- is the only zone of low conodont CAIs. This plate contains the Chainman Shale.

Maturation studies from the UE17e core in the Chainman at Syncline Ridge indicate that many of the samples have been heated past the best temperatures for oil production. However, there are scattered immature results, including some near the bottom of the core, which demonstrates that the heating recorded by the other samples is a local, not a regional, event. (These data are presented in our 1994 annual report; we have no new maturation data this year.) For the rocks that are "cooked" (many of which still have TOCs over 1%), the implication is that the rock generated something, and that the liquid hydrocarbons have been driven off. If this is the case, where did they go?

We have not attempted to constrain burial histories combining what we now know about thrust geometries and maximum temperatures reached (based on conodont CAIs) -- e.g., at Syncline Ridge, Mine Mountain, Calico Hills, drillhole data from the western side of Yucca Flat, etc. This would be a useful exercise, and might result in insights about the thrusting as well as about the burial histories.

Reservoirs

Many kinds of rocks, and many kinds of porosity, provide the reservoirs in Nevada's producing oil fields (see earlier annual reports). Most of these rock types and porosity types can also be found at the NTS. For example, potential reservoirs include (1) vesicles and fractures in Tertiary volcanic rocks, (2) solution porosity in carbonates (e.g., the karsted Guilmette at Shoshone Mtn or Mine Mtn), (3) primary porosity in carbonates or clastics, (4) fracture porosity in any competent rocks .

Traps

Many kinds of traps have been proposed for Nevada's producing fields (see earlier annual reports); most of these can be found at the NTS also. Notably, the recognition of low-angle thrusting in the Calico Hills -- placing the Devonian dolomite section and the overlying Eleana clastics over the Chainman Shale -- is an example of the kind of "thrust play" structure that has been proposed elsewhere in the state, but has not yet resulted in a producing field.

Summary: Remaining Areas of Uncertainty

(1) Tertiary source rocks: Tertiary sedimentary rocks that are rich in organic material occur locally, and could be hydrocarbon source rocks. These include sediments under northwestern Yucca Flat, sediments west of Yucca Mountain, and possibly the "rocks of Joshua Hollow" at the northeast edge of Bare Mountain.

(2) The westward extent of Chainman (past the Calico Hills) under volcanic cover -- structural question.

(3) The original geometry of Chainman basin (and therefore of organic-rich potential source rocks) -- this could be a stratigraphic problem (note the paradox of transitional sections apparently deposited east of the Chainman at Syncline Ridge) or a structural problem (note the possibility of an unrecognized fault between Syncline Ridge and Mine Mountain).

(4) Hydrocarbon generation history of Chainman source rocks -- if these rocks have generated hydrocarbons, where did they go?; how widespread was this generation? -- have all potential source rocks generated all that they can?

(5) Timing of thrusting: This will be important when calculating thermal maturity of potential source rocks in different structural positions -- both the depth of burial (which depends on the stratigraphic thickness of the overlying thrust sheet) and the length of time the source rocks were buried are important.

(6) Geometry of thrusting, continuity of individual structures, amount of slip on thrusts: These have important implications for calculations of source rock extent and volume, amount of tectonic burial, etc.

PUBLICATIONS

Trexler, J. H., Jr., Snyder, W. S., Schwarz, D., Kurka, M. T., & Crosbie, R. A. (1995). An overview of the Mississippian Chainman Shale. In M. W. Hansen, J. P. Walker, & J. H. Trexler, Jr. (Eds.), Mississippian Source Rocks in the Antler Basin of Nevada and Associated Structural Traps (pp. 45-60). Reno: Nevada Petroleum Society.

Trexler, James H., Jr., and Patricia H. Cashman, in review, A Southern Antler Submarine-Fan: the Mississippian Eleana Formation, Nevada Test Site: submitted to the Journal of Sedimentary Research

Trexler, James H., Jr., Patricia H. Cashman, and James C. Cole, in review, The Southern Antler Foreland Basin: Mississippian Stratigraphy on and near the Nevada Test Site: submitted to the American Association of Petroleum Geologists Bulletin

INVITED PRESENTATIONS

November 17: Cashman presented an invited lecture on our work at NTS at Brigham Young University (Provo, Utah)

July 20: Trexler gave an invited lecture on the Chainman Shale in an evening session associated with the AAPG field trip to eastern and central Nevada

MEETINGS/WORKSHOPS

October 23 - 27: Cashman and Trexler attended the Geological Society of America annual meeting in Seattle, WA

April 12: Cashman and Trexler attended the Nevada Petroleum Society meeting to hear AAPG Distinguished Lecturer Kenneth McClay, "3D Fault Systems in Rifts"

May 4: Trexler and students attended the Nevada Petroleum Society meeting to hear Tamra Schiappa speak on "Tectonic Implications of Ammonoid Biostratigraphy - Paleoecology within the Dry Mountain Trough"

May 2 - 5: Kurka visited Dr. Gary Webster in Pullman, WA, to review her conodont identifications and work with Webster's collection

June 19 - 23: Kurka visited Dr. Carl Rexroad in Bloomington, IN, to review her conodont identifications and work with Rexroad's collection

July 17 - 19: Cashman, Trexler, Kurka and students attended the AAPG Rocky Mountain Section meeting in Reno

July 20 - 23: Cashman, Trexler, Kurka and students; attended the AAPG field trip in central and eastern Nevada; Trexler was one of the leaders on the trip

FIELD WORK

November 8 - 13: Cashman, Trexler, Kurka and Taylor; mapping in the Calico Hills (Cashman), measured section and conodont sampling at Carbonate Wash (Trexler and Cashman), conodont sampling at Mine Mountain (Kurka and Taylor)

December 27 - 30: Cashman with Cole (USGS); mapping in the Calico Hills, one day looking at the ER-6-2 core from the CP Hills

March 24 - 26: Trexler, Kurka and Hookway; measured section and biostratigraphic sampling at Bare Mountain

March 27 - 29: Trexler and Cashman with Cole (USGS); stratigraphy and conodont sampling, Calico Hills and Spotted Range

March 30 - April 2: Cashman and Fontaine; mapping in the Calico Hills and southern Quartzite Ridge

May 3 - 8: Cashman; mapping and collection of structural data in the Calico Hills; one day looking at the UE25a-3 core from the Calico Hills with Cole (USGS)

May 21 - 24: Cashman and Hookway; mapping and collection of structural data in the Calico Hills and North Syncline Ridge

May 31 - June 5: Trexler and Kurka, with Cole (USGS), Snyder (Boise State University) and Ritter (Brigham Young University); measuring a section and collecting

biostratigraphic samples in the Spotted Range; collecting biostratigraphic samples in the Devonian/Mississippian section at Bare Mountain and the Calico Hills, collecting biostratigraphic samples in the Mississippian/Permian section at Syncline Ridge and the CP Hills

June 18 - 22: Cashman with Cole (USGS); mapping and collection of structural data in the southern Eleana Range

August 24 - 25: Trexler with Cole (USGS); stratigraphic description and biostratigraphic sampling in the Bullfrog Hills and Bare Mountain

Figure Captions

Figure 1: Correlation diagram showing the Eleana Formation and stratigraphic equivalents in Nevada; includes new measured sections at Bare Mountain, the Spotted Range, and the base of the Eleana Formation at Carbonate Wash. Figure from Trexler and Cashman, in review.

Figure 2: Simplified measured sections in the Tongue Wash and Castle structural plates of the Eleana Formation in the Eleana Range, and of the Eleana Formation at Bare Mountain. Figure from Trexler and Cashman, in review.

Figure 3: Measured section from Carbonate Wash.

Figure 4: Measured section from Bare Mountain.

Figure 5: Measured section from the Spotted Range.

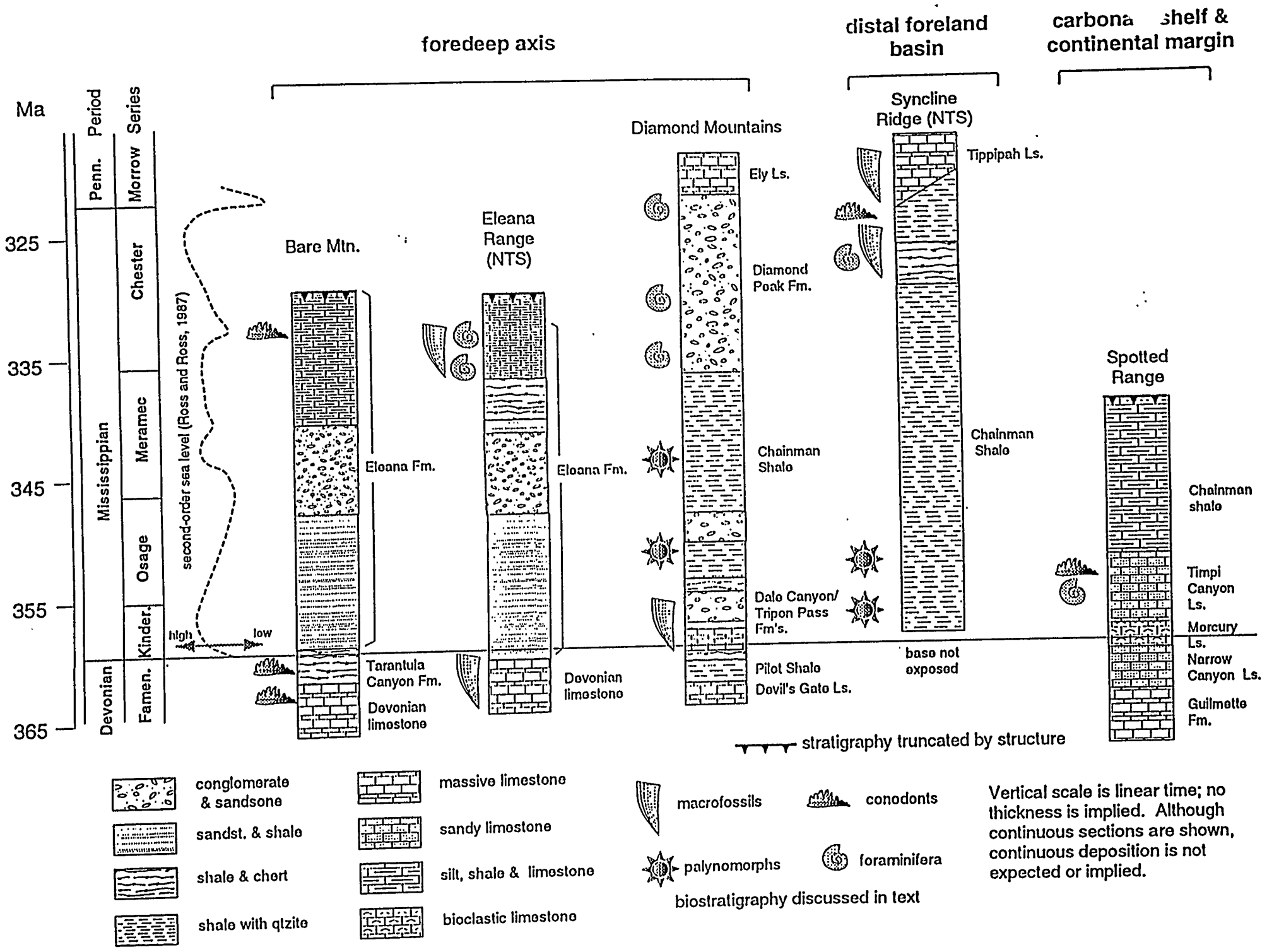
foredeep axis
distal foreland basin
carbona shelf & continental margin
Ma
Period
Series
Penn.
Morrow
Chester
Meramec
Osage
Kinder.
Famen.
Mississippian
Devonian
325
335
345
355
365
second-order sea level (Ross and Ross, 1987)
high
low
Bare Mtn.
Eleana Range (NTS)
Diamond Mountains
Syncline Ridge (NTS)
Spotted Range
Eleana Fm.
Eleana Fm.
Tarantula Canyon Fm.
Devonian limestone
Devonian limestone
Ely Ls.
Diamond Peak Fm.
Chainman Shale
Dale Canyon/ Tripon Pass Fm's.
Pilot Shale
Devil's Gate Ls.
Tippipah Ls.
Chainman Shale
base not exposed
Chainman shale
Timpi Canyon Ls.
Mercury Ls.
Narrow Canyon Ls.
Guilmette Fm.
stratigraphy truncated by structure
conglomerate & sandsone
sandst. & shale
shale & chert
shale with qtzite
massive limestone
sandy limestone
silt, shale & limestone
bioclastic limestone
macrofossils
conodonts
palynomorphs
foraminifera
biostratigraphy discussed in text
Vertical scale is linear time; no thickness is implied. Although continuous sections are shown, continuous deposition is not expected or implied.

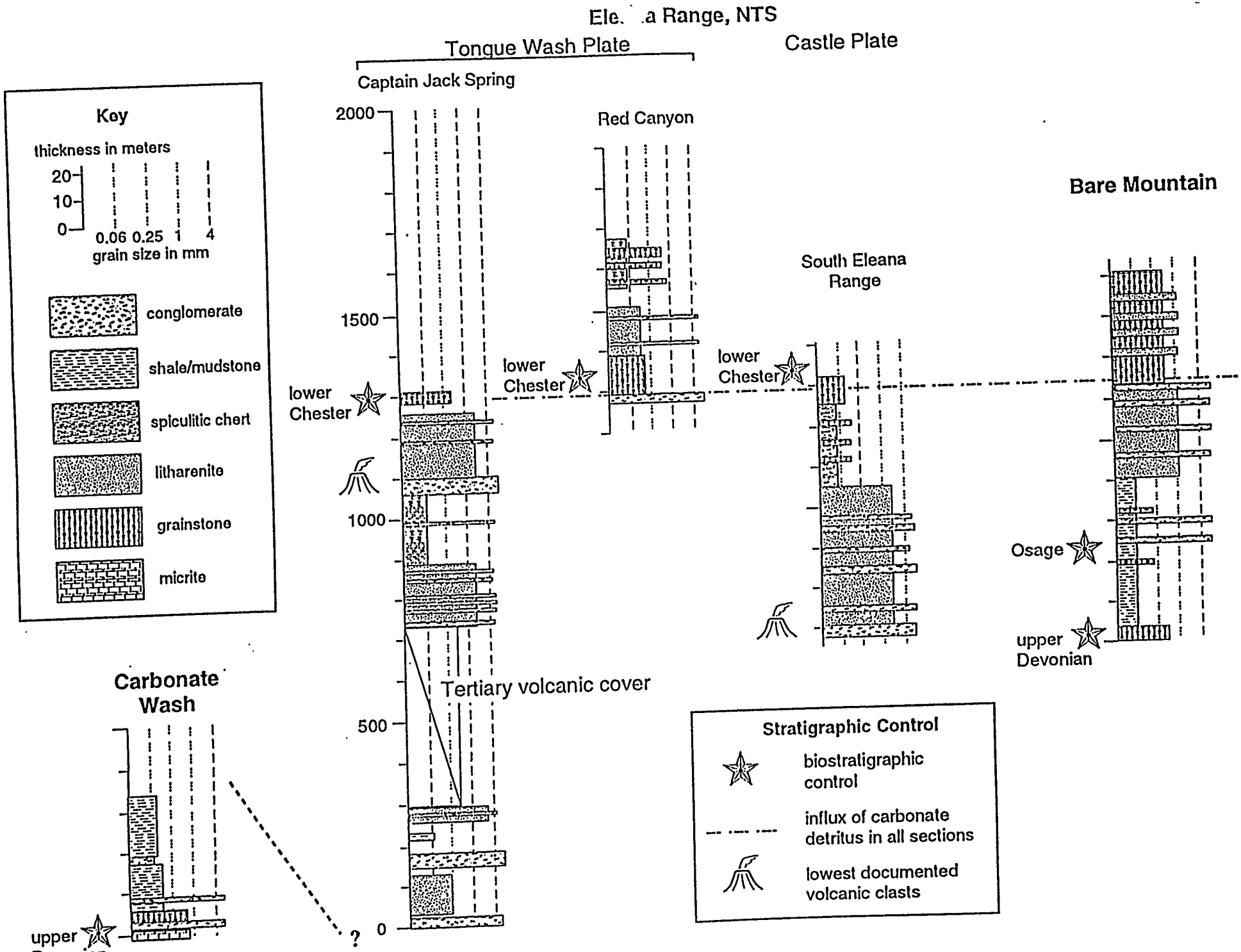
Ele. .a Range, NTS
Tongue Wash Plate
Castle Plate
Captain Jack Spring
Red Canyon
Bare Mountain
South Eleana Range
Key
thickness in meters
20
10
0
0.06 0.25 1 4
grain size in mm
conglomerate
shale/mudstone
spiculitic chert
litharenite
grainstone
micrite
2000
1500
1000
500
0
lower Chester
lower Chester
lower Chester
Osage
upper Devonian
Carbonate Wash
upper Devonian
?
Tertiary volcanic cover
Stratigraphic Control
biostratigraphic control
influx of carbonate detritus in all sections
lowest documented volcanic clasts

dmg/5-22-93

Location Carbonate Wash Oak Spgs Butte 7½

Name Carbonate Wash

Date 11/11/94 Initials JT; PHC

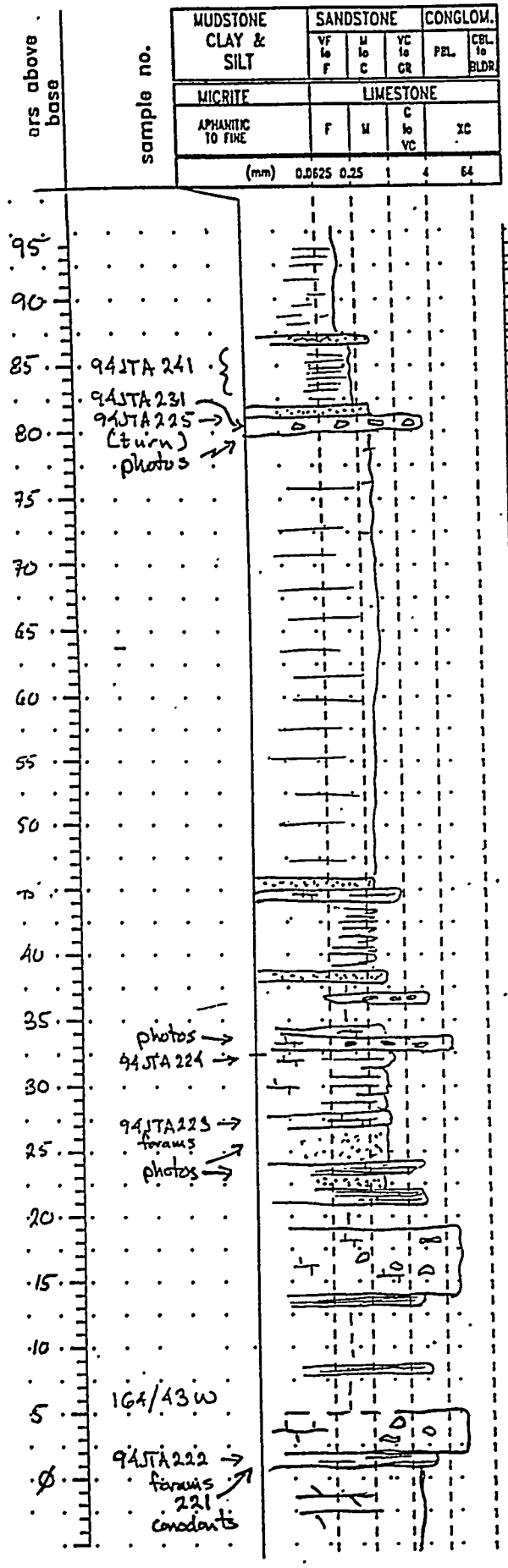

orange/yellow siltstone

qtzite

laminated siliz grainstone, poss. chert grains too

qtzite carb clast breccia, v. coarse ↖? (offset section south)

poorly exposed:
slabby grainstone & qtzite interbeds, yellow to orange
laminated planar bedding, some is very siliceous

laminated grainstone ↖?

slabby wx carb & sand, planar laminated

qtzite (breccia)

coarse carb breccia

lamin coarse carb & thin breccias

lamin grainstone

qtzite - v. clean, no bedding, burrows

massive, vitreous qtzite, med grain wvrd, clean & prob. burrowed

lamin qtz ss & grainstone

carb clast breccia; soft sed def., ls clasts are intraclasts

lamin siltst. & grainstone

lamin carb & siltstone

carb. clast breccia, ls clasts up to 30 cm+, corals & brachs

lamin. grainstone &/ wackestone ← dol/ls bdry (base of "A")

coarse, xtline dolomite

Interp Notes:
- high energy & steep? All upper flow regime & slump debris flows

dmg/5-22-93

Location Carbonate Wash Oak Spgs Butte 7½'

Name Carbonate Wash

Date 11/11/94 Initials JT / PHC

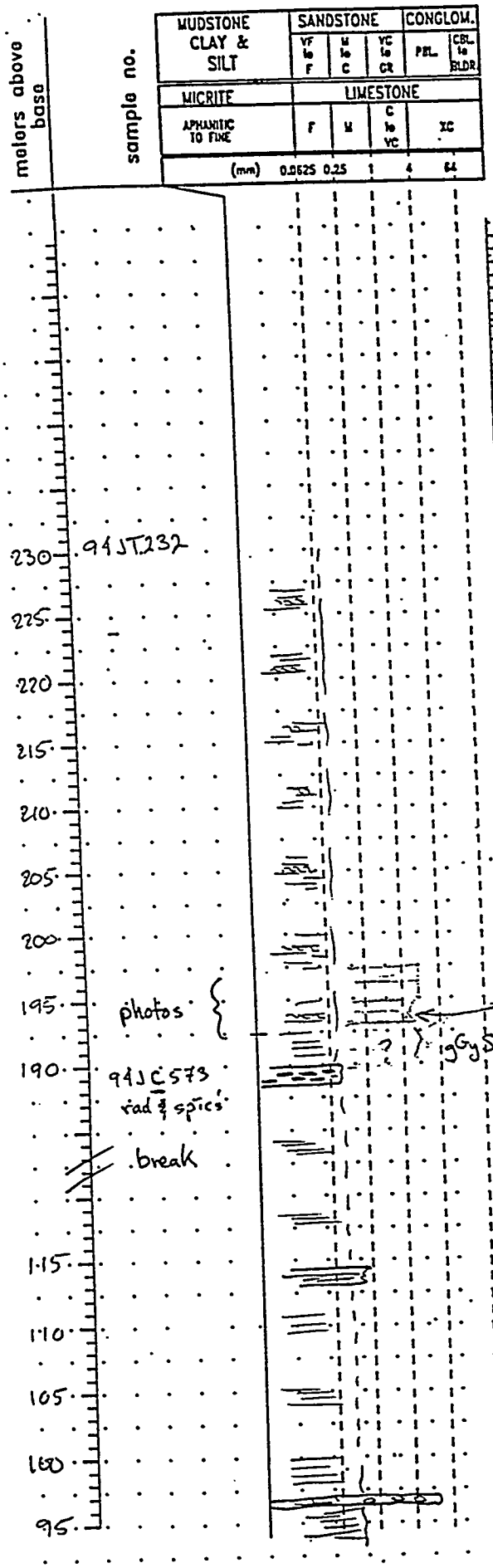

End for now in talus cover

thin qtzites (rare)

flaggy yellow / tan siltstone, mostly covered
ripple lamin dominates – climbing ripples and convolute beds
= abundant sed ↓ in stable slope but more stable than below

20 m to south of section (blue) ~ 2 m of lithic cgl & litharenite as amalg. turbidites ÷ channel fill ? pinches out laterally
* lowest chert lith seds.

thinly bedded chert & cherty argillite

occas. small outcrop yellow to pale rose siltstone

← rare exposure
poor exposure – laminate siltstone, yellow wx, slabby, not calcareous

carb clast breccia, thin; 7-10 cm rip-ups

Fig 4

Location Tarantula Canyon, Bare Mtn

Name Tarantula Canyon Section

Date 3/25/95 Initials JT

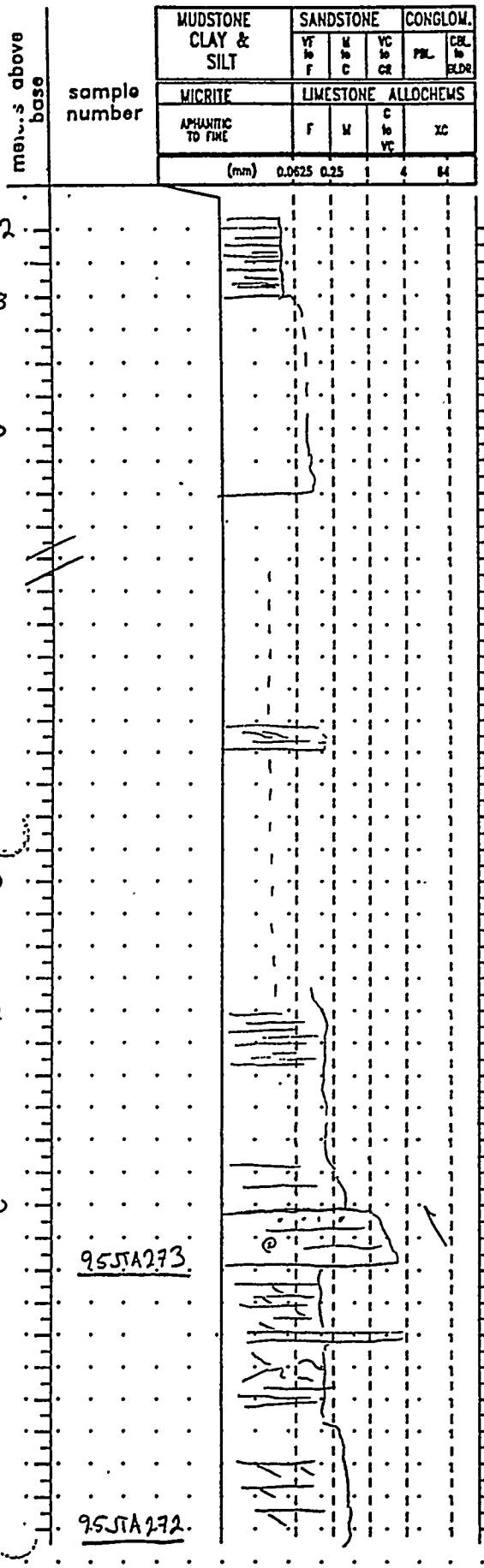

3-5 cm beds
chert/argillite, black w/ rusty wx surfaces

* Snyder: orig. section much lower, silicified now

Lite gray siltic. mudst & siltstone

cover

red clayey siltstone, v. poor exposure

lavender gray siltstone, slightly calcareous

† see notes: 95JTA360.

covered

laminated purple & gray dolomite

more laminated upward

silty dolomite

vc grainstone w/ rugose corals, brachs; well bedded

lamin. dolomite, red & gray (hematite?). Lime. upward

coarse: fossil hash

slumped

} incipient brecciation and rip-ups, scarce of breccias.

Dolomite, laminated & some slumping, graded beds

Location Baine Mtns

Name Tarantula Canyon

Date 3/25 Initials

meters above base	sample number	MUDSTONE CLAY & SILT	SANDSTONE VF to F	SANDSTONE M to C	SANDSTONE VC to CR	CONGLOM. PEBL	CONGLOM. CBL to BLDR	Sedimentary Structures/ Taxa/ Notes
		MICRITE	LIMESTONE F	LIMESTONE M	LIMESTONE C to VC	LIMESTONE ALLOCHEMS XC		
		APHANITIC TO FINE						
		(mm)	0.0625	0.25	1	4	64	

192

laminated purple siltstone

purple siltstone

180 — 95JTA 281

calcareous siltstone / silty limestone sampled for conodonts

160

more silt & fine sand in lamin. beds, thin & well bedded w/ argillite / chert, dark gray w/ rusty wx

influx of fine sand as thin beds: < 1 cm interval w/ chert

140

black, well bedded chert & argillite + silicified silty micrite (Snyder)

120

prominent rib

95JTA274

sampled for rads. / spicules

"ribbon" chert

Location Bare Mtn

Name Tarantula Canyon

Date 3/25 Initials JT

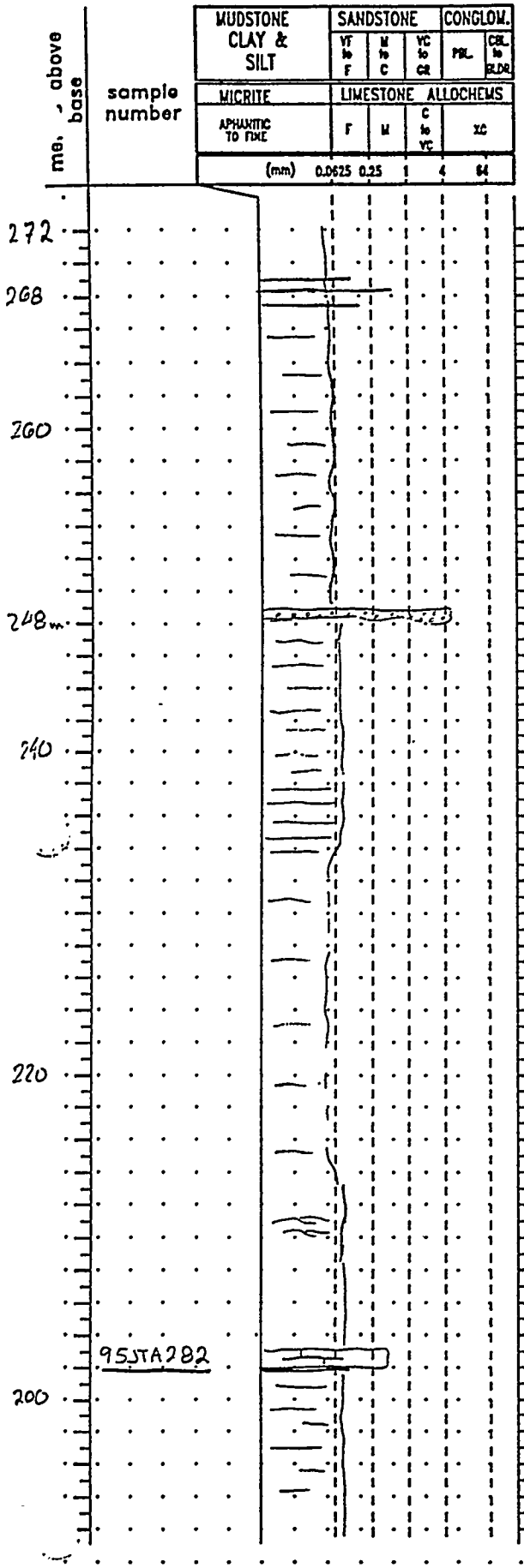

Location Baro Mtn

Name Tarantula Canyon

Date 3/25/95 Initials JT

meters above base

sample number

MUDSTONE CLAY & SILT	SANDSTONE VF to F	SANDSTONE M to C	SANDSTONE VC to GR	CONGLOM. PEBL	CONGLOM. CBL to BLDR
MICRITE	LIMESTONE ALLOCHEMS				
APHANITIC TO FINE	F	M	C to VC	XC	
(mm) 0.0625	0.25	1	4	64	

Sedimentary Structures/ Taxa/ Notes

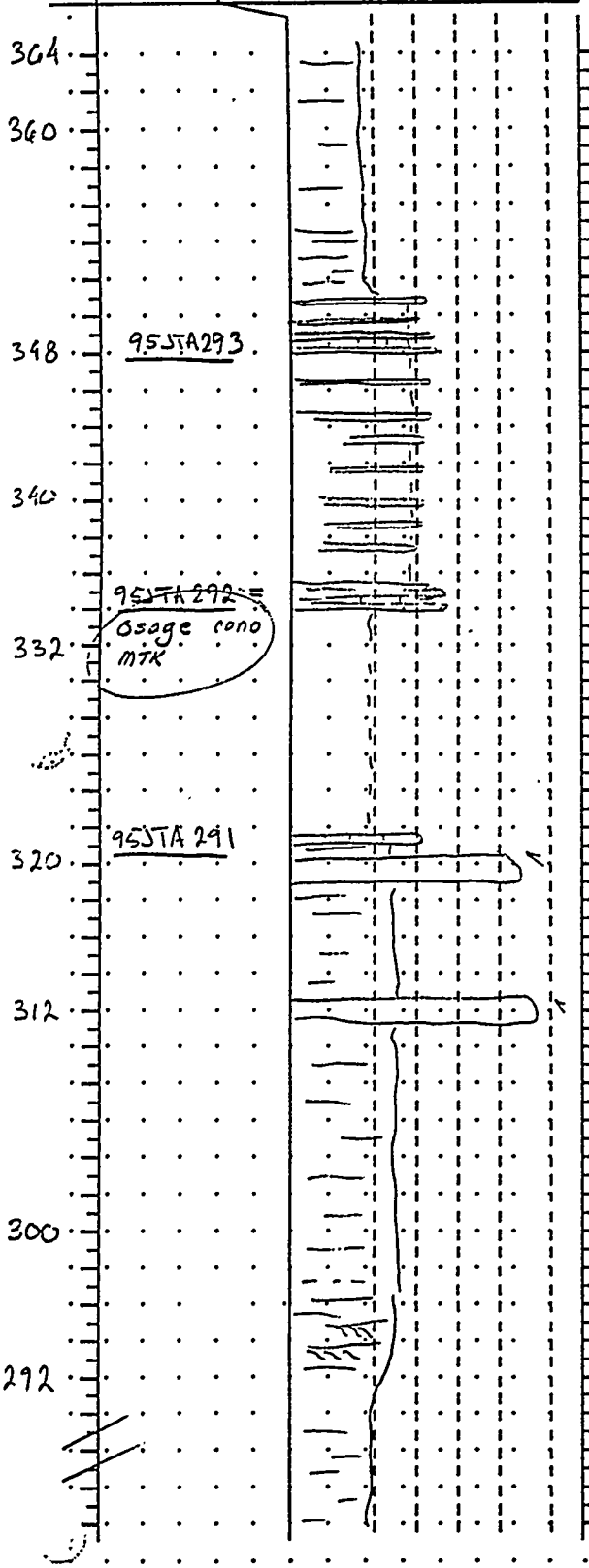

mostly cover

gray siltstone

↑ conodont sample

cont section of calc grainstone & silic interbeds

↓

interbeds of calc grit & silic siltstone conodont sample
± qtz sandstone beds, wrd, wsrt, clean qtzite

cover

grainstone, orange wx; interbeds of silt & ss { sample for conodonts
gradid chert-lithic cgl to arenite
well bedded ss & siltstone

chert-lithic cgl w/ large ripups of siltstone
chert is bleached

laminated fine sand & silt

sandier, w/ ripple & convolute laminae

siltstone

Location Bare Mtn

Name Tarantula Canyon

Date 3/25/95 Initials JT

meters above base	sample number	MUDSTONE CLAY & SILT	SANDSTONE VF to F	SANDSTONE M to C	SANDSTONE VC to GR	CONGLOM. PEBL	CONGLOM. CBL to BLDR	Sedimentary Structures/ Taxa/ Notes
		MICRITE	LIMESTONE F	LIMESTONE M	LIMESTONE C to VC	ALLOCHEMS XC		
		APHANITIC TO FINE						
		(mm)	0.0625	0.25	1	4	64	

464

460

interval of cgl turbs

3-5 cm. clasts

440 95JTA301

grainstone - sample for conodonts

cover

cgl interval - clean silic. cgl, mostly grit to 3 cm clasts, poorly bedded, poorly sorted

v. large (5-7 cm) mudst rip-ups

ridge top 4450' →

420 2-5 cm clasts

coarsening-up sequence

cgl - <5m thick turbidites, pea-gravel at base

qtzite - clean, med gr wkd & worted

cover

lithic cgl (turbidites) clasts < 1 cm

400

silty & sandier

396

394

siltstone & argillite, well bedded

Location Bare Mtn

Name Tarantula Canyon

Date 3/25/05 Initials JT

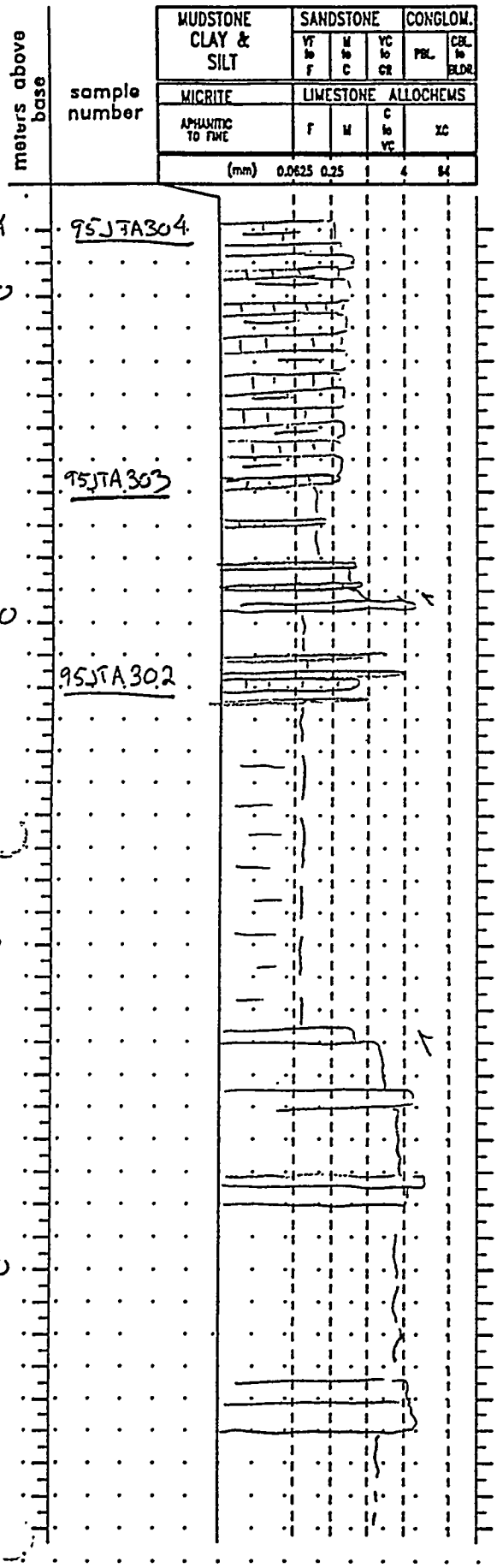

meters above base	sample number	MUDSTONE CLAY & SILT / MICRITE APHANITIC TO FINE	SANDSTONE VF to F / M to C / VC to GR; LIMESTONE ALLOCHEMS F / M / C to VC	CONGLOM. PBL / CBL to BLDR; XC	Sedimentary Structures/ Taxa/ Notes
		(mm)	0.0625 0.25 1	4 64	

Location Bare Mtn

Name Tarantula Canyon

Date 3/26 Initials JT

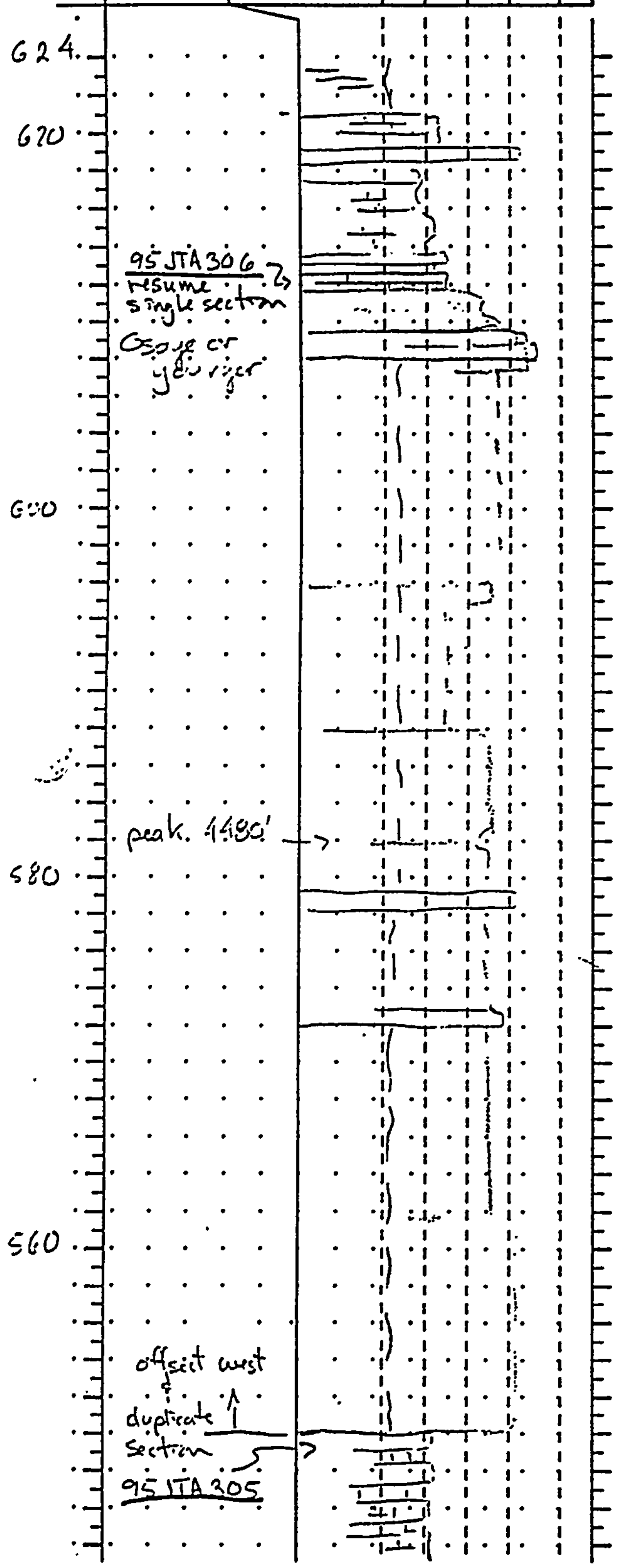

lite gray siltstone

interbedded ls & litharenite

grainstone – conodont sample

v coarse cgl w/ siltstone rip-ups (offset on ridge).

blue: v. coarse & v. poorly exposed

siltstone & fine ss rubble

{ sections lack carbonate }

blue: coarse cgl rubble

lithic grit

Note: much coarser section on strike ... implies rapid lateral facies changes & channel-domin syst

rubble – lithic grit & arenite

blue: coarse litharenite & cgl in rubble

mostly cover

blue: cgl, lamin. litharenite – poor exposure

gray-white siltstone, siliceous alteration. ↑ doubled section in blue

potential conodont sample

calc/sil beds cont.

Location Bare Mtn

Name Tarantula Canyon

Date 3/20/95 Initials JT

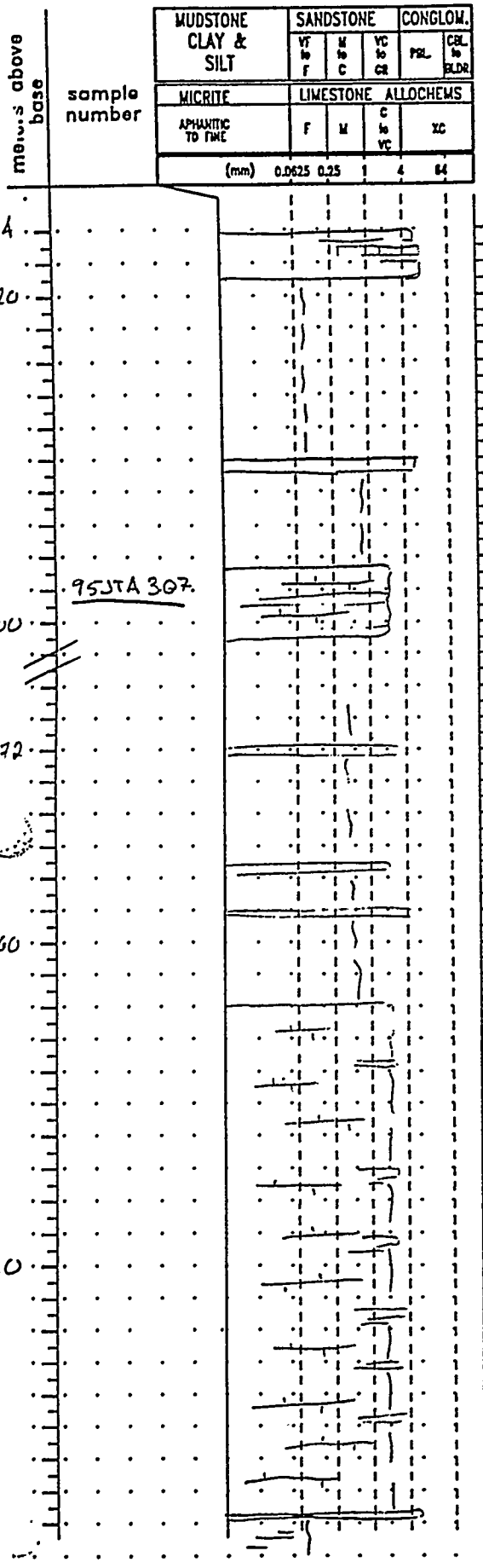

Sedimentary Structures/ Taxa/ Notes

interval of grainstone/grit beds

Lite tan siltstone

conodonts sample

interbedded grainstone & grits

rubble & cover

lacks carbonate

siliceous mudstone, litharenite & grit

mixed/interbedded calc-silicate grits & grainstones 20-50 cm beds, grainstones laminated

Location Bare Mtn

Name Tarantula Canyon

Date 3/26 Initials JT

meters above base	sample number	MUDSTONE CLAY & SILT	SANDSTONE VF to F	SANDSTONE M to C	SANDSTONE VC to GR	CONGLOM. PEBL	CONGLOM. CBL to BLDR	Sedimentary Structures/ Taxa/ Notes
		MICRITE	LIMESTONE ALLOCHEMS					
		APHANITIC TO FINE	F	M	C to VC	XC		
		(mm)	0.0625	0.25	1	4	64	

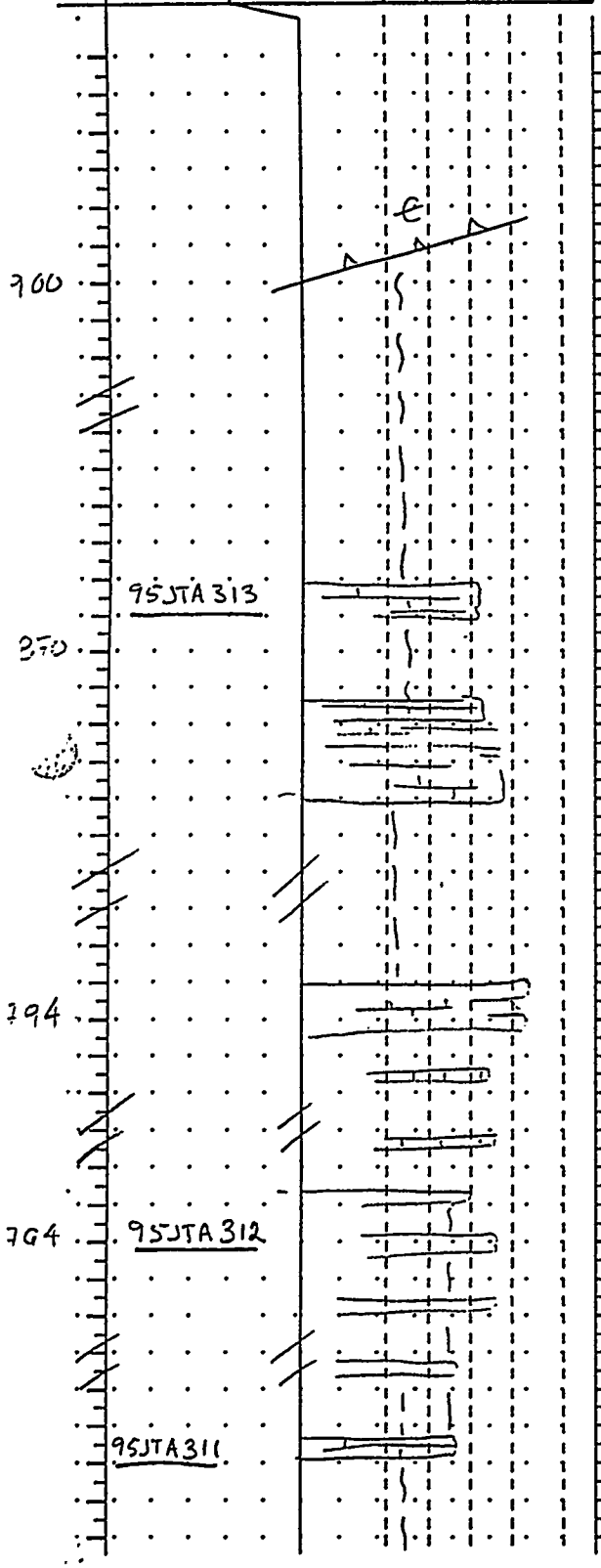

700

cover & talus

cover & talus

95JTA313 conodont sample

370

silic. mudrx

grainstone & silic. muddy interbeds

lithe gray siltstone & siliceous mudrx, litharenites (rubble)

coarse grit, several grainstones

794

lite gray siltstone w/ occ grainstone, tan-orange litharenite

764 95JTA312 v. coarse, gritty grainstone – conodont sample

interbeds grainstone & grit.

95JTA311 grainstone – conodont sample

Tarantula Canyon area (1.4X 1:24,000) 40' contours

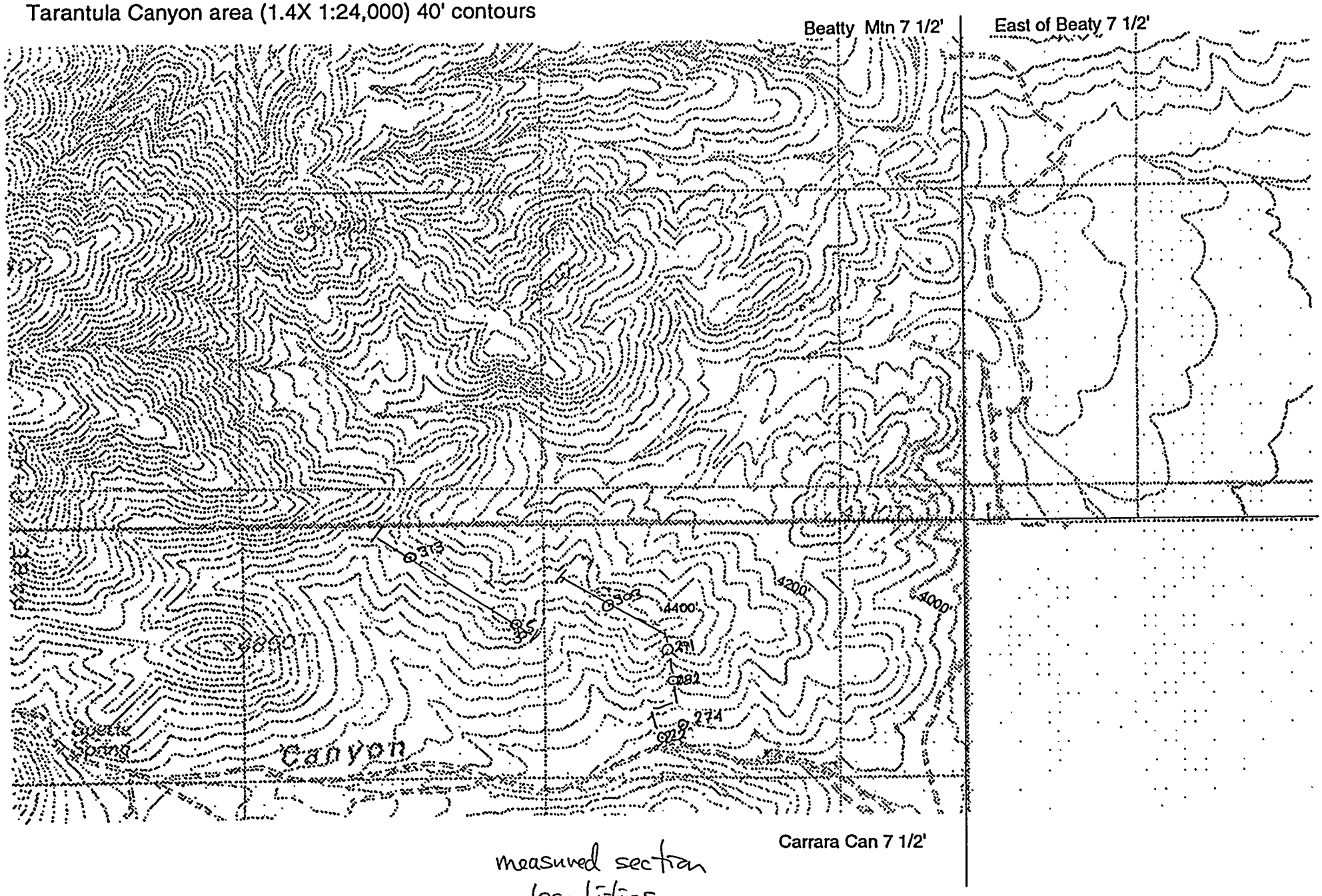

measured section localities

dmg/5-22-93

Location Spotted Range, Mercury Quad

Name Tinpi Canyon Section

Date 6/2/95 Initials JT/WS/JC

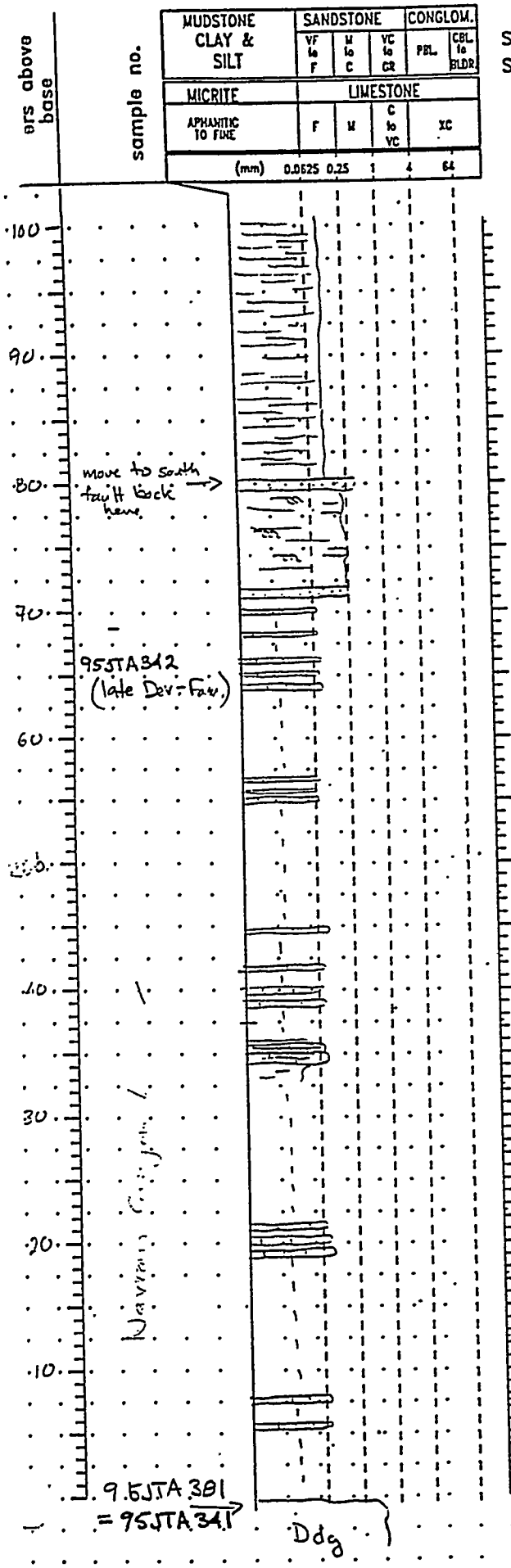

somewhat anoxic - note lack of burrows & fossils

2nd replacement of micrite makes "fake" qtzite beds

Distinctive flaggy silty ls., orange wx

silty micrite & micritic siltstone, flaggy & orange wx, thin sandy beds
less bioturb, no macrofossils

- some "scolithos" burrows, wvd, invert

well-bedded qtzite-dominated interval, ripple lamin & burrows

qtzite - fine grained, highly bioturbed, may have been calcareous, ripple lam?

silty ls w/ fossil debris (brachs, gastros etc.)

limonite on bedding planes * = sample for conodonts

less silty ledges

ledges of less silty ls.

intensly bioturbated wackestone
↓ silt

less silty beds crop out, silty beds dominate cover

less silty ledges of micrite / wackestone

background - limey siltstone
scm beds silty wackestone, highly bioturbated* - a distinctive feature

fine gr. dark micrite in gully. Mapped Devil's Gate

Ø - 80 m measured in northern fault block & then checked & repeated in next block south. When 341 & 342 were collected, it was not recognized that 341 was actually uppermost Devil's Gate;

dmg/5-22-93

Location Spotted Range, Mercury Quad.
Name Timpi Canyon Section
Date 6/2/95 Initials JT/WS/JC
Page 2 of 4

MUDSTONE CLAY & SILT	SANDSTONE VF to F	SANDSTONE M to C	SANDSTONE VC to GR	CONGLOM. PEBL	CONGLOM. CBL to BLDR
MICRITE	LIMESTONE				
APHANITIC TO FINE	F	M	C to VC	XC	
(mm)	0.0625	0.25	1	4	64

ors above base | sample no. | Sedimentary Structures/ Taxa

200
190
180
170
160
150
140
130
120
110

re-locate exist along fin →
Mercury Ls
Narrow Canyon Ls
talus
talus
95JTA351 → conodonts

crinoidal grainstone beds

abundant horn & colonial corals, silicified

cross-beds in coarser beds, muddy beds are bioturbated
mud-dominated section

chert nodules as stringers

– bedding attitudes variable –

graded wackest to packstone intervals 10-15cm tempestites

fine to med grain wackestone & packstone, horn corals
variable & irreg bedding, some laminination

(colonial corals)

irreg bedded Ls

bioclastic grainstone

↑ Upper Narrow Canyon Ls. is transitional to Mercury Ls

fine grain wackestone / packstone in prom. ridge

micrite & wackestone, occ. grainstone, silty intervals

grainstones & wackestones

(ridge flank) abundant burrows in muddier / silt. beds

bioclastic grainst. 2-8cm beds, coarse debris, grain-size sorted, reworked

(ridge crest) transition to ↑ more bioclastic beds

laminated silty micrite w/ occ bioclastic grain-packstone

dmg/5-22-93

Location Spotted Range, Mercury Quad

Name Timp. Canyon Section

Date 6/2/95 Initials JT/WS/JC

MUDSTONE CLAY & SILT	SANDSTONE VF to F	SANDSTONE M to C	SANDSTONE VC to GR	CONGLOM. PEB.	CONGLOM. CBL. to BLDR
MICRITE	LIMESTONE				
APHANITIC TO FINE	F	M	C to VC	XC	
(mm)	0.0625	0.25	1	4	64

ers above base | sample no. | Sedimentary Structures/ Taxa

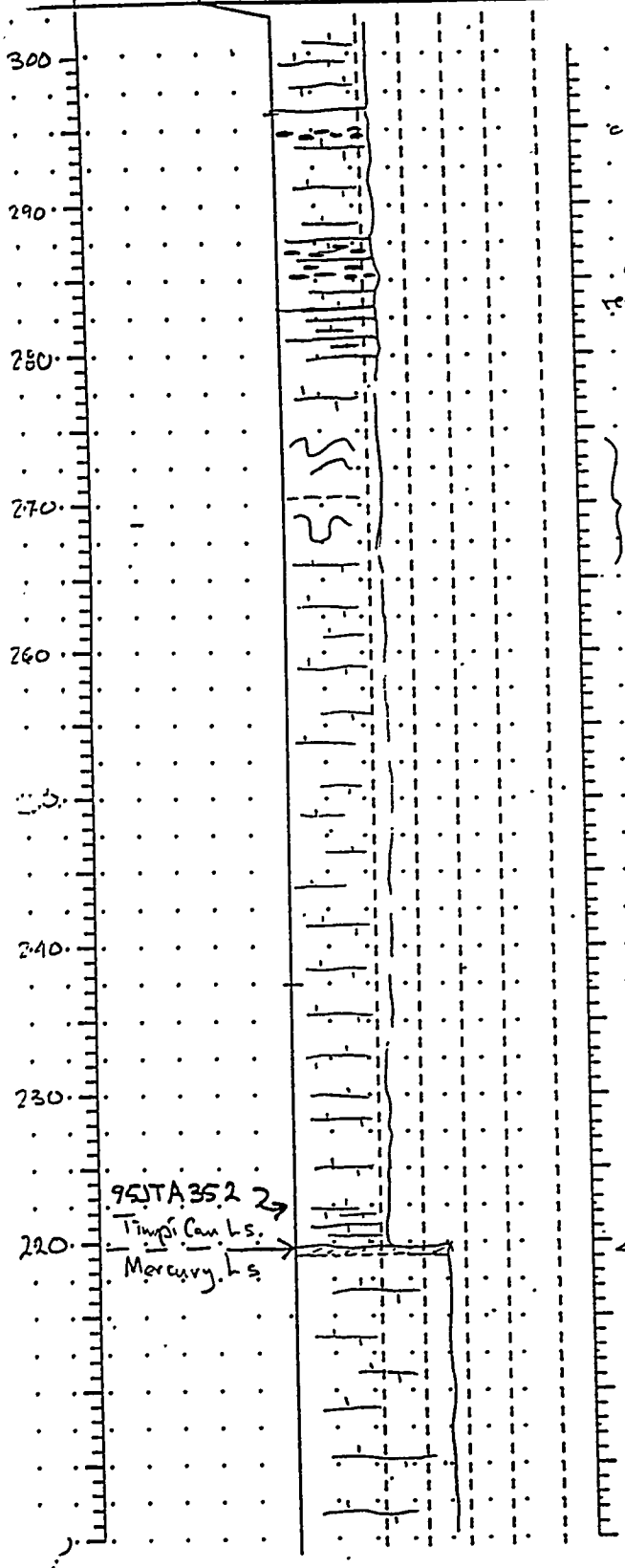

chert nodule zone

chert nodule horiz

resistant, small cliff former has thinner & fewer silt beds

less silt in ledgy, massive micrite beds

structurally crumpled & thickened slightly

30-50 cm beds

silt intervals become somewhat thicker & more common

Distinctive "stair-step" outcrop pattern

thin silty intervals make bed-breaks

ledgy micrite & muddy wackestone, bioturbated, occ black

* abrupt transition to micrite block (fresh) & lite gray (wx), recessive ledgys

interp: lowstand, subaerial exposure

oxidized / leached zone, silicified, iron oxide, grades down to unaltered l.s
30 cm altered zone

thick bedded grainstone / packstone, macrofossil incl. corals

> 90 grainstone beds

Outcrops as massive cliffs

dmg/5-22-93

Location Spotted Range Mercury Quad

Name Timpi Canyon Section

Date 6/2/95 Initials JT | WS | JC

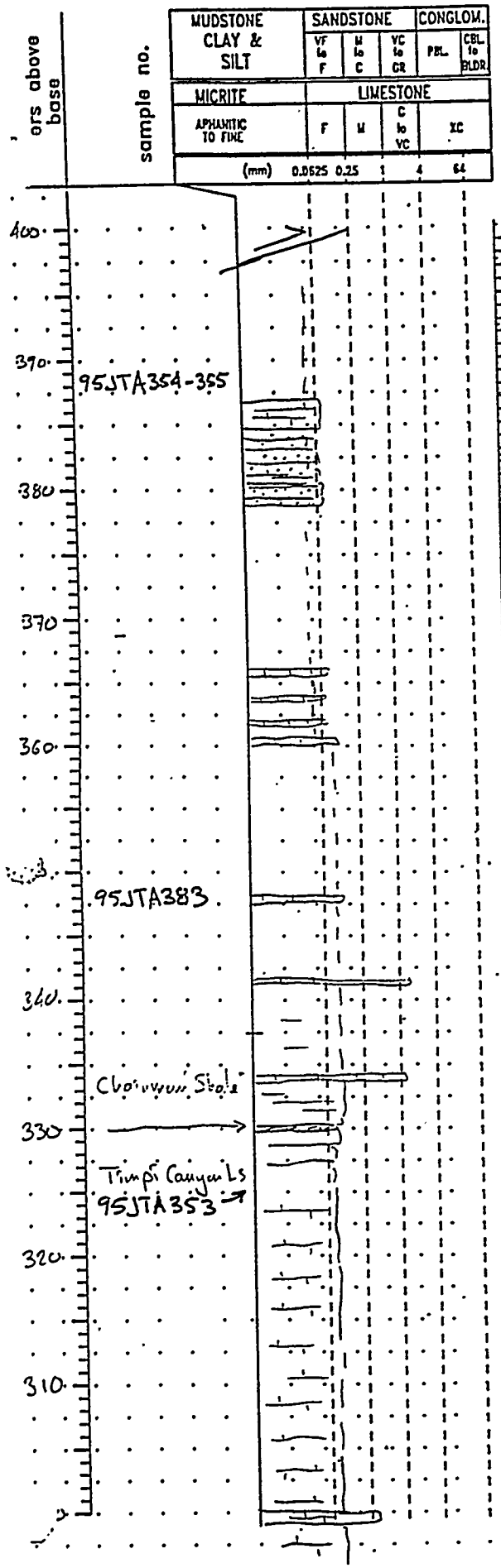

Mira Teru Kurka
Department of Geological Sciences
University of Nevada, Reno
Reno, NV 89557

27 September 1995

SUMMARY OF CONODONT BIOSTRATIGRAPHY FOR THE NEVADA TEST SITE

October 1994 - October 1995

The following samples have been processed and analyzed for conodont biostratigraphy. Samples followed by asterisks have been processed to completion: 1) acid digestion of rocks, 2) heavy liquid separation of residue, 3) picking and identifying conodonts from heavy residue, and 4) biostratigraphic analysis.

Shoshone Mountain	sample
	94JTA123 *
	94JTA126B *
Mine Mountain	94JTA143 *
	94JTA146 *
Carbonate Wash	94JTA221
	94JTA222 *
	94JC575 *
Bare Mountain (Tarantula Canyon)	95JTA271
	95JTA272
	95JTA273
	95JTA281
	95JTA282
	95JTA291 *
	95JTA292 *
	95JTA293
	95JTA301
	95JTA302
	95JTA303
	95JTA304
95JTA311	95JTA305
95JTA312	95JTA306 *
95JTA313	95JTA307

Calico Hills	sample
	JC10678 *
	JC10601 *
	95JC718 *
	94PC2182 *
	94PC2153 *
	94PC2154 *
	JC10757
	JC10638
	JC10623 *
	95JC848
	JC10612 *
	JC10612B *
Spotted Range	95JTA341
	95JTA342 *
	95JTA351
	95JTA352
	95JTA353 *
	95JTA354
	95JTA355
	95JTA383
South Syncline Ridge	95JTA391
CP Hills	95JTA462
	95JTA463

Mira Teru Kurka

sample number	94JTA123
rock type	limestone
purpose	paleo
storage	conodont slide in LMR358; residue dumped.
map locality	
descriptive locality	Shoshone Mtn: (NTS), measured section at 46m
strat unit	"Ml" on GQ-746, overlies Guilmette; Miss. Joana (?)
outcrop description	lowest sandy limestone above the Guilmette; common shell fragments
process	for conodonts
results	Mississippian; Kinderhookian; lower *crenulata* through isosticha-upper *crenulata* zones. *Gnathodus delicatus?, Gn. punctatus, Siphonodella istosticha, Palmatolepis* sp. * may be reworked. MTK (5/19/95); Webster (5/95); Rexroad (6/95) Skipp (6/95): no call

sample number	94JTA126B
rock type	limestone
purpose	paleo
storage	conodont slide in LMR358; residue dumped.
map locality	
descriptive locality	Shoshone Mtn: (NTS)
strat unit	Miss. Joana (?)
outcrop description	
process	for conodonts
results	Mississippian; Kinderhookian; isosticha-upper *crenulata* zone: *Polygnathus communis communis, Siphonodella obsoleta, Gnathodus typicus (M1), Gn. simplicatus?, Gn. punctatus, Hindeodus crassidentatus. Palmatolepis gracilis sigmoidalis, Pa. gracilis subsp., Pa. perlobata** may be reworked.

sample number	94JTA143
rock type	limestone
purpose	paleo
storage	conodont slide in LMR 358; residue dumped.
map locality	
descriptive locality	Mine Mountain: (NTS); Mine Mountain Pass measured section at 830m above the top of the Guilmette
strat unit	Miss. Eleana Fm.
outcrop description	calcareous turbidite; sandy limestone, chert and quartz clasts
process	for conodonts
results	Mississippian; late Osagean; *mehli* - lower *texanus* zone. *Gnathodus texanus, Polygnathus nodomarginata* MTK (5/19/95) ; Rexroad (6/95) Skipp (6/95): no call, no obvious biota CAI = 2 (A. Harris. 2/8/95)

sample number	94JTA146
rock type	bioclastic limestone;mixed calc./silic. turbidite
purpose	paleo, conodonts and forams
storage	conodont slide in LMR 358; residue dumped.
map locality	
descriptive locality	Mine Mountain: (NTS); Mine Mountain Pass measured section at 1015m above the Guilmette
strat unit	Miss. Eleana Fm.
outcrop description	calcareous turbidite
process	processed to completion
results	Mississippian; late Meramecian-Chesterian; lower *Cavusgnathus* through *muricatus* zones. *Lochreia commutatus, Gnathodus girtyi?* MTK (5/19/95); Webster (5/95) Skipp (6/95): no call; silicified pelmatazoan-bryozoan algal wackestone/packstone, medium to coarse-grained. radiolarian algae

sample number	94JTA221
rock type	limestone
purpose	paleo, conodonts
storage	
map locality	Oak Springs Butte 7 1/2'
descriptive locality	Carbonate Wash (NTS), measured section, 0m
strat unit	basal Eleana Fm. (?)
outcrop description	lowest carbonate breccia unit, arbitrary base of measured section
process	
results	in process

sample number	94JTA222
rock type	limestone
purpose	paleo, conodonts
storage	split processed;
map locality	Oak Springs Butte 7 1/2'
descriptive locality	Carbonate Wash (NTS), measured section
strat unit	basal Eleana Fm. (?)
outcrop description	lowest carbonate breccia unit, just below arbitrary base of measured section
process	split processed; separated
results	*BARREN* of conodonts

sample number	94JC575
rock type	limestone
purpose	conodonts
storage	1 vial to pick in LMR358
map locality	
descriptive locality	Carbonate Wash (NTS); Oak Springs Butte
strat unit	
outcrop description	
process	separated in part 8-4-95
results	*BARREN* of conodonts

sample number	95JTA271
rock type	limestone breccia
purpose	paleo, conodonts
storage	split processed; remaining sample in 355A LMR; residue to be separated
map locality	Carrara Canyon 7 1/2', T12S, R48E, unsurveyed; Monsen et al, 1992, Geol map
descriptive locality	Bare Mtn, Tarantula Canyon, offset from base of measured section, (NTS)
strat unit	Dtc, "Rocks of Tarantula Canyon, Devonian"
outcrop description	Prominent breccia along the road at the base of the Eleana section, = 94JTA 61
process	split processed for conodonts
results	in process

sample number	95JTA272
rock type	dolomite
purpose	paleo, conodonts
storage	split processed (355A LMR); 2 bags residue; 3 vials to pick.
map locality	Carrara Canyon 7 1/2', T12S, R48E, unsurveyed; Monsen et al, 1992, Geol map
descriptive locality	Bare Mtn, Tarantula Canyon, measured section, 0m, (NTS)
strat unit	Dtc, "Rocks of Tarantula Canyon, Devonian"
outcrop description	Thinly bedded / laminated dolomite with intraclasts
process	split process for conodonts.
results	in process

sample number	95JTA273
rock type	dolomite
purpose	paleo, conodonts
storage	split processed (355A LMR); 2 bags residue; 10 vials to pick.
map locality	Carrara Canyon 7 1/2', T12S, R48E, unsurveyed; Monsen et al, 1992, Geol map
descriptive locality	Bare Mtn, Tarantula Canyon, measured section, 17m, (NTS)
strat unit	Dtc, "Rocks of Tarantula Canyon, Devonian", poss Eleana
outcrop description	bedded grainstone with visible fossils
process	split processed for conodonts.
results	in process

sample number	95JTA281
rock type	limestone
purpose	paleo, conodonts
storage	split processed (355A LMR); bag residue.
map locality	Carrara Canyon 7 1/2', T12S, R48E, unsurveyed; Monsen et al, 1992, Geol map
descriptive locality	Bare Mtn, Tarantula Canyon, measured section, 182m, (NTS)
strat unit	MDe, Eleana Fm.
outcrop description	laminated silty limestone
process	split processed.
results	in process

sample number	95JTA291
rock type	limestone
purpose	paleo, conodonts
storage	split processed (355LMR).
map locality	Carrara Canyon 7 1/2', T12S, R48E, unsurveyed; Monsen et al, 1992, Geol map
descriptive locality	Bare Mtn, Tarantula Canyon, measured section, 321m, (NTS)
strat unit	MDe, Eleana Fm.
outcrop description	orange-tan limestone interbedded with siliceous beds
process	split processed.
results	*BARREN* of conodonts.

sample number	95JTA292
rock type	limestone
purpose	paleo, conodonts
storage	conodont slide in LMR 358; split processed (355A LMR); bag residue; 1+vial to pick
map locality	Carrara Canyon 7 1/2', T12S, R48E, unsurveyed; Monsen et al, 1992, Geol map
descriptive locality	Bare Mtn, Tarantula Canyon, measured section, 334m, (NTS)
strat unit	Miss., MDe, Eleana Fm.
outcrop description	calcareous grit interbedded with siltstone, x-beds, channeled into siltstone below
process	for conodonts
results	Mississppian; Osagean; upper *typicus* zone. *Polygnathus communis communis, P. cf. P. longiposticus, P. inornatus, P. symmetricus, Gnathodus typicus, ?Doliognathus latus* (M 3) MTK (5/19/95); G. Webster (5/95)

sample number	95JTA293
rock type	limestone
purpose	paleo, conodonts
storage	split processed (355A LMR); bag residue.
map locality	Carrara Canyon 7 1/2', T12S, R48E, unsurveyed; Monsen et al, 1992, Geol map
descriptive locality	Bare Mtn, Tarantula Canyon, measured section, 348m, (NTS)
strat unit	MDe, Eleana Fm.
outcrop description	gray grainstone with siliceous interbeds
process	split processed for conodonts
results	in process

sample number	95JTA301
rock type	limestone
purpose	paleo, conodonts
storage	split processed (355A LMR); bag residue.
map locality	Carrara Canyon 7 1/2', T12S, R48E, unsurveyed; Monsen et al, 1992, Geol map
descriptive locality	Bare Mtn, Tarantula Canyon, measured section, 440m, (NTS)
strat unit	MDe, Eleana Fm.
outcrop description	orange weathering grainstone
process	split processed.
results	in process

sample number	95JTA302
rock type	limestone
purpose	paleo, conodonts
storage	split processed (355A LMR); bag residue.
map locality	Carrara Canyon 7 1/2', T12S, R48E, unsurveyed; Monsen et al, 1992, Geol map
descriptive locality	Bare Mtn, Tarantula Canyon, measured section, 517m, (NTS)
strat unit	MDe, Eleana Fm.
outcrop description	med. grainstone interbedded with siliceous grit
process	split processed.
results	in process

sample number	95JTA303
rock type	limestone
purpose	paleo, conodonts
storage	split processed (355A LMR); bag residue.
map locality	Carrara Canyon 7 1/2', T12S, R48E, unsurveyed; Monsen et al, 1992, Geol map
descriptive locality	Bare Mtn, Tarantula Canyon, measured section, 529m, (NTS)
strat unit	MDe, Eleana Fm.
outcrop description	med. grainstone interbedded with siliceous grit
process	split processed for conodonts.
results	in process

sample number	95JTA304
rock type	limestone
purpose	paleo, conodonts
storage	conodont slide in 358LMR; split processed (355A LMR); bag residue; 7 vials to pick
map locality	Carrara Canyon 7 1/2', T12S, R48E, unsurveyed; Monsen et al, 1992, Geol map
descriptive locality	Bare Mtn, Tarantula Canyon, measured section, 544m, (NTS)
strat unit	MDe, Eleana Fm.
outcrop description	med. grainstone interbedded with siliceous grit
process	split processed for conodonts
results	in process

sample number	95JTA305
rock type	limestone
purpose	paleo, conodonts
storage	split processed (355A LMR); bag residue.
map locality	Carrara Canyon 7 1/2', T12S, R48E, unsurveyed; Monsen et al, 1992, Geol map
descriptive locality	Bare Mtn, Tarantula Canyon, measured section, 549m, (NTS)
strat unit	MDe, Eleana Fm.
outcrop description	med. grainstone interbedded with siliceous grit
process	split processed for conodonts.
results	in process

sample number	95JTA305
rock type	limestone
purpose	paleo, conodonts
storage	
map locality	Carrara Canyon 7 1/2', T12S, R48E, unsurveyed; Monsen et al, 1992, Geol map
descriptive locality	Bare Mtn, Tarantula Canyon, measured section, 549m, (NTS)
strat unit	MDe, Eleana Fm.
outcrop description	med. grainstone interbedded with siliceous grit
process	
results	

sample number	95JTA306
rock type	limestone
purpose	paleo, conodonts
storage	conodont slide in 358LMR; split processed (355A LMR); bag residue.
map locality	Carrara Canyon 7 1/2', T12S, R48E, unsurveyed; Monsen et al, 1992, Geol map
descriptive locality	Bare Mtn, Tarantula Canyon, measured section, 612m, (NTS)
strat unit	MDe, Eleana Fm.
outcrop description	med. grainstone interbedded with siliceous grit
process	split processed for conodonts.
results	Mississippian; Osage or younger. species: *Gnathodus texanus; Polygnathus communis communis.* MTK (6/95); Rexroad (6/95)

sample number	95JTA311
rock type	limestone
purpose	paleo, conodonts
storage	split processed (355A LMR); bag residue.
map locality	Carrara Canyon 7 1/2', T12S, R48E, unsurveyed; Monsen et al, 1992, Geol map
descriptive locality	Bare Mtn, Tarantula Canyon, measured section, 729m, (NTS)
strat unit	MDe, Eleana Fm.
outcrop description	med. grainstone interbedded with siliceous grit
process	split processed for conodonts
results	in process

sample number	JC10678
rock type	
purpose	paleo
storage	split processed;conodont slide in LMR 358; bag residue
map locality	
descriptive locality	Calico Hills, Unit 5 (NTS)
strat unit	Miss. Eleana Fm.
outcrop description	
process	for conodonts; petroliferous when processed.
results	Mississippian; Kinderhookian; lower *crenulata* through *isosticha* upper *crenulata* zones. *Siphonodella isosticha, Si. obsoleta, Palmatolepis gracilis sigmoidalis, Pa. gracilis* sp., *Polygnathus communis communis, Gnathodus punctatus.* MTK (5/19/95)

sample number	JC10601
rock type	
purpose	paleo, conodonts
storage	conodont slide in LMR 358; residue dumped.
map locality	
descriptive locality	Calico Hills, NTS
strat unit	Miss. Eleana Fm.
outcrop description	
process	for conodonts
results	*BARREN* MTK (5/19/95)

sample number	95JC718 (=95JC10718)
rock type	limestone
purpose	paleo
storage	vial to be picked in LMR 358
map locality	
descriptive locality	ne part of Calico Hills (NTS)
strat unit	Unit 1
outcrop description	micrite
process	processed for conodonts
results	in process

sample number	94PC2182
rock type	l
purpose	conodont extraction
storage	conodont slide in LMR 358
map locality	
descriptive locality	Calico Hills (NTS)
strat unit	Unit 3
outcrop description	
process	processed to completion
results	Middle Devonian; Mid-Eifelian through Lower Givetian; *Tortodus australis* zone through Lower *varcus* zone. species: *Polygnathus parawebbi* Chatterton, 1974, beta morphotype.

sample number	94PC2182
rock type	limestone
purpose	conodonts
storage	LMR 358
map locality	
descriptive locality	Calico Hills
strat unit	
outcrop description	
process	dissolved 7-31-95
results	

sample number	94PC2153
rock type	limestone
purpose	conodonts
storage	1 vial ready to pick in LMR358
map locality	
descriptive locality	Calico Hills(NTS); above black siliceous siltstone
strat unit	
outcrop description	
process	separated in part 8-3-94
results	Mississippian; Kinderhookian; *sandbergi* - Upper *crenulata* zone. species found: *Siphonodella obsoleta, S. sandbergi, S. duplicata, Polygnathus inornatus, P. communis communis.*

sample number	94PC2154
rock type	limestone
purpose	conodonts
storage	1 small vial ready to pick in LMR 358
map locality	
descriptive locality	
strat unit	Calico Hills (NTS)
outcrop description	
process	separated completely
results	Mississippian; Kinderhookian; *sandbergi* through Upper *crenulata-isosticha* zone. species: *Siphonodella quadruplicata;* MTK (8/95)

sample number	JC10757
rock type	limestone
purpose	conodont extraction
storage	2 vials to pick in LMR 358
map locality	
descriptive locality	Topopah spring
strat unit	
outcrop description	
process	split processed 7-25-95 (separation)
results	in process

sample number	JC10638
rock type	limestone
purpose	conodont extraction
storage	2 vials to pick in LMR 358 residue bag and sample bag
map locality	
descriptive locality	Calico Hills
strat unit	
outcrop description	
process	separated in part 7-26-95
results	in process

sample number	JC10623
rock type	limestone
purpose	conodont extraction
storage	conodont slide in LMR 358
map locality	
descriptive locality	Calico Hills
strat unit	
outcrop description	
process	split processed 7-24-95 (separation)
results	inconclusive

sample number	95JC848
rock type	limestone
purpose	conodont extraction
storage	2 vials to pick in LMR 358 in residue bag and in sample bag
map locality	
descriptive locality	Calico Hills
strat unit	
outcrop description	
process	dissolved 7-26-95
results	in process

sample number	95JC848
rock type	limestone
purpose	conodonts
storage	LMR 358 residue bag
map locality	
descriptive locality	Calico Hills
strat unit	
outcrop description	
process	separated in part 7-28-95
results	

sample number	JC10612
rock type	limestone
purpose	conodont extraction
storage	conodont slide in LMR 358, 3 vials to pick.
map locality	
descriptive locality	Calico Hills
strat unit	Unit 1
outcrop description	limestone bed from upper part of lower flaggy unit
process	separated in part 7-26-95
results	Devonian; jury still out on this one

sample number	JC10612-B
rock type	limestone
purpose	conodont extraction
storage	LMR 358 residue bag
map locality	
descriptive locality	W. Calico Hills
strat unit	
outcrop description	
process	separated completely 8-11-95
results	

sample number	95JTA341
rock type	limestone
purpose	paleo, conodonts
storage	LMR 358
map locality	Mercury 7 1/2'; Barns et al, 1981 Geologic Map
descriptive locality	Spotted Range (NTS): traverse in Miss. section beneath thrust complex, Timpi Canyon measured section, base in Dev. carbonates
strat unit	Narrow Canyon Fm.
outcrop description	ledgy limestone beds interpreted as structurally repeated Dev. Devil's Gate
process	
results	in process

sample number	95JTA342
rock type	limestone
purpose	paleo, conodonts
storage	conodont slide in LMR358; half sample on floor in LMR 358
map locality	Mercury 7 1/2'; Barns et al, 1981 Geologic Map
descriptive locality	Spotted Range (NTS): traverse in Miss. section beneath thrust complex, Timpi Canyon measured section, at 68m
strat unit	Narrow Canyon Fm.
outcrop description	ledgy limestone beds below important quartzite interval, low in unit
process	split processed for conodonts.
results	Late Devonian; Famennian?

sample number	95JTA351
rock type	limestone
purpose	paleo, conodonts
storage	
map locality	Mercury 7 1/2'; Barns et al, 1981 Geologic Map
descriptive locality	Spotted Range (NTS): traverse in Miss. section beneath thrust complex, Timpi Canyon measured section, at 115m
strat unit	Narrow Canyon Fm. to Mercury Ls. transition zone
outcrop description	beds of grainstone with thin quartzites
process	
results	in process

sample number	95JTA352
rock type	limestone
purpose	paleo, conodonts
storage	
map locality	Mercury 7 1/2'; Barns et al, 1981 Geologic Map
descriptive locality	Spotted Range (NTS): traverse in Miss. section beneath thrust complex, Timpi Canyon measured section, at 222m
strat unit	Timpi Canyon Ls., lowest beds
outcrop description	dull gray micrite in recessive ledges
process	
results	in process

sample number	95JTA353
rock type	limestone
purpose	paleo, conodonts
storage	conodont slide in 358LMR; split processed (355A LMR); vial to pick.
map locality	Mercury 7 1/2'; Barns et al, 1981 Geologic Map
descriptive locality	Spotted Range(NTS): traverse in Miss. section beneath thrust complex, Timpi Canyon measured section, at 325m
strat unit	Timpi Canyon Ls., upper beds
outcrop description	dull gray micrite in ledges, with silty laminae, rythmic outcrops
process	split processed for conodonts.
results	Mississippian; late Kinderhookian. species: *Gnathodus punctatus; Gn.* cf *G. simplicatus; Polygnathus communis* subsp.; MTK (6/95); Rexroad (6/95)

sample number	95JTA354
rock type	limestone
purpose	paleo, conodonts
storage	
map locality	Mercury 7 1/2'; Barns et al, 1981 Geologic Map
descriptive locality	Spotted Range (NTS): traverse in Miss. section beneath thrust complex, Timpi Canyon measured section, at 390m
strat unit	Chainman Fm.
outcrop description	purple slabby limestone below thrust fault, collected near 355
process	
results	in process

sample number	95JTA355
rock type	limestone
purpose	paleo, conodonts
storage	
map locality	Mercury 7 1/2'; Barns et al, 1981 Geologic Map
descriptive locality	Spotted Range (NTS): traverse in Miss. section beneath thrust complex, Timpi Canyon measured section, at 390m
strat unit	Chainman Fm.
outcrop description	bioclastic grainstone with large mudrock ripups, collected near 345
process	
results	in process

sample number	95JTA383
rock type	limestone
purpose	paleo, conodonts
storage	
map locality	Mercury 7 1/2'; Barns et al, 1981 Geologic Map
descriptive locality	Spotted Range (NTS): traverse in Miss. section beneath thrust complex, Timpi Canyon measured section, at 348m
strat unit	Miss. Chainman Fm.
outcrop description	bioclastic grainstone, silty
process	
results	in process

sample number	95JTA391
rock type	limestone
purpose	paleo, conodonts
storage	
map locality	Tippipah Springs 7 1/2', no T&R
descriptive locality	NTS, southern Syncline Ridge, northern Shoshone Mountain, 1 mile ENE from Tippipah Point
strat unit	Miss. Eleana Fm.
outcrop description	locallized outcrops of pebbly mudstone and thinnly bedded siliceous mudrocks, rare limestone bed about 10m up section from pebble beds
process	
results	in process

sample number	95JTA462
rock type	limestone
purpose	paleo
storage	LMR 358 in yellow envelope
map locality	Yucca Lake 7 1/2'
descriptive locality	C.P. Hills (CP), NTS, southeast flank above DAF building, lower plate to CP thrust
strat unit	Miss or Penn, Chainman or Tippipah
outcrop description	lowest limestone outcrop above last quartzite
process	dissolved 7-21-95
results	in process

sample number	95JTA462
rock type	limestone
purpose	conodont extraction
storage	sample bag LMR 358
map locality	
descriptive locality	basal Tippipah, CP Hills (NTS).
strat unit	
outcrop description	
process	
results	

sample number	95JTA463
rock type	limestone
purpose	paleo
storage	LMR 358 in yellow envelope
map locality	Yucca Lake 7 1/2'
descriptive locality	C.P. Hills (CP), NTS, southeast flank above DAF building, lower plate to CP thrust
strat unit	Miss or Penn, Chainman or Tippipah
outcrop description	limestone outcrop above last quartzite, 2nd parasequence
process	dissolved 7-21-95
results	in process

Selected Core Chip Sample Descriptions from the UE17e Core Hole, Nevada Test Site

TABLE OF CONTENTS

17 January 1995

Donna M. Herring
Petroleum Geologist

• Donna M. Herring • P.O. Box 13652, Reno NV 89507-3652 • (702) 786-5620 •

Selected Core Chip Sample Descriptions from the UE17e Core Hole, Nevada Test Site

EXECUTIVE SUMMARY

Core chip samples were examined microscopically and described in geologic detail, as a continuation of a study of petroleum source-rock potential of the Chainman Formation in the 3,000'-deep NTS core hole UE17e.

The paucity of silt in the mudrocks above about 1500' is probably related to a change in provenance or other sedimentological condition. The anhydritic or gypsiferous nature of the entire interval is likely to be primary, and as such would reflect restricted circulation in the Chainman depositional basin. The dolomitic zones which correlate in part with evaporitic zones are probably primary and may be correlatable to outcrop. The erratic highly-smectitic zones may be correlatable and might be datable.

When integrated with previously collected data, the core chip sample descriptions will aid correlation of the UE17e core to adjacent outcrops and extrapolation within the Test Site. Description of existing thin sections is the major work remaining to be done for the UE17e core analysis, followed by synthesis and interpretation of all the data relative to hydrocarbon generation in the UE17e core hole area.

INTRODUCTION AND METHODS

This report is a continuation of a study, under subcontract from Dr. Patricia H. Cashman, Principal Investigator, of the hydrocarbon potential of the Chainman Formation as cored in the Nevada Test Site UE17e core hole. The core has been previously described in general terms, some intervals have been described in detail, and implications of results through the fall of 1993 have been discussed (Herring, 1993). The present report details only the examination of core chip samples; analyses of organic carbon and various age determinations have been completed since 1993, and are discussed by the Principal Investigator elsewhere.

One hundred and seventy core chip samples were collected in 1993 at the U.S.G.S. Mercury Core Library from core UE17e. These samples comprised lithologies ranging from fossiliferous carbonate and sandstone to clayshale, though the core below a depth

• Donna M. Herring • P.O. Box 13652, Reno NV 89507-3652 • (702) 786-5620 •

of about 240' is almost entirely mudstone and shale. The emphasis of the continuing study is the source-rock potential of the Chainman Formation, and only the mudrocks of the cored interval have petroleum source potential. Fifty-eight mudrock samples of the total 170 samples were selected for this report, chosen to represent significant changes in mudrock lithology and to sample thick zones of similar lithology at 40-60' intervals where possible.

Binocular microscope examination of core chip samples was undertaken to identify basic mineralogical changes within the cored interval, especially as a basis for correlation and a guide to thin section study. The descriptions presented in Appendix A are as detailed as possible in the absence of additional destructive testing, such as X-ray diffraction or other intensive mineral-identification methods.

For each sample, that portion of the core chip required to yield about 10ml volume was crushed to a maximum piece size of about 6mm, and all resulting fragments were placed in the examination tray. Parting and fracture were then noted, UV fluorescence was tested, hardness was tested on several fragments with a steel probe, and siltiness and taste were tested on one or two fragments by mouth (standard procedures per numerous authors, see References and Appendix). The samples were then water-wetted in the examination tray, and color and luster were noted. Two to four representative chips were removed and heat-dried while the remaining sample soaked several minutes in water. Half of the representative dried chips were reacted with about 1ml cold hydrochloric acid, then heated in the acid until dry. Half of the representative dried chips were reacted with about 1ml of naptha under UV light and allowed to air-dry. The remaining wet sample was examined under tungsten and UV light for mineralogic and sedimentologic indicators, then heated until dry. Then all these re-dried portions of the sample (reacted with acid, water, or naptha) were reexamined. The results of the reactions and drying were recorded and interpreted.

The water-wetted portions of the samples were saved for possible further study, in small envelopes marked with their depth, date of collection, date of examination, and the fact that they had been previously examined water-wet. Grains were cut from vein material in three samples (at 1765.1', 2346.0', and 2492.0') for possible further study.

DISCUSSION AND SUMMARY

No hydrocarbon stain, cut, fluorescence, or odor was observed in these samples. Black to near-black color is typical of most samples below about 700', and is indicative of organic

carbon content greater than 0.5% (see discussion of black color in Herring, 1993). Rare mineral fluorescence was observed in some vein material.

Apparent sedimentology of the chips is fairly straightforward, with the majority of samples above about 1500' being silt-free clayshale or claystone, and samples below that depth being more or less silty and dominantly mudshale or mudstone. Bioturbation was not recognized, though lamination is indistinct. The presence of siltstone in only one sample is an artifact of the sampling focus on mudrocks.

Mineralogy of the core is more variable, with 100-400' zones being non-calcareous to very slightly dolomitic, and much thinner zones (typically 50-100') being moderately to very dolomitic. Most of the core is at least moderately anhydritic (see further discussion below). Water-soluble evaporite minerals appear to be present in several zones about 50' thick occurring between depths of about 1900' and 2900'. Vein mineralogy varies throughout the core, including quartz, calcite, dolomite, anhydrite/gypsum, and kaolinite, generally in various combinations. The present study is insufficient to determine whether vein mineralogy varies systematically with depth.

The presence of anhydrite is indicated by the precipitation of acicular crystals during the hot-acid test (Swanson, 1981:14). Acicular crystals may also be precipitated by this test as gypsum polymorphs of anhydrite, if gypsum is the native sulfate in the rock (see Hurlbut and Klein, 1977:322). Therefore, for the purposes of this report, "anhydrite" must be considered an imprecise term which refers to calcium sulfate in either the hydrous or the anhydrous state.

In many of the examined samples, "very slightly dolomitic" was the interpretive term applied when the acid test yielded few bubbles and trains of small bubbles as the acid warmed. It is possible that liberated sulfur dioxide from dissolution of gypsum/anhydrite was in some cases the source of these bubbles, instead of carbon dioxide liberated in the dissolution of dolomite and calcite. However, these results did not always coincide with a sulfurous smell or anhydritic character, and so were typically interpreted as dolomite dissolution.

Below a depth of about 1900' and near 2400', unknown minerals with non-acicular crystal habits also precipitated from several samples during the hot-acid test. Unknown evaporite minerals also were precipitated rarely from the hot-water test, at depths above 1300', between 1900' and 2400', and below 2800'. The core hole was drilled with freshwater bentonite mud, and these evaporites are therefore unlikely to be contamination of the formation by mud filtrates. The evaporitic zone near 1900'

correlates with a dolomitic zone, which is another indication that these anomalous minerals are native to the core mineralogy.

The majority of samples were at least slightly water-sensitive, indicating the presence of smectite or interlayered illite/smectite. The erratically-occurring highly-smectitic zones do not have any obvious correlation to siltiness or to other mineralogical variations. Except for the presence of kaolinite in some veins, no other specific clay mineralogy is apparent. Analyses from other UE17e samples (Herring, 1993) indicate that clay-size quartz and feldspar are common constituents, and that chlorite is in some zones nearly as abundant as illite/smectite among the clay minerals present.

CONCLUSIONS

The paucity of silt in the mudrocks above about 1500' is probably related to a change in provenance or other sedimentological condition. The anhydritic or gypsiferous nature of the entire interval is likely to be primary, and as such would reflect restricted circulation in the Chainman depositional basin. The dolomitic zones which correlate in part with evaporitic zones are probably primary and may be correlatable to outcrop. The erratic highly-smectitic zones, whether they are provenance-controlled (unlikely, if the systematic silt distribution reflects provenance control) or a product of airborne volcanic ash, may be correlatable and might be datable.

When integrated with the previous general and interval-detailed descriptions of the whole core, the attached selected core chip sample descriptions should aid correlation of the UE17e core to adjacent outcrops. Description of existing thin sections is the major work remaining to be done for the UE17e core analysis, followed by synthesis and interpretation of all the data relative to hydrocarbon generation in the UE17e core hole area.

Donna M. Herring, 17 January 95
Petroleum Geologist
Certified Professional Earth Scientist

REFERENCES CITED

Blatt, H., G. Middleton and R.C. Murray, 1980. Origin of Sedimentary Rocks: Prentice-Hall, Englewood Cliffs, New Jersey, 782 pp.

Herring, D.M., 1993. Hydrocarbon potential of the UE17e core hole, Nevada Test Site: Interim report: Nevada Nuclear Waste Project Office, Carson City, 67 pp.

Hurlbut, C. S., Jr. and C. Klein, 1977. Manual of Mineralogy: John Wiley & Sons, New York, 532 pp.

LeRoy, L.W., D.O. LeRoy and J.W. Raese, 1977. Subsurface Geology - Petroleum, Mining, Construction: Colorado School of Mines, Golden, Colorado, 941 pp.

Potter, P.E., J.B. Maynard and W.A. Pryor, 1980. Sedimentology of Shale: Springer-Verlag, New York, 310 pp.

Rock Color Chart Committee, 1980. Rock Color Chart of the Geological Society of America: Geological Society of America (G.S.A.), Boulder, Colorado, 6 pl.

Swanson, R.G., 1981. Sample Examination Manual: American Association of Petroleum Geologists, Tulsa Oklahoma, 106 pp.

KEY TO CORE CHIP SAMPLE DESCRIPTIONS

Sample depth
As estimated from marked core at the USGS Mercury Core Library.

Rock type Using classifications by Potter et al (1980:14-16) for mudrocks.

Color Corresponding to the G.S.A. Rock Color Chart color names. Described water-wet in tungsten lamp reflected light, under magnification of 7x for most samples and to 30x where necessary for very fine included or exsolved grains or crystals.

Minerals Determined from visual examination in tungsten and UV light at magnifications to 30x, plus interpretation from reactions to hydrochloric acid and drinking water detailed below, plus resistance to hardened steel probe, plus interpretation using field criteria of Blatt et al (1980:382), all with reference to Hurlbut and Klein (1977).

Hardness Subjective analysis using the method of Swanson (1981:12), determined on dry-crushed sample.

Parting Using the criteria of Potter et al (1980:15-16, 24, 90), description of parting and fracturing characteristics of the dry-crushed sample.

Luster Using terminology of Hurlbut and Klein (1977) and LeRoy and LeRoy (1977:291), description of water-wet sample.

Misc Including mineral UV fluorescence, hydrocarbon stain and/or UV fluorescence, fossils, unusual tastes, and any other characteristic not discussed elsewhere in the description.

Rxn HCl Reaction with 10% hydrochloric acid, after water-wetting and redrying. Acid and sample were initially at room temperature ("cold" reaction, approximately 25°C), and were then heated to approximately 100°C ("hot" reaction).

Rxn H2O Reaction with drinking water from the Reno city water supply. Sample and water were initially at room temperature (25°C as for acid), and were then heated to approximately 100°C until sample was dry.

Other analyses Test results or additional data available for the described sample or on a sample within 1.0 foot of this sample, to the author's knowledge.

SRF date Date a USGS Sample Removal Form was completed for this sample.

Exam date Date this author examined the sample under a binocular microscope and recorded the above observations.

• Donna M. Herring • P.O. Box 13652, Reno NV 89507-3652 • (702) 786-5620 •

SUMMARY OF SAMPLES EXAMINED FOR THIS REPORT

Sample depth	Rock type	Color	SRF date
66.7 ft	Mudstone;	dark yellow brown;	2-19-93
82.7 ft	Claystone;	moderate brown grey;	2-19-93
102.9 ft	Claystone;	brown grey;	2-19-93
136.4 ft	Claystone;	brown grey;	2-19-93
179.0 ft	Mudstone;	brown grey, 30x magnification shows	2-19-93
189.0 ft	Mudstone;	brown grey;	2-19-93
192.0 ft	Mudstone;	brownish olive grey, rare indistinct thin to	2-19-93
205.9 ft	Claystone;	brown grey;	2-19-93
218.5 ft	Claystone;	brownish grey;	2-19-93
240.0 ft	Claystone;	brown grey;	2-19-93
252.5 ft	Claystone;	olive grey;	2-19-93
266.6 ft	Claystone;	olive grey;	2-19-93
324.5 ft	Clayshale;	medium dark grey to dark grey;	2-19-93
494.5 ft	Clayshale;	olive grey;	9-23-93
507.7 ft	Clayshale;	olive grey;	9-23-93
535.3 ft	Mudstone;	olive grey;	2-19-93
564.5 ft	Mudstone;	olive black;	2-19-93
597.0 ft	Mudstone and Siltstone;	olive grey to dark olive grey;	2-19-93
616.0 ft	Clayshale;	olive grey;	2-19-93
664.0 ft	Mudshale;	olive grey;	2-19-93
698.0 ft	Clayshale;	olive grey to olive black;	2-19-93
801.4 ft	Clayshale;	olive grey to olive black;	9-23-93
860.5 ft	Mudstone;	olive black;	2-19-93
970.0 ft	Clayshale;	olive grey;	9-23-93
995.0 ft	Clayshale;	olive grey to olive black;	9-23-93
1050.5 ft	Clayshale;	olive grey;	9-23-93
1105.8 ft	Clayshale;	olive black;	9-23-93
1128.8 ft	Mudshale;	olive grey;	9-23-93
1198.8 ft	Clayshale;	olive black;	9-23-93
1222.0 ft	Clayshale;	olive black;	9-23-93
1281.5 ft	Clayshale;	olive black;	9-23-93
1300.5 ft	Clayshale;	olive grey to olive black;	9-23-93
1339.0 ft	Clayshale;	olive grey to olive black;	9-23-93
1549.0 ft	Mudstone;	olive grey to olive black;	2-19-93

SUMMARY OF SAMPLES EXAMINED FOR THIS REPORT

Sample depth	Rock type	Color	SRF date
1596.0 ft	Mudstone;	olive black to olive grey;	2-19-93
1626.7 ft	Mudstone;	olive black;	2-19-93
1697.3 ft	Mudstone;	olive black;	2-19-93
1735.4 ft	Mudstone;	olive grey;	2-19-93
1765.1 ft	Mudstone;	olive black;	2-19-93
1809.2 ft	Mudstone;	olive black;	2-19-93
1847.9 ft	Mudstone;	olive black;	2-19-93
1901.7 ft	Mudstone;	olive black;	2-19-93
1947.2 ft	Mudshale;	olive black;	2-19-93
1985.5 ft	Mudshale;	olive black;	1-14-93
2029.5 ft	Mudstone;	olive grey to olive black;	2-19-93
2061.1 ft	Mudstone;	olive grey to olive black;	2-19-93
2158.0 ft	Mudstone;	olive black;	1-14-93
2224.8 ft	Clayshale;	grey black to black;	1-14-93
2295.0 ft	Mudshale;	olive black;	2-19-93
2346.0 ft	Mudstone;	olive grey to olive black;	2-19-93
2420.1 ft	Mudshale;	olive grey to olive black;	2-19-93
2453.8 ft	Mudshale;	brown black;	2-19-93
2492.0 ft	Mudshale;	grey black to black;	2-19-93
2523.9 ft	Mudstone;	olive grey to olive black;	1-14-93
2654.0 ft	Mudshale;	olive black;	1-14-93
2691.7 ft	Mudstone;	olive black to grey black;	1-14-93
2834.5 ft	Mudshale;	olive grey to grey black;	2-19-93
2871.5 ft	Clayshale;	dark grey to grey black;	1-14-93

Sample depth		
66.7 ft	Rock type	Mudstone;
	Color	dark yellow brown;
	Minerals	slightly to moderately dolomitic, rarely slightly silty, trace very fine-grained glauconite, abundantly anhydritic;
	Hardness	firm;
	Parting	sub-platy to sub-blocky;
	Luster	sub-earthy;
	Misc	no observed;
	Rxn HCl	slow effervescence, sulfurous odor, abundant residual acicular crystals;
	Rxn H2O	becoming soft, disaggregating in cold H2O, when dried has trace to common soft translucent white to light brown minute fibrous radial evaporitic crystal clusters;
	Other analyses	unknown;
	SRF date 2-19-93	Exam date 1-1-95

Sample depth		
82.7 ft	Rock type	Claystone;
	Color	moderate brown grey;
	Minerals	non-silty, moderately dolomitic, rarely limey (possibly calcite replacement of fine fossil debris), rare silty-looking laminae apparently rich in diagenetic dolomite, very abundantly anhydritic;
	Hardness	firm to hard;
	Parting	sub-blocky to sub-platy;
	Luster	sub-earthy;
	Misc	bitter taste, possible unidentifiable fine-size fossil fragments;
	Rxn HCl	slow effervescence, sulfurous odor, very abundant residual acicular crystals;
	Rxn H2O	platy disaggregation in cold H2O, trace to common radial evaporitic clusters as above;
	Other analyses	unknown;
	SRF date 2-19-93	Exam date 1-1-95

Sample depth		
102.9 ft	Rock type	Claystone;
	Color	brown grey;
	Minerals	non-silty, moderately dolomitic with very dolomitic laminae, rare silty-looking laminae apparently rich in diagenetic dolomite, abundantly anhydritic;
	Hardness	firm to hard;
	Parting	sub-blocky to sub-pencilly;
	Luster	sub-earthy;
	Misc	no observed;
	Rxn HCl	slow effervescence, sulfurous odor, abundant residual acicular crystals;
	Rxn H2O	platy disaggregation in cold H2O, trace to common radial evaporitic clusters as above;
	Other analyses	unknown;
		SRF date 2-19-93 Exam date 1-1-95

Sample depth		
136.4 ft	Rock type	Claystone;
	Color	brown grey;
	Minerals	non-silty, rarely very slightly dolomitic, common silty-looking laminae ?not detrital (probably diagenetic anhydrite and/or dolomite crystals), moderately anhydritic;
	Hardness	firm to hard;
	Parting	sub-blocky;
	Luster	sub-earthy to sub-waxy;
	Misc	no observed;
	Rxn HCl	very slow effervescence, sulfurous odor, common residual acicular crystals;
	Rxn H2O	fissile to platy disaggregation and becoming soft in cold H2O, trace to common radial evaporitic clusters as above;
	Other analyses	unknown;
		SRF date 2-19-93 Exam date 1-1-95

Sample depth		
179.0 ft	Rock type	Mudstone;
	Color	brown grey, 30x magnification shows speckled black-white-yellow-grey thick indistinct laminae in part;
	Minerals	slightly to moderately silty, slightly dolomitic, moderately anhydritic;
	Hardness	firm to hard;
	Parting	blocky to sub-blocky;
	Luster	sub-earthy to sub-waxy;
	Misc	no observed;
	Rxn HCl	slow effervescence, sulfurous odor, common residual acicular crystals;
	Rxn H2O	platy parting and becoming firm in cold H2O, trace to common radial evaporitic clusters as above;
	Other analyses	unknown;
		SRF date 2-19-93 Exam date 1-1-95

Sample depth		
189.0 ft	Rock type	Mudstone;
	Color	brown grey;
	Minerals	non-silty, ?micaceous (silt-size), slightly to moderately dolomitic with rare laminae moderately to very dolomitic, abundantly anhydritic;
	Hardness	firm;
	Parting	sub-platy to sub-blocky;
	Luster	sub-earthy;
	Misc	no observed;
	Rxn HCl	slow effervescence, sulfurous odor, abundant residual acicular crystals;
	Rxn H2O	platy parting and becoming soft in cold H2O, abundant radial evaporitic clusters as above;
	Other analyses	unknown;
		SRF date 2-19-93 Exam date 1-1-95

Sample depth		
192.0 ft	Rock type	Mudstone;
	Color	brownish olive grey, rare indistinct thin to thick laminae speckled black-white-yellow-grey;
	Minerals	non-silty, non-calcareous, abundantly anhydritic;
	Hardness	firm;
	Parting	sub-blocky;
	Luster	sub-earthy;
	Misc	indistinct laminae to 3mm thick;
	Rxn HCl	slight sulfurous odor, very abundant residual acicular crystals;
	Rxn H2O	becoming soft in cold H2O with platy and pencilly parting, rare radial evaporitic clusters as above and rare very fine-grained opaque white blocky evaporite crystals;
	Other analyses	unknown;
		SRF date 2-19-93 Exam date 1-1-95

Sample depth		
205.9 ft	Rock type	Claystone;
	Color	brown grey;
	Minerals	non-silty, non-calcareous, abundantly anhydritic;
	Hardness	firm;
	Parting	sub-blocky;
	Luster	sub-earthy;
	Misc	slightly bitter taste;
	Rxn HCl	slight sulfurous odor, very abundant residual acicular crystals;
	Rxn H2O	becoming soft to very soft in cold H2O and immediately disaggregating, common radial evaporitic clusters as above;
	Other analyses	unknown;
		SRF date 2-19-93 Exam date 1-1-95

Sample depth		
218.5 ft	Rock type	Claystone;
	Color	brownish grey;
	Minerals	non-silty, non-calcareous, moderately anhydritic, rare very thin white veins microcrystalline dolomite;
	Hardness	firm to moderately soft;
	Parting	sub-blocky to sub-platy;
	Luster	sub-earthy to sub-waxy;
	Misc	no observed;
	Rxn HCl	slight sulfurous odor, common residual acicular crystals;
	Rxn H2O	becoming very soft and fissile in cold H2O and immediately disaggregating, rare to common radial evaporitic clusters as above becoming stubby, and opaque white evaporite crystals as above;
	Other analyses	unknown;
		SRF date 2-19-93 Exam date 1-1-95

Sample depth		
240.0 ft	Rock type	Claystone;
	Color	brown grey;
	Minerals	non-silty, slightly dolomitic, moderately anhydritic, rare indistinct thick laminae with common very fine-grained disseminated pyrite;
	Hardness	firm to very firm;
	Parting	sub-pencilly to sub-blocky;
	Luster	sub-earthy to sub-waxy;
	Misc	no observed;
	Rxn HCl	slow effervescence, slight sulfurous odor, common residual acicular crystals;
	Rxn H2O	becoming very soft andplaty-splitting in cold H2O and immediately disaggregating, rare to common radial evaporitic stubby clusters and opaque white evaporite crystals as above, pyritic laminae exsolve rare white very fine acicular crystals;
	Other analyses	unknown;
		SRF date 2-19-93 Exam date 1-1-95

Sample depth		
252.5 ft	Rock type	Claystone;
	Color	olive grey;
	Minerals	non-silty, non-calcareous, moderately anhydritic;
	Hardness	firm to very firm;
	Parting	sub-platy to sub-blocky;
	Luster	sub-earthy to sub-waxy;
	Misc	no observed;
	Rxn HCl	slight sulfurous odor, common residual acicular crystals;
	Rxn H2O	becoming soft and platy-splitting in cold H2O and rarely disaggregating, rare to common radial evaporitic stubby clusters and opaque white evaporite crystals as above;
	Other analyses	unknown;
	SRF date	2-19-93 Exam date 1-1-95

Sample depth		
266.6 ft	Rock type	Claystone;
	Color	olive grey;
	Minerals	non-silty, slightly to moderately dolomitic, microbrecciated in part with white to light blue vitreous microcrystalline dolomite matrix, abundantly anhydritic;
	Hardness	firm to very firm, brittle;
	Parting	sub-blocky;
	Luster	sub-earthy to earthy;
	Misc	slightly bitter taste;
	Rxn HCl	slow effervescence, slight sulfurous odor, abundant residual acicular crystals;
	Rxn H2O	becoming firm and platy-splitting in cold H2O;
	Other analyses	unknown;
	SRF date	2-19-93 Exam date 1-1-95

Sample depth		
324.5 ft	Rock type	Clayshale;
	Color	medium dark grey to dark grey;
	Minerals	non-silty, slightly dolomitic, abundantly anhydritic;
	Hardness	firm;
	Parting	sub-fissile;
	Luster	sub-earthy;
	Misc	metallic taste;
	Rxn HCl	slow effervescence in cold HCl, disaggregates in hot HCl, abundant residual acicular crystals;
	Rxn H2O	becoming soft in cold H2O;
	Other analyses	unknown;
		SRF date 2-19-93 Exam date 1-1-95

Sample depth		
494.5 ft	Rock type	Clayshale;
	Color	olive grey;
	Minerals	non-silty, non-calcareous, abundantly anhydritic;
	Hardness	firm;
	Parting	fissile to sub-blocky;
	Luster	sub-earthy;
	Misc	no observed;
	Rxn HCl	very abundant residual acicular crystals;
	Rxn H2O	immediately becoming very soft in cold H2O;
	Other analyses	unknown;
		SRF date 9-23-93 Exam date 1-1-95

Sample depth		
507.7 ft	Rock type	Clayshale;
	Color	olive grey;
	Minerals	non-silty, very slightly dolomitic, abundantly anhydritic;
	Hardness	soft to firm;
	Parting	sub-fissile to sub-blocky;
	Luster	earthy;
	Misc	metallic taste;
	Rxn HCl	slow effervescence in hot HCl, abundant residual acicular crystals;
	Rxn H2O	becoming very soft in cold H2O;
	Other analyses	conodont age;
		SRF date 9-23-93 Exam date 1-1-95

Sample depth		
535.3 ft	Rock type	Mudstone;
	Color	olive grey;
	Minerals	slightly to moderately silty, slightly dolomitic, moderately anhydritic, indistinct laminae, some thin laminae with common very fine-grained disseminated pyrite, rare fine-grained quartz sand laminae;
	Hardness	firm;
	Parting	sub-blocky to sub-platy;
	Luster	earthy;
	Misc	no observed;
	Rxn HCl	slow effervescence in cold HCl, becoming very soft and disaggregating in hot HCl, slightly sulfurous odor, common residual acicular crystals;
	Rxn H2O	becoming soft to firm in cold H2O with rare zones disaggregating;
	Other analyses	unknown;
		SRF date 2-19-93 Exam date 1-2-95

Sample depth		
564.5 ft	Rock type	Mudstone;
	Color	olive black;
	Minerals	non-silty to slightly silty in part, moderately dolomitic to very dolomitic in part, rare thin light green fine-crystalline dolomite veins, moderately anhydritic;
	Hardness	very firm to hard;
	Parting	sub-blocky to hackly, rare sub-platy;
	Luster	waxy to sub-waxy;
	Misc	rare white to light blue mineral fluorescence in dolomite veins;
	Rxn HCl	slow effervescence in cold HCl, becoming soft in hot HCl, sulfurous odor with common residual acicular crystals;
	Rxn H2O	becoming sub-platy in cold H2O;
	Other analyses	unknown;
		SRF date 2-19-93 Exam date 1-2-95

Sample depth		
597.0 ft	Rock type	Mudstone and Siltstone;
	Color	olive grey to dark olive grey;
	Minerals	moderately to very silty, moderately to very dolomitic, rare disseminated very fine-grained quartz sand, abundantly anhydritic;
	Hardness	firm to hard;
	Parting	sub-blocky;
	Luster	earthy, sub-waxy in part;
	Misc	metallic taste;
	Rxn HCl	slow effervescence, sulfurous odor with abundant residual acicular crystals, becoming soft in hot HCl;
	Rxn H2O	becoming firm and platy-splitting in part in cold H2O;
	Other analyses	total organic carbon;
		SRF date 2-19-93 Exam date 1-2-95

Sample depth		
616.0 ft	Rock type	Clayshale;
	Color	olive grey;
	Minerals	very slightly silty in part, moderately dolomitic, abundantly anhydritic;
	Hardness	firm;
	Parting	sub-platy to fissile;
	Luster	earthy;
	Misc	no observed;
	Rxn HCl	slow effervescence, strong sulfurous odor, abundant residual acicular crystals, becoming soft in hot HCl;
	Rxn H2O	becoming soft in cold H2O;
	Other analyses	unknown;
		SRF date 2-19-93 Exam date 1-2-95

Sample depth		
664.0 ft	Rock type	Mudshale;
	Color	olive grey;
	Minerals	slightly to very slightly silty in part, abundantly anhydritic, thin indistinct silt laminae, rare to common siliceous spicules, non-calcareous;
	Hardness	firm to hard;
	Parting	blocky to sub-platy;
	Luster	earthy to sub-waxy;
	Misc	no observed;
	Rxn HCl	sulfurous odor with abundant residual acicular crystals;
	Rxn H2O	becoming soft to firm in cold H2O;
	Other analyses	unknown;
		SRF date 2-19-93 Exam date 1-2-95

Sample depth		
698.0 ft	Rock type	Clayshale;
	Color	olive grey to olive black;
	Minerals	non-silty, slightly dolomitic, moderately anhydritic;
	Hardness	firm;
	Parting	fissile to sub-blocky;
	Luster	sub-earthy to sub-waxy;
	Misc	no observed;
	Rxn HCl	slow effervescence, disaggregates rapidly in hot HCl, common very fine-grained residual acicular crystals;
	Rxn H2O	becoming soft to very soft and disaggregating in cold H2O;
	Other analyses	unknown;
		SRF date 2-19-93 Exam date 1-2-95

Sample depth		
801.4 ft	Rock type	Clayshale;
	Color	olive grey to olive black;
	Minerals	non-silty, very slightly dolomitic, moderately anhydritic;
	Hardness	firm;
	Parting	fissile to sub-blocky;
	Luster	sub-waxy to sub-earthy;
	Misc	no observed;
	Rxn HCl	very slow effervescence, disaggregates in hot HCl, common residual very fine-grained acicular crystals;
	Rxn H2O	becoming soft to very soft and disaggregating in cold H2O;
	Other analyses	total organic carbon;
		SRF date 9-23-93 Exam date 1-2-95

Sample depth		
860.5 ft	Rock type	Mudstone;
	Color	olive black;
	Minerals	slightly silty, moderately dolomitic, moderately anhydritic, rare disseminated very fine siliceous spicules in part;
	Hardness	hard to firm;
	Parting	sub-blocky;
	Luster	earthy;
	Misc	metallic taste;
	Rxn HCl	slow effervescence, exfoliates in hot HCl, common residual acicular crystals;
	Rxn H2O	rare evaporitic very fine-grained fibrous white radial crystal clusters;
	Other analyses	unknown;
		SRF date 2-19-93 Exam date 1-3-95

Sample depth		
970.0 ft	Rock type	Clayshale;
	Color	olive grey;
	Minerals	non-silty, slightly to moderately dolomitic, slightly anhydritic, common fragments white milky opaque quartz veins to 2mm thick, trace fragments white fine-crystalline dolomite veins to .5mm thick;
	Hardness	soft to firm;
	Parting	sub-fissile to platy;
	Luster	earthy;
	Misc	no observed;
	Rxn HCl	slow effervescence, uncommon residual acicular crystals;
	Rxn H2O	becoming very soft and disaggregating in part, becoming colloidal in part, in cold H2O;
	Other analyses	unknown;
		SRF date 9-23-93 Exam date 1-3-95

Sample depth		
995.0 ft	Rock type	Clayshale;
	Color	olive grey to olive black;
	Minerals	non-silty, slightly dolomitic, moderately anhydritic;
	Hardness	soft to firm;
	Parting	fissile to sub-platy;
	Luster	earthy;
	Misc	metallic taste;
	Rxn HCl	slow effervescence, sulfurous odor, common residual acicular crystals;
	Rxn H2O	becoming very soft in cold H2O, with some disaggregation, trace fibrous white very fine-grained evaporitic crystals;
	Other analyses	unknown;
		SRF date 9-23-93 Exam date 1-3-95

Sample depth		
1050.5 ft	Rock type	Clayshale;
	Color	olive grey;
	Minerals	non-silty, non-calcareous, abundantly anhydritic;
	Hardness	soft;
	Parting	fissile to sub-blocky;
	Luster	earthy;
	Misc	no observed;
	Rxn HCl	expands violently in hot HCl with no to very slight slow effervescence, strong sulfurous odor and abundant residual acicular crystals;
	Rxn H2O	disaggregates completely to colloid in cold H2O;
	Other analyses	unknown;
		SRF date 9-23-93 Exam date 1-3-95

Sample depth		
1105.8 ft	Rock type	Clayshale;
	Color	olive black;
	Minerals	non-silty, very slightly dolomitic in part, abundantly anhydritic;
	Hardness	firm to very firm;
	Parting	fissile to sub-pencilly, hackly in part;
	Luster	sub-waxy;
	Misc	no observed;
	Rxn HCl	very slow effervescence, strong sulfurous odor and abundant residual acicular crystals, disaggregates in hot HCl;
	Rxn H2O	becoming soft to firm in cold H2O with platy and hackly parting;
	Other analyses	unknown;
		SRF date 9-23-93 Exam date 1-3-95

Sample depth		
1128.8 ft	Rock type	Mudshale;
	Color	olive grey;
	Minerals	slightly silty in part, abundantly anhydritic, rare white opaque calcite and dolomite fracture filling/slickensided in part, rare very soft very thin white opaque veins possibly anhydrite or kaolinite;
	Hardness	moderately firm;
	Parting	fissile to sub-platy;
	Luster	sub-waxy;
	Misc	no observed;
	Rxn HCl	abundant residual acicular crystals, disaggregates rapidly in hot HCl;
	Rxn H2O	becoming soft in cold H2O, disaggregating and becoming colloidal in part;
	Other analyses	unknown;
		SRF date 9-23-93 Exam date 1-3-95

Sample depth		
1198.8 ft	Rock type	Clayshale;
	Color	olive black;
	Minerals	non-silty, very slightly dolomitic, abundantly anhydritic;
	Hardness	firm to very firm;
	Parting	fissile to sub-platy to hackly;
	Luster	earthy to sub-waxy;
	Misc	no observed;
	Rxn HCl	abundant residual acicular crystals, disaggregates rapidly in hot HCl;
	Rxn H2O	becoming soft and platy-parting in cold H2O, becoming colloidal in part;
	Other analyses	bulk chemistry, trace elements;
		SRF date 9-23-93 Exam date 1-3-95

Sample depth		
1222.0 ft	Rock type	Clayshale;
	Color	olive black;
	Minerals	non-silty, non-calcareous, abundantly anhydritic;
	Hardness	firm to very firm;
	Parting	fissile to sub-blocky to hackly;
	Luster	earthy to sub-waxy;
	Misc	no observed;
	Rxn HCl	abundant residual acicular crystals, disaggregates rapidly in hot HCl;
	Rxn H2O	becoming soft and platy-parting in cold H2O, rarely becoming colloidal;
	Other analyses	unknown;
		SRF date 9-23-93 Exam date 1-3-95

Sample depth		
1281.5 ft	Rock type	Clayshale;
	Color	olive black;
	Minerals	non-silty, very slightly dolomitic, moderately anhydritic, rare to common very fine white opaque imbedded grains dissolve in hot HCl without effervescence;
	Hardness	very firm;
	Parting	sub-fissile to sub-platy to hackly, slickensided and polished in part;
	Luster	waxy to sub-waxy;
	Misc	?authigenic very fine-grained grey ?dolomite crystals raft on bubbles;
	Rxn HCl	sulfurous odor and common residual acicular crystals, becoming platy-parting in hot HCl, imbedded grain dissolution as noted in "Minerals" section;
	Rxn H2O	becoming firm and sub-platy-parting in cold H2O, rare white elongate tabular evaporite crystals;
	Other analyses	total organic carbon;
		SRF date 9-23-93 Exam date 1-3-95

Sample depth		
1300.5 ft	Rock type	Clayshale;
	Color	olive grey to olive black;
	Minerals	non-silty, very slightly dolomitic, abundantly anhydritic;
	Hardness	firm;
	Parting	sub-fissile to sub-platy;
	Luster	sub-waxy to earthy;
	Misc	no observed;
	Rxn HCl	strong sulfurous odor and abundant residual acicular crystals, slow to rapid disaggregation in hot HCl;
	Rxn H2O	becoming soft in cold H2O, disaggregating in part, becoming colloidal in part;
	Other analyses	total organic carbon;
		SRF date 9-23-93 Exam date 1-3-95

Sample depth		
1339.0 ft	Rock type	Clayshale;
	Color	olive grey to olive black;
	Minerals	non-silty, very slightly dolomitic, abundantly anhydritic;
	Hardness	firm;
	Parting	sub-fissile to sub-platy;
	Luster	sub-waxy to earthy;
	Misc	no observed;
	Rxn HCl	strong sulfurous odor and abundant residual acicular crystals, slow to rapid disaggregation in hot HCl;
	Rxn H2O	becoming soft in cold H2O, disaggregating in part, becoming colloidal in part;
	Other analyses	conodont age;
		SRF date 9-23-93 Exam date 1-3-95

Sample depth		
1549.0 ft	Rock type	Mudstone;
	Color	olive grey to olive black;
	Minerals	slightly silty, very slightly dolomitic, slightly to moderately anhydritic;
	Hardness	firm;
	Parting	sub-blocky to hackly;
	Luster	sub-waxy to waxy;
	Misc	slightly metallic taste;
	Rxn HCl	sparse to common small residual acicular crystals;
	Rxn H2O	becoming soft and platy- to hackly-parting in cold H2O;
	Other analyses	total organic carbon;
		SRF date 2-19-93 Exam date 1-3-95

Sample depth		
1596.0 ft	Rock type	Mudstone;
	Color	olive black to olive grey;
	Minerals	moderately silty, non-calcareous, abundantly anhydritic, some pieces with common very fine-grained disseminated pyrite, common slickensided veins of calcite/dolomite/quartz/anhydrite/?chlorite;
	Hardness	very firm;
	Parting	blocky;
	Luster	earthy to sub-waxy;
	Misc	slightly metallic taste, veins have common metallic inclusions;
	Rxn HCl	very slow exfoliation in hot HCl without effervescence, abundant small residual acicular crystals;
	Rxn H2O	becoming soft and platy- to hackly-parting in cold H2O;
	Other analyses	unknown;
	SRF date 2-19-93	Exam date 1-3-95

Sample depth		
1626.7 ft	Rock type	Mudstone;
	Color	olive black;
	Minerals	very silty, slightly dolomitic, moderately anhydritic, common very fine-grained disseminated pyrite;
	Hardness	very firm;
	Parting	blocky to hackly;
	Luster	sub-waxy, to pearly in part;
	Misc	no observed;
	Rxn HCl	slow effervescence, common small residual acicular crystals;
	Rxn H2O	none;
	Other analyses	unknown;
	SRF date 2-19-93	Exam date 1-4-95

Sample depth		
1697.3 ft	Rock type	Mudstone;
	Color	olive black;
	Minerals	very silty, very slightly dolomitic, abundantly anhydritic;
	Hardness	very firm;
	Parting	blocky to hackly;
	Luster	earthy to sub-waxy;
	Misc	slightly metallic taste;
	Rxn HCl	slow effervescence, abundant residual acicular crystals;
	Rxn H2O	becoming soft to firm in part, platy parting in cold H2O;
	Other analyses	unknown;
		SRF date 2-19-93 Exam date 1-4-95

Sample depth		
1735.4 ft	Rock type	Mudstone;
	Color	olive grey;
	Minerals	very to moderately silty, very to moderately dolomitic, abundantly anhydritic;
	Hardness	firm to very firm;
	Parting	sub-platy;
	Luster	earthy to sub-waxy;
	Misc	no observed;
	Rxn HCl	slow effervescence, abundant residual acicular crystals, rapid disaggregation in hot HCl;
	Rxn H2O	platy parting and some disaggregation in cold H2O;
	Other analyses	unknown;
		SRF date 2-19-93 Exam date 1-4-95

Sample depth		
1765.1 ft	Rock type	Mudstone;
	Color	olive black;
	Minerals	moderately silty, abundantly anhydritic, non-calcareous except for common very thin non-parallel wavy dolomitic laminae, common white to light green soft fine-crystalline thin veins of H2O-soluble mineral;
	Hardness	very firm;
	Parting	sub-platy to sub-blocky, slickensided in part;
	Luster	earthy to sub-waxy;
	Misc	no observed;
	Rxn HCl	abundant residual acicular crystals;
	Rxn H2O	becoming slightly to moderately firm in cold H2O, veins soluble as noted in "Minerals" section;
	Other analyses	unknown;
		SRF date 2-19-93 Exam date 1-4-95

Sample depth		
1809.2 ft	Rock type	Mudstone;
	Color	olive black;
	Minerals	very silty, moderately anhydritic, very slightly dolomitic;
	Hardness	very firm;
	Parting	sub-blocky to sub-platy;
	Luster	earthy;
	Misc	no observed;
	Rxn HCl	very slow effervescence, common residual acicular crystals;
	Rxn H2O	becoming firm with some platy parting in cold H2O;
	Other analyses	unknown;
		SRF date 2-19-93 Exam date 1-4-95

Sample depth		
1847.9 ft	Rock type	Mudstone;
	Color	olive black;
	Minerals	very slightly silty, slightly anhydritic, very slightly dolomitic;
	Hardness	very firm;
	Parting	sub-blocky to hackly;
	Luster	sub-waxy;
	Misc	no observed;
	Rxn HCl	very slow effervescence, sparse residual acicular crystals, slow disaggregation in hot HCl;
	Rxn H2O	becoming soft to slightly firm with common platy parting in cold H2O, becoming colloidal in small part;
	Other analyses	unknown;
	SRF date 2-19-93	Exam date 1-4-95

Sample depth		
1901.7 ft	Rock type	Mudstone;
	Color	olive black;
	Minerals	non-silty, moderately anhydritic, moderately dolomitic, abundant veins very fine crystalline white/yellow/light green and white/light green (slickensided in part) dominantly quartz with calcite and dolomite;
	Hardness	firm;
	Parting	sub-blocky to hackly;
	Luster	earthy;
	Misc	veins noted above may be recrystallized thin quartz-sand beds, folded;
	Rxn HCl	slow effervescence, common residual acicular crystals;
	Rxn H2O	becoming soft/colloidal in part in cold H2O, rare very fine white bladed evaporite crystals in petal-shaped clusters of four;
	Other analyses	unknown;
	SRF date 2-19-93	Exam date 1-4-95

Sample depth		
1947.2 ft	Rock type	Mudshale;
	Color	olive black;
	Minerals	very slightly silty, moderately anhydritic, very slightly dolomitic;
	Hardness	firm;
	Parting	sub-fissile to sub-platy, slickensided in part;
	Luster	earthy to waxy;
	Misc	no observed;
	Rxn HCl	very slow effervescence, common residual acicular crystals, sparse white opaque very fine bladed residual crystals;
	Rxn H2O	becoming slightly firm to soft in cold H2O, rare very fine white bladed evaporite crystals in petal-shaped clusters of four and less organized aggregations;
	Other analyses	unknown;
		SRF date 2-19-93 Exam date 1-4-95

Sample depth		
1985.5 ft	Rock type	Mudshale;
	Color	olive black;
	Minerals	slightly silty, abundantly anhydritic, very slightly dolomitic;
	Hardness	very firm;
	Parting	sub-blocky to sub-fissile, common wavy sub-parallel lamination;
	Luster	earthy to sub-waxy;
	Misc	no observed;
	Rxn HCl	very slow effervescence, sulfurous odor and abundant residual acicular crystals;
	Rxn H2O	becoming soft in cold H2O, disaggregating with fissile to papery parting;
	Other analyses	total organic carbon;
		SRF date 1-14-93 Exam date 1-4-95

Sample depth		
2029.5 ft	Rock type	Mudstone;
	Color	olive grey to olive black;
	Minerals	very silty, abundantly anhydritic, very slightly dolomitic, common fine-crystalline veins (slickensided in part) of white/yellow/light green (quartz/dolomite/calcite mineralogy) as above;
	Hardness	very firm;
	Parting	sub-blocky to hackly, common slickensides;
	Luster	earthy to waxy;
	Misc	rare spotty dull purple mineral fluorescence in crystalline vein material;
	Rxn HCl	very slow effervescence, abundant residual acicular crystals;
	Rxn H2O	becoming firm in cold H2O, common white very fine bladed evaporite crystals as above;
	Other analyses	unknown;
		SRF date 2-19-93 Exam date 1-4-95

Sample depth		
2061.1 ft	Rock type	Mudstone;
	Color	olive grey to olive black;
	Minerals	very silty, abundantly anhydritic, very slightly dolomitic;
	Hardness	very firm;
	Parting	sub-blocky to hackly;
	Luster	waxy to pearly;
	Misc	no observed;
	Rxn HCl	very slow effervescence, abundant residual acicular crystals;
	Rxn H2O	becoming firm in cold H2O, common white very fine bladed evaporite crystals as above;
	Other analyses	unknown;
		SRF date 2-19-93 Exam date 1-4-95

Sample depth		
2158.0 ft	Rock type	Mudstone;
	Color	olive black;
	Minerals	slightly silty, moderately to very dolomitic, slightly anhydritic;
	Hardness	very firm;
	Parting	sub-blocky to pencilly;
	Luster	earthy to sub-waxy;
	Misc	metallic taste, indistinct thick laminae;
	Rxn HCl	slow effervescence, sparse residual small acicular and bladed crystals;
	Rxn H2O	developing common blocky parting in cold H2O;
	Other analyses	total organic carbon, thin section;
		SRF date 1-14-93 Exam date 1-4-95

Sample depth		
2224.8 ft	Rock type	Clayshale;
	Color	grey black to black;
	Minerals	non-silty, slightly to moderately dolomitic, moderately anhydritic, abundant veins of white/light yellow/light green fine- to medium-crystalline calcite/dolomite/quartz as above;
	Hardness	firm;
	Parting	fissile to hackly, sheared in part;
	Luster	sub-waxy to waxy to pearly;
	Misc	metallic taste;
	Rxn HCl	slow effervescence, common residual acicular crystals;
	Rxn H2O	becoming firm to moderately soft in cold H2O;
	Other analyses	unknown;
		SRF date 1-14-93 Exam date 1-4-95

Sample depth		
2295.0 ft	Rock type	Mudshale;
	Color	olive black;
	Minerals	slightly silty, non-calcareous, moderately anhydritic;
	Hardness	firm;
	Parting	sub-fissile to sub-hackly, with indistinct thick laminae;
	Luster	earthy to sub-waxy;
	Misc	no observed;
	Rxn HCl	common residual acicular crystals;
	Rxn H2O	becoming fissile, moderately soft in part, in cold H2O;
	Other analyses	unknown;
		SRF date 2-19-93 Exam date 1-4-95

Sample depth		
2346.0 ft	Rock type	Mudstone;
	Color	olive grey to olive black;
	Minerals	very silty, very slightly dolomitic, abundantly anhydritic, common slickensided veins of soft light yellow green mineral (?gypsum) with metallic inclusions;
	Hardness	very firm;
	Parting	sub-blocky, with indistinct thick laminae;
	Luster	earthy to sub-waxy;
	Misc	no observed;
	Rxn HCl	very slow effervescence, very abundant residual acicular crystals;
	Rxn H2O	becoming firm in cold H2O, with rare white very fine evaporite crystals;
	Other analyses	unknown;
		SRF date 2-19-93 Exam date 1-4-95

Sample depth		
2420.1 ft	Rock type	Mudshale;
	Color	olive grey to olive black;
	Minerals	slightly silty, non-calcareous, moderately ?anhydritic, fine sand-size mudshale intraclasts;
	Hardness	very firm;
	Parting	pencilly to sub-fissile, thick indistinct laminae, commonly slickensided;
	Luster	sub-waxy to sub-earthy;
	Misc	no observed;
	Rxn HCl	common white opaque very fine-crystalline blades and pencils (not acicular or radial) on sample after drying (not in residual ring), very soft;
	Rxn H2O	becoming firm and disaggregating in part in cold H2O, with very rare white very fine evaporite crystals as above;
	Other analyses	unknown;
	SRF date 2-19-93	Exam date 1-5-95

Sample depth		
2453.8 ft	Rock type	Mudshale;
	Color	brown black;
	Minerals	slightly silty, slightly to very slightly dolomitic, moderately ?anhydritic;
	Hardness	firm;
	Parting	pencilly to sub-fissile, thick indistinct laminae;
	Luster	sub-waxy to sub-earthy;
	Misc	no observed;
	Rxn HCl	very slow effervescence, common very soft white opaque very fine-crystalline blades and pencils on sample after drying;
	Rxn H2O	becoming firm to soft and platy-parting in cold H2O, disaggregating in part;
	Other analyses	unknown;
	SRF date 2-19-93	Exam date 1-5-95

Sample depth		
2492.0 ft	Rock type	Mudshale;
	Color	grey black to black;
	Minerals	slightly silty, moderately dolomitic, moderately ?anhydritic, very abundant slickensided veins of light green/yellow green soft mineral (?gypsum) with metallic inclusions;
	Hardness	firm to hard;
	Parting	fissile to sub-platy;
	Luster	sub-waxy to waxy;
	Misc	moderately bright spotty blue mineral fluorescence in vein material;
	Rxn HCl	slow effervescence, common very soft white opaque very fine-crystalline blades and pencils on sample after drying;
	Rxn H2O	none;
	Other analyses	unknown;
		SRF date 2-19-93 Exam date 1-5-95

Sample depth		
2523.9 ft	Rock type	Mudstone;
	Color	olive grey to olive black;
	Minerals	slightly silty, slightly to moderately dolomitic, abundantly anhydritic;
	Hardness	very firm;
	Parting	sub-blocky;
	Luster	sub-earthy;
	Misc	no observed;
	Rxn HCl	slow effervescence, abundant residual acicular crystals, and abundant very soft white opaque very fine-crystalline blades and pencils on sample after drying;
	Rxn H2O	becoming firm to very firm with some sub-platy parting in cold H2O;
	Other analyses	thin section;
		SRF date 1-14-93 Exam date 1-5-95

Sample depth		
2654.0 ft	Rock type	Mudshale;
	Color	olive black;
	Minerals	moderately silty in part, slightly silty in part, very slightly dolomitic, abundantly anhydritic;
	Hardness	very firm;
	Parting	sub-fissile to sub-platy;
	Luster	earthy to sub-waxy;
	Misc	no observed;
	Rxn HCl	very slow effervescence, abundant residual acicular crystals, and abundant very soft white opaque very fine crystalline blades and pencils on sample after drying;
	Rxn H2O	becoming firm/platy-parting in part and soft/papery-parting in part in cold H2O;
	Other analyses	total organic carbon;
		SRF date 1-14-93 Exam date 1-5-95

Sample depth		
2691.7 ft	Rock type	Mudstone;
	Color	olive black to grey black;
	Minerals	slightly to moderately silty, very slightly dolomitic, moderately anhydritic;
	Hardness	very firm;
	Parting	sub-blocky;
	Luster	sub-waxy to earthy;
	Misc	no observed;
	Rxn HCl	very slow effervescence, common residual acicular crystals, common very soft white opaque very fine crystalline blades and pencils on sample after drying;
	Rxn H2O	becoming firm in cold H2O, platy-parting in part;
	Other analyses	total organic carbon, thin section;
		SRF date 1-14-93 Exam date 1-5-95

Sample depth		
2834.5 ft	Rock type	Mudshale;
	Color	olive grey to grey black;
	Minerals	slightly silty, very slightly dolomitic, moderately anhydritic;
	Hardness	very firm;
	Parting	sub-platy to fissile, slickensided in part;
	Luster	waxy to pearly;
	Misc	no observed;
	Rxn HCl	very slow effervescence, common residual acicular crystals, common very soft white opaque very fine crystalline blades and pencils on sample after drying;
	Rxn H2O	becoming platy-parting in cold H2O, dried sample has common very fine drusy ?cubic white opaque crystals with salty taste;
	Other analyses	unknown;
		SRF date 2-19-93 Exam date 1-5-95

Sample depth		
2871.5 ft	Rock type	Clayshale;
	Color	dark grey to grey black;
	Minerals	non-silty, slightly dolomitic in part, moderately anhydritic, common veins white translucent gypsum;
	Hardness	firm;
	Parting	fissile to sub-platy, commonly slickensided;
	Luster	waxy to pearly;
	Misc	no observed;
	Rxn HCl	very slow effervescence, common residual acicular crystals, common very soft white opaque very fine crystalline blades and pencils on sample after drying;
	Rxn H2O	becoming soft and disaggregating in part in cold H2O, dried sample has abundant very fine drusy ?cubic white opaque crystals with salty taste;
	Other analyses	total organic carbon;
		SRF date 1-14-93 Exam date 1-5-95